USGS
science for a changing world

Prepared in cooperation with the
Georgia Department of Natural Resources
Environmental Protection Division

Simulated Effects of Seasonal Ground-Water Pumpage for Irrigation on Hydrologic Conditions in the Lower Apalachicola–Chattahoochee–Flint River Basin, Southwestern Georgia and Parts of Alabama and Florida, 1999–2002

Scientific Investigations Report 2006-5234

U.S. Department of the Interior
U.S. Geological Survey

Cover photograph: Center-pivot irrigation system in peanut field, Baker County, Georgia.

Photograph by L. Elliott Jones, U.S. Geological Survey

Simulated Effects of Seasonal Ground-Water Pumpage for Irrigation on Hydrologic Conditions in the Lower Apalachicola–Chattahoochee–Flint River Basin, Southwestern Georgia and Parts of Alabama and Florida, 1999–2002

By L. Elliott Jones and Lynn J. Torak

Prepared in cooperation with the
Georgia Department of Natural Resources,
Environmental Protection Division

Scientific Investigations Report 2006-5234

U.S. Department of the Interior
U.S. Geological Survey

U.S. Department of the Interior
DIRK KEMPTHORNE, Secretary

U.S. Geological Survey
Mark D. Myers, Director

U.S. Geological Survey, Reston, Virginia: 2006

This report is a Web-only publication: ***http://pubs.usgs.gov/sir/2006/5234/***

For more information on the USGS—the Federal source for science about the Earth, its natural and living resources, natural hazards, and the environment:
World Wide Web: *http://www.usgs.gov/*

Suggested citation:
Jones, L.E., and, Torak, L.J., 2006, Simulated efects of seasonal ground-water pumpage for irrigation on hydrologic conditions in the lower Apalachicola–Chattahoochee–Flint River Basin, southwestern Georgia and parts of Alabama and Florida, 1999–2002: U.S. Geological Survey Scientific Investigations Report 2006-5234, 115 p., a Web-only publication at *http://pubs.usgs.gov/sir/2006/5234/*.

Contents

Figures

Figures—Continued

Figures—Continued

Figures—Continued

Tables

Tables—Continued

Conversion Factors

Multiply	By	To obtain
	Length	
inch (in.)	2.54	centimeter (cm)
foot (ft)	0.3048	meter (m)
mile (mi)	1.609	kilometer (km)
	Area	
acre	0.4047	hectare (ha)
square mile (mi^2)	2.590	square kilometer (km^2)
	Volume	
gallon (gal)	3.785	liter (L)
cubic mile (mi^3)	4.168	cubic kilometer (km^3)
	Flow rate	
foot per day (ft/d)	0.3048	meter per day (m/d)
cubic foot per second (ft^3/s)	0.02832	cubic meter per second (m^3/s)
gallon per minute (gal/min)	0.06309	liter per second (L/s)
million gallons per day (Mgal/d)	0.04381	cubic meter per second (m^3/s)
inch per year (in/yr)	2.54	centimeter per year (cm/yr)
	Hydraulic conductivity	
foot per day (ft/d)	0.3048	meter per day (m/d)
	Transmissivity*	
foot squared per day (ft^2/d)	0.09290	meter squared per day (m^2/d)

Temperature in degrees Fahrenheit (°F) may be converted to degrees Celsius (°C) as follows:

$$°C = (°F - 32) / 1.8$$

Vertical coordinate information is referenced to the North American Vertical Datum of 1988 (NAVD 88).

Horizontal coordinate information is referenced to the North American Datum of 1983 (NAD 83).

Altitude, as used in this report, refers to distance above the vertical datum.

*Transmissivity: The standard unit for transmissivity is cubic foot per day per square foot times foot of aquifer thickness [$(ft^3/d)/ft^2$]ft. In this report, the mathematically reduced form, foot squared per day (ft^2/d), is used for convenience.

Specific conductance is given in microsiemens per centimeter at 25 degrees Celsius (µS/cm at 25 °C).

Concentrations of chemical constituents in water are given either in milligrams per liter (mg/L) or micrograms per liter (µg/L).

NOTE TO USGS USERS: Use of liter (L) as a special name for cubic decimeter (dm^3) is restricted to the measurement of liquids and gases. No prefix other than milli should be used with liter.

Simulated Effects of Seasonal Ground-Water Pumpage for Irrigation on Hydrologic Conditions in the Lower Apalachicola–Chattahoochee–Flint River Basin, Southwestern Georgia and Parts of Alabama and Florida, 1999–2002

By L. Elliott Jones and Lynn J. Torak

Abstract

To determine the effects of seasonal ground-water pumpage for irrigation, a finite-element ground-water flow model was developed for the Upper Floridan aquifer in the lower Flint River Basin area, including adjacent parts of the Chattahoochee and Apalachicola River Basins. The model simulates withdrawal from the aquifer at 3,280 irrigation, municipal, and industrial wells; stream-aquifer flow between the aquifer and 36 area streams; leakage to and from the overlying upper semiconfining unit; regional ground-water flow at the lateral boundaries of the model; and water-table recharge in areas where the aquifer is at or near land surface. Steady-state calibration to drought conditions of October 1999 indicated that the model could adequately simulate measured ground-water levels at 275 well locations and streamflow gains and losses along 53 reaches of area streams. A transient simulation having 12 monthly stress periods from March 2001 to February 2002 incorporated time-varying stress from irrigation pumpage, stream and lake stage, head in the overlying upper semiconfining unit, and infiltration rates.

Analysis of simulated water budgets of the Upper Floridan aquifer provides estimates of the source of water pumped for irrigation. During October 1999, an estimated 127 million gallons per day (Mgal/d) of irrigation pumpage from the Upper Floridan aquifer in the model area were simulated to be derived from changes in: stream-aquifer flux (about 56 Mgal/d, or 44 percent); leakage to or from the upper semiconfining unit (about 49 Mgal/d, or 39 percent); regional flow (about 18 Mgal/d, or 14 percent); leakage to or from Lakes Seminole and Blackshear (about 2.7 Mgal/d, or 2 percent); and flux at the Upper Floridan aquifer updip boundary (about 1.8 Mgal/d, or 1percent). During the 2001 growing season (May–August), estimated irrigation pumpage ranged from about 310 to 830 Mgal/d, about 79 percent of the 12-month total. During the growing season, irrigation pumpage was derived from decreased discharge or increased recharge of stream-aquifer flux (from about 23 to 39 percent), leakage to or from the upper semiconfining unit (from about 30 to 36 percent), regional flow (from about 8 to 11 percent), Lakes Seminole and Blackshear (about 2 percent), and flux at the Upper Floridan aquifer updip boundary (about 1 percent). Storage effects (decreased storage gain or increased storage loss) contributed from about 11 to 36 percent of irrigation pumpage during the growing season.

Water managers can use the model to determine where and how much additional ground-water pumpage for irrigation should be permitted based on a variety of hydrologic constraints. For example, the model results may indicate that in some critical locations, additional ground-water pumpage during a prolonged drought might reduce stream-aquifer flux enough to cause noncompliance of established minimum in-stream flow conditions.

Introduction

The Apalachicola–Chattahoochee–Flint (ACF) River Basin encompasses a long, narrow area of about 19,256 square miles (mi^2), mostly in western Georgia and partly in southeastern Alabama and northwestern Florida (see inset map in fig. 1). About 17,230 mi^2 of the ACF River Basin are contained in Georgia and Alabama, and this area is nearly equally divided between the Chattahoochee and Flint Rivers. The remaining 2,026 mi^2 of drainage area in the ACF River Basin are tributary directly to the Apalachicola River in Florida (U.S. Army Corps of Engineers, 1973). Flow from the Chattahoochee and Flint Rivers is tributary to Lake Seminole, a human-made impoundment located at the Georgia-Florida State line that provides headwater to the Apalachicola River (fig. 1). The Apalachicola River flows from Lake Seminole about 107 miles (mi) southward through the panhandle of northwestern Florida to the Gulf of Mexico. Flow in the Apalachicola River is important to the ecology and economy of the region surrounding the floodplain and estuary.

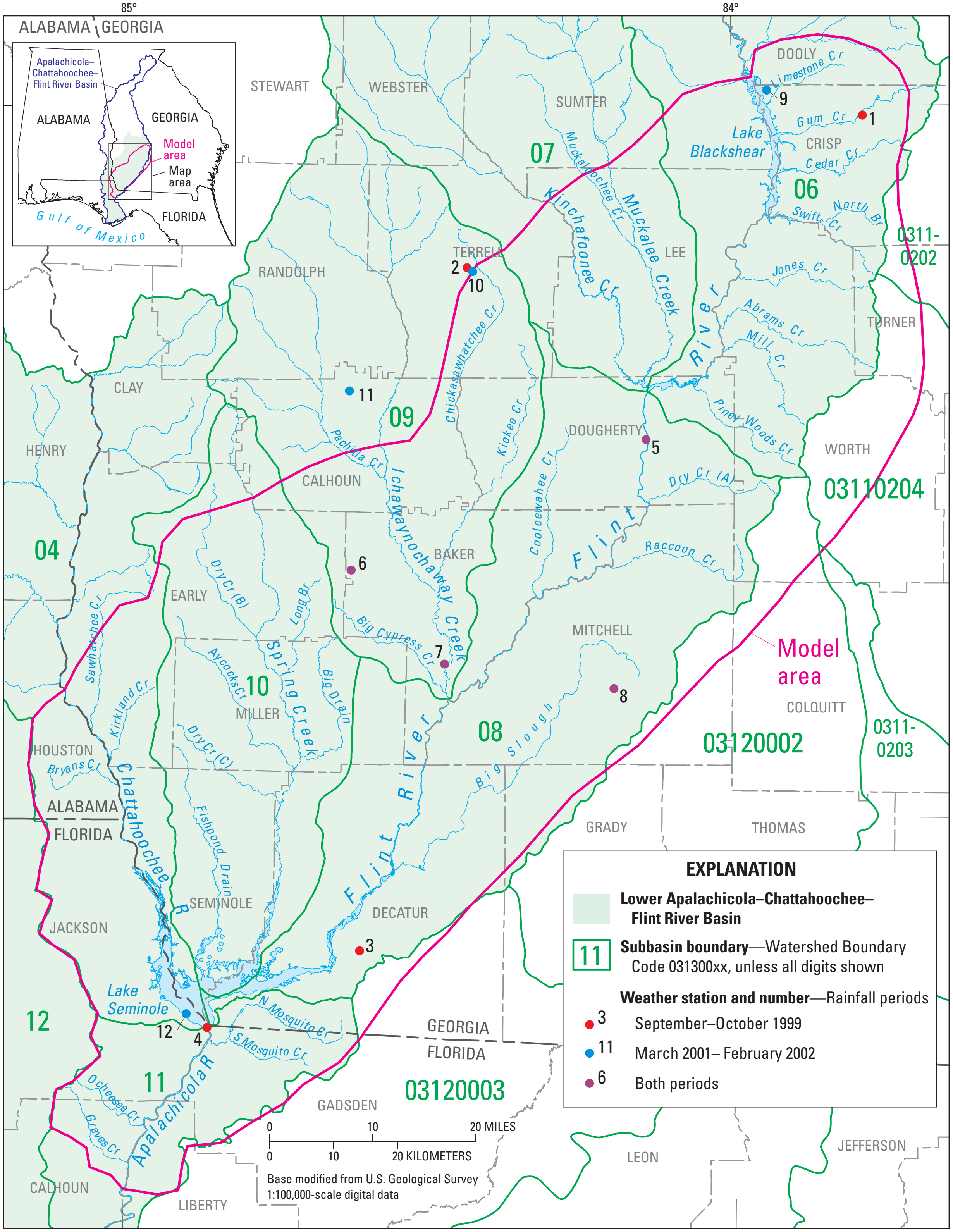

Figure 1. Ground-water flow model area, lower Apalachicola–Chattahoochee–Flint River Basin, subbasin boundaries, major streams, and weather stations used for model input (identified in table A1) in southwest Georgia and adjacent parts of Alabama and Florida.

The principal rivers and tributaries of the lower ACF River Basin (fig. 1) drain karstic and fluvial plains, which are hydraulically connected to the Upper Floridan aquifer, one of the most productive aquifers in the United States. The Upper Floridan aquifer contains nearly 100,000 cubic miles of predominantly karst limestone (Bush and Johnston, 1988) and is the primary source of ground water for agriculture, industry, and public supply in the lower ACF River Basin. Irrigation pumpage is the major use of ground water in this heavily agricultural region. Nearly 500,000 acres are irrigated with ground water from about 4,000 wells completed in the Upper Floridan aquifer (James E. Hook, National Environmentally Sound Production Agricultural Laboratory, written commun., November 2002). During 2002, ground-water withdrawal from the Upper Floridan aquifer in the Flint River Basin averaged about 340 million gallons per day (Mgal/d) (Hook and others, 2005).

Hydraulic connection of the Upper Floridan aquifer with surface water in the lower ACF River Basin occurs directly through many karst sinks, sinkhole ponds, and conduits that expose limestone at land surface. Indirect hydraulic connection of the aquifer with surface water occurs by leakage through undifferentiated overburden consisting of alluvium and chemically weathered limestone (residuum), which mantles the aquifer throughout much of the area. Many springs feed streams that flow directly on limestone of the Upper Floridan aquifer. Streams contain gaining and losing reaches that change seasonally and along relatively short distances. Some streams disappear into limestone sinks and caverns, flow underground in the aquifer, and reappear in solution openings in the limestone.

During the early and mid-1990s, the ACF River Basin gained prominence as Georgia, Florida, and Alabama competed within the judicial system for the basin's finite water resources (U.S. Army Corps of Engineers, 1997). Increases in population, agriculture, and industry and the drought from 1998 to 2002 made water supply and use in the lower ACF River Basin a major concern for environmental managers. To avert a potentially costly and time-consuming court battle concerning water, the three States signed the ACF River Basin Compact[1] during 1997, intending to ensure equitable use and availability of water resources in the region while protecting river ecology. After 6 years of negotiations, the States failed to reach a water-sharing agreement by the deadline of July 2003, and the tri-state decision of water allocation in the ACF River Basin reverted to the courts (Shelton, 2005).

During October 1999, the Georgia Environmental Protection Division (GaEPD) initiated the Flint River Basin Regional Water Development and Conservation Plan (Flint River Basin Plan) under the authority of two Georgia statutes that regulate water withdrawal permitting in Georgia: the Water Quality Act and the Ground-Water Use Act [Official Code of Georgia Annotated, subsections 12-5-31(h) and 12-5-96(e), respectively; from Georgia Environmental Protection Division, 2005]. The Water Quality Act states that such plans "shall promote the conservation and reuse of water, guard against a shortage of water, and promote efficient use of the water resource." Initiation of such plans allows GaEPD to suspend issuance of permits until completion of the plan, after which all permits must be consistent with the plan. Thus, as part of the Flint River Basin Plan, and because agricultural water use is by far the largest use category in the Flint River Basin, the Director of GaEPD announced that the GaEPD would not process farm-use permit applications for withdrawals from the Upper Floridan aquifer in the lower Flint River Basin and for surface-water withdrawals in the entire Flint River Basin after November 30, 1999. This moratorium remained in place until GaEPD adopted the Flint River Basin Plan (Georgia Environmental Protection Division, 2006).

Implementation of the Flint River Basin Plan includes a hydrologic assessment of the Upper Floridan aquifer in southwestern Georgia and an update of an existing digital model of ground-water flow (William H. McLemore, Georgia State Geologist, Georgia Department of Natural Resources, Environmental Protection Division, Geologic Survey Branch, Atlanta, Ga., written commun., May 2000). During 1999, the GaEPD requested that the U.S. Geological Survey (USGS) engage in a cooperative investigation to "develop considerable new data" in support of the hydrologic assessment of the Upper Floridan aquifer. The investigation incorporated site-specific hydrologic measurements into an updated version of the digital model developed by Torak and McDowell (1996) to simulate time-variant (transient) ground-water flow and stream-aquifer interaction (Harold F. Reheis, Director, Georgia Environmental Protection Division, Atlanta, Ga., written commun., April 1999). State water officials intend to use the model as a management tool to provide an early indication of low-streamflow and ground-water level conditions that might occur within the basin, and as a predictor of low streamflow in the Apalachicola River at the Georgia–Florida State line at Chattahoochee, Florida. Analysis of model results would provide the basis of a method to notify specific agricultural water users early in the year of possible restrictions on irrigation withdrawal during the upcoming growing season (Harold F. Reheis, Director, Georgia Environmental Protection Division, Atlanta, Ga., written commun., April 1999).

The following objectives represent the role of the USGS in addressing part of the State's water issues through implementation of the Flint River Basin Plan:

- Increase current understanding of the hydrogeologic framework that controls stream-aquifer relations and flow-system processes in the lower ACF River Basin

---

[1]As adopted by: the Alabama Legislature on February 18, 1997, and signed by the Governor of Alabama on February 25, 1997, as Alabama Acts 97-67, Alabama Code, Title 33-19-1 et seq.; the Florida Legislature on April 14, 1997, and signed by the Governor of Florida on April 24, 1997, as Chapter 97-25, Laws of Florida, Section 373.71, Florida Statutes (1997); the Georgia Legislature on February 11, 1997, as Georgia Acts No. 7, and signed by the Governor of Georgia on February 25, 1997, as Georgia Code Annual Section 12-10-100 et seq., and passed by the United States Congress on November 7, 1997, and signed by the President of the United States on November 20, 1997, as Public Law Number 105-104, 111 Statute 2219; accessed December 19, 2006, at *http://www.legis.state.ga.us/legis/1997_98/fulltext/hb149.htm*

through analysis of recent subsurface geologic, geophysical, and hydrologic data.

- Devise and direct a program of boring, well drilling and installation, and aquifer testing to acquire hydrogeologic information in areas where data are lacking.
- Establish a hydrologic data-collection network suitable for assessing stream-aquifer relations, recharge, and withdrawal from the Upper Floridan aquifer.
- Incorporate newly acquired and existing hydrologic data into a transient finite-element model of ground-water flow capable of simulating seasonal ground-water level and streamflow conditions and pumpage-induced streamflow reduction (William H. McLemore, Georgia State Geologist, Georgia Department of Natural Resources, Environmental Protection Division, Geologic Survey Branch, Atlanta, Ga., written commun., May 2000).

Purpose and Scope

This report is the third in a series of three reports describing work performed by the USGS that contributes to a hydrologic assessment of the Upper Floridan aquifer in southwestern Georgia, as part of the State of Georgia's Flint River Basin Plan. The first report by Mosner (2002) partially addressed the first previously listed objective by describing stream-aquifer relations in the lower ACF River Basin, effects of drought on the ground-water level of the Upper Floridan aquifer, and ground-water discharge to (or baseflow of) streams. In the second report, Torak and Painter (2006) addressed the first three objectives listed in the previous section by describing the geologic and hydrologic setting of the stream-aquifer flow system comprising the Upper Floridan aquifer, overlying and underlying hydrologic units, and surface water. This report addresses the final objectives listed in the previous section; namely, the development of a transient, finite-element model of ground-water flow capable of simulating seasonal ground-water flow conditions.

This report documents technical aspects of a finite-element model used to simulate effects of seasonal ground-water pumpage for irrigation on hydrologic conditions in the stream-lake-aquifer flow system located in the lower ACF River Basin in southwestern Georgia and adjacent parts of Alabama and Florida. Thus, the report contains maps, tables, charts, and diagrams that describe relevant hydrologic components of the flow system and flow-system conceptualization, areal and vertical representation of flow-system components in the digital model, analysis of model results, and discussions pertinent to resource management based on simulated changes to hydrologic components. Results presented are focused specifically on drought conditions that existed during the study period extending from March 2001 to February 2002. General background of these and historical drought conditions are referenced to reports by Torak and others (1993 and 1996), Torak and McDowell (1996), and Torak and Painter (2006), and are cited where appropriate.

The ground-water model described in this report is based on an earlier model of the lower ACF River Basin (Torak and others, 1996), which was calibrated using a steady-state simulation of drought conditions (ground-water levels and streamflow) during October 1986. Using hydrologic data collected since the previous model was developed, including data collected recently during this study, the new model was developed and was calibrated using a steady-state simulation based on ground-water level and streamflow conditions of October 1999. Drought conditions of October 1999 allowed streamflow conditions to be considered in calibration, by assuming that the difference in streamflow between successive gaging stations is attributable only to stream-aquifer flux. The model was then applied to simulation of seasonal conditions during a 12-month period, including a 6-month irrigation season and a 6-month off-season having relatively little irrigation pumpage.

Previous Studies

Many investigators have studied the regional geology, physiography, geohydrology, and ground-water resources of the Upper Floridan aquifer in the lower ACF River Basin since the 1890s. A study by McCallie (1898) first described the general geology and ground-water resources of the Coastal Plain; this was followed by similar studies by Stephenson and Veatch (1915), Cooke (1939, 1943), and Herrick (1961).

Wait (1963), Sever (1965a, b), Pollard and others (1978), and Hicks and others (1981, 1987) described detailed investigations of geologic formations, water-bearing properties, and the hydrology of selected parts of the lower ACF River Basin. Moore (1955), Kwader and Schmidt (1978), Schmidt (1978, 1979, 1984), Schmidt and Coe (1978), Schmidt and Clark (1980), and Schmidt and others (1980) investigated the geology of parts of the lower ACF River Basin in Florida near Lake Seminole. Arthur and Rupert (1989) investigated details of basin physiography. A preimpoundment survey identified details of the geology, hydrogeology, and structural integrity of foundation material to Jim Woodruff Lock and Dam (U.S. Army Corps of Engineers, 1948). Hayes and others (1983) defined geohydrologic and hydraulic characteristics of the Floridan aquifer system (formerly called the *principal artesian aquifer system*) in southwestern Georgia, and developed a hydrologic budget and digital model that quantified aquifer-system response to real and hypothetical increases in ground-water withdrawal. Torak and others (1993, 1996) and Torak and McDowell (1996) updated the geohydrology of parts of the lower ACF River Basin from that described by Hayes and others (1983), investigated stream-aquifer relations, and simulated the effects of ground-water withdrawal on streamflow and water levels in the Upper Floridan aquifer.

Mosner (2002) described stream-aquifer relations and ground-water level conditions in the lower ACF River Basin during the drought years of 1999 and 2000, and computed aquifer contribution to streamflow for specific reaches. Jones and Torak (2004) described the geohydrology of the area surrounding Lake Seminole in southwestern Georgia and simulated the effects of impoundment on ground-water flow in the Upper Floridan aquifer. Torak and others (2006) cited physical and hydrochemical evidence of hydraulic connection between surface water and ground water beneath and around Lake Seminole and Jim Woodruff Lock and Dam and documented the complex exchange of surface water and ground water among the lake, streams, and aquifer. Torak and Painter (2006) described the geologic and hydrologic framework of the lower ACF River Basin, incorporating borehole and aquifer-test data collected for this study.

Model Area

The model area is located in the lower ACF River Basin and adjacent areas of the Coastal Plain physiographic province in parts of southwestern Georgia, northwestern Florida, and southeastern Alabama, and consists of the land area that contributes ground water and surface water to the Upper Floridan aquifer, about 4,632 mi^2 (fig. 1). In Georgia, the model area includes all or parts of the following counties: Baker, Calhoun, Colquitt, Crisp, Decatur, Dooly, Dougherty, Early, Grady, Lee, Miller, Mitchell, Seminole, Sumter, Terrell, Turner, and Worth. In Florida, the model area is contained within Calhoun, Gadsden, Jackson, and Liberty Counties; in Alabama, a small part of the model area is located in Houston County.

Climate

The climate of the lower ACF River Basin is humid subtropical, defined by long summers and mild winters. Temperature and precipitation vary seasonally and areally across the basin as a result of the proximity of the basin to the Gulf of Mexico and the length of the basin, which spans about 150 mi in a northeast-to-southwest direction (Torak and Painter, 2006). The coldest months, December and January, average about 51.4 degrees Fahrenheit (°F) in the southern part of the basin (near Colquitt, Ga., fig. 2) and about 44.7°F to the north (near Plains, Ga.); freezing temperatures, however, can occur during this time. The warmest months, July and August, average about 80°F at both locations, although temperatures near 100°F are common. The mean annual air temperature at Colquitt, Ga., is about 66.4°F for the 47-year period from 1957 to 2003, and the mean annual air temperature is about 64°F at Plains, Ga., for the 48-year period from 1956 to 2003 (Torak and Painter, 2006).

Normal[2] annual precipitation ranges from about 49.4 inches at Plains, Ga., in the northern part of the model area, to about 53.2 inches at Colquitt, Ga., in the southern part of the model area, for the climate-averaging period from 1961 to 1990 (National Oceanic and Atmospheric Administration, 2003). Although precipitation is fairly uniformly distributed throughout the year, most of the recharge to the aquifer occurs during December through March, when storms associated with frontal passages bring relatively long-duration (from 2 to 3 days), low-intensity rainfall to the model area, and evapotranspiration rates are low. Rainfall events of this type are conducive to high infiltration and low runoff, in contrast with summer rainfall, which is usually of short duration and high intensity, derived from convective-type thunderstorms that cause high runoff and low infiltration (Torak and Painter, 2006).

The extent and severity of the drought from 1998 to 2002 affected several parts of the lower ACF River Basin differently than others (Torak and Painter, 2006). Although monthly precipitation and departure from normal precipitation recovered slightly from the drought during the first half of 2001 in areas near Americus, Camilla, and Morgan, Ga. (fig. 2), drought conditions persisted for the remainder of 2001 and through the first half of 2002. Normal to above-normal precipitation occurred by the last half of 2002, although cumulative departures from normal precipitation during 2001 and 2002 remained negative, with some locations indicating precipitation deficits from 12 to 13 inches. An exception to negative departures from normal precipitation for 2002 occurred in Colquitt, Ga., which overcame a 7-inch deficit during May to finish the year with a 15-inch surplus (Torak and Painter, 2006).

[2]Climate data normals: The average value of the meteorological element (for example, precipitation and temperature) during a time period. Effective January 1, 1993, the averaging period is from 1961 to 1990. The normals for National Weather Service localities have been adjusted so as to be representative for the current observation site (National Oceanic and Atmospheric Administration, 2003).

Physiography and Drainage

The model area is located in the Coastal Plain physiographic province and can be divided into four distinct regions: (1) a region of rolling hills and dendritic drainage; (2) a low-lying karstic region; (3) a region of dissected remnant hills and sand-hill ridges; and (4) a flat, low-lying, coastal-sediment region. The rolling hills comprise the Fall Line Hills District along the northwestern model boundary (fig. 2). The karstic region includes the Dougherty Plain, Marianna Lowlands, and Tifton Upland physiographic districts (fig. 2). In the Florida panhandle, the Dougherty Plain District is called the Marianna Lowlands District, and the Tifton Upland District is called the Tallahassee Hills District (Puri and Vernon, 1964). The boundary between the Dougherty Plain and Tifton Upland Districts in Georgia is a regionally prominent northwest-facing escarpment called the Solution Escarpment (MacNeil, 1947), or Pelham Escarpment (Hayes and others, 1983). In the southernmost part of the model area in Florida, the Holmes Valley Scarp separates the Marianna Lowlands District from the Grand Ridge region, a topographically high area containing dissected remnant hills and sand-hill ridges (Schmidt and Coe, 1978). Along the Apalachicola River in Florida, the Gulf Coastal Lowlands contains the flat, low-lying coastal-sediment region.

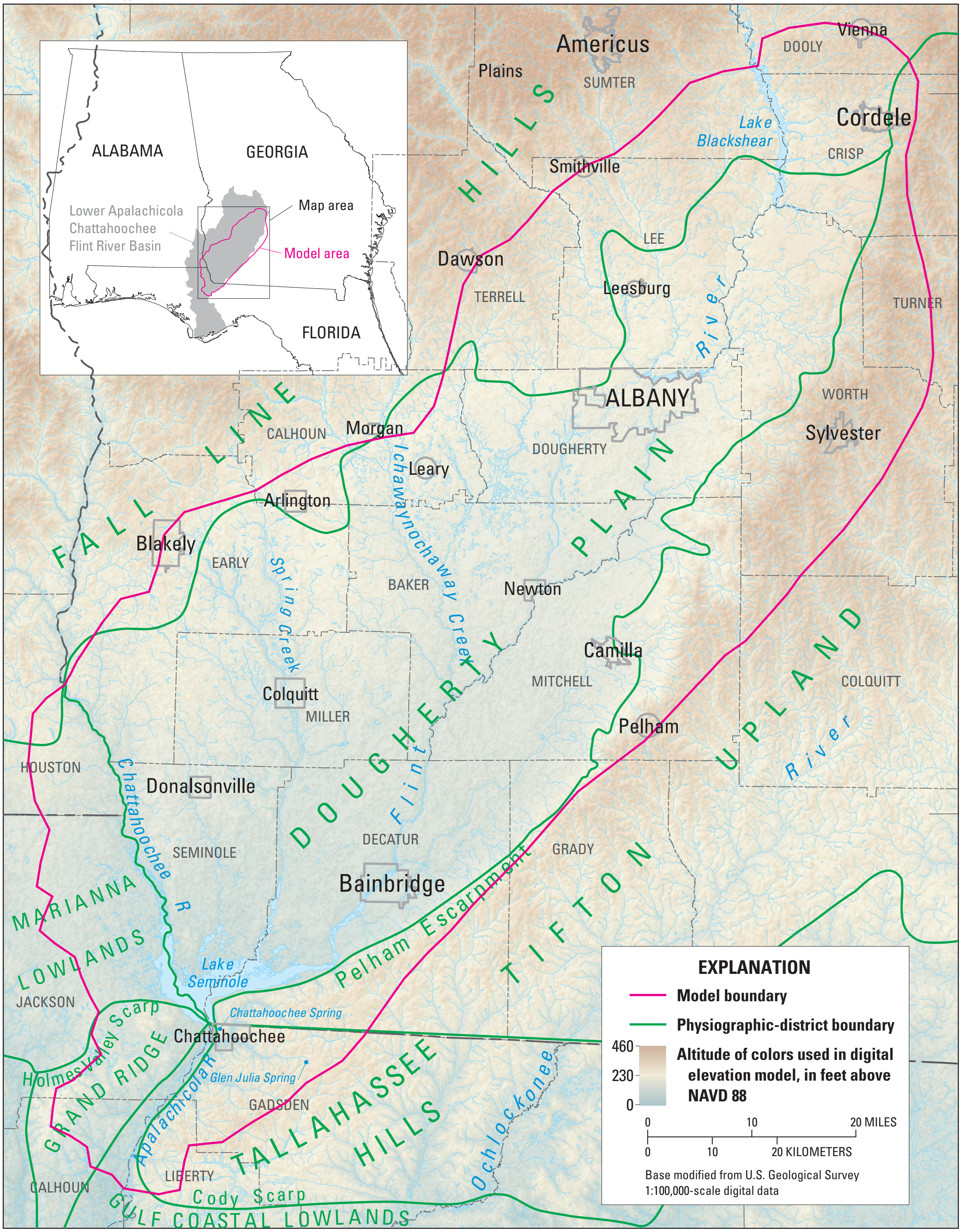

Figure 2. Physiographic districts and features, topography, and municipalities in the model area in southwest Georgia and adjacent parts of Alabama and Florida.

The Fall Line Hills District is a highly dissected series of ridges and valleys, having little level land except the marshy floodplains and their better drained, narrow stream terraces (Clark and Zisa, 1976). Stream valleys lie from 50 to 250 feet (ft) below adjacent ridgetops, and relief gradually diminishes to the southeast. The southeastern boundary separates the district from the Dougherty Plain and approximates the line having a land-surface altitude of about 250 ft (fig. 2).

The Dougherty Plain spans most of the model area and is a relatively flat, internally drained, inner lowland having an irregular and undulating surface characterized by heterogeneous stream-channel development and karst topography (fig. 2). Land-surface altitudes range from about 250 ft along parts of the northwestern boundary, to about 150 ft along the southeastern boundary with the Tifton Upland, and to about 50 ft near Lake Seminole. Limestone dissolution exerts the greatest influence on shaping the landscape and surface-water drainage in the Dougherty Plain and occurs where Eocene limestone crops out beneath the overburden. Many shallow sinks and depressions—ranging in size from a few tens of feet in diameter to several hundred acres, with some containing water year-round—dot the landscape and provide evidence of active solutioning in the limestone aquifer. The Dougherty Plain contains subsurface, internal drainage, typical of karst topography, and mainstem streams flow in terraced valleys and cut shallow channels through the overburden to the underlying limestone of the Upper Floridan aquifer.

Evidence of active-limestone solutioning exists on and beneath the landscape in the form of sinkholes, sinkhole ponds, marshes, and underground channels that capture surface drainage. Active solutioning of limestone interrupts the relatively flat terrane of the Dougherty Plain in western Baker and Early Counties, Ga., by forming a ridge that separates surface-water drainage between Ichawaynochaway and Spring Creeks (Torak and Painter, 2006). Formed between two elongated depressions (uvalas) created by limestone sinks, this "interuvala" ridge represents topography that is physiographically younger than the remainder of the Dougherty Plain (Hendricks and Goodwin, 1952). Many sinkholes collect runoff from rainfall, providing direct recharge to the Upper Floridan aquifer; and small tributary streams are scarce (Sever, 1965a).

Between the Dougherty Plain and Tifton Upland Districts lies the Pelham Escarpment, a steeply-sloping escarpment along the southeastern shore of the Flint River impoundment arm to Lake Seminole that continues northeastward across Decatur, Grady, and Mitchell Counties, Ga. (fig. 2). The escarpment produces as much as 125 ft of local relief, and the ridge of the escarpment forms a topographic and surface-water divide between the Flint River Basin and the Ochlockonee River Basin to the east. The slope of the Pelham Escarpment faces west to northwest, and small streams flow northwestward down the escarpment into caves and sinkholes along the eastern edge of the Dougherty Plain (Sever, 1965a). The base of the escarpment contains cavities and sinkholes, but solution features that exist are deeper and more narrow than those on the Dougherty Plain (Hicks and others, 1987).

In northwestern Florida, Vernon (1951) subdivided the Coastal Plain province into a minor geomorphic unit called the Marianna River Valley Lowlands, or, as proposed by Cooke (1939), the Marianna Lowlands (fig. 2). The Marianna Lowlands contains low, generally flat or rolling topography that resulted from a complicated sequence of stream erosion, deposition, and capture by several streams, including the Apalachicola and Chattahoochee Rivers, and to a lesser extent from lowering of the surface by limestone solutioning. During recent times, however, the surface has been modified by processes related to the dissolving of limestone (Schmidt and Coe, 1978). The formation of the lowland has been ongoing since early Pleistocene by removal and dissection of Miocene clastic sediments, exposing underlying limestone units at the surface. Normal topography of a coastal plain rather than karst topography resulted from this erosion (Moore, 1955); well-developed sinkholes and gently-sloping depressions indicative of internal drainage, however, are common (Schmidt and Coe, 1978).

The Marianna Lowlands extends eastward in the panhandle of Florida to the Chattahoochee River and is bounded in southeastern Jackson County, Fla., by the Grand Ridge region, a topographically high section similar in structure and relief to the Tifton Upland and Tallahassee Hills (fig. 2). Land surface in the Grand Ridge region rises above 250 ft altitude and consist of a series of remnant hills and sand-hill ridges dissected by stream valleys (Puri and Vernon, 1964). The ridges are composed of clayey sands, probably Miocene to Pleistocene, that cover the underlying limestone to depths ranging from 100 to 200 ft below the surface (Schmidt and Coe, 1978). The transition from the Marianna Lowlands to the Grand Ridge region occurs across an abrupt north-facing slope, termed the *Holmes Valley Scarp* (Schmidt and Coe, 1978), much like in Georgia where the Pelham Escarpment separates the Dougherty Plain from the Tifton Upland (fig. 2).

The Tifton Upland in Georgia and Tallahassee Hills in Florida are hilly regions between the low-lying Dougherty Plain and Gulf Coastal Lowlands, consisting of narrow, rounded plateaus and well-developed drainage. These regions contain high hills composed largely of resistant clayey sands, silts, and clays (Arthur and Rupert, 1989), which slope gently to the southeast. Land-surface altitudes range from about 330 ft near the Florida-Georgia State line to about 100 ft at the southern edge of the zone. Dendritic drainage and erosion by running water dissect the hills and form deeply incised valleys and ravines (Rupert, 1990) in the otherwise broad, flat plain. Many surface streams are present, and sinkholes and other solution features are absent (Sever, 1965a). The Tifton Upland and Tallahassee Hills are incised at the Flint and Apalachicola Rivers, respectively, in steep bluffs that produce relief from about 150 to 200 ft above the floodplain (Torak and others, 1996) and expose Miocene to Holocene sediments. The Grand Ridge region of southeastern Jackson County, Fla., extends this hilly region westward.

The Gulf Coastal Lowlands (fig. 2) is a sandy, flat, seaward-sloping feature shaped mostly by wave and current activity from high sea-level stands during the Pleistocene Epoch

(Arthur and Rupert, 1989). Land surface in the lowlands contains relic Pleistocene marine bars, terraces, spits, and sandbar dunes. The floodplain of the Apalachicola River occupies the lowlands, which separates the Grand Ridge region to the west of the river in Jackson and Liberty Counties, Fla., from the Tallahassee Hills to the east.

Geohydrologic Setting

The geohyrologic setting coincides with the area described in Torak and Painter (2006), which is in the same series of reports as the current report. Torak and Painter (2006) focused on geohydrology and fluid-flow aspects of ground water in the Upper Floridan aquifer and in overlying and underlying geohydrologic units; the reader is referred to that work for detail. Torak and Painter (2006) contains maps, tables, charts, and diagrams pertinent for describing the areal and vertical extent of geohydrologic units and corresponding hydraulic properties, aquifer-recharge mechanisms, interaction of geohydrologic units with surface water, and ground-water level fluctuations, which are assumed to govern ground-water flow and affect water-resource potential of the Upper Floridan aquifer. Discussions contained in that report use subsurface sections that depict geologic and geohydrologic units in the southern part of the lower ACF River Basin, developed previously by Torak and others (2006), to increase current understanding of the hydrogeologic framework that controls stream-aquifer relations and flow-system processes. Newly acquired geologic and geohydrologic information from recent test boring, well drilling, and aquifer testing, which supplemented and refined similar information compiled during and since the investigation performed by Torak and McDowell (1996), aided in the development of geohydrologic descriptions and illustrations contained in this report. Figure 3 correlates the geologic and geohydrologic units described in greater detail in Torak and Painter (2006).

SERIES	GEORGIA AND FLORIDA NORTHWEST OF PELHAM ESCARPMENT			FLORIDA AND GEORGIA SOUTHEAST OF PELHAM ESCARPMENT		
	Geologic unit	Geohydrologic unit	Ground-water quality	Geologic unit	Geohydrologic unit	Ground-water quality
Holocene and Pleistocene	Terrace and undifferentiated (surficial) deposits	Surficial aquifer system / Upper semiconfining unit	Not determined	Terrace and undifferentiated (surficial) deposits	Surficial aquifer system / Upper semiconfining unit	Not determined
Miocene	Undifferentiated overburden (residuum)	Upper semiconfining unit	Not determined	Hawthorn Group	Upper semiconfining unit	Corrosive
Miocene	Undifferentiated overburden (residuum)	Upper semiconfining unit	Not determined	Tampa Limestone / Chattahoochee Formation / St. Marks Formation	Upper semiconfining unit / Upper Floridan aquifer	Moderately soft to moderately hard, high magnesium
Oligocene	Undifferentiated overburden (residuum) / Suwannee Limestone	Upper Floridan aquifer	Moderately hard	Suwannee Limestone; Marianna Limestone	Upper Floridan aquifer	Moderately hard to hard, high magnesium and sulfate
Eocene	Ocala Limestone / Clinchfield Sand	Upper Floridan aquifer	Moderately hard, good quality	Ocala Limestone	Upper Floridan aquifer	Hard to very hard, high magnesium and sulfate; high iron along Solution Escarpment
Eocene	Lisbon Formation	Lower confining unit	Moderately hard, fair quality but sulphurous	Lisbon Formation	Lower confining unit	Moderately hard, sulphurous

Figure 3. Geologic and geohydrologic units and general ground-water quality of the Upper Floridan aquifer in the lower Apalachicola–Chattahoochee–Flint River Basin (modified from Torak and others, 2006).

The geohydrology of the model area is separated into two general regions by Lake Seminole and the Pelham Escarpment (figs. 2 and 3). Most of the area included in the ground-water model developed for this study is in the Dougherty Plain northwest of this dividing line. In this area, the Upper Floridan aquifer consists of Eocene sediments identified as the Clinchfield Sand and the Ocala Limestone and Oligocene sediments identified as the Suwannee Limestone and locally undifferentiated overburden. The aquifer is overlain by undifferentiated overburden or weathered residuum, and in some areas the Hawthorn Group, that form a semiconfining unit. Overlying the overburden are Pliestocene and Holocene terrace and undifferentiated (surficial) deposits that locally may contain water-bearing zones. These water-bearing sediments have been called the surficial aquifer system, but for the ground-water model all the sediments overlying the Upper Floridan aquifer are lumped together and called the upper semiconfining unit. Throughout the model area, the Upper Floridan aquifer is underlain by the Eocene Lisbon Formation, which forms the lower confining unit.

Southeast of the dividing line formed by Lake Seminole and the Pelham Escarpment are the upland physiographic districts, the Tifton Upland in Georgia and the Tallahassee Hills in Florida (fig. 2). In this area the stratigraphy is more complicated than to the northwest, and the Upper Floridan aquifer comprises Oligocene and Miocene geologic units that are not present in the Dougherty Plain (fig. 3). These geologic units include the Oligocene Marianna Limestone, which lies above the Eocene Ocala Limestone and below the Oligocene Suwannee Limestone, and the Miocene Tampa Limestone, Chattahoochee Formation, and St. Marks Formation, which intermittently overly the Suwannee Limestone. The Hawthorn Group comprises the shallower Miocene sediments overlying the Upper Floridan aquifer, which is overlain by Holocene and Pliestocene terrace and undifferentiated (surficial) deposits. For the ground-water model, the Hawthorn Group and terrace and undifferentiated deposits also are lumped together and called the upper semiconfining unit. More detailed discussion of the lithologic composition and the stratigraphic and structural relations of the geologic units that control the hydrologic connectivity of the system is contained in Torak and Painter (2006).

Well and Surface-Water Station Numbering System

Wells in Georgia are numbered by a system based on USGS topographic maps. Each 7½-minute topographic quadrangle map in Georgia has been given a number and letter designation beginning at the southwest corner of the State. Numbers increase eastward through 39; letters advance northward through "Z," then double-letter designations "AA" through "PP" are used. The letters "I," "O," "II," and "OO" are not used. Wells inventoried in each quadrangle are numbered sequentially beginning with "1." Thus, the 48th well inventoried in the Albany West quadrangle (designated 12L) in Dougherty County is designated 12L048. Wells in Florida are numbered with a four-digit code that is assigned by the Northwest Florida Water Management District, for example, 8038 (Christopher J. Richards, Senior Hydrogeologist, Northwest Florida Water Management District, Havana, Fla., written commun., April 2000).

Partial- and continuous-record surface-water stations are given a station-identification number, which is assigned in "downstream order" (Stokes and others, 1990). No distinction is made between partial-record stations and other stations; therefore, the station number for a partial-record station indicates downstream-order position in a list made up of both types of stations. The complete number for each station includes a 2-digit part number "02" plus the downstream-order number, which can contain from 6 to 12 digits.

Acknowledgments

The authors thank all who contributed to this study. Past and current officials of the GaEPD, who made this study possible and maintained constructive dialog throughout, include Harold F. Reheis, William H. McLemore, Robin J. McDowell, and Carol A. Couch. This study supports the GaEPD Flint River Basin Plan, which is being developed considering the counsel of two steering committees—a technical advisory committee and a stakeholder advisory committee. The authors were invited to all meetings of the two committees throughout the study, and acknowledge the technical advisory committee for considering this hydrological study within the broader scientific context of agricultural and biological studies, and the stakeholder advisory committee for considering this hydrological study within the process of public policy development. The authors would like to thank David W. Hicks and Lindsay R. Boring of the Joseph W. Jones Ecological Research Center at Ichauway for hosting meetings of the technical advisory committee of the Georgia Flint River Basin Plan.

James E. Hook (National Environmentally Sound Production Agriculture Laboratory) provided daily agricultural pumpage measurements, without which the transient simulation in this study would not have been possible. Menghong Wen (GaEPD) consulted with the authors on ground-water modeling procedures and provided supplemental agricultural permit data; Vicki Trent (GaEPD) and Derek Fussel (GaEPD) provided primary agricultural permit data. David C. Leeth (USGS) used kriging to analyze the areal distribution of hydraulic conductivity of the Upper Floridan aquifer in the model area.

Jaime A. Painter (USGS) compiled geologic and geohydrologic data in a geographic information system database. Caryl J. Wipperfurth (USGS) and Bonnie Turcott (USGS) assisted with the numerous figures, and Patricia L. Nobles (USGS) was responsible for the final report layout.

Simulated Effects of Seasonal Ground-Water Pumpage

The effects of seasonal ground-water pumpage for agricultural irrigation relate to changes in the interaction of the ground-water flow system of the Upper Floridan aquifer at various hydrologic boundaries and to changes in the amount of water in storage. In the lower ACF River Basin, ground-water flow mechanisms at boundaries of the Upper Floridan aquifer consist of regional ground-water flow to and from other parts of the Upper Floridan aquifer at lateral margins of the model area, flow to and from streams and lakes within the model area, vertical leakage to and from the overlying upper semiconfining unit, direct infiltration of precipitation to the aquifer in areas where the upper semiconfining unit is thin or absent, and flow from the aquifer at springs. Rates of ground-water flow within the Upper Floridan aquifer depend on characteristics of sediments comprising the aquifer, including hydraulic conductivity, storage coefficient, and thickness. Aquifer water levels indicate the amount of water in storage. A finite-element ground-water flow model was constructed that is capable of simulating ground-water flow within the Upper Floridan aquifer and inflows and outflows at the various aquifer boundaries.

Steady-state simulation of October 1999 conditions was used to refine the performance of the model by successively comparing simulated and observed conditions and adjusting model parameters. Transient simulation was then used to evaluate the effects of seasonal ground-water pumpage on the hydrology of the lower ACF River Basin. Hydrologic data, measured during the period from March 2001 to February 2002, were used to develop model-input data representing stresses and boundary conditions that varied during the course of an irrigation season during a prolonged drought period. Time-varying input data included irrigation pumpage from the aquifer, stage in streams and lake water levels within the model area, water levels in the undifferentiated overburden, and rates of direct infiltration from precipitation. The effect of seasonal irrigation pumpage on the ground-water flow system is indicated by simulated components of the ground-water budget of the Upper Floridan aquifer, including stream-aquifer flux, vertical leakage to and from the upper semiconfining unit and lakes, and flux at the lateral margins of the model area.

Ground-Water Flow Model Development

Based on available hydrogeologic and hydrologic information, a conceptual model of the hydrologic flow system in the lower ACF River Basin was developed that included ground-water flow in the Upper Floridan aquifer, stream-aquifer flow, irrigation pumpage, and inflows and outflows at other vertical and lateral boundaries of the aquifer. Mathematical equations described each aspect of the conceptual model in the framework of a numerical finite-element ground-water flow model. A finite-element mesh was designed that could simulate accurately the effect of irrigation pumpage on ground-water flow within the Upper Floridan aquifer and at hydrologic boundaries. Hydrologic properties of boundaries and the aquifer were discretized as numerical parameters across the finite-element mesh.

Conceptualization of Geohydrologic Flow System

The geohydrologic flow system of the lower Flint River Basin in the model area was conceptualized based on hydrogeologic information in previous studies (including Hayes and others, 1983; Hicks and others, 1987; and Torak and others, 1996) and supported by more recent information collected and in association with the current study (Mosner, 2002; and Torak and Painter, 2006). The resulting conceptual model of the flow system in the model area (idealized section shown in fig. 4) is similar to the northern part of the model area of Torak and others (1996, figs. 16 and 17), and the following description is equally applicable to this model (Torak and others, 1996, p. 28):

> [T]he Upper Floridan aquifer * * * is semiconfined above by alluvium containing undifferentiated overburden and terrace deposits * * * [upper semiconfining unit in fig. 4]. The northern boundary is defined as the saturated, updip limit (outcrop) of the aquifer. Surface-water features (streams, reservoirs, and lakes) are in hydraulic connection with the Upper Floridan aquifer and alluvium * * *. The Lisbon Formation, underlying the Upper Floridan aquifer, functions as an impermeable base, and is termed the lower confining unit * * *.
>
> Clayey sediments in the lower half of the undifferentiated overburden serve as a limited source of water to the Upper Floridan aquifer by vertical downward leakage [fig. 4]. The low hydraulic conductivity of the clayey sediments inhibits lateral flow to streams and vertical leakage to the aquifer. Variations in thickness and content of sand and clay in the overburden (Hayes and others, 1983) create areas of locally large and small leakage rates across this upper vertical boundary of the aquifer with the semiconfining unit * * *.
>
> The Upper Floridan aquifer is well drained in the northern part of the lower ACF River Basin by the Chattahoochee and Flint Rivers and by numerous tributary streams. There is direct hydraulic connection of the aquifer with surface water where rivers and streams cut into and expose aquifer material [fig. 4]. Hydraulic connection is less direct in other areas where the overlying semiconfining unit in the undifferentiated alluvium separates the aquifer from surface water * * *.

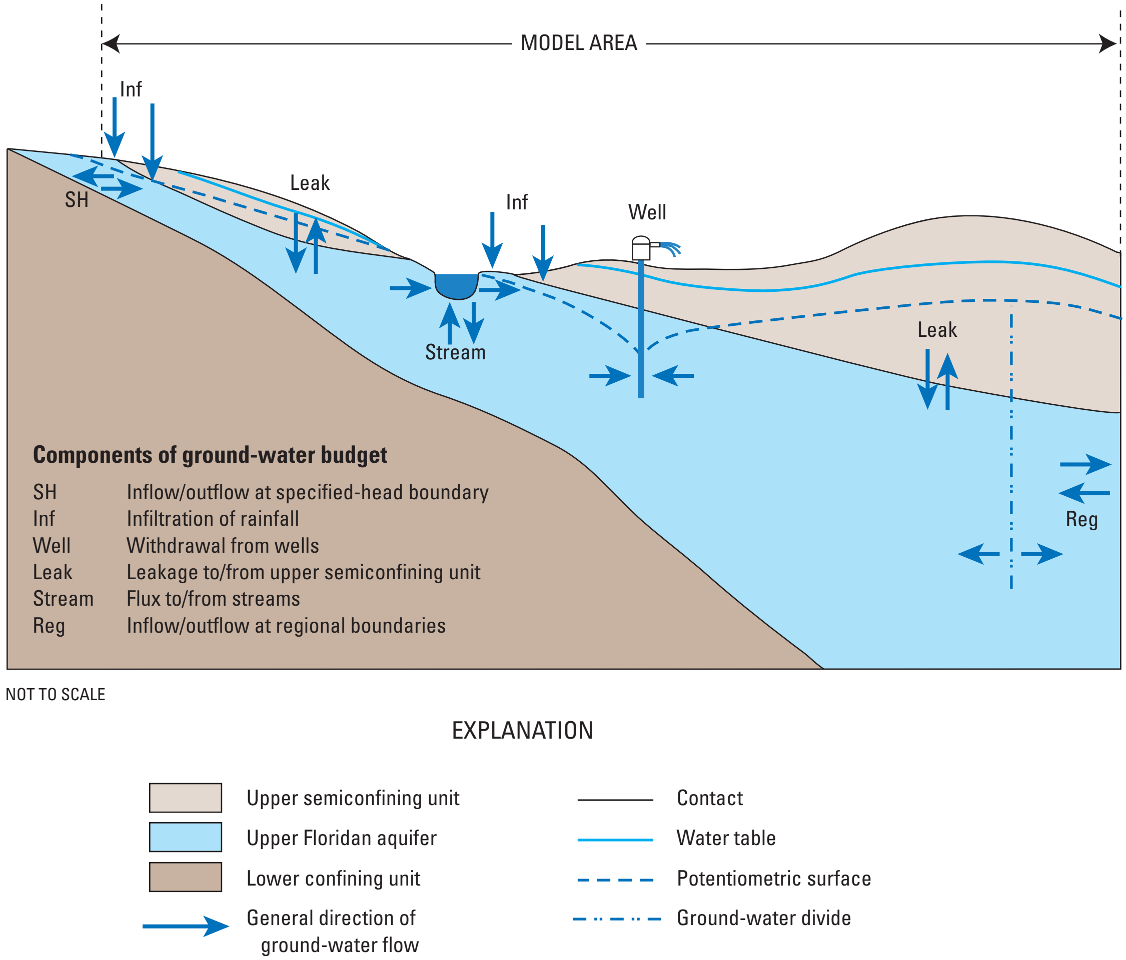

Figure 4. Idealized section of the ground-water flow system of the Upper Floridan aquifer in the lower Apalachicola–Chattahoochee–Flint River Basin showing components of the ground-water budget simulated by the model.

> Regional and local inflows and outflows affect ground-water flow in the northern part of the study area, primarily in the Upper Floridan aquifer. Regional ground-water inflow to the aquifer occurs across the eastern study-area boundary in upland areas of the * * * [Pelham] Escarpment.

Like the model of Torak and others (1996), steady-state conditions are assumed for model calibration. October 1999 was chosen for the calibration because the model area was under drought conditions similar to the drought that included October 1986, which was described in Torak and others (1996, p. 28):

> Water levels in wells completed in the Upper Floridan aquifer * * * and semiconfining units were either at or near seasonal or record lows in October 1986, and had been maintained there for a period of time necessary for the surface- and ground-water flow system to equilibrate, or achieve steady-state. The extremely dry climatic conditions in the lower ACF River Basin during most of the year virtually eliminated significant recharge to the stream-aquifer system by infiltration of precipitation; vertical leakage from clayey sediments in the semi-confining units provided one of the few sources of water to the aquifer for October 1986. Other aquifer recharge included lateral flow across surface-water divides and vertical leakage from surface water. Aquifer recharge was balanced identically by discharge to surface water and pumped wells, and by discharge across lateral and vertical flow boundaries. These hydrologic mechanisms produced stable ground-water-level conditions that defined a steady-state condition for the flow system.

Hydrologic data collected to support the October 1999 calibration (mostly during the period from October 18–22, 1999) included 275 water-level measurements in wells open to the Upper Floridan aquifer and 64 streamflow measurements collected from throughout the model area. The procedure for using these data to refine the steady-state simulation is described in the section Calibration Strategy.

Unlike the conceptualized hydrologic flow system in Torak and others (1996), the current conceptualization is not limited to steady-state flow. Fully transient conditions are simulated using time-varying stress to the ground-water system and time-varying boundary conditions. Transient simulation allows evaluation of the effects on the hydrologic system of changes in ground-water pumpage that typically occur during an agricultural irrigation season, and the effect of other changes related to lake levels and naturally varying factors such as rainfall, direct infiltration, water level in the overlying upper semiconfining unit, and stream stage. Because Torak and others (1996) considered drought conditions during a period of little or no rainfall, the only inflow of water to the Upper Floridan aquifer from above occurred in areas where the overlying upper semiconfining unit was thick and clayey enough to support a permanent water table that could provide a source of water. Simulation for the current study requires an additional boundary representing direct infiltration of rainfall in parts of the model area where the upper semiconfining unit is absent, thin, or has insufficient clay content to support a permanent water table.

A 12-month transient simulation was intended to estimate the variations in ground-water flow through a typical year, consisting of an irrigation period (the growing season in southwest Georgia lasts from about April to October or November) followed by a period of little or no agricultural irrigation (October or November through March). Considering a long-term drought affecting the model area (1999–2003), and the availability of short-term measured daily pumping rates for a 5-percent sample of agricultural irrigation systems in the model area (from March 2001 to May 2003); March 2001 through February 2002 was chosen for transient simulation. Irrigation pumpage was expected to be greater than average during a drought; and, thus, more representative of worst-case conditions than wetter years having less than average irrigation pumpage.

Governing Equations and Simulation Approach

The mathematical model code used to simulate ground-water flow in the Upper Floridan aquifer in the lower ACF River Basin is the USGS MODular Finite-Element model (MODFE) (Cooley, 1992; Torak, 1993a,b). The equations solved by MODFE consist of partial-differential equations and the appropriate boundary and initial conditions that are assumed to describe the physics of fluid flow in porous media. The governing equation and boundary and initial conditions given in Cooley (1992) are presented as they apply to flow in the Upper Floridan aquifer. Ground-water flow conditions within the aquifer and flow at various physical boundaries of the aquifer in the lower ACF River Basin are then related to the governing equation and boundary and initial conditions. Details of preparing model input for the boundaries are discussed in subsequent sections.

Ground-water flow in the Upper Floridan aquifer, within boundaries of any discontinuities in transmissivity or within external boundaries, is to be governed by the following two-dimensional, steady-state flow equation

$$\frac{\partial}{\partial x}\left(T_{xx}\frac{\partial h}{\partial x}+T_{xy}\frac{\partial h}{\partial y}\right)+\frac{\partial}{\partial y}\left(T_{yx}\frac{\partial h}{\partial x}+T_{yy}\frac{\partial h}{\partial y}\right)+$$

$$+R(H-h)+W+P=S\frac{\partial h}{\partial t}, \quad (1)$$

where

(x,y) = Cartesian coordinate directions [length];

t = time [time];

$h(x,y,t)$ = aquifer hydraulic head [length];

$H(x,y,t)$ = hydraulic head in the source layer [length];

$\begin{bmatrix} T_{xx}\ (x,\ y,\ t) & T_{xy}\ (x,\ y,\ t) \\ T_{yx}\ (x,\ y,\ t) & T_{yy}\ (x,\ y,\ t)\end{bmatrix}$ = symmetric transmissivity tensor written in matrix form [length^2/time];

$R(x,y,t)$ = vertical hydraulic conductance (vertical hydraulic conductivity divided by thickness) of a confining bed, [time^{-1}];

$W(x,y,t)$ = unit areal recharge or discharge rate [length/time] (positive for recharge; and negative for discharge);

$P(x,y,t)=\sum_{j=1}^{p}\delta\left(x-a'_j\right)\delta\left(y-b'_j\right)Q_j(t)$ = Dirac-delta designation for p point sources or sinks, each having strength Q_j [length/time] (positive for injection) and located at (a'_j, b'_j); and

$S(x,y,t)$ = storage coefficient.

Equation 1 is subject to the following boundary and initial conditions:

- At a discontinuity in transmissivity within the aquifer, hydraulic head and the component of flow normal to the discontinuity are unchanged as the discontinuity is crossed (Bear, 1979, p. 100–102). Thus, at a discontinuity in transmissivity between transmissivity zones a and b,

$$h\big|_a = h\big|_b \quad (2)$$

and

$$q_n\big|_a = q_n\big|_b, \quad (3)$$

where $\big|_a$ and $\big|_b$ indicate evaluation just within the a and b sides of the discontinuity, respectively, and $q_n(x,y,t)$ is the normal component of flow (specific discharge times aquifer thickness).

- The normal component of flow across a boundary of the aquifer is given by the sum of specified and head-dependent flux components (Bear, 1979, p. 117–120). Thus, on this type of boundary

$$q_n = q_B + \alpha(H_B - h) \quad (4)$$

where

$q_B(x,y,t)$ = specified flux (specific discharge times aquifer thickness) normal to the boundary [length^2/time] (positive for inflow),

$\alpha(x,y,t)$ = a conductance parameter that approaches infinity for a specified-head (Dirichlet) condition, is zero for a specified-flux (Neumann) condition, and is finite and positive for a general or mixed head-dependent flux (Cauchy) condition [length/time], and

$H_B(x,y,t)$ = specified head at the boundary [length].

- The hydraulic head is known everywhere at the initial instant of time, or

$$h = H_0 \quad (5)$$

where

$H_0(x,y)$ = initial head [length].

The following explanation of the linear and nonlinear conditions of the governing equation and boundary conditions in the model area is from Torak and others (1996, p. 34–35) and applies to the current model (equation numbers are the same):

> Artesian (linear) and water-table (nonlinear) conditions exist in the Upper Floridan aquifer * * *, and both are represented by equation 1. Ground-water flow under artesian conditions is linear (having linear boundary conditions), because terms in equation 1 that multiply either aquifer hydraulic head, $h(x,y)$, or derivatives of head are not functionally dependent on head. Water-table or semiconfined conditions cause nonlinear ground-water flow, as some terms in equation 1 are functionally dependent on aquifer hydraulic head. Transmissivity is a function of saturated aquifer thickness, which in turn is a function of hydraulic head, and steady-vertical leakage, expressed as $R(H - h)$ in equation 1 for the linear case, is a function of the difference between head in the overlying semiconfining unit and either the altitude of the top of the aquifer or aquifer head, whichever is lower. The changing form of the leakage expression causes the nonlinear condition.
>
> Likewise, boundary conditions in the study area are expressed by using linear and nonlinear forms of equation 4. A unit discharge across and normal to the outer boundary of the aquifer is represented by equation 4, and is positive for inflow. The sum of specified and head-dependent components on the right side of this equation is termed a Cauchy-type boundary, for convenience, because each component represents a special case of the Cauchy-boundary condition (Norrie and deVries, 1973; Cooley, 1983).

MODFE approximates the governing equation and boundary and initial conditions (equations 1–5) by using the extended Galerkin finite-element method with triangular elements and linear coordinate (basis) functions in space (Cooley, 1983; Zienkiewicz, 1977, chap. 3). Approximate solutions to the governing equation are obtained at intersections of element sides, which are called nodes. In the model area, two-dimensional, horizontal, ground-water flow in the Upper Floridan aquifer was simulated by computing hydraulic head for this unit, which was represented in MODFE as a single active model layer.

In parts of the model area where the overlying upper semiconfining unit is thicker than 30 ft, recharge to and discharge from the Upper Floridan aquifer was simulated in MODFE using a vertical leakage function and a head-dependent flux boundary. Vertical leakage is based on the difference between head in the upper semiconfining unit and simulated head in the Upper Floridan aquifer ($R(H - h)$ in equation 1), but does not account for storage effects in the upper semiconfining unit. In parts of the model area where the upper semiconfining unit is thinner than 30 ft, precipitation was assumed to infiltrate directly to the Upper Floridan aquifer and was temporally and areally distributed, based on a seasonally varying percentage (from 10 to 30 percent) of measured rainfall. Direct infiltration of precipitation is represented in equation 1 by the term $W(x,y,t)$. Rationale for using both a head-dependent flux boundary and an areally distributed stress boundary to simulate interaction with materials above the Upper Floridan aquifer and details of model implementation are discussed in subsequent sections on boundary conditions.

The vertical boundary of the simulated aquifer with the lower confining unit (Lisbon Formation, Torak and Painter, 2006) was simulated as a no-flow boundary because the Lisbon Formation creates an effective impermeable base to the stream-aquifer system. The details of the simulation approach are summarized as follows:

Hydrologic unit	Simulation approach
Infiltrated precipitation	Areally distributed stress
Semiconfining unit	Vertical leakage (no storage effects)
Upper Floridan aquifer	Simulated model layer
Lower confining unit	No-flow boundary

Other hydrologic characteristics of regional and stream-aquifer flow and springflow in the current model are identical to those described by Torak and others (1996, p. 35–36, equation numbers the same), namely:

> [R]egional ground-water flow, flow across streambeds, and springflow, were simulated in MODFE by using mathematical boundary conditions to ground-water-flow equation 1 that account for recharge to, or discharge from, the simulated Upper Floridan aquifer. In addition, the * * * [updip limit] of the Upper Floridan aquifer was represented with specified-head boundaries. Regional inflows and outflows were represented with computations that simulated lateral flow across boundaries of the Upper Floridan aquifer with aquifer material located beyond the model area. Flow across streambeds was simulated in MODFE as either aquifer discharge to, or recharge from, streams by using computations that involve the hydraulic properties and general geometry of the streambed, and relative head differences between stream stage and the Upper Floridan aquifer. Simulation of in-channel springflow was combined with flow across streambeds, as hydrologically, and mathematically, both are identical features that cause aquifer discharge to streams. Off-channel springflow was simulated in a manner identical to well discharge, because both of these features are point discharges from the aquifer. Thus, a point-discharge function in MODFE was used to represent these hydrologic features for simulation.

Finite-Element Mesh

A finite-element mesh, a network of triangular elements, was constructed for the model area in the lower ACF River Basin and surrounding areas to represent variations in hydraulic properties, boundary geometry, surface-water features, and hydraulic head. The mesh for the model consists of 37,587 elements and 18,951 nodes. The model area contained within the finite-element mesh is about 4,632 mi^2, and consists of all or parts of seven Watershed Boundary Dataset (WBD) subbasins (formerly 8-digit Hydrologic Unit Code [HUC] cataloging units; Seaber and others, 1987) within the ACF Basin (formerly 6-digit HUC accounting unit 031300—Apalachicola) and smaller parts of five WBD subbasins within the Suwannee and Ochlockonee River Basins (031102 and 031200, respectively). The 12 WBD subbasins are identified in table 1, and shown in figure 1.

Physical boundaries of the lower ACF River Basin were used as limits for the finite-element mesh (fig. 5). Lateral hydrologic boundaries generally were defined from patterns of ground-water movement: (1) the northwestern boundary, extending from west of the Chattahoochee River in Houston County, Ala., to northeast of Lake Blackshear in Dooly County, Ga., is the updip limit of the Upper Floridan aquifer (simulated as a specified-head boundary); (2) the eastern and southeastern boundaries (simulated as linear head-dependent flux boundary, roughly zones 46–49) are beyond the boundary of the Flint River Basin near a ground-water divide in the potentiometric surface of the Upper Floridan aquifer, roughly coinciding with

Table 1. Subbasins partially contained within the model.

Watershed Boundary Dataset code	Subbasin name
03110202	Alapaha River
03110203	Withlacoochee River
03110204	Little River
03120002	Upper Ochlockonee River
03120003	Lower Ochlockonee River
03130004	Lower Chattahoochee River
03130006	Middle Flint River
03130007	Muckalee–Kinchafoonee Creeks
03130008	Lower Flint River
03130009	Ichawaynochaway Creek
03130010	Spring Creek
03130011	Upper Apalachicola River

the Tifton Upland; (3) the northern and southern boundaries (linear head-dependent flux boundary, roughly zones 45, 50, and 51), correspond to small watershed divides between tributaries of the Flint and Apalachicola Rivers, respectively; and (4) the western boundary (linear head-dependent flux boundary, zone 52) roughly follows the boundary between subbasins 03130004 and 03130011 to the east and subbasin 03130012 (Chipola River) to the west (the Chipola River, west of the model area, does not appear in figures). Characteristics of these boundaries are discussed in greater detail in subsequent sections on specified-head and head-dependent flux boundary conditions.

Using a ground-water modeling Geographic Information System (GIS) software package, ArgusONE®, a triangular mesh was developed that has a wide range of element sizes, from small (fine mesh discretization) to large (coarse mesh discretization), by varying the geometric detail of the boundaries that were incorporated in the mesh. Considering that stream-aquifer interaction is a focus of the study, stream boundaries were constructed to have more detail (smaller elements) and lateral hydrologic boundaries (the Upper Floridan updip limit and regional flow boundaries) less detail (larger elements). The mesh has the finest discretization within subbasin 03130008 (lower Flint River); thus, providing the most accurate estimations of aquifer head and the most sensitive response to time-varying stresses and boundary conditions. The desired range of element sizes was accomplished by providing the ArgusONE® meshing algorithm more detailed stream traces within subbasin 03130008, where stream traces were lines having average vertex spacing of 0.45 mi or less, and less detailed stream traces outside subbasin 03130008, where stream traces were lines having vertices spaced generally from 0.95 to 1.55 mi. The resulting mesh contains triangles (elements) ranging more than three orders of magnitude in area, from about 0.002 mi^2 (1.3 acres) adjacent to the Flint River within subbasin 03130008 to about 2.6 mi^2 (1,680 acres) near the easternmost boundary. The resulting stream boundaries (streams are represented by zones of element sides) averaged about 0.2 mi or less inside subbasin 03130008 and generally from 0.3 to 0.6 mi outside subbasin 03130008.

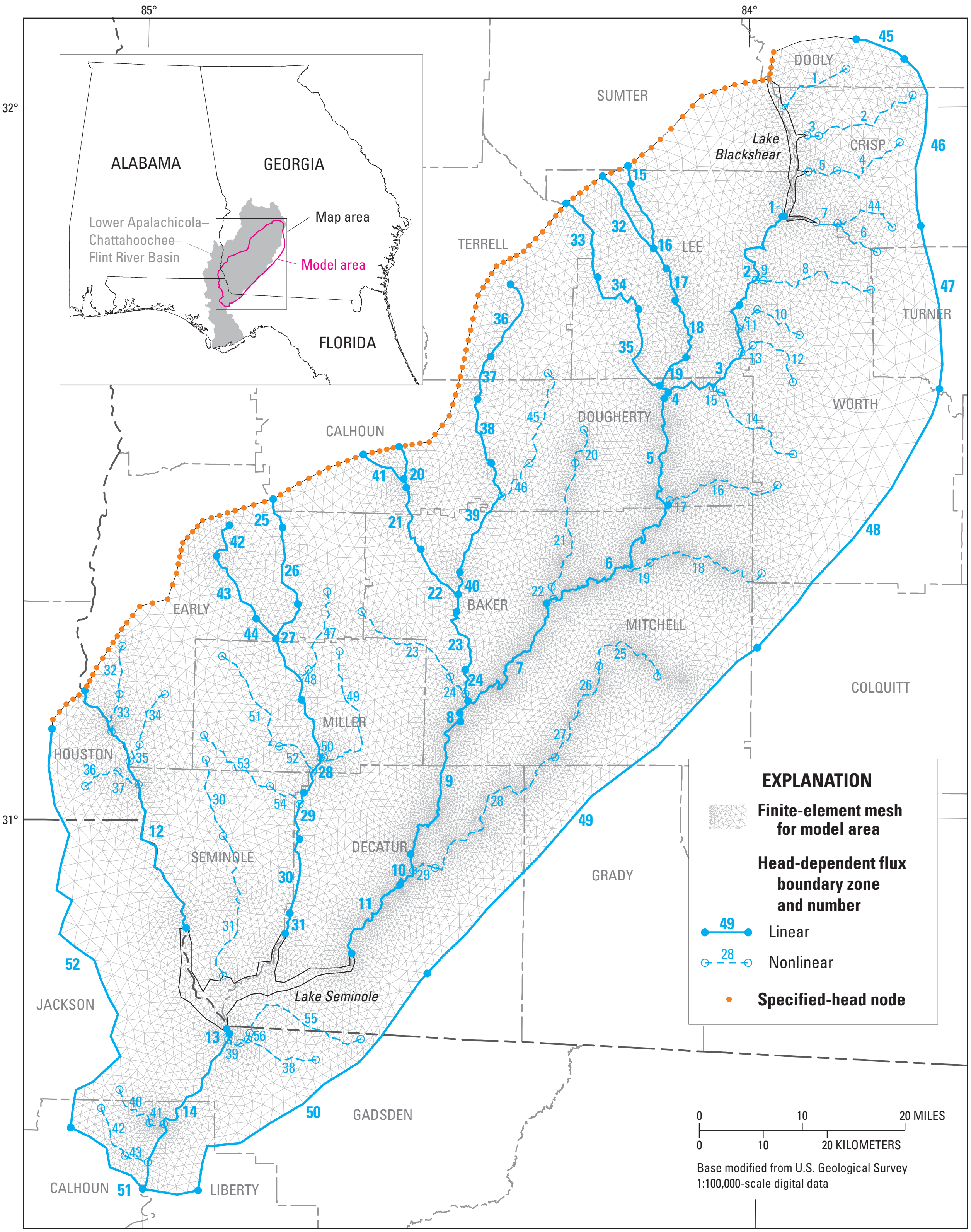

Figure 5. Finite-element mesh, linear and nonlinear head-dependent flux boundary zones of element sides, and specified-head nodes in southwest Georgia and adjacent parts of Alabama and Florida.

The finite-element mesh designed for the current study represents an important improvement in the representation of flow and boundary-condition geometry from the meshes designed for previous studies in the lower ACF River Basin by Torak and others (1993 and 1996) and Torak and McDowell (1996). Smooth transitions in discretization utilizing nearly equilateral triangles minimize approximation error within each element by minimizing the distance between nodal locations and the interior of any element, allowing curved geometric boundaries, such as stream courses and the areal extent of the model area, to be represented with better detail than in previous models. For example, the model by Torak and others (1993), representing nearly the same area as the current model, contained 12,295 elements and 12,113 nodes, in comparison with 37,587 elements and 18,951 nodes contained in the current model. Stream reaches were represented in the previous model by Torak and others (1993) by using element sides varying in length from 0.21 to 0.9 mi, compared with from less than 0.2 to 1.55 mi used in the current model.

Specified-Head Boundary: Upper Floridan Aquifer Updip Limit

Specified-head boundaries were used to represent ground-water level and regional flow conditions near the updip limit of the Upper Floridan aquifer. The location of the model boundary near the updip limit does not necessarily correspond to the location where the Upper Floridan aquifer pinches out, rather it is the location where the aquifer is at land surface and is thin enough not to be used as a water source. Long-term water-level records indicate that hydraulic head in the area of the updip limit, where there is little or no pumpage, fluctuates only a few feet during the year and has not changed appreciably from year to year. In the current model, the specified-head boundary is in the same location as the corresponding boundary in the Ocala model of Torak and others (1996); thus, the hydraulic-head distribution at the specified-head boundary from the Ocala model was retained in the current model for both the October 1999 steady-state simulation and the subsequent March 2001–February 2003 transient simulation (fig. 5).

Specified-Flux Boundaries

Two types of specified-flux boundary functions were used in the model, point functions applied at node points and areally distributed functions applied across elemental areas. Irrigation pumpage, municipal pumpage, and off-channel springflow were simulated using point specified-flux boundaries, and direct infiltration of precipitation was simulated using areally distributed specified-flux boundaries.

Irrigation Pumpage

Construction of input data representing seasonal withdrawal from about 4,000 irrigation systems in the model area involved the manipulation of three voluminous sets of data, which is described in detail below. Based on the data and the needs of the cooperator, GaEPD, average monthly irrigation pumpage applied for a 12-month simulation period (March 2001–February 2002) was determined to be the most reasonable approach for the transient simulation. Irrigation pumpage input for the steady-state October 1999 calibration simulation (before detailed irrigation pumpage data were collected) was assumed to be similar to irrigation pumpage input for October 2001. A step-by-step procedure for determining node-wise, steady-state and time-varying irrigation-pumpage input data is:

1. Description of metered pumpage data at a subset of irrigation systems in model area,
2. Determination of an average monthly irrigated depth at the subset of irrigation systems,
3. Description of permitted well data and data of mapped, irrigated acreage,
4. Relation of permitted wells to irrigated acreage,
5. Culling of permitted wells assumed not open to the Upper Floridan aquifer,
6. Mapping of acreage by well location to closest node of finite-element mesh, and
7. Construction of irrigation input datasets based on irrigated depth and nodal acreage.

Short-term measurements of irrigation pumpage in the model area during the 1999–2003 drought were made in a related study—Agricultural Water: Potential Use and Management Program in Georgia—called Ag Water Pumping (two research projects of the University of Georgia, College of Agricultural and Environmental Sciences, funded by GaEPD). In Phase II of this program, daily agricultural pumpage was measured at about 200 irrigation systems in the model area, beginning during July 2000 and extending through March 2004 (National Environmentally Sound Production Agriculture Laboratory Web site *http://nespal.cpes.peachnet.edu/awp/*, accessed September 9, 2005). After an initial start-up period of several months during which the meters were being installed, the period March 2001 through February 2002 was chosen as a 12-month irrigation season and off-season suitable for a 1-year transient simulation. During this period, 192 systems were monitored, which represent about a 5-percent sampling of the about 4,000 irrigation wells permitted to withdraw water from the Upper Floridan aquifer in the model area (James E. Hook, National Environmentally Sound Production Agriculture Laboratory, written commun., 2003).

Considering that the approximate number of irrigated acres was known for both the monitored systems and for the permitted systems, an average monthly irrigated depth was calculated from the daily measured flow volumes of the monitored systems, and that depth was applied by irrigated acres of the permitted systems to estimate total irrigation pumpage rate by month in the model area. For each month, the total pumpage was summed for each day of the month and for each system. Missing records of daily pumpage at any of the monitored systems were considered in the computation of the average monthly irrigation rate by prorating the acreage of a system by the percentage of days. In the case of a missing daily pumpage record, it is unknown whether the system was operated or not, and that day should not be considered. For example, if a 300-acre system was missing six daily pumpage rates in April, then the prorated acreage of that system for April would have been calculated as 300 acres times 24 daily pumping records divided by 30 possible records, or 240 acres. The sum of all the pumping in any month, divided by the sum of all the prorated acreages for each system for that month, resulted in an average monthly irrigated depth for all the actual records from the 192 systems (fig. 6).

Average monthly irrigation depths for the 12-month transient simulation period, March 2001–February 2002, ranged from 0.01 inch during March 2001 to 2.24 inches during July 2001, totaled 8.74 inches for the 12-month period, and averaged 0.73 inch per month. The 2001 irrigation season—months having average monthly irrigation depths of 0.25 inch or more—lasted April through November 2001. Peak months—months having average monthly depths of nearly 1 inch or more—were May through August 2001. The average irrigation depth during June 2001, 0.82 inch, is lowest of the peak months because average rainfall in the model area during June 2001 (7.04 inches) was higher than in other peak irrigation months (average monthly rainfall from 2.29 to 3.53 inches, fig. 7). The average monthly rainfall depths in figure 7 were derived from total monthly precipitation at eight stations given in table 2.

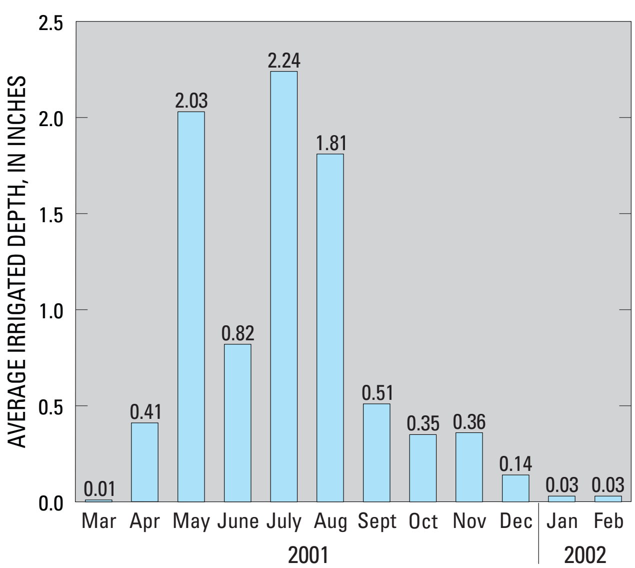

Figure 6. Average monthly irrigated depth in the model area during March 2001–February 2002, based on measured daily flow at 192 irrigation systems (James E. Hook, National Environmentally Sound Production Agriculture Laboratory, written commun., 2003).

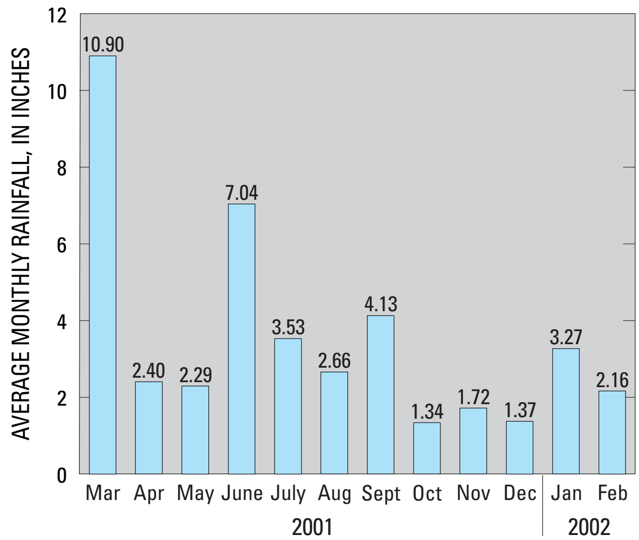

Figure 7. Average monthly rainfall at eight weather stations in model area during March 2001–February 2002 (see figure 1 for station location, table A1 for identification, and table 2 for data).

Estimating irrigation pumpage for the model depended on the construction of a reliable and accurate database that included each permitted ground-water irrigation well by location, and the irrigated acres associated with each permitted well. Each well also had to be withdrawing most of its yield from the Upper Floridan aquifer; several deeper aquifers provide reliable sources of water in the model area. Two sets of data were provided by GaEPD (Vicki Trent and Derek Fussel, Georgia Environmental Protection Division, written commun., November 2004): one was a database of 5,062 permitted irrigation wells in the model area, and other was a database of 7,738 records of irrigated fields in the model area, mapped using GIS, most of which also listed a permit number. The permit number was the only common record to relate these two databases into the format that could be used to create model input; that is, well location and an estimate of irrigated acreage.

Initially, the salient characteristics of the two databases were inspected for verification. Inconsistencies in the 5,062 permitted-well records included: (1) 290 records lacked a permit number; (2) 60 records were duplicate entries; and (3) 18 records lacked latitude and longitude, but most were outside the model area. Culling those records having unverifiable characteristics resulted in a new database of 4,695 permitted-well records. Relating the permitted-well records to the 7,738 mapped, irrigated field records revealed other inconsistencies including: (1) fields associated to permitted wells whose locations were unknown (most of these were outside the model area); and (2) permitted wells that were not associated with any of the mapped fields (764 permitted wells lacked any irrigated acreage). The result of relating the two databases was a new database of 3,931 permitted wells that had associated irrigated acres (one or often many more of the 7,738 mapped fields) of which 3,456 were in the model area.

Table 2. Precipitation totals from weather stations used for model input.[1]

[—, precipitation data not used as model input for station and period]

Station number (figure 1, table A1)	Total precipitation for period, in inches												
	Sept. 19–Oct. 18, 1999	2001										2002	
		Mar.	Apr.	May	June	July	Aug.	Sept.	Oct.	Nov.	Dec.	Jan.	Feb.
1	3.89	—	—	—	—	—	—	—	—	—	—	—	—
2	3.10	—	—	—	—	—	—	—	—	—	—	—	—
3	5.16	—	—	—	—	—	—	—	—	—	—	—	—
4	5.85	—	—	—	—	—	—	—	—	—	—	—	—
5	3.12	9.93	2.09	1.42	5.52	0.92	3.94	4.23	1.51	1.02	0.88	3.24	2.17
6	1.82	10.20	2.61	2.99	5.92	2.15	2.07	2.32	0.78	1.65	1.11	2.82	2.10
7	1.89	13.87	3.83	2.02	9.25	2.68	2.14	7.15	1.09	2.93	1.03	3.54	1.84
8	3.79	12.59	2.15	3.15	9.58	5.58	4.01	5.81	1.68	0.24	0.58	4.38	1.82
9	—	9.48	1.62	1.65	7.95	2.61	1.33	4.42	0.50	1.43	1.56	2.54	2.22
10	—	9.00	1.71	2.75	5.64	3.37	1.45	3.84	1.49	2.80	2.64	2.54	2.47
11	—	11.51	3.97	3.86	5.38	2.15	1.95	2.29	1.20	1.21	2.82	2.96	2.42
12	—	10.58	1.24	0.46	7.10	8.80	4.38	3.00	2.49	2.48	0.32	4.12	2.21
Average	**3.58**	**10.90**	**2.40**	**2.29**	**7.04**	**3.53**	**2.66**	**4.13**	**1.34**	**1.72**	**1.37**	**3.27**	**2.16**
Standard deviation	**1.42**	**1.66**	**1.01**	**1.10**	**1.71**	**2.51**	**1.24**	**1.69**	**0.61**	**0.94**	**0.92**	**0.70**	**0.24**

[1] National Oceanic and Atmospheric Administration, 2002, 2003

Determining whether or not an irrigation well withdraws from the Upper Floridan aquifer involved careful inspection of the construction information for each well in relation to the estimates of the top and thickness of the Upper Floridan aquifer. Because of the variability of well construction and the lack of well-construction data, it was often difficult to determine whether a well was primarily an Upper Floridan aquifer well or whether a well derived most of its water from other aquifers. It also should be noted that drilling records generally were not available and reported well-construction information was not always reliable, as it was typically provided by the permit holder, who may or may not have been present when the well was drilled. Based on available information, 462 additional wells for which the Upper Floridan aquifer was apparently not the primary source of water were eliminated, leaving 2,994 wells that likely produced primarily from the Upper Floridan aquifer. One last amendment to the irrigation well database was the addition of 148 permitted wells and associated irrigated acreages that were within the model area but east of the lower ACF River Basin in Turner, Worth, Mitchell and Decatur Counties (Menghong Wen, Georgia Environmental Protection Division, written commun., July 2005), resulting in 3,142 irrigation wells in the model area in Georgia. In addition to the irrigation wells in Georgia, acreages for 72 wells in Florida and 29 wells in Alabama were determined based on pumping rates in the October 1986 calibrated Ocala model of Torak and others (1996) and an irrigated depth of 0.35 inch, assuming the irrigated depth for October 1986 was similar to the irrigated depth determined for October 2001. These 101 wells and acreages in Florida and Alabama were treated like the 3,142 wells and acreages in Georgia, as variable-rate irrigation wells, and were assigned pumpage rates as described below. In total, 3,243 irrigation wells in Alabama, Florida, and Georgia were associated with about 421,000 irrigated acres in the model.

Acreage for each of the 3,243 Upper Floridan aquifer irrigation wells in Georgia, Florida and Alabama was assigned to the closest finite-element node in the model. Because many of the wells were assigned to the same node, acreage often was accumulated for multiple systems at the same node; figure 8 shows the 2,518 irrigation-pumpage nodes and the associated acreage ranges that are used for the model. For the October 1999 calibration, the irrigated depth computed for October 2001, 0.35 inch, was multiplied by the acreages represented in figure 8 to develop the irrigation pumping input data. For the March 2001–February 2002 transient simulation, time-varying irrigation pumping rates were computed using the average monthly irrigated depths in figure 6. For reference, a 350-acre irrigation system would have an average pumpage rate of 110,000 gallons per day (gal/d) for the October 1999 calibration simulation, and in the transient simulation would have a range of average monthly pumping rates from 3,200 gal/d during March 2001 to 690,000 gal/d during July 2001.

Pumping rates from irrigation wells were varied during the March 2001–February 2002 transient simulation of the model. Total irrigation pumping in the model was about 130 Mgal/d for the October 1999 calibration simulation, and in the transient simulation ranged from about 3.5 Mgal/d during March 2001 to about 830 Mgal/d during July 2001.

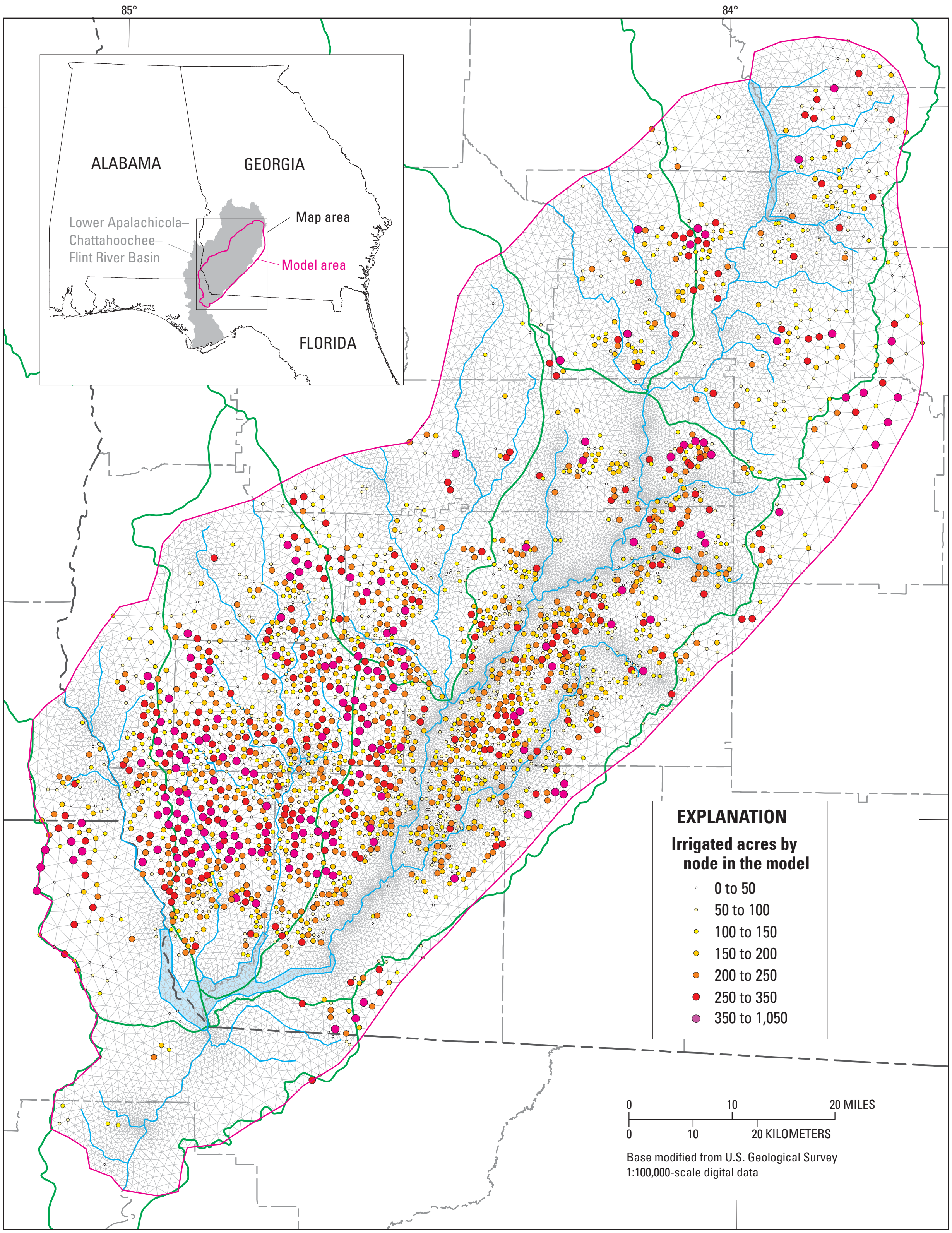

Figure 8. Distribution of nodes in the model simulating irrigation wells pumping from the Upper Floridan aquifer in southwest Georgia and adjacent parts of Alabama and Florida and ranges of irrigated acres.

Industrial and Municipal Pumpage and Off-Channel Springflow

Industrial and municipal pumpage was applied at several localities within the model area (fig. 9). These pumping rates vary little over time, and for the both the October 1999 calibration simulation and the March 2001–February 2002 transient simulation the rates were maintained constant at about 30 Mgal/d. Most of the industrial and municipal pumpage in the model area was in Georgia (about 26 Mgal/d), and the rates are based on GaEPD records of reported usage by 20 permit holders in six Georgia counties (Menghong Wen, Georgia Environmental Protection Division, written commun., March 2005).

Off-channel springs were simulated in the model as point-discharge function, which represents springflow in the identical manner as point withdrawal from wells. There are two off-channel springs located in Gadsden County, Fla., Chattahoochee Spring and Glen Julia Spring (figs. 2 and 9), which discharge 0.02 and 0.37 Mgal/d, respectively (Torak and others, 1996). Time-varying discharge measurements for these springs were not available; but, considering the small discharge relative to irrigation pumpage, maintaining discharge at a constant rate during the March 2001–February 2002 transient simulation would not introduce substantial error.

Infiltration

In areas where the upper semiconfining unit is absent, has a total thickness less than 30 ft, or has a clay thickness of zero, it was assumed that the unit could neither supply enough water nor act as a semiconfining unit to the Upper Floridan aquifer. In these areas, leakage to or from the upper semiconfining unit was not simulated, and elements were assigned a zero value of vertical hydraulic conductance, R^e (fig. 10); however, precipitation was allowed to infiltrate directly to the Upper Floridan aquifer as an areally distributed source, W, in equation 1. Under these circumstances, the material overlying Upper Floridan aquifer was assumed to be aquifer material and was lumped together with the aquifer. Recharge from infiltration was applied directly to a water table that is positioned either in the aquifer or in the overlying aquifer-equivalent material. Herein this recharge mechanism is called infiltration. Figure 10 shows the three sets of elements in the model having different vertical flow boundaries above the Upper Floridan aquifer: (1) an area of infiltration only, no leakage; (2) a transition area of no infiltration and vertical leakage only during periods wet enough that the saturated part of the upper semiconfining unit was between 10 and 30 ft; and (3) an area of leakage only, no infiltration.

Infiltration rates to the Upper Floridan aquifer in the model area vary; based on digital modeling, Hayes and others (1983) reported that mean annual recharge is about 10 inches per year (in/yr) (about 20 percent of mean annual rainfall), and late-summer recharge is about 6 in/yr (about 12 percent of mean annual rainfall). To simulate infiltration as direct recharge to the Upper Floridan aquifer, areally distributed source terms were applied to elements used as an infiltration boundary (fig. 10).

Ground-water levels and streamflows for the October 1999 model calibration mostly were measured in the period October 18–October 22, 1999. Infiltration was estimated from daily rainfall measurements from eight weather stations (fig. 1) in the model area having complete records for the prior 30-day period, September 19–October 18, 1999. The average rainfall for the period, 3.58 inches (table 2), and an infiltration rate of 30 percent of precipitation (explained below), results in an infiltration rate of 0.036 inches per day (about 13 in/yr).

For the transient simulation period, March 2001–February 2002, average monthly rainfall in the model area (fig. 7) was estimated from daily rainfall measurements from eight weather stations (fig. 1) having complete records for the period. Average monthly rainfall ranged from 1.34 inches during October 2001 to 10.90 inches during March 2001 (table 2), and totaled 42.81 inches for the 12-month period. The areal distribution of monthly rainfall varied slightly within the model area, indicating less variation during the months of October through March (0.84 inches, average standard deviation of monthly rainfall) than during April through September (1.54 inches, average standard deviation of monthly rainfall). In comparison, the standard deviation of rainfall for the 30-day period, September 19–October 18, 1999, used for the steady state simulation of October 1999 conditions, was 1.42 inches (table 2). The sparse and non-uniform distribution of available rainfall estimates in the model area precluded the use of a detailed areal representation of infiltration as model input. Infiltration was applied, therefore, as areally distributed source terms using the average monthly precipitation and infiltration rates of 10 percent of precipitation in the late spring and summer months (from April to August) when evapotranspiration is highest, 20 percent in the transition months (March and September), and 30 percent in the fall and winter months (from October to February) when evapotranspiration is lowest.

Conversion of average monthly precipitation to infiltration rates that vary somewhat seasonally by 10, 20 and 30 percent of the precipitation rate allows variable recharge to be simulated according to the type of storms and associated runoff, in addition to month-to-month rainfall variations, that occur during the year. That is, relatively high infiltration associated with long-duration precipitation from frontal passages (Torak and Painter, 2006) is represented by using 30 percent of average monthly rainfall during the fall and winter months as the simulated infiltration rate. Similarly, relatively low infiltration corresponding to summer convective storms, which usually are high intensity and short duration, is represented in the model as 10 percent of average monthly rainfall. Both types of storms can occur during the transition months of March and September, thus requiring the model to contain slightly more infiltration than occurs during summer and slightly less than occurs during the winter; hence, 20 percent of the average monthly rainfall is applied in those months.

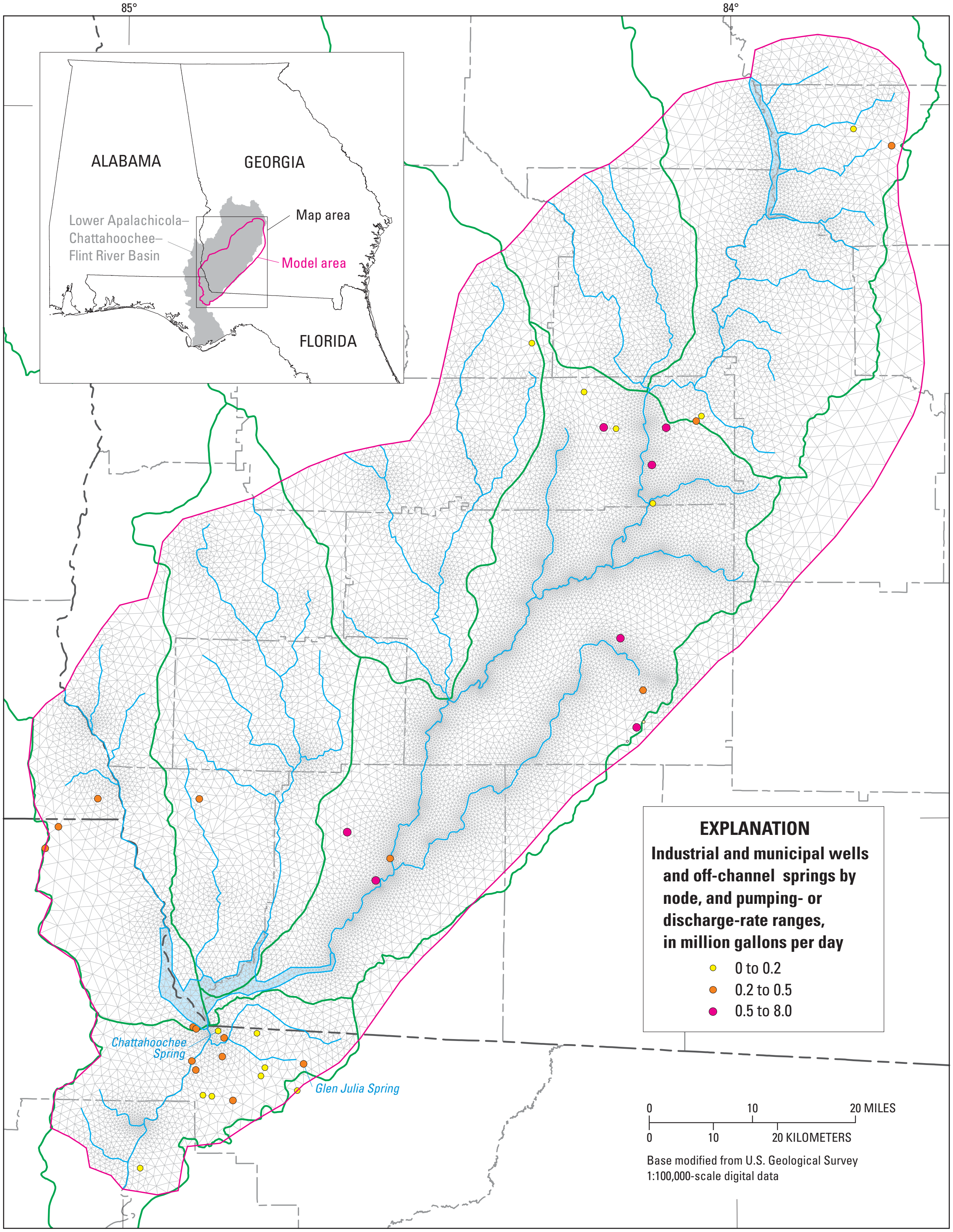

Figure 9. Distribution of nodes in the model simulating industrial and municipal wells and off-channel springs in southwest Georgia and adjacent parts of Alabama and Florida, and pumping- or discharge-rate ranges from the Upper Floridan aquifer.

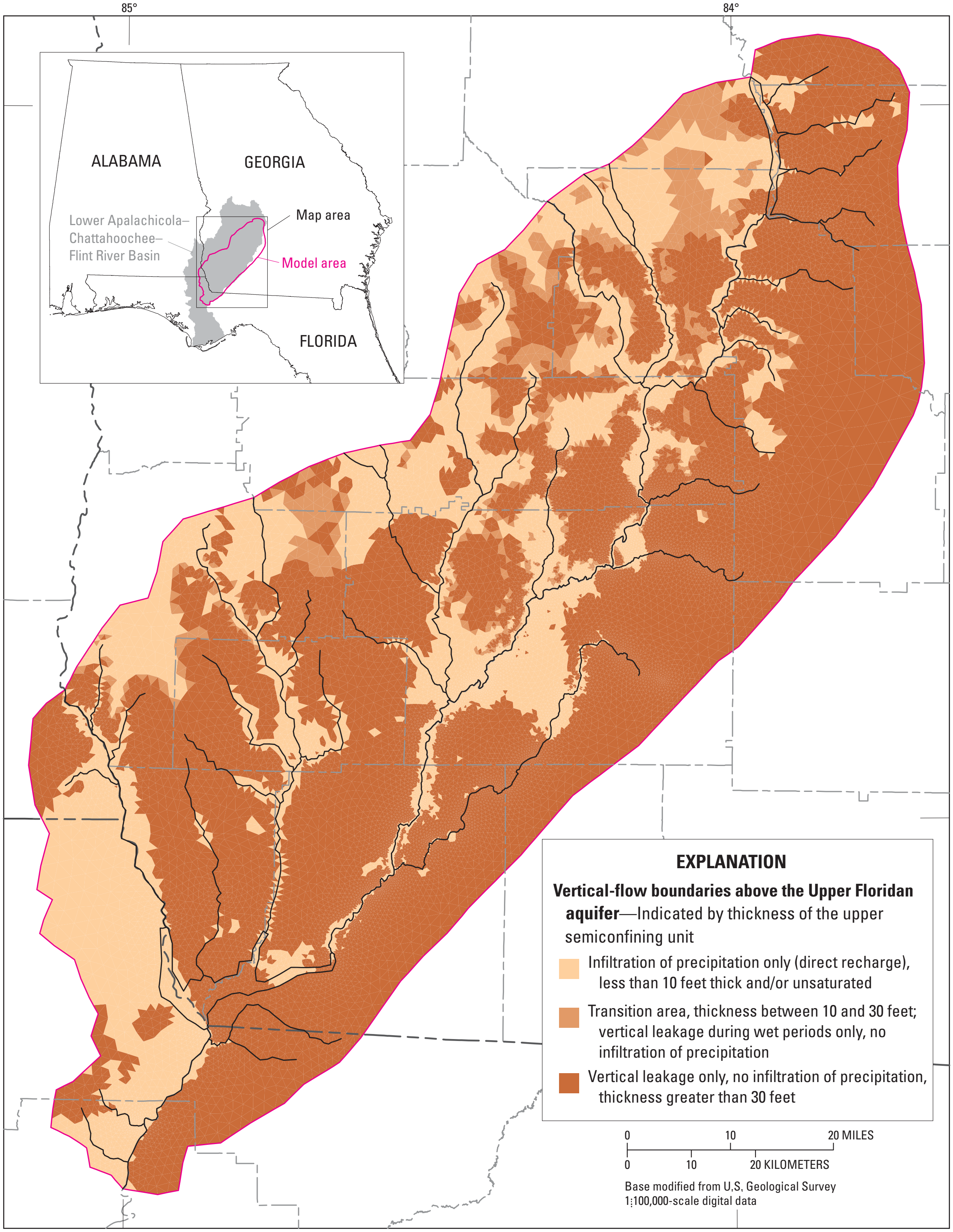

Figure 10. Vertical-flow boundaries above the Upper Floridan aquifer by element in the model in southwest Georgia and adjacent parts of Alabama and Florida.

Head-Dependent Flux Boundaries

Two general types of head-dependent flux boundary functions were used in the model, linear functions applied along element sides, and areally distributed functions applied across elemental areas. Regional ground-water flow into or out of the model area within the Upper Floridan aquifer (except at the aquifer updip boundary) and flow across streambeds were simulated using linear head-dependent flux boundaries, and vertical leakage to and from the overlying semiconfining unit and across areally extensive lake beds such as Lakes Seminole and Blackshear was simulated using an areally distributed, head-dependent flux boundary.

Regional Ground-Water Flow

Regional ground-water inflow and outflow across lateral model boundaries not at the Upper Floridan updip boundary was simulated with the head-dependent flux part of a Cauchy boundary, given by equation 4. The general form of the head-dependent flux boundary condition is expressed as the right side of equation 4 with q_B set to zero. For regional flow not at the Upper Floridan updip boundary, the controlling head, H_B, of equation 4 is located in the aquifer but external to the model area, situated transverse to and at a distance L from the boundary (or element) side so that it is unaffected by water-level changes in the model area (Torak, 1993a, p. 27). Each node defining an element side on a head-dependent flux boundary has an external (or controlling) head, H_B, associated with it. Ground water is allowed to flow across this boundary, as dictated by the difference between the external head and computed hydraulic head at the node located on the boundary, and by the value of a leakage coefficient that accounts for aquifer thickness and hydraulic conductivity of the external area to the model, thus simulating changes in location of the ground-water divide that occur with changes in hydrologic conditions within the model area. The region external to the model area is not simulated *per se*, only the flow rate across the model boundary is computed, exclusive of storage effects from this external area. Thus, for an element side defined by nodes k and l, the nodal flow rate across the boundary is expressed as

$$Q_B = (\tfrac{1}{2})\alpha L_{kl}(H_{Bi} - h_i),\ i = k \text{ or } l, \qquad (6)$$

and the boundary conductance term, α in equation 4, is defined as

$$\alpha = \frac{Kb}{L} \qquad (7)$$

for which K and b are, respectively, the average (estimated) hydraulic conductivity and thickness of the aquifer between the model boundary and H_B, that is, within the distance, L, from the boundary, and L_{kl} is the length of the element side. A distance of 3 mi was used for L to separate the external head, H_B, from the model boundary and to compute α. Values of H_{Bi} for each node i (=k or l) on the boundary side were interpolated from water-level measurements made in October 1986 (Torak and others, 1996) and May 1998 (Peck and others, 1999).

Element sides that simulate regional flow within the extended Upper Floridan aquifer using the head-dependent flux boundary were grouped into zones according to α values that were calculated from equation 7. Of the 52 zones representing the linear form of this boundary condition, eight represent regional flow in the model (table 3 and fig. 5, linear zones 45–52); the other zones represent flow across streambeds (discussed in the following section). [Note: there are three streams named Dry Creek simulated in the model, herein differentiated by the letters A, B, and C, as: (A) tributary to the Flint River in southwestern Worth and southeastern Dougherty Counties; (B) tributary to Spring Creek in Early County; and (C) tributary to Spring Creek in southwestern Miller, northeastern Seminole, and northwestern Decatur Counties. See figure 1.]

Flow Across Streambeds

Flow across streambeds was simulated with the head-dependent flux part of a Cauchy boundary, which is similar to the representation of regional flow discussed previously. For flow across streambeds, however, the streambed conductance term, α, in equations 4 and 6, is defined as

$$\alpha = \frac{K_r W_r}{b_r}, \qquad (8)$$

where K_r is vertical hydraulic conductivity of the streambed, W_r is streambed width, and b_r is streambed thickness. Values for α were specified individually by element side. Controlling head, H_{Bi}, in equation 6 is the stream stage (or lake level), associated with node i (=k or l) defining the element side on the boundary. Nodes are aligned along the stream or other surface-water feature and width, W_r, is the average width of the surface-water feature, measured transverse to the element side (fig. 5).

A nonlinear form of the head-dependent flux boundary condition was used to simulate small streams that would go dry if the water level in the aquifer was below the altitude of the bottom of the streambed. The boundary condition is nonlinear because the mathematical expression of streambed leakage is dependent on the relative positions of the nodal aquifer head, h_i, and the altitude of the bottom of the streambed, z_r. Thus, for node i (=k or l) on an element side that represents the surface-water feature as a nonlinear head-dependent flux (Cauchy-type) boundary, leakage expressions are given as

$$Q_{ri} = \begin{cases} C_{ri}\,(h_{ri} - h_i), & h_i > Z_{ri} \\ C_{ri}\,(h_{ri} - z_{ri}), & h_i > Z_{ri} \end{cases} \qquad (9)$$

where

Q_{ri} = volumetric flow rate [length^3/time];

C_{ri} = coefficient, given as (½)αL_{kl} [length^2/time];

h_{ri} = stream stage [length], and;

z_{ri} = controlling head (altitude of streambed bottom) [length];

the streambed conductance term, α, and L_{kl} have been defined previously for equations 8 and 6, respectively.

Table 3. Linear head-dependent flux boundary zones.

[α values, in feet per day, from calibrated model; 8-digit numbers are streamgage numbers in table A2]

Zone (figure 5)	Boundary coefficient, α	Description
		Zones representing stream reaches
1	0.75	Flint River: Crisp Co. Dam to 02350405
2	0.75	Flint River: 02350405 to 02350512
3	0.06–5	Flint River: 02350512 to Georgia Power Dam
4	200	Flint River: Georgia Power Dam to 02352500
5	600	Flint River: 02352500 to 02352790
6	25–50	Flint River: 02352790 to 02353000
7	1,000	Flint River: 02353000 to 02355660
8	1,500	Flint River: 02355660 to 02355662
9	1,500	Flint River: 02355662 to 02355700
10	170	Flint River: 02355700 to 02356000
11	170–200	Flint River: 02356000 to Lake Seminole
12	2–150	Chattahoochee River: model boundary to Lake Seminole
13	65	Apalachicola River: Jim Woodruff Dam to 02358000
14	65	Apalachicola River: 02358000 to model boundary
15	15	Muckalee Creek: model boundary to 02351700
16	15	Muckalee Creek: 02351700 to 02351890
17	5	Muckalee Creek: 02351890 to 02351900
18	3–4.5	Muckalee Creek: 02351900 to 02351930
19	2–6	Muckalee Creek: 02351930 to Flint River
20	0.5	Ichawaynochaway Creek: 02353265 (model boundary) to 02353460
21	5	Ichawaynochaway Creek: 02353460 to 02353500
22	600	Ichawaynochaway Creek: 02353500 to 02354800
23	350	Ichawaynochaway Creek: 02354800 to 02355350
24	300	Ichawaynochaway Creek: 02355350 to Flint River
25	0.5	Spring Creek: model boundary to 02356100
26	0.5	Spring Creek: 02356100 to 02356220
27	2	Spring Creek: 02356220 to 02356640
28	1.5	Spring Creek: 02356640 to 02357000
29	5–27	Spring Creek: 02357000 to 02357050
30	32	Spring Creek: 02357050 to 02357150
31	32	Spring Creek: 02357150 to Lake Seminole
32	35	Muckaloochee Creek: 02351800 (model boundary) to Muckalee Creek
33	0.5–0.7	Kinchafoonee Creek: 02350860 (model boundary) to 02350900
34	20	Kinchafoonee Creek: 02350900 to 02351000
35	20	Kinchafoonee Creek: 02351000 to Muckalee Creek
36	2.5	Chickasawhatchee Creek: headwaters to 02354300
37	1.25	Chickasawhatchee Creek: 02354300 to 02354350
38	1.5	Chickasawhatchee Creek: 02354350 to 02354410
39	1.5	Chickasawhatchee Creek: 02354410 to 02354500
40	1.8	Chickasawhatchee Creek: 02354500 to Ichawaynochaway Creek
41	5	Pachitla Creek: model boundary to Ichawaynochaway Creek
42	0.5	Dry Creek (B): headwaters to 02356290
43	1.25	Dry Creek (B): 02356290 to 02356460
44	2.5	Dry Creek (B): 02356460 to Spring Creek
		Zones representing regional boundaries
45	0–34	Northern Model Boundary
46	45	Northeastern Model Boundary
47	100	Eastern Model Boundary
48	120	North Pelham Model Boundary
49	55	South Pelham Model Boundary
50	55	Southeastern Model Boundary
51	30	Southern Model Boundary
52	30	Southwestern Model Boundary

Table 4. Nonlinear head-dependent flux boundary zones.

[α values, in feet per day, from calibrated model; 8-digit numbers are streamgage numbers in table A2]

Zone (figure 5)	Boundary coefficient, α	Description
1	0.5	Limestone Creek: headwaters to Lake Blackshear
2	3.5	Gum Creek: headwaters to 02350220
3	3.5	Gum Creek: 02350220 to Lake Blackshear
4	4	Cedar Creek: headwaters to 02350300
5	4	Cedar Creek: 02350300 to Lake Blackshear
6	20	Swift Creek: headwaters to 02350360
7	20	Swift Creek: 02350360 to Lake Blackshear
8	1.7	Jones Creek: headwaters to 02350509
9	1.7	Jones Creek: 02350509 to Flint River
10	2.8	Abrams Creek: headwaters to 02350524
11	2.8	Abrams Creek: 02350524 to Flint River
12	3.5	Mill Creek: headwaters to 02350527
13	3.5	Mill Creek: 02350527 to Flint River
14	2	Piney Woods Creek: headwaters to 02350543
15	2	Piney Woods Creek: 02350543 to Ichawaynochaway Creek
16	2	Dry Creek (A): headwaters to 02352760
17	2	Dry Creek (A): 02352760 to Flint River
18	2	Raccoon Creek: headwaters to 02352920
19	2	Raccoon Creek: 02352920 to Flint River
20	2	Cooleewahee Creek: headwaters to 02352970
21	5	Cooleewahee Creek: 02352970 to 02352980
22	5	Cooleewahee Creek: 02352980 to Flint River
23	2	Big Cypress Creek: headwaters to 02355600
24	2	Big Cypress Creek: 02355600 to Ichawaynochaway Creek
25	2	Big Slough: headwaters to 02355785
26	2	Big Slough: 02355785 to 02355830
27	2	Big Slough: 02355830 to 02355880
28	2	Big Slough: 02355880 to 02355950
29	2	Big Slough: 02355950 to Flint River
30	2	Fishpond Drain: headwaters to 02357310
31	2	Fishpond Drain: 02357310 to Lake Seminole
32	2.5	Sawhatchee Creek: headwaters to 02343940
33	2.5	Sawhatchee Creek: 02343940 to Chattahoochee River
34	0	Kirkland Creek: headwaters to 02344009
35	0	Kirkland Creek: 02344009 to Chattahoochee River
36	0	Bryans Creek: headwaters to 02344025
37	0	Bryans Creek: 02344025 to Chattahoochee River
38	5	Mosquito Creek: headwaters to 02358519
39	5	Mosquito Creek: 02358519 to Apalachicola River
40	50	Ocheesee Creek: headwaters to 02358661
41	25	Ocheesee Creek: 02358661 to Apalachicola River
42	200	Graves Creek: headwaters to 02358683
43	200	Graves Creek: 02358683 to Apalachicola River
44	20	North Branch: headwaters to Swift Creek
45	2	Kiokee Creek: headwaters to 02354440
46	2	Kiokee Creek: 02354440 to Chickasawhatchee Creek
47	2	Long Creek: headwaters to 02356600
48	2	Long Creek: 02356600 to Spring Creek
49	2	Big Drain: headwaters to 02356860
50	2	Big Drain: 02356860 to Spring Creek
51	2	Aycocks Creek: headwaters to 02356970
52	2	Aycocks Creek: 02356970 to Spring Creek
53	2	Dry Creek (C): headwaters to 02357025
54	2	Dry Creek (C): 02357025 to Spring Creek
55	5	North Mosquito Creek: headwaters to 02358500
56	5	North Mosquito Creek: 02358500 to Mosquito Creek

Simulated streams originated at either the stream headwaters where the stream was small, at the model boundary, or at the tailwater of an impoundment, and terminated at the point of discharge to another stream or lake, or at the model boundary. Most streams were divided into zones (table 3, zones 1–44, and table 4) based on the locations of 64 streamgaging stations having a record of measured streamflow or stage during the October 1999 calibration period (October 18–22, 1999; see table A2 in Appendix A).

Initial values of the boundary coefficient, α, were based on estimates of a similar parameter used in previous digital-modeling studies that were performed in the Dougherty Plain (Hayes and others, 1983; Torak and others, 1996). These values were adjusted during calibration to account for differences in simulation techniques used to represent surface-water features in both models; finite-differences used by Hayes and others (1983), and the finite-element model, MODFE, used in this study. Because three physical properties of linear surface-water features—vertical hydraulic conductivity of the streambed, stream width, and sediment thickness—are combined in one term, α, variations in any of these properties change the value of α. All streams used as head-dependent flux boundaries are shown in figure 5. Values of the boundary coefficient that were used in the calibrated models are listed by zone in table 3 for linear head-dependent flux boundaries, and in table 4 for nonlinear head-dependent flux boundaries.

Intermittent streams were assigned a controlling head, z_{ri}, representing the altitude of the streambed. During dry conditions, stage, h_{ri}, in these streams was set at the same level as the controlling head, and it was assumed that the stream could only receive water discharging from the aquifers, but could not recharge the aquifer, thus creating, in dry conditions, nonlinear discharge-only conditions in the aquifer. During wet conditions, however, stage in these streams was set at some level higher than the controlling head based on measured stream stage, if available, or the interpolated stage of the lower order stream where the tributary stream flows into it; and if ground-water levels in the aquifer were lower than stream stage, the stream was allowed to recharge the aquifer.

For the October 1999 steady-state calibration, values of H_B (stream stage) for all nodes representing a stream were obtained by interpolation between measured stream-stage records at 13 gaging stations having continuous records and measured levels of Lakes Seminole and Blackshear (in Appendix A, the bold, italicized stations shown in figure A1; see table A2 for location and name of gaging stations). Local variations in slope of the stream surface were estimated by measuring the distance along the stream trace between other gaging stations having instantaneous measurements of stage during October 1999 and points on topographic maps where contours crossed the stream channel. These slope values were the basis for the piece-wise linear interpolation of nodal values of stream stage, H_B, which was varied monthly throughout the March 2001–February 2002 transient simulation based on monthly averages of stream stage at 13 gaging stations having continuous records and the two lake levels (see table A3 in Appendix A).

Upper Semiconfining Unit and Lake-Bed Leakage

Vertical leakage between the Upper Floridan aquifer and the overlying upper semiconfining unit and Lakes Seminole and Blackshear was simulated using a nonlinear form of a steady vertical-leakage function, expressed generally by the term $R(H - h)$ in equation 1 (Cooley, 1992; Torak, 1993a,b). Lateral and vertical discontinuities in permeable zones contained in the upper semiconfining unit, along with variable sand and clay content, total thickness, and ground-water level fluctuations influence the rate of vertical leakage of ground water into or out of the Upper Floridan aquifer (Torak and Painter, 2006) and preclude representation of the upper semiconfining unit as a distinct model layer; thus, requiring use of nonlinear leakage functions to simulate water exchange between the Upper Floridan aquifer, surface water, and land surface.

The nonlinear form of the steady vertical-leakage function limits recharge by vertical leakage for water-level declines that cause water-table conditions in the Upper Floridan aquifer and hydraulic separation from the upper semiconfining unit. The volumetric-flow rate, Q_{ai}, across the vertical boundary of the Upper Floridan aquifer with the upper semiconfining unit is expressed for node i as

$$Q_{ai} = \begin{cases} C_{ai}\,(H_i - h_i), & h_i > z_{ti} \\ C_{ai}\,(H_i - z_{ti}), & h_i > z_{ti} \end{cases} \quad (10)$$

where

Q_{ai} = volumetric flow rate for steady vertical leakage [length^3/time];$(1/3)\sum_{e_i} R^e \Delta^e$;

C_{ai} = nodal vertical-leakage coefficient [length^2/time], given as

h_i = nodal hydraulic head in the Upper Floridan aquifer [length];

H_i = nodal head in upper semiconfining unit [length], and;

z_{ti} = nodal altitude of top of Upper Floridan aquifer or base of upper semiconfining unit [length];

and R^e and Δ^e are vertical hydraulic conductance [time^{-1}] and area [length^2], respectively, of element e. Aquifer recharge is limited to a maximum rate by equation 10 when aquifer head drops below the base of the upper semiconfining unit or top of the Upper Floridan aquifer. Discharge from the Upper Floridan aquifer to the upper semiconfining unit is not limited by the nonlinear function.

Thickness variations, lithology, and water-level fluctuations in the upper semiconfining unit as well as other factors—such as proximity to streams and lakes, pumped wells, topography, and rainfall distribution—affect the hydrologic function of this unit (Torak and Painter, 2006); hence, its areal representation in the model as nonlinear, steady vertical leakage. As noted by Torak and Painter (2006), these factors uniquely combine at each location in the study area, yielding uncertain results with regard to vertical leakage and recharge from and through the upper semiconfining unit to the Upper Floridan aquifer. Torak and Painter (2006, fig. 11) developed 14 geohydrologic zones in the upper semiconfining unit on the basis of unique combinations of hydrologic factors, mentioned previously, and the temporal distribution of saturated upper semiconfining unit thickness (fig. 11 and table 5), which served as a guide to identify areas where vertical leakage was represented in the model with the nonlinear, steady vertical-leakage function.

Areas where the upper semiconfining unit is more than 30 ft thick (fig. 12), generally contain a clay layer near the lower-half thickness, or base, of the unit (described in Torak and Painter, 2006) and were assigned a value of vertical hydraulic conductance, R^e, based on the thickness and vertical hydraulic conductivity of the basal clay. This clay layer forms a semiconfining unit between the upper part of the upper semiconfining unit, which locally is a water-bearing zone, and the Upper Floridan aquifer. The distribution and thickness of the clay layer was established from data collected during studies by Hayes and others (1983), Hicks and others (1987), and Torak and Painter (2006), and from other data on file at either the USGS Georgia Water Science Center, Atlanta, Ga., or the Florida Bureau of Geology, Tallahassee, Fla. As Torak and Painter (2006, p. 27) noted:

> Geohydrologic zones containing less than 30 ft of total upper semiconfining unit thickness (fig. 7) and having a proportional saturation of total thickness that corresponds to less than 10 ft of saturated thickness (that is, less than about 0.3) indicate a low potential for recharge to the Upper Floridan aquifer by vertical leakage through the upper semiconfining unit or by the release of water in storage from this unit (fig. 12, medium-shaded areas). In the upland interstream, interstream karst swamp, and upland outcrop areas (fig. 11), the combination of relatively high proportional saturation of total upper semiconfining unit thickness (from 0.6 to 0.7, fig. 11) and relatively small total thickness (less than 30 ft) corresponds to a saturated thickness of less than about 21 ft that can dewater rapidly during dry climatic conditions, especially where the upper semiconfining unit contains a silty and sandy lithology (table 4).

For the upper semiconfining unit, elements were assigned a zero value of vertical hydraulic conductance in areas where the unit was absent, had a total thickness less than 30 ft, or had a clay thickness of zero. In these areas, infiltration was applied as a percentage of average monthly precipitation as described in the previous section on “Infiltration.”

Table 5. Geohydrologic zones in the upper semiconfining unit overlying the Upper Floridan aquifer and generalized saturated proportion of total upper semiconfining unit thickness from March 2001 to February 2002 (from Torak and Painter, 2006).

[Saturated proportion expressed as a fraction of total thickness of upper semiconfining unit; NAVD 88, North American Vertical Datum of 1988]

Upper semiconfining unit geohydrologic zone (figure 11)	Proportional saturation of total semiconfining unit thickness by month											
	2001										2002	
	Mar.	Apr.	May	June	July	Aug.	Sept.	Oct.	Nov.	Dec.	Jan.	Feb.
Upland outcrop	0.25	0.25	0.25	0.25	0.25	0.25	0.25	0.25	0.35	0.35	0.35	0.5
Upland, dry	0	0	0	0	0	0	0	0	0	0	0	0
Interstream karst swamp	.35	.35	.35	.35	.35	.35	.35	.35	.5	.5	.6	.6
Upland interstream	.9	.9	.75	.75	.75	.75	.75	.69	.69	.65	.76	.9
Interstream karst	.45	.45	.45	.45	.45	.45	.45	.45	.45	.45	.45	.45
Flint River upstream of Lake Seminole to Cooleewahee Creek, and Apalachicola River	.25	.12	.1	0	0	0	0	0	0	0	0	0
Northeast of Lake Seminole, east of Flint River to 150 above NAVD 88	.25	.25	.25	.25	.25	.25	.25	.25	.25	.25	.25	.25
Pelham Escarpment	.5	.5	.5	.5	.5	.5	.5	.5	.68	.6	.6	.5
Upland interstream karst	.5	.5	.5	.5	.5	.5	.5	.5	.4	.4	.3	.3
Headwater upland	.2	.3	.3	.3	.3	.3	.2	.2	.2	.6	.6	.6
Upland, east of Lake Blackshear	.85	.85	.85	.83	.83	.8	.8	.8	.76	.76	.76	.78
Pelham Escarpment upland	.6	.6	.6	.6	.6	.6	.6	.6	.7	.7	.8	.8
Terrace and undifferentiated deposits	0	0	0	0	0	0	0	0	0	0	0	0
Marine and fluvial terrace deposits	0.2	0.2	0.2	0.2	0.2	0.2	0.2	0.2	0.2	0.2	0.2	0.2

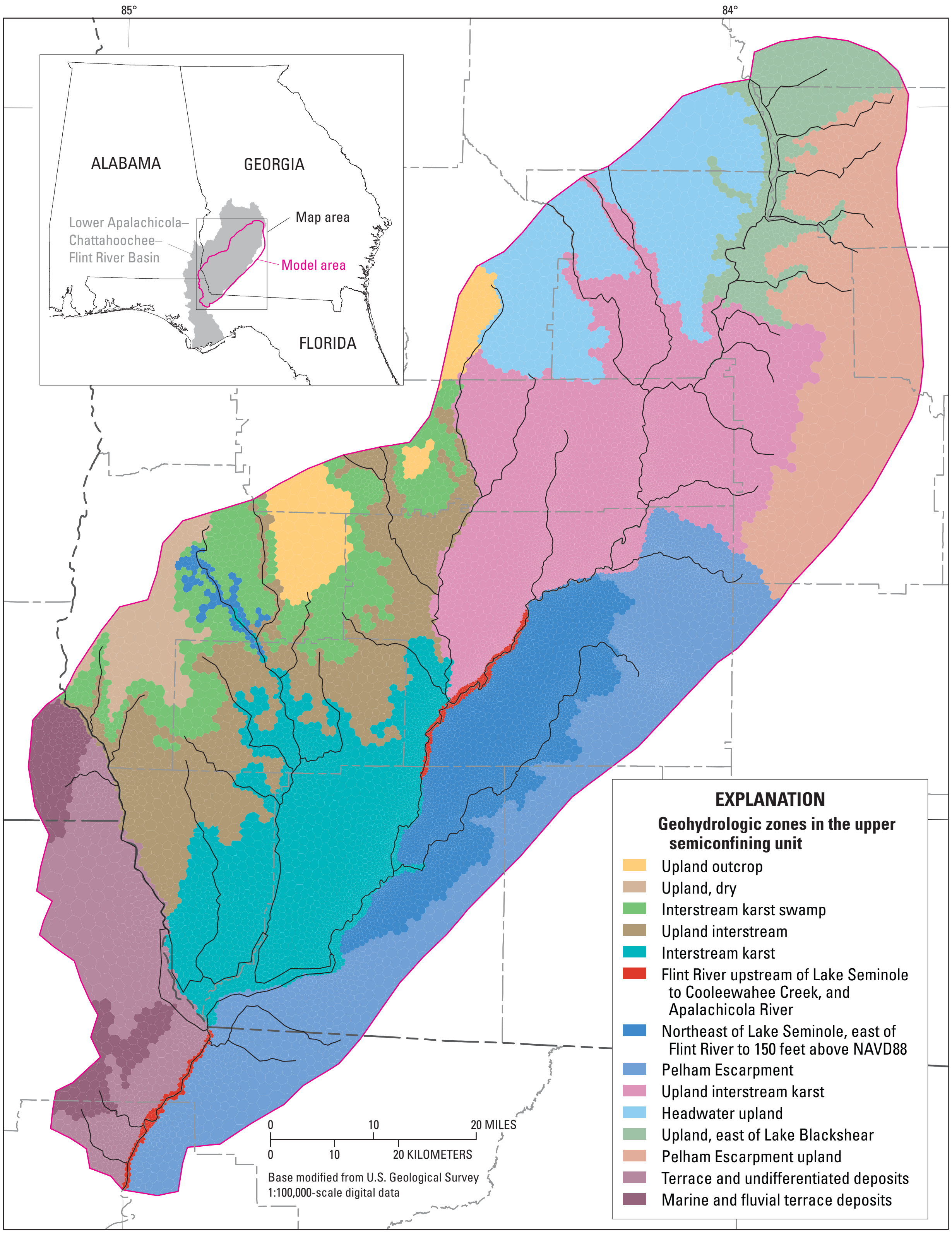

Figure 11. Geohydrologic zones in the upper semiconfining unit overlying the Upper Floridan aquifer by nodal area in the model in southwest Georgia and adjacent parts of Alabama and Florida (modified from Torak and Painter, 2006).

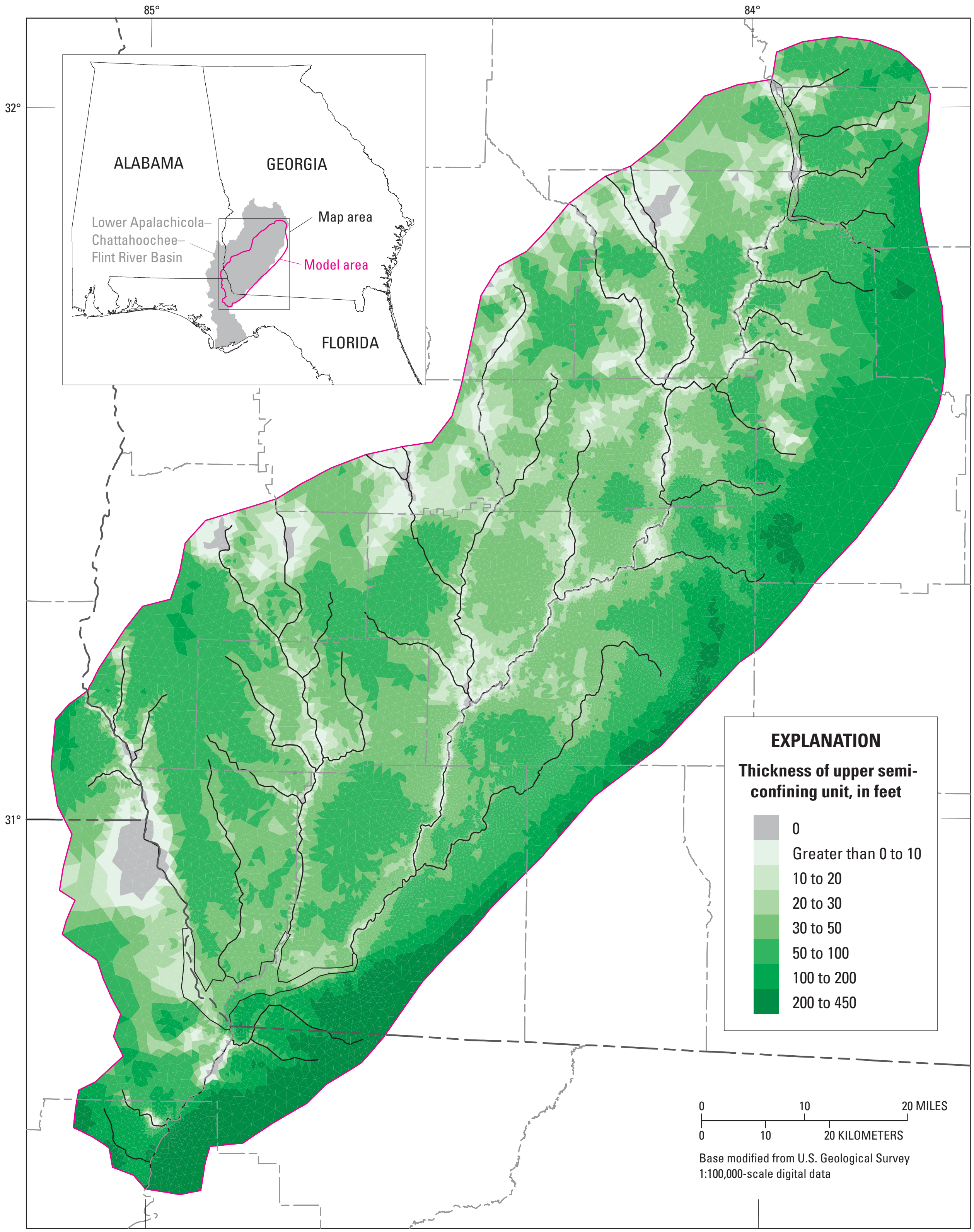

Figure 12. Thickness of upper semiconfining unit overlying the Upper Floridan aquifer by element in the model in southwest Georgia and adjacent parts of Alabama and Florida (modified from Torak and Painter, 2006).

Values for source-layer head, *H*, of equation 1, for vertical leakage to and from the upper semiconfining unit were input to the model by node. An extensive discussion of the determination of these head values and their fluctuation during the transient simulation period from March 2001 to February 2002 is provided in Torak and Painter (2006).

Considerable uncertainty is associated with the estimation of model-input values of vertical hydraulic conductance, R^e, and source-layer head, *H*, for the upper semiconfining unit. Torak and Painter (2006) cited values of vertical hydraulic conductivity, K_v, which were used to compute input values of R^e, that range over four or five orders of magnitude. The calibrated value of K_v, 0.0075 feet per day (ft/d), is within the ranges cited, but only can be considered a very rough estimate of the average value for a parameter that probably varies widely across the model area. There are no available data to provide a more accurate distribution of K_v. Similarly, scarcity of continuous water-level data in wells open to the upper semiconfining unit (only four wells in the model area) limit the accuracy of saturation percentages given in table 5.

The hydrologic interaction between the Upper Floridan aquifer and Lakes Seminole and Blackshear was simulated in the model in the same manner as the leakage between the aquifer and the upper semiconfining unit. Lake-bed sediments, however, are assumed to be far more transmissive than the clays in the lower part of the upper semiconfining unit, as the lakes were impounded in river valleys containing a thin veneer of relatively sandy to silty terrace and undifferentiated deposits and residuum (Torak and Painter, 2006). The value of R^e assigned to elements representing both lakes was 8.0×10^{-3} day^{-1} (as in Torak and others, 1996). Average lake levels for October 1999 of 76.89 ft and 233.3 ft for Lakes Seminole and Blackshear, respectively, were used for the October 1999 calibrated model. During the March 2001–February 2002 transient simulation, lake levels were varied monthly based on average monthly lake levels (U.S. Army Corps of Engineers, Mobile District, Mobile, Alabama, Web site *http://water.sam.usace.army.mil/gage/acfhist.htm,* accessed May 6, 2005; and Marcus Waters, Crisp County Power Company, written commun., 2005).

Upper Floridan Aquifer Characteristics

Hydrologic characteristics of the Upper Floridan aquifer used in the construction of the model primarily were derived from Torak and Painter (2006), which considers the most recent data available, much of which was collected for the current study. Hydrologic data presented and discussed by Torak and Painter (2006) were modified only slightly to allow it to be prepared as model input. For example, the contoured nodal values of the altitude of the top of the Upper Floridan aquifer model (fig. 13) correspond to the surface map of Torak and Painter (2006, fig. 8), except along some stream reaches where stream-stage data used in the model indicated that the Upper Floridan aquifer was incised by the stream. Thus, lower altitude values for the top of the Upper Floridan aquifer were input to the model along some stream traces in areas where the Upper Floridan aquifer crops out (for example, along the Muckalee, Muckaloochee, and Kinchafoonee Creeks in northern Lee and Terrell Counties) and along major streams crossing the Dougherty Plain and Marianna Lowlands (for example, the Flint River and Ichawaynochaway Creek in Baker and Mitchell Counties, and the Chattahoochee River in Houston County, Ala., and Early County, Ga.).

Some of the adjustments based on stream incisions discussed above are also reflected in nodal values of thickness of the Upper Floridan aquifer (fig. 14). Because the thickness of the Upper Floridan was estimated by subtracting the altitude of the base of the aquifer from the altitude of the top, there is some commensurate thinning of the aquifer in the same areas where the top of the aquifer is incised by streams.

Initial values of hydraulic conductivity of the Upper Floridan aquifer were based on the kriged distribution in Torak and Painter (2006, fig. 16). These values were adjusted during the calibration process as described in that section below. Few data are available for approximating storage coefficient of the Upper Floridan aquifer, and a value of 5×10^{-4} was assumed throughout the model area. In the parts of the Upper Floridan aquifer that are under water-table conditions, the aquifer is not used for water supply, and there were no measured values of specific yield. A value of 0.2 was assumed for specific yield throughout the model area, in case water-table conditions occur and have to be simulated.

Ground-Water Flow Model Performance and Analysis

The performance of the ground-water flow model is refined through calibration in steady-state mode to conditions of October 1999. Ground-water level residuals (simulated minus measured ground-water levels) and simulated and measured stream-aquifer fluxes were used to achieve calibration. Sensitivity analysis is used to provide an understanding of the relative importance of values of various model parameters on ground-water level residuals and simulated components of the ground-water budget, followed by a discussion of model uncertainty. A ground-water flow net is illustrated for the steady-state October 1999 calibrated model and for subbasin 03130008 (lower Flint River).

Steady-State Calibration, October 1999

Substantial hydrologic field data were collected from the model area during October 1999 expressly for calibrating a ground-water flow model. During October 1999, the model area was in a long-term drought that persisted from 1998 through the first half of 2002. By calibrating the ground-water flow model to hydrologic data collected during a period of little or no rainfall, it could be reasonably assumed that increases in streamflow from upstream to downstream gages could be

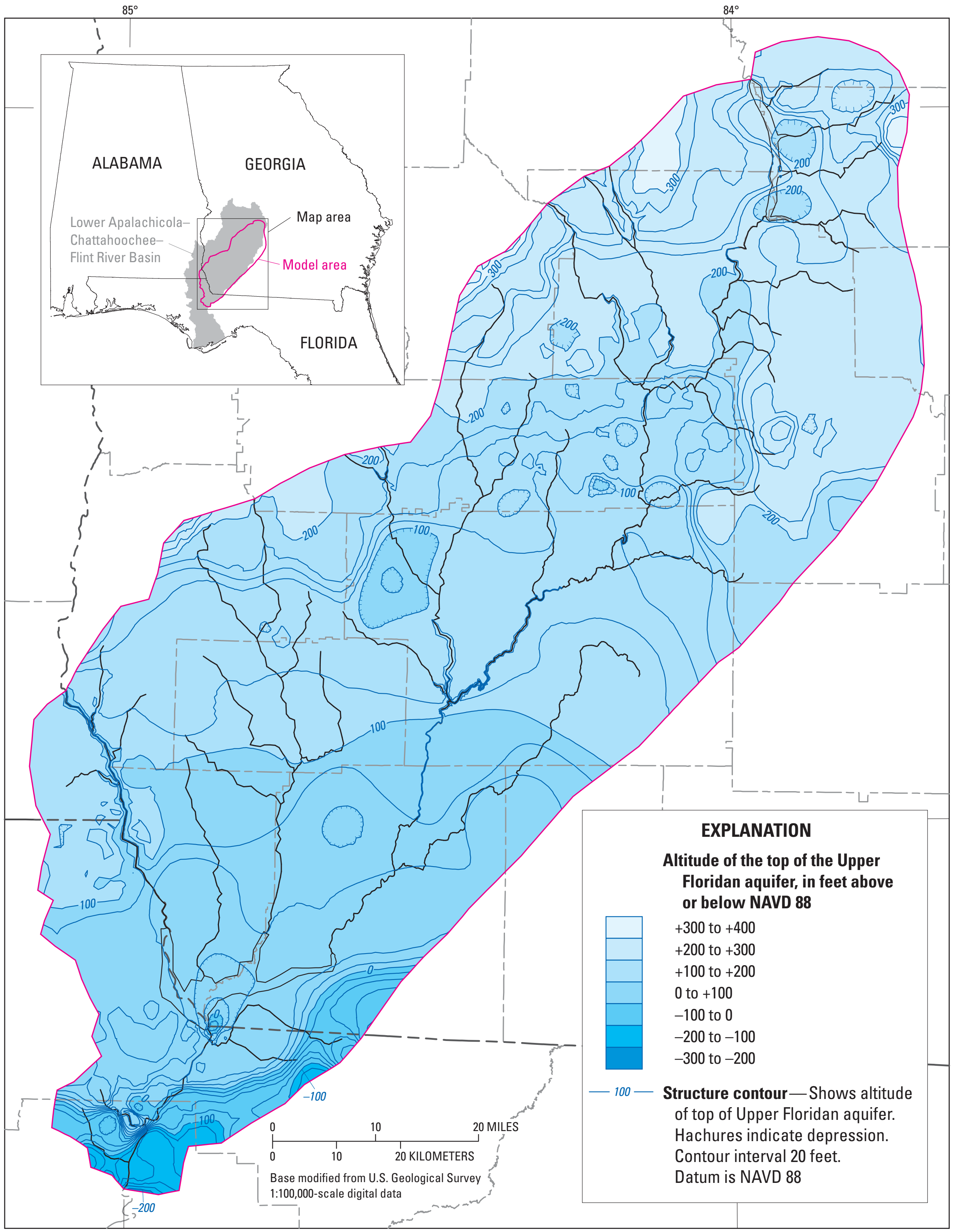

Figure 13. Altitude of the top of the Upper Floridan aquifer in the model area in southwest Georgia and adjacent parts of Alabama and Florida (modified from Torak and Painter, 2006).

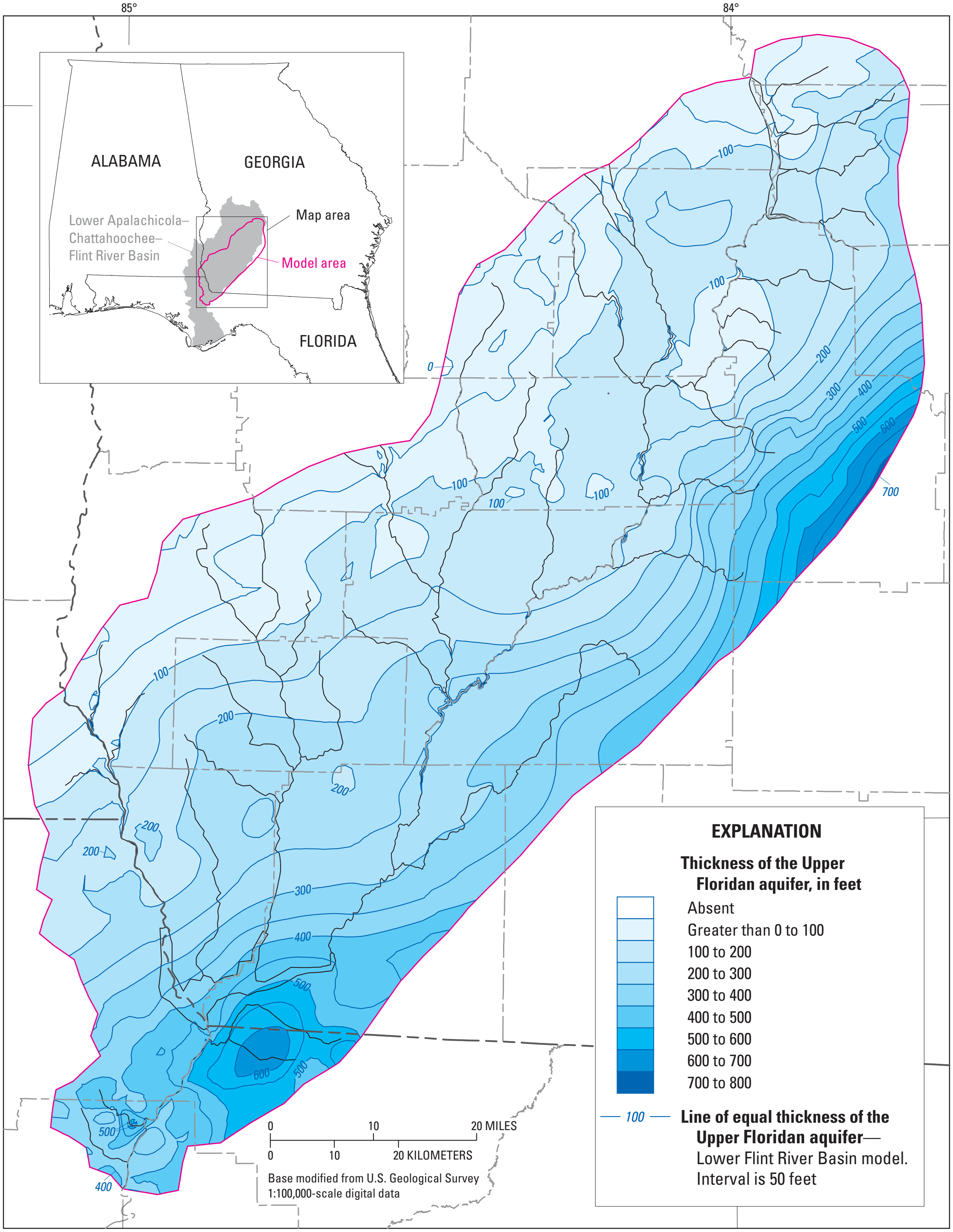

Figure 14. Thickness of the Upper Floridan aquifer in the model area in southwest Georgia and adjacent parts of Alabama and Florida (modified from Torak and Painter, 2006).

attributed entirely to baseflow from the ground-water system, because little or no overland runoff would have occurred. In the model area, ground-water level was measured in 275 wells open to the Upper Floridan aquifer in the model area (table A4 in Appendix A) and streamflow was measured at 64 stream-gaging stations on 33 streams in the model area (table A1 in Appendix A). These data were compared to model results to achieve calibration.

Calibration Strategy

Acceptance of model results for evaluating stream-aquifer relations in the lower Flint River Basin depends on the accuracy of the model in simulating ground-water levels and associated stream-aquifer processes during October 1999 when extensive hydrologic data were collected during an earlier part of this study. The process of adjusting model inputs of hydraulic properties, within plausible limits, to produce a computed solution that satisfies error criteria established with regard to observations of the hydrologic system during the historical period is termed calibration. The objective of model calibration was to refine input parameters so that the model simulates, within acceptable error bounds, ground-water levels and flow and stream-aquifer interaction in the Upper Floridan aquifer for October 1999, as indicated by comparison to measurements of pertinent hydrologic phenomena (Torak and others, 1996).

The criteria for accepting simulated water levels were based on the accuracy of model input parameters and water-level measurements used for comparison. The accuracy of the water-level measurements depends on whether the land-surface altitude at the well was estimated from leveling or from a topographic map. Of the 275 ground-water level measurements, 19 of the well altitudes were leveled (15 are accurate to within 0.01 ft and 4 are accurate to within 1.0 ft), and the remaining 256 well altitudes were estimated from a topographic map (to within 5 ft, or one half the contour interval of 10 ft). Thus, the average accuracy of the ground-water level measurements is 4.7 ft. Most of the well locations that were estimated from a topographic map were also located without modern global positioning systems (GPS), thereby introducing further possible loss of accuracy. Geometry of the ground-water model (aquifer thickness, aquifer top, thickness of the upper semiconfining unit) was derived from well data that have land-surface accuracy similar to that of the 275 measured ground-water levels. Aquifer geometry actually is subject to much greater errors associated with subjective picks of aquifer boundaries based on drill cuttings and geophysical logs, but the accuracy of those picks is impossible to quantify. Conservatively, aquifer geometry is assumed to have accuracy similar to measured ground-water levels. Combining the two potential errors, a good fit of average simulated and measured ground-water levels should be within 9.4 ft (two times the average accuracy of the measured ground-water levels). Additionally, the range of the 275 measured ground-water levels was from about 62 ft to 294 ft above NAVD 88. Generally, a fit is considered good if the ratio of the standard deviation of the residual (simulated minus measured) ground-water levels divided by the range of measured ground-water levels is less than 0.1. The range of measured ground-water levels is 232 ft; thus, the standard deviation of the ground-water level residual should be less than 23 ft.

The calibration procedure involved trial-and-error adjustments to hydraulic properties that affected simulated values of ground-water levels and volumetric flow rates across streambeds, termed *stream-aquifer fluxes*. Comparisons were made of simulated ground-water levels with measured levels at 275 discrete points (wells), and of simulated stream-aquifer fluxes with fluxes that were estimated on the basis of streamflow measurements for 53 selected reaches (the same type of calibration criteria used by Torak and others, 1996). Adjustments to the following two hydraulic properties were made within plausible limits to achieve calibration: (1) hydraulic conductivity of Upper Floridan aquifer and (2) vertical hydraulic conductivity of overlying semiconfining unit. Often, calibration involved trade-offs between these two primary parameters, and the parameters were adjusted until a reasonable minimum value of the root-mean square of ground-water level residuals (simulated minus measured water levels) was achieved, as discussed in the next section. Leakage coefficients for head-dependent flux boundaries that represent streams also were adjusted to achieve a good fit of simulated and measured values of stream aquifer flux, also discussed in a subsequent section.

Hydraulic conductivity of the Upper Floridan aquifer, K, is input by element, and values initially were taken from a kriged hydraulic conductivity distribution in the model area based on 119 test values of hydraulic conductivity (David C. Leeth, U.S. Geological Survey, written commun., 2004; Torak and Painter, 2006, fig. 16). Because all of the point values of K were derived from localized tests, which generally underestimate regional K (Rovey and Cherkauer, 1995), the kriged values of K were systematically raised and adjusted (along with other calibration parameters) until a minimum root-mean-square error of 275 ground-water level residuals (simulated minus measured water level) was achieved. The calibrated multiplier for raising the local kriged values of K to an effective regional value was 9.2.

One of the effects of using kriging to estimate and distribute values of any spatial parameter is that in areas that are beyond the range of the variogram developed for the parameter an average value is assigned. In reality, at any of the locations assigned an average value, the actual value of the parameter could be anywhere within or even beyond the range of measured data, there are simply no available data to indicate it. For the present geostatistical analysis of K the range of the variogram was about 4.5 mi (David C. Leeth, U.S. Geological Survey, written commun., 2004). Thus, in areas more than 4.5 mi from a measured point (see Torak and Painter, 2006, fig 16), where there is any other plausible hydrologic evidence for adjusting the values of K that also would lower the root-mean-square error of the ground-water-level residuals, that evidence should be considered and K adjusted accordingly.

A generalized potentiometric surface of the Upper Floridan aquifer in the model area for October 1999 (Mosner, 2002, fig. 19) was used to adjust the kriged distribution of *K*. In four areas, contours of the October 1999 potentiometric surface are more closely spaced than on average elsewhere, indicating a steeper hydraulic gradient. One explanation for such a steepening is lower hydraulic conductivity, *K*, at that location. To account for this in the model, *K* of the Upper Floridan aquifer was lowered from 0.5 to 1.0 order of magnitude in four roughly oval areas having steeper than average hydraulic gradients: (1) an east-west trending oval from Spring Creek through western Miller and southern Early Counties, Ga., across the Chattahoochee River into Houston County, Ala.; (2) in an east-west trending oval from western Baker to eastern Early Counties, Ga.; (3) in a east-northeast-west-southwest trending oval from southwestern Lee through southeastern Terrell to northwestern Dougherty Counties, Ga.; and (4) in a north-south trending oval in western Worth County, Ga., just east of the Worth-Dougherty and Worth-Mitchell county lines in Georgia. Lowering *K* in each of these areas reduced the mean-square-error of the residual water levels; and the resulting distribution of *K* values by element in the model is shown in figure 15.

Initial values of vertical hydraulic conductance, R^e, were computed from values of vertical hydraulic conductivity, K_v [length/time], discussed in Torak and Painter (2006). K_v was systematically adjusted within a feasible range during calibration of the steady-state simulation (discussed in subsequent sections). R^e values, which are input to the model by element, were computed using the relation $R^e = K_v / b_u$, where b_u is the thickness of upper semiconfining unit by element based on the average of the thickness of the semiconfining unit at three nodes comprising the element. The calibrated value of K_v was 0.0075 ft/d, and the distribution of values of R^e of the upper semiconfining unit by element are shown in figure 16.

Ground-Water Level Residuals

Ground-water level residuals were calculated at 275 well locations in the model (fig. 17). Values of simulated water level for well locations used in calibration were obtained by applying the finite-element concept of linear variation of water level in an element (Zienkiewicz, 1977, p. 93–95) to those elements containing wells. Thus, simulated water levels at nodes were used to compute the water level at locations in an element corresponding to the measured water levels in wells used for comparison during calibration. Residuals from the calibrated model are listed in table A4 and the well locations are shown in figures A2–A7 in Appendix A.

A commonly used indicator of the quality of a model simulation with regard to ground-water level residuals is the root-mean square (*RMS*) of residuals, similar to the standard deviation of residuals, and defined as:

$$RMS = \left[\frac{1}{N} \sum_{i=1}^{N} (h_{i\,sim} - h_{i\,mes})^2 \right]^{1/2}, \qquad (11)$$

where *N* is the number of residuals (275), and $h_{i\,sim}$ and $h_{i\,mes}$ are, respectively, the simulated and measured hydraulic head for the i^{th} residual. *RMS* of ground-water level residuals was 8.18 ft for the steady-state October 1999 calibrated simulation (table 6). The arithmetic average of ground-water level residuals was 0.29 ft, and the standard deviation of residuals was 8.19 ft. The standard deviation and *RMS* of residuals are essentially equal, as expected for a sample from a population having a mean of zero, which ground-water level residuals should have. The *RMS* of residuals (8.18 ft) is within the water-level error criteria of 9.4 ft discussed in the previous section. The ratio of standard deviation of the residual errors divided by the range of water levels (8.19/232) is 0.035, well below the value of 0.1 considered to be a good fit. For the 95 residuals in subbasin 03130008 (lower Flint River), the *RMS* of residuals was 6.47 ft, indicating a marginally better fit than for the entire model; the standard deviation was 6.43 ft, and the average was 0.96 ft. The *RMS* of residuals in subbasin 03130008 also is within the water-level error criteria of 9.4 ft. Measured water levels in subbasin 03130008 range from about 63 ft to about 213 ft; thus, the ratio of standard deviation of the residual errors divided by the range of water levels in the subbasin (6.43/150) is 0.043, which also is well below the value 0.1 considered to be a good fit.

Frequency histograms of ground-water level residuals from the calibrated model (table 6 and fig. 18) indicate how normally distributed residuals are about zero, which cannot be determined by evaluating RMS of residuals alone. Of the 275 ground-water level residuals from the October 1999 calibrated model, 143 values (52 percent) were within 5 ft of zero, 21 values (8 percent) deviated from zero by more than 15 ft, and the largest residual was –39.40 ft (table 6 and table A4 in Appendix A). Of the 95 water-level residuals in subbasin 03130008, 52 values (55 percent) were within 5 ft of zero and only one value (1 percent) deviated from zero by more than 15 ft, which was also the largest residual at 15.26 ft. Figure 19 is a comparison of 275 measured and simulated water levels using graphs of (*A*) measured versus simulated ground-water levels, (*B*) measured versus residual ground-water levels, and (*C*) cumulative probability plots of residuals from the calibrated model and subbasin 03130008. Several characteristics of the graphs indicate that the ground-water residuals are normally distributed, including the bell shape of the histograms shown in figure 18, the close fit of data to the diagonal in figure 19*A*, the even spread of data in figure 19*B*, and the linearity of data in figure 19*C*. Standard-normal distributions defined by statistics in table 6, shown in figure 19*C*, indicate that the five lowest residual water levels in the model could be considered outliers from a normal distribution.

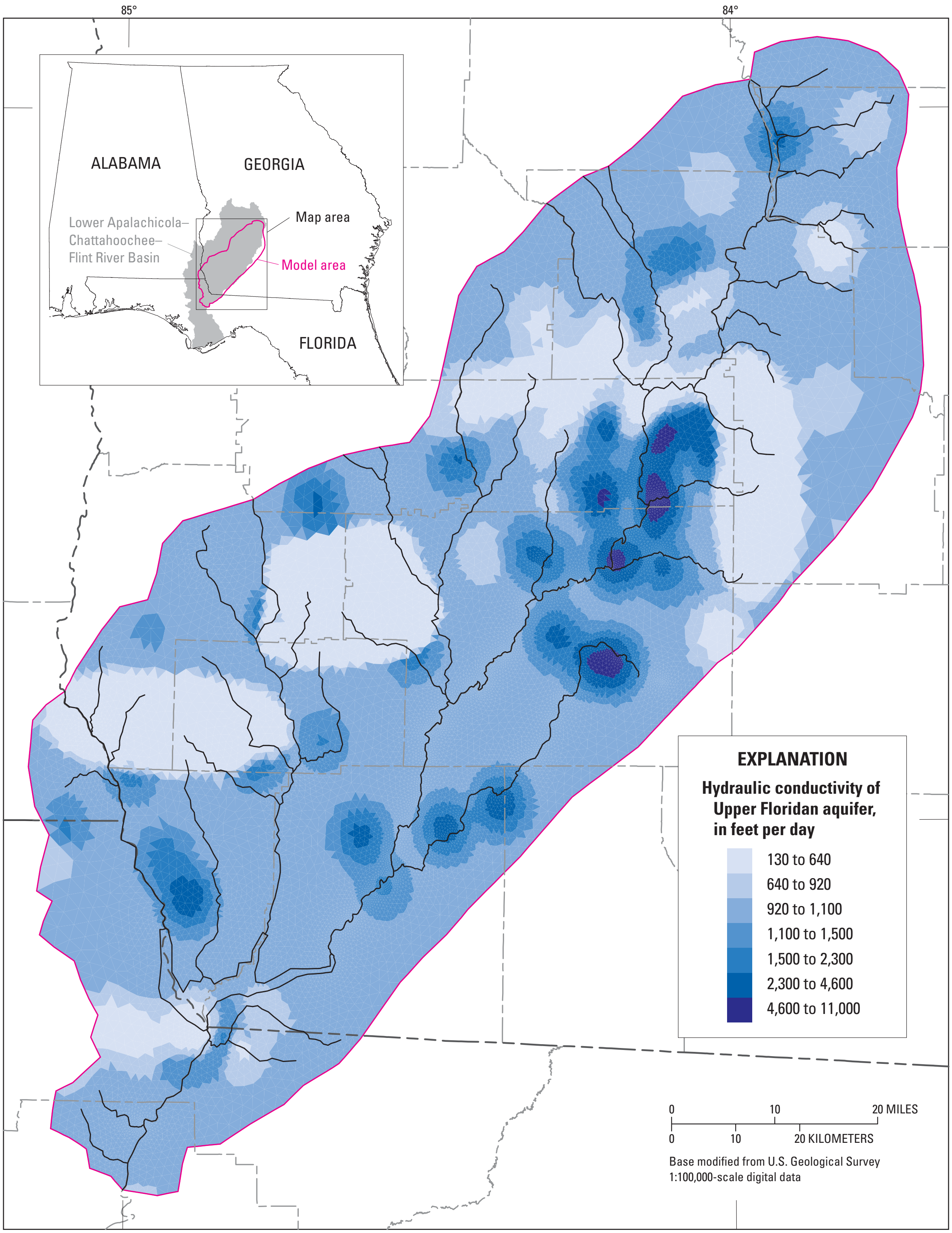

Figure 15. Distribution of hydraulic-conductivity values of the Upper Floridan aquifer by element in the model in southwest Georgia and adjacent parts of Alabama and Florida.

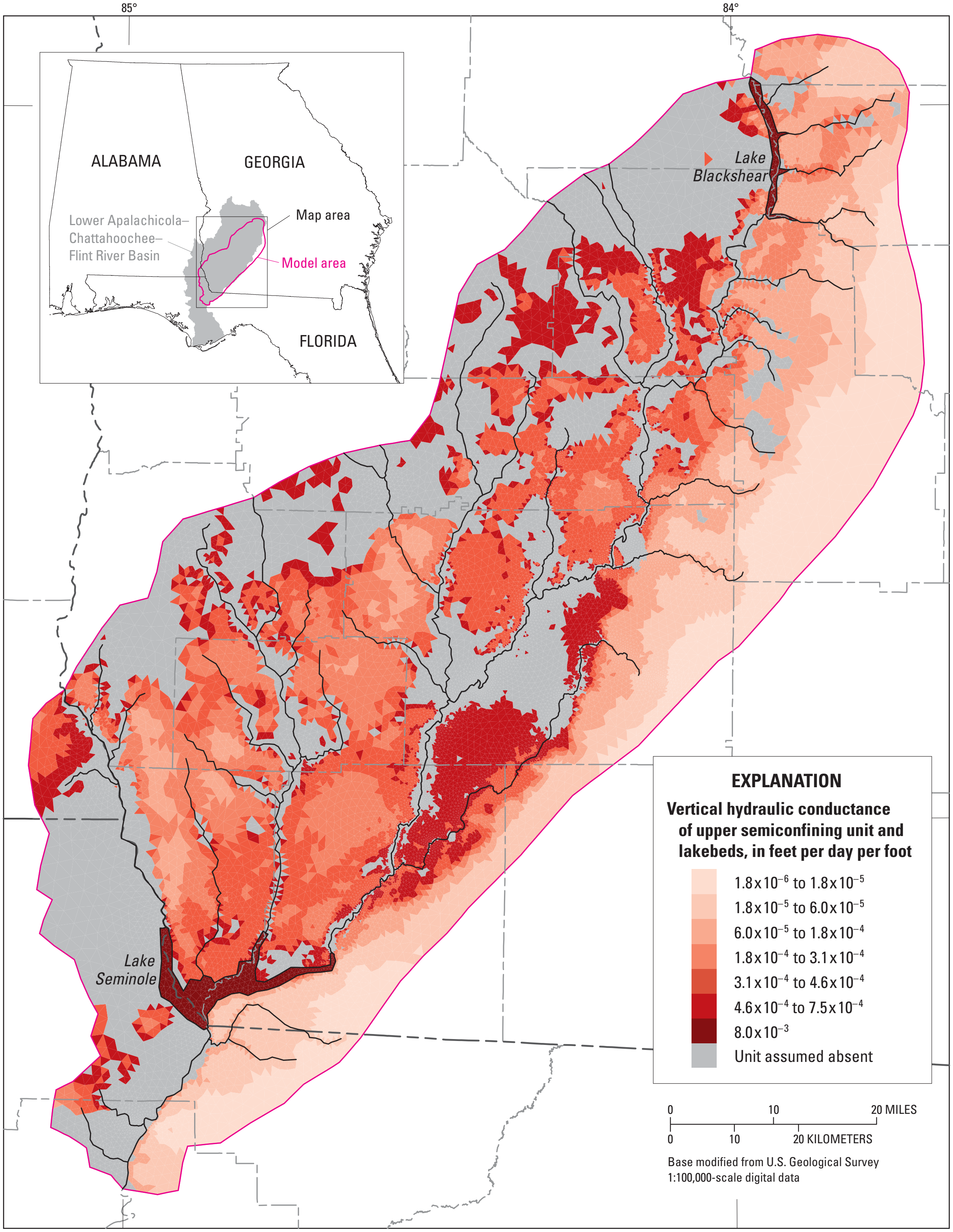

Figure 16. Distribution of values of vertical hydraulic conductance of the upper semiconfining unit and the beds of Lakes Seminole and Blackshear by element in the model in southwest Georgia and adjacent parts of Alabama and Florida.

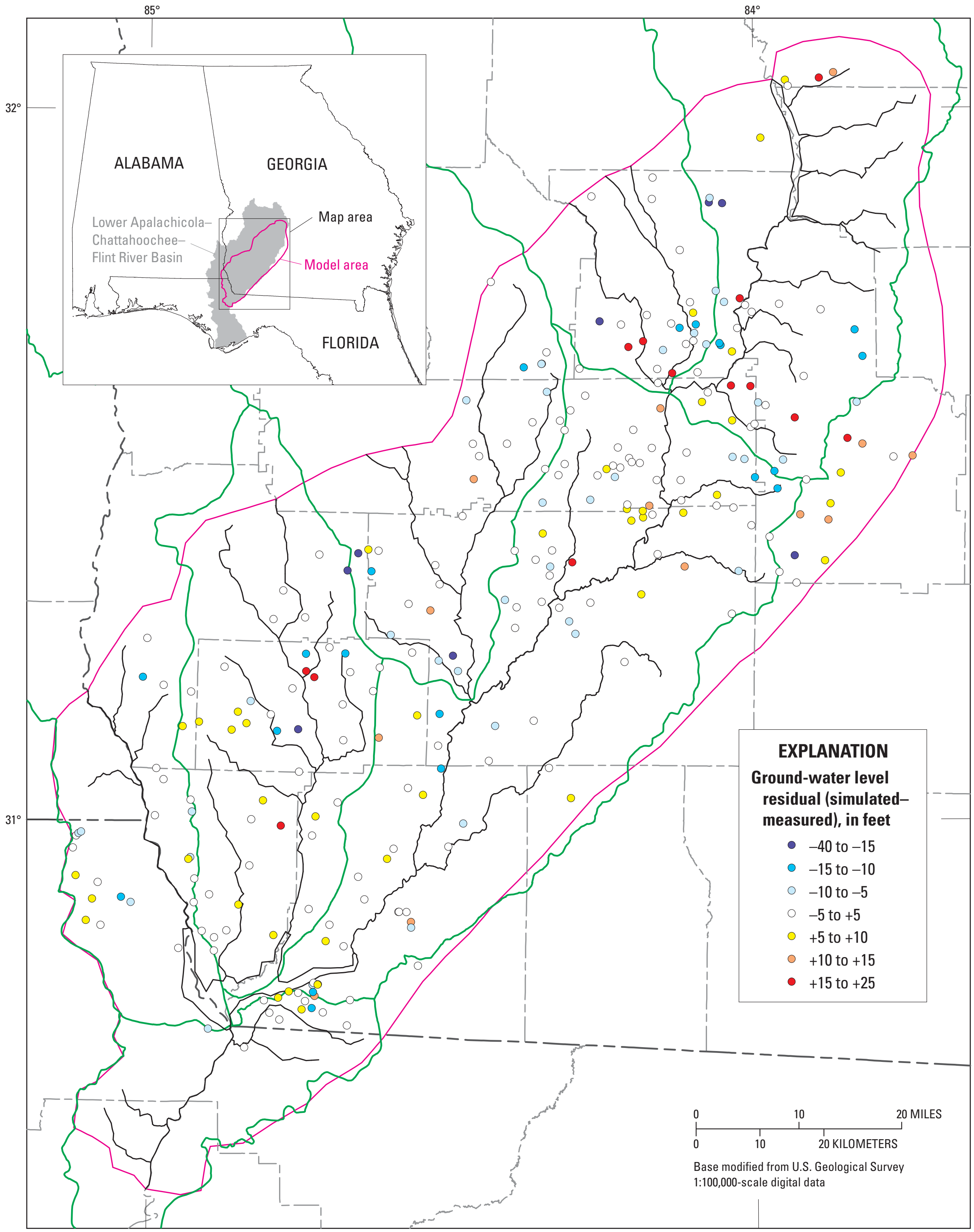

Figure 17. Ground-water level residuals (simulated minus measured) from the October 1999 calibrated model in southwest Georgia and adjacent parts of Alabama and Florida. (See figures A2–A7 for well identification and table A4 for water-level data.)

Table 6. Statistics for ground-water level residuals from the October 1999 calibrated model and subbasin 03130008.

[ft², foot squared; ft, foot; *RMS*, root-mean square of residuals; –, minus]

Statistic	Calibrated model	Subbasin 03130008
Number of terms	275	95
Sum of squared residuals (ft^2)	18,403	3,975
RMS (ft)	8.18	6.47
Standard deviation (ft)	8.19	6.43
Average residual (ft)	0.29	0.96
Percentage of residuals within standard deviations		
1 standard deviation	72.7	65.3
2 standard deviations	95.6	94.7
3 standard deviations	99.3	100
Water-level residuals by class		
Class interval (foot)	**Number of occurrences**	
	Calibrated model	**Subbasin 03130008**
–40 to –35	1	0
–35 to –30	0	0
–30 to –25	1	0
–25 to –20	2	0
–20 to –15	4	0
–15 to –10	20	5
–10 to –5	36	14
–5 to 0	58	18
0 to 5	85	34
5 to 10	42	17
10 to 15	13	6
15 to 20	10	1
20 to 25	3	0
25 to 30	0	0
30 to 35	0	0
35 to 40	0	0

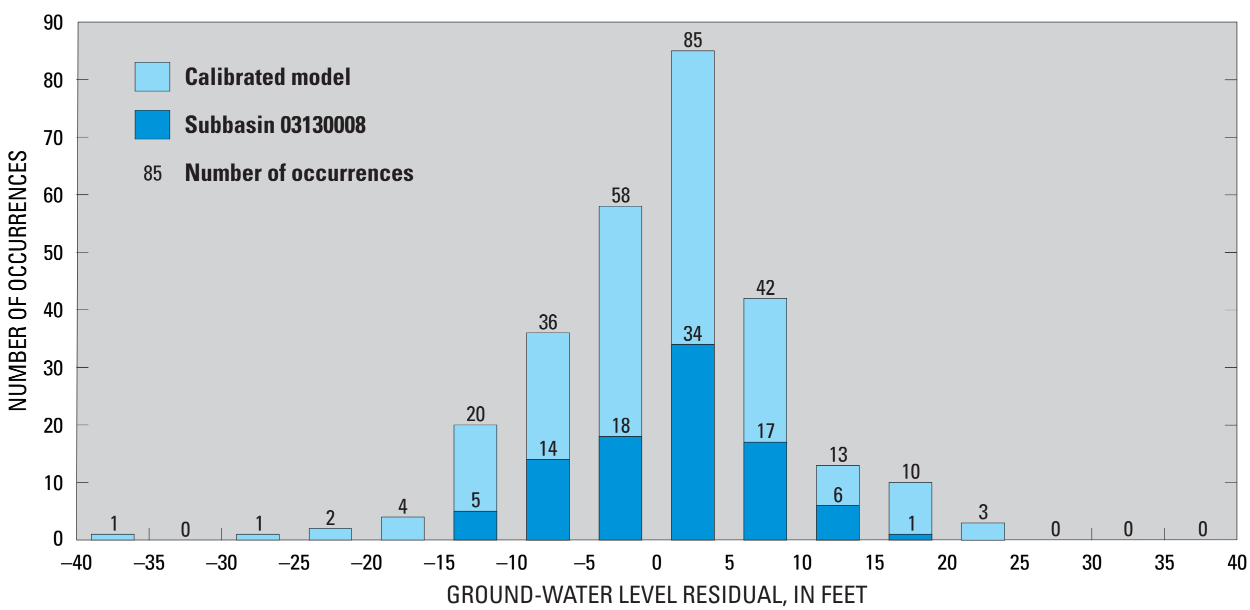

Figure 18. Frequency of ground-water-level residuals (simulated minus measured) from the October 1999 calibrated model and subbasin 03130008.

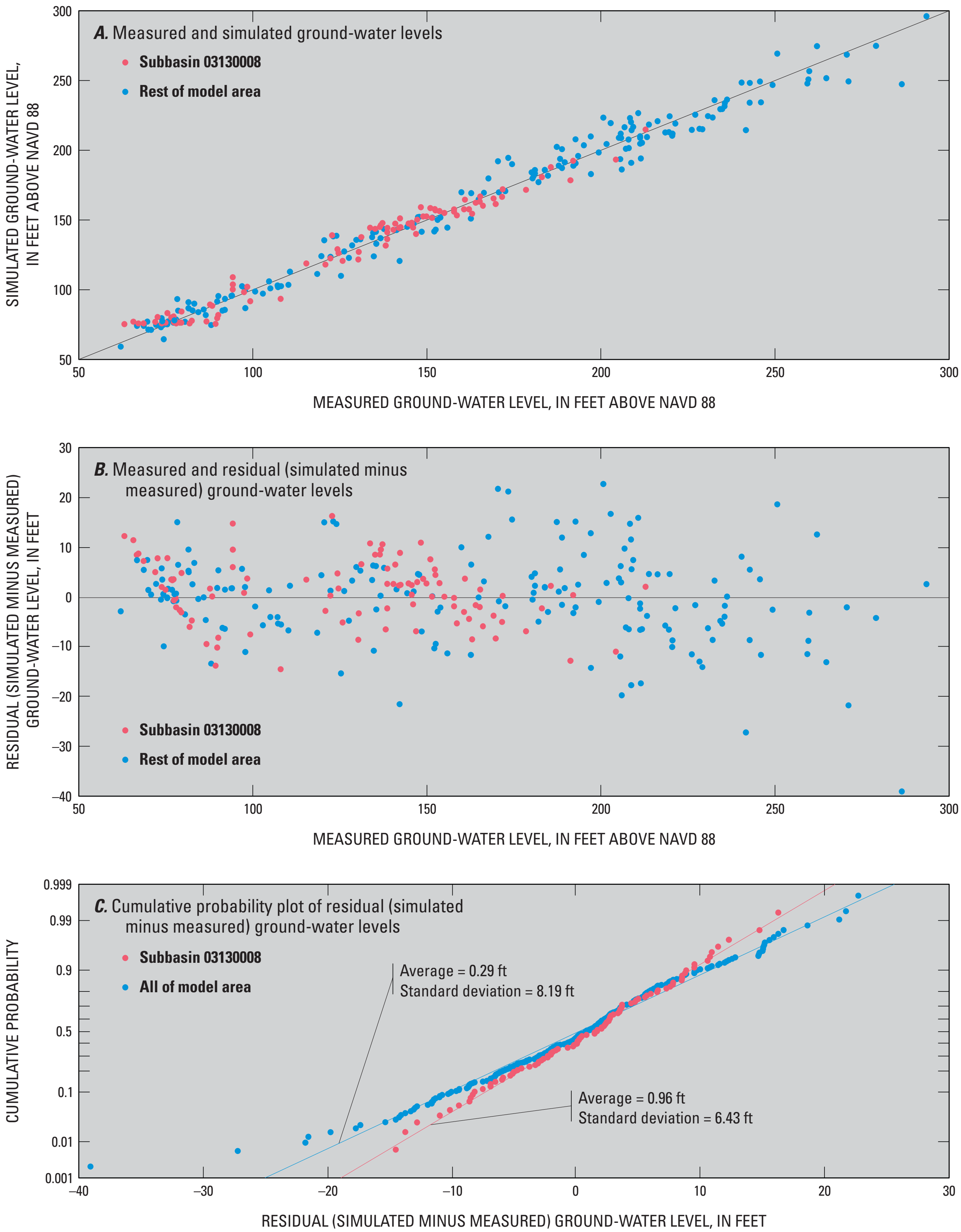

Figure 19. Comparison of 275 simulated and measured ground-water levels in the model area, including 95 in subbasin 03130008, for the October 1999 model calibration.

The *RMS* of ground-water-level residuals for the October 1999 calibrated model, 8.18 ft, is slightly greater than the *RMS* of water-level residuals, 6.95 ft, of the October 1986 calibrated Ocala model of Torak and others (1996), which the current model is intended to replace. The calibration procedure used for the current model, however, allowed the variation of fewer parameters that are known to vary widely in field studies, and those parameters were varied only on a global or subregional scale from the best estimates available from measured field data. The resulting calibrated model is more general and more reproducible than its predecessor.

Stream-Aquifer Flow

Following to the procedure described in Torak and others (1996), the flow rate across streambeds into and out of aquifers, termed *stream-aquifer flow*, was estimated for 53 reaches in the lower ACF River Basin (fig. 20 and table 7) by using streamflow data collected during October 1999 (in table A1 in Appendix A). A brief discussion of the terms in table 7 is included here. Positive values of stream-aquifer flow indicate that, within the reach, the stream is gaining water from the aquifer (ground water discharges to streams); negative values indicate that the stream is losing water to the aquifer (stream recharges the aquifer). Streamflow, Q, is the average of upstream, Q_u, and downstream, Q_d, flow measurements. For reaches having an average flow of less than 250 cubic feet per second (ft^3/s), the target range was computed by applying an error factor, EF, of 0.1 (10-percent error) to measurements at the upstream and downstream ends of the reach, Q_u and Q_d, respectively; for streams having an average flow greater than 250 ft^3/s, an EF of 0.05 (5-percent error) was applied (Torak and others, 1996). A lower limit of the target range, $Flow_{min}$, was computed by adjusting upstream and downstream flow measurements with the error factor to give the smallest streamflow gain (stream-aquifer flow) along the reach when upstream flow is subtracted from downstream flow. This is demonstrated in the expression for $Flow_{min}$:

$$Flow_{\min} = (Q_d - EF \times Q_d) - (Q_u + EF \times Q_u) \qquad (12)$$

Similarly, an upper limit of the target range, $Flow_{max}$, is calculated by using EF to adjust upstream and downstream flow measurements to give the largest stream-aquifer flow along the reach. The calculation of $Flow_{max}$ is given as

$$Flow_{\max} = (Q_d + EF \times Q_d) - (Q_u - EF \times Q_u) \qquad (13)$$

Simulated flows, qs, were compared with corresponding target ranges and measured flows, qm, to evaluate model acceptance. Measured flow, qm, is the average of $Flow_{max}$ and $Flow_{min}$.

Two error terms associated with stream-aquifer flow were computed to evaluate the accuracy of simulated stream-aquifer flows and to evaluate the relative significance of discrepancies from measured values. One error term, EQ, normalizes the difference between simulated and measured stream-aquifer flows as a percentage of streamflow, Q, for the reach:

$$EQ = \frac{(qs_i - qm_i)}{Q} \times 100, \qquad (14)$$

where qs_i and qm_i are the simulated and measured flows, respectively, for reach i, in figure 20 and table 7. Therefore, EQ represents the magnitude of error in simulated stream-aquifer flow relative to average streamflow, Q, in the reach. Another error term, $EqeTOT$, normalizes the difference in simulated and measured stream-aquifer flow as a percentage of the total simulated stream-aquifer flow, **Total** $qs = \sum_{i=1}^{53} qs_i$, for all reaches in the model area:

$$EqeTOT = \frac{|(qs_i - qm_i)|}{\sum_{i=1}^{53} qs} \times 100, \qquad (15)$$

where all terms have been defined previously. Values of $EqeTOT$ are listed by reach in table 7. The term $EqeTOT$ attempts to assess the significance of discrepancies between simulated and measured stream-aquifer flow relative to the total stream-aquifer flow in the flow system of the model area.

Stream reaches in table 7 were grouped into five classes according to magnitude of streamflow to facilitate interpretation of model results and to determine if acceptability criteria for stream-aquifer flow are satisfied on the basis of streamflow magnitude. The streamflow classes, corresponding reach numbers, and flow ranges are as follows:

A. 15 reaches; reach numbers 1–15: 0 (“dry streams”)
B. 19 reaches; reach numbers 16–34: 0 to 25 ft^3/s (“small streams”)
C. 10 reaches; reach numbers 35–44: 25 ft^3/s to 250 ft^3/s (“major tributaries”)
D. 6 reaches; reach numbers 45–50: 250 ft^3/s to 2,500 ft^3/s (Ichawaynochaway Creek and Flint River)
E. 2 reaches; reach numbers 51, 52: 2,500 ft^3/s and greater (lowest reach of Flint and Apalachicola Rivers)

For the October 1999 calibrated model, the number and percentage of reaches in each class having simulated flow within their target ranges (table 7) are: (*A*) 11 of 15 reaches, or 73 percent; (*B*) 14 of 19 reaches, or 74 percent; (*C*) 10 of 11 reaches, or 91 percent; (*D*) 6 of 6 reaches, or 100 percent; and (*E*) 2 of 2 reaches, or 100 percent. For the entire model, 42 of 52 reaches (81 percent) had simulated stream-aquifer flows within their target ranges.

Most of the streams in Class A “dry streams” were not included in the Ocala model of Torak and others (1996). These streams are small and intermittent, and have no real function in a model based on drought conditions when they typically have no flow. The current model, however, is being developed as a transient model that should be able to provide reasonable results during all types of hydrologic conditions. None of these streams had measurable flow during the calibration period of October 1999, but it is assumed there could be flow in these streams during transient simulations when hydrologic conditions are wetter.

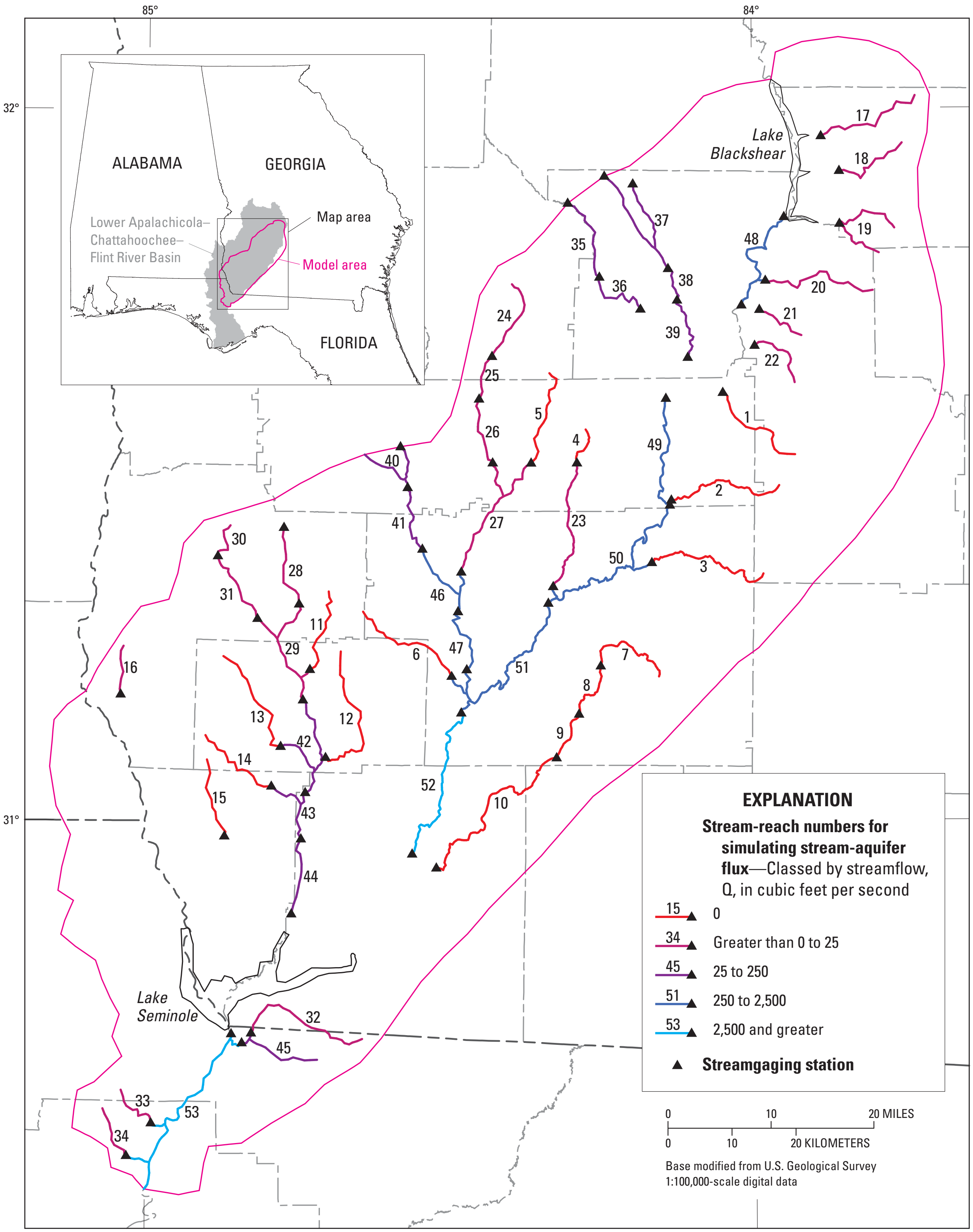

Figure 20. Stream reaches having measured and simulated stream-aquifer flux along sides of finite elements in the October 1999 calibrated model in southwest Georgia and adjacent parts of Alabama and Florida. (Stream-aquifer flow listed by reach in table 7. See figure A1 for streamgaging station identification and table A2 for measured streamflow data.)

Table 7. Stream-aquifer flow for selected stream reaches from the October 1999 calibrated model.

[n/a, not applicable; –, minus; streamflow, measured flow, target range, and simulated flow, in cubic feet per second (ft^3/s); measured streamflow data in table A1 in Appendix A; totals may be inexact due to rounding]

Reach number (figure 20)	Stream reach	[1]Streamflow, *Q*	[2]Measured flow, *qm*	Target range		[5]Simulated flow, *qs*	Error, in percent	
				[3]$Flow_{min}$	[4]$Flow_{max}$		[6]*EQ*	[7]*EqeTOT*
Class A reaches—dry streams								
1	Piney Woods Creek[8]	0.0	0.0	0.0	0.0	0.0	n/a	0.0
2	Dry Creek (A)[8]	0.0	0.0	0.0	0.0	0.0	n/a	0.0
3	Raccoon Creek[8]	0.0	0.0	0.0	0.0	0.0	n/a	0.0
4	Cooleewahee Creek[8]	0.0	0.0	0.0	0.0	0.0	n/a	0.0
5	Kiokee Creek[8]	0.0	0.0	0.0	0.0	0.2	n/a	0.0
6	Big Cypress Creek[8]	0.0	0.0	0.0	0.0	0.0	n/a	0.0
7	Big Slough[8]	0.0	0.0	0.0	0.0	0.0	n/a	0.0
8	Big Slough[8]	0.0	0.0	0.0	0.0	0.0	n/a	0.0
9	Big Slough[8]	0.0	0.0	0.0	0.0	0.0	n/a	0.0
10	Big Slough[8]	0.0	0.0	0.0	0.0	0.0	n/a	0.0
11	Long Creek[8]	0.0	0.0	0.0	0.0	0.1	n/a	0.0
12	Big Drain[8]	0.0	0.0	0.0	0.0	0.3	n/a	0.0
13	Aycocks Creek[8]	0.0	0.0	0.0	0.0	1.9	n/a	0.1
14	Dry Creek (C)[8]	0.0	0.0	0.0	0.0	0.0	n/a	0.0
15	Fishpond Drain[8]	0.0	0.0	0.0	0.0	0.0	n/a	0.0
Class B reaches—small streams								
16	Sawhatchee Creek[8]	5.3	10.6	9.5	11.7	10.5	–2.3	0.0
17	Gum Creek[8]	5.1	10.1	9.1	11.1	10.3	4.8	0.0
18	Cedar Creek[8]	0.7	1.4	1.3	1.6	1.3	–15.4	0.0
19	Swift Creek[8]	5.5	10.9	9.8	12.0	8.4	–45.9	0.1
20	Jones Creek[8]	2.3	4.7	4.2	5.2	4.3	–18.3	0.0
21	Abrams Creek[8]	4.8	9.6	8.7	10.6	10.1	10.6	0.0
22	Mill Creek[8]	5.4	10.8	9.7	11.9	10.7	–1.9	0.0
23	Cooleewahee Creek[8]	1.0	1.9	1.7	2.1	1.8	–9.3	0.0
24	Chickasawhatchee Creek	6.5	13.0	11.7	14.3	12.3	–10.3	0.0
25	Chickasawhatchee Creek	15.1	4.2	1.2	7.2	5.0	5.0	0.0
26	Chickasawhatchee Creek	10.1	–14.2	–16.2	–12.2	0.8	148.8	0.6
27	Chickasawhatchee Creek	5.7	5.5	4.4	6.7	6.1	9.6	0.0
28	Spring Creek	2.0	3.3	2.9	3.7	3.0	–15.8	0.0
29	Spring Creek	18.4	14.3	10.7	18.0	13.4	–5.3	0.0
30	Dry Creek (B)[8]	0.6	1.2	1.1	1.3	1.3	18.8	0.0
31	Dry Creek (B)	4.4	6.5	5.6	7.4	6.9	9.8	0.0
32	North Mosquito Creek[8]	22.2	44.4	40.0	48.8	0.0	–200.0	1.8
33	Ocheesee Creek[8]	3.9	7.7	7.0	8.5	0.5	–188.1	0.3
34	Graves Creek[8]	7.5	14.9	13.4	16.4	0.1	–198.5	0.6

Table 7. Stream-aquifer flow for selected stream reaches from the October 1999 calibrated model.—Continued

[n/a, not applicable; –, minus; streamflow, measured flow, target range, and simulated flow, in cubic feet per second (ft^3/s); measured streamflow data in table A1 in Appendix A; totals may be inexact due to rounding]

Reach number (figure 20)	Stream reach	[1]Streamflow, Q	[2]Measured flow, qm	Target range		[5]Simulated flow, qs	Error, in percent	
				[3]$Flow_{min}$	[4]$Flow_{max}$		[6]EQ	[7]$EqeTOT$
			Class C reaches—major tributaries					
35	Kinchafoonee Creek	143.0	–10.0	–38.6	18.6	5.5	10.8	0.6
36	Kinchafoonee Creek	174.0	72.0	37.2	106.8	71.3	–0.4	0.0
37	Muckalee Creek	129.8	42.5	16.6	68.5	42.9	0.3	0.0
38	Muckalee Creek	150.0	–2.0	–32.0	28.0	9.1	7.4	0.4
39	Muckalee Creek	137.5	–23.0	–50.5	4.5	16.4	28.6	1.6
40	Ichawaynochaway Creek	204.5	13.0	–27.9	53.9	19.1	3.0	0.2
41	Ichawaynochaway Creek	225.0	28.0	–17.0	73.0	26.9	–0.5	0.0
42	Spring Creek	29.9	8.6	2.6	14.6	12.2	12.1	0.1
43	Spring Creek	61.3	54.2	41.9	66.5	54.7	0.8	0.0
44	Spring Creek	123.2	69.6	45.0	94.2	50.8	–15.3	0.8
45	Mosquito Creek	45.3	1.8	–7.3	10.9	0.7	–2.4	0.0
			Class D reaches—Ichawaynochaway Creek and upper reaches of Flint River					
46	Ichawaynochaway Creek	269.8	44.5	17.5	71.5	26.2	–6.8	0.7
47	Ichawaynochaway Creek	299.5	15.0	–15.0	45.0	13.1	–0.6	0.1
48	Flint River	867.8	24.3	–62.5	111.1	26.1	0.2	0.1
49	Flint River	1,215.0	310.0	188.5	431.5	324.2	1.2	0.6
50	Flint River	1,486.0	228.1	79.5	376.7	232.7	0.3	0.2
51	Flint River	2,088.5	363.0	154.2	571.9	355.5	–0.4	0.3
			Class E reaches—lowest reach of Flint River and Apalachicola River					
52	Flint River	2,510.0	480	229.0	731.0	444.1	–1.4	1.4
53	Apalachicola River	6,077.5	645.0	37.2	1,252.7	644.2	0.0	0.0
	TOTAL		**2,455.9**			**2,484.8**		**11.1**

1. Streamflow, $Q = \frac{Q_u + Q_d}{2}$, ft^3/s, where Q_u and Q_d are measured streamflows at the upstream and downstream ends of each reach, respectively.

2. Measured flow, $qm = \frac{Flow_{min} + Flow_{max}}{2}$, ft^3/s.

3. $Flow_{min} = (Q_d - EF \times Q_d) - (Q_u + EF \times Q_u)$, ft^3/s.

4. $Flow_{max} = (Q_d + EF \times Q_d) - (Q_u - EF \times Q_u)$, ft^3/s.

5. Simulated flow, $qs = \alpha(h_B - h)$, ft^3/s; $qs = \alpha(h_B - h)$, where estimates are used to define average hydraulic conductivity, K_r, width, W_r, and thickness, b_r, of streambed sediments; stream stage, h_B, and aquifer head, h, obtained from calibrated model; and length of reach, L, from finite-element mesh.

6. $EQ = \frac{qs - qm}{Q} \times 100$, percent.

7. $EqeTOT = \frac{qs - qm}{\sum_{1}^{53} qs} \times 100$, percent.

8. Reach originates within study area or discharge at one end of reach equals zero.

Using the best estimates available to represent hydrologic conditions during the drought period of October 1999, the model had small positive simulated flows along 4 of the 15 reaches in this class of streams that were assumed to be dry during October 1999. Despite the apparent inaccuracy, the regional impact of the small simulated ground-water discharge to these streams is negligible. If data were available to calibrate the model in wetter hydrologic conditions, simulation of these small streams could improve the understanding of the flow system.

Among the Class B "small streams," reach 26 appears to be a losing reach based on measured streamflow (17.20 ft^3/s at upstream gage [02354350] and 2.97 ft^3/s at downstream gage [02354410]), but was simulated as a gaining reach. Reach 26 is within the Chickasawhatchee Swamp, where streamflow of the Chickasawhatchee Creek is braided in numerous ephemeral channels, and flow at these two individual streamgages may not always indicate the entire flow of the creek. Also, during low-flow conditions, streamflow measurements may not be accurate; 2.97 ft^3/s is less than the instantaneous low-flow rate for the entire 2003 water year (October 2002 through September 2003) at station 02354410.

Simulated flow was well below measured flow along three reaches (32–34) on tributary streams to the Apalachicola River (North Mosquito, Ocheesee, and Graves Creeks). The upper semiconfining unit is relatively thick along these reaches (fig. 12), and they may gain water from water-bearing units above the Upper Floridan aquifer that were not included in the model.

Within subbasin 03130007 (Kinchafoonee-Muckalee Creeks), streamflow measurements indicate three losing reaches of Class C "major tributary" streams (table 7), one on Kinchafoonee Creek (reach 35) and two on Muckalee Creek (reaches 38 and 39); each of the three reaches was simulated as gaining. Simulated flows for reaches 35 and 38 were within the target ranges, but the simulated flow for reach 39 was outside the target range. Stage elevations are higher and gradients steeper in this subbasin than in any other subbasin containing streams this large. Because of the greater relief, it is possible that estimates of stage along these streams are less accurate, which could cause a reversal of simulated stream-aquifer flow. Simulated flows for the larger streams in Classes D and E are reasonably similar to measured flow.

Sensitivity Analysis

To evaluate the relative sensitivity of model parameters on simulation results, *RMS* of residuals and ground-water budget components were examined for simulations performed using ranges of values of 12 different model parameters. Sensitivity parameters were grouped into three categories: (1) flow rates at specified-flux boundaries (infiltration rate, irrigation pumpage, and municipal and industrial pumpage); (2) conductivity parameters (vertical hydraulic conductivity, K_v, of the upper semiconfining unit; hydraulic conductivity, K, of the Upper Floridan aquifer; streambed conductance, α; regional-boundary conductance, α; and vertical hydraulic conductivity, K_v, of beds of Lakes Seminole and Blackshear); and (3) head parameters (head in the upper semiconfining unit, head [stage] in streams, head at regional boundaries, and specified head at the Upper Floridan aquifer updip boundary). Flow and conductance parameters (categories 1 and 2) were varied using a multiplier, F, from 0.2 to 5.0 times the calibrated value; head parameters (category 3) were varied using a head change, dh, from 20 ft less than to 20 ft more than the calibrated value ($dh = -20$ and $dh = +20$, respectively). Sensitivity plots showing the simulated variation of *RMS* of residuals and budget-component flows for each of the varied parameters are in figures A8–A19 in Appendix A.

Changes in simulated budget components in response to changes in the values of 12 selected parameters are summarized in table 8. For each selected parameter, the sensitivity of each budget component is indicated by the simulated change in the budget component resulting from two simulations in which the selected parameter was assigned a lower value and a higher value. For flux and conductivity parameters, values were halved and doubled; that is, the multiplier, F, applied to each value of the parameter in the data-input file was 0.5 or 2.0. For head parameters, the value of head change, dh, was –10 or +10 ft. Calibrated values of flow for discharge and recharge components are given in the first row of the table. In each subsequent row are the changes in flow for each budget component. For example, applying $F = 0.5$ to (halving) the infiltration rate resulted in a 137-Mgal/d reduction in discharge to streams, a 51-Mgal/d reduction in discharge to the upper semiconfining unit and Lakes Seminole and Blackshear, and reductions of 6 and 11 Mgal/d, respectively, to the regional boundary and the Upper Floridan updip boundary. The same halving of the infiltration rate increased recharge: from the upper semiconfining unit and lakes by 66 Mgal/d, from the regional boundary by 16 Mgal/d, from the Upper Floridan updip boundary by 26 Mgal/d, and from streams by 13 Mgal/d; recharge from infiltration was reduced by 326 Mgal/d, half of the calibrated rate of 652 Mgal/d.

Shading in table 8 indicates direct association of specific budget components to the varied parameter and the relative sensitivity of the other budget components to changes in the varied parameter. Tan shading indicates that the budget component is directly associated with the varied parameter; for example, in the columns for "Leakage," defined as flow to and from the upper semiconfining unit and Lakes Seminole and Blackshear, cells are shaded tan in rows corresponding to: vertical hydraulic conductivity of both the upper semiconfining unit and lake beds, and head in the upper semiconfining unit. (Head in the lakes was not tested in the sensitivity analysis because lake levels were known more accurately than ±10 ft.) Blue shading indicates the relative sensitivity of the budget components to the varied parameter, and is based on the percentage of change in each budget component to total change, which is the sum of increased discharge and decreased recharge. No shading indicates negligible sensitivity (flow change less than 10 percent of total change), light blue indicates minimal sensitivity (flow change from 10 to 20 percent of total change), medium blue indicates moderate sensitivity (flow

Table 8. Sensitivity of simulated ground-water budget components to variations in values of selected model parameters.

[*F*, multiplier for specified fluxes and conductivity parameters; *dh*, head change for head parameters; "Leakage," flow to and from the upper semiconfining unit and Lakes Seminole and Blackshear; "Wells" includes spring flow; "Updip," flow at the specified-head boundary to the northwest; "Infiltrat.," infiltration; 'Calibrated flow,' in million gallons per day; "Total change," sum of increased discharge and decreased recharge; Shading: tan, budget component directly associated with varied parameter; none, flow change less than 10 percent of total change; light blue, flow change from 10 to 20 percent of total change; medium blue, flow change from 20 to 50 percent of total change; dark blue, flow change 50 percent of total change and greater; –, minus; +, plus]

Varied parameter	*F* or *dh*	Discharge components					Recharge components					Total	Total change
		Streams	Leakage	Wells	Regional	Updip	Leakage	Infiltrat.	Regional	Updip	Streams		
Calibrated flow		–2046	–473	–157	–130	–44	1,435	652	607	142	16	2,851	
Specified flux (multiplier, F, from 0.5 to 2.0); change in flow, in million gallons per day													
Infiltration rate	0.5	–137	–51	0	–6	–11	66	–326	16	26	13	–205	**326**
	2.0	292	120	0	20	37	–111	652	–24	–39	–10	469	**652**
Irrigation pumpage	0.5	27	8	–64	3	0	–18	0	–6	–1	–1	–26	**64**
	2.0	–54	–15	127	–5	0	37	0	13	1	2	52	**127**
Municipal & industrial pumpage	0.5	10	0	–15	0	0	–2	0	–2	0	0	–4	**15**
	2.0	–20	–1	30	–1	0	4	0	4	0	0	8	**30**
Conductivity parameters (multiplier, F, from 0.5 to 2.0); change in flow, in million gallons per day													
Vertical hydraulic conductivity of upper semiconfining unit	0.5	–274	–193	0	–25	–8	–575	0	67	–4	12	–500	**579**
	2.0	386	367	0	50	15	918	0	–103	8	–5	817	**925**
Hydraulic conductivity of Upper Floridan aquifer	0.5	–545	–25	0	–23	–4	–218	0	–289	–80	–10	–597	**597**
	2.0	785	39	0	29	13	206	0	450	173	37	866	**866**
Streambed conductance	0.5	–270	52	0	10	3	–104	0	–82	–9	–10	–205	**270**
	2.0	241	–47	0	–7	–3	95	0	64	11	14	184	**241**
Regional-boundary conductance	0.5	–40	–4	0	–32	0	11	0	–87	0	0	–76	**87**
	2.0	29	2	0	28	0	–6	0	66	0	0	59	**66**
Vertical hydraulic conductivity of lakebeds	0.5	–4	–19	0	0	2	–23	0	3	–1	0	–21	**26**
	2.0	4	17	0	0	–2	20	0	–2	0	0	18	**23**
Head parameters (head change, dh, from –10 to +10 ft); change in flow, in million gallons per day													
Head in upper semiconfining unit	–10	–636	372	0	–33	–22	–620	0	177	48	76	–320	**992**
	+10	699	–189	0	76	34	787	0	–128	–31	–8	620	**976**
Head (stage) in streams	–10	814	–135	0	–26	–3	415	0	221	23	–10	649	**824**
	+10	–728	232	0	71	8	–350	0	–170	–20	123	–417	**851**
Head at regional boundary	–10	–241	–48	0	163	–1	127	0	–260	1	7	–126	**424**
	+10	250	71	0	–42	1	–107	0	388	–1	–1	280	**430**
Specified head at Upper Floridan updip boundary	–10	–23	–29	0	0	37	30	0	1	–54	8	–16	**91**
	+10	27	41	0	0	–18	–22	0	–1	78	–4	51	**96**

change from 20 to 50 percent of total change), and dark blue indicates maximal sensitivity (flow change 50 percent of total change and greater). Within each group representing the types of varied parameters, parameters are ordered by total change.

Using the shading in table 8, the relative sensitivity of simulated budget components to variations in the values of a specific model parameters is indicated in each row. For example, the effect of changes in infiltration rate on leakage (discharge) to the upper semiconfining unit and lakes is minimal (light blue shading); increased infiltration rate has a minimal effect on leakage (recharge) from above (light blue shading), but decreased infiltration has a moderate effect on leakage (recharge) from above (medium blue shading); and changes in infiltration have a moderate effect on discharge to streams (medium blue shading). Also, for a given budget component, the parameters affecting the component and the relative sensitivity of the effect can be identified in each column. In this study, for example, simulated discharge from the ground-water system to streams has a greater relative sensitivity to most parameter variations (except head at the specified head boundary) than other components, as indicated by the larger values of flow change in the first column relative to the other columns. Table 8 also indicates that the varied parameters having the maximal relative effect (dark blue shading) on, for example, stream discharge are municipal and industrial pumpage (these pumped locations are close to major streams), hydraulic conductivity of the Upper Floridan aquifer, head in the upper semiconfining unit, and head at the regional boundary. The varied parameters that have a moderate relative effect (medium blue shading) on stream discharge are infiltration rate, irrigation pumpage, vertical hydraulic conductivity of the upper semiconfining unit, regional conductance term, and specified head at the Upper Floridan updip boundary. Vertical hydraulic conductivity of lake beds has a minimal relative effect (light blue shading) on stream discharge. Two parameters, streambed conductance term, α, and head (stage) in streams, are directly related to discharge to streams, as indicated by tan shading.

Parameter Uncertainty

Uncertainty inherent to the model originates in all phases of model development, including conceptualization of the hydrologic flow system, estimation and discretization of hydrologic parameters, estimation and discretization of boundary conditions, and calibration based on measured conditions. Discussion of the several sources of uncertainty is important, not only with respect to understanding the limitations that uncertainty imposes on the model, but also with respect to determining if and how the various sources of uncertainty could be reduced and the reliability and accuracy of the model improved.

The simplest and probably the most pervasive source of uncertainty is in the estimation of land-surface altitude of wells, streamgages, and other features from topographic maps. The uncertainty typically associated with estimating land-surface altitude from a topographic map is plus or minus one-half the contour interval. Topographic maps in the model area have contour intervals of 5 or 10 ft; thus any estimate of land-surface altitude has an accuracy of ±2.5 ft at best and ±5 ft at worst. If land-surface altitude of a well is estimated from topographic maps, this uncertainty applies to all measured level data from the well, including water levels and depths to any geologic or hydrologic contact. Most of the 275 wells used for the October 1999 calibration of the model have land-surface altitudes that were estimated more precisely than from a topographic map (estimated by leveling or GPS), but most of the wells used to estimate the altitude of the top and bottom of the Upper Floridan have land-surface altitudes that were estimated from topographic maps.

Some streamgage datums in the model area also were estimated from topographic maps. The same uncertainty (±2.5 ft at best and ±5 ft at worst) applies to estimates of stage altitude at those streamgages. There are also some streamgages that have gage datums reported in Gotvald and others (2005) that produced unreasonable results if used to estimate stream stage for head-dependent flux boundaries representing streams. All streamgages reported to have gage datums estimated from topographic maps were checked for accuracy; more reasonable gage datums were estimated from topographic maps for four streamgaging stations used in this study (station number in italics in table A4 in Appendix A).

The Upper Floridan aquifer in the model area is productive and properly constructed wells deliver high yields. Thus, in an aquifer-performance tests used to determine aquifer transmissivity or hydraulic conductivity, it is difficult to pump enough water to create more than a localized effect. All of the values of hydraulic conductivity of the Upper Floridan aquifer, *K*, that were used to develop model input were derived from such localized tests, which are well known to underestimate regional *K* (Rovey and Cherkauer, 1995). Consequently, after an areal distribution of the widely dispersed measured values of *K* was estimated using kriging, the areally distributed values were systematically raised and adjusted (along with other calibration parameters) until a minimum root-mean-square error of the ground-water level residuals was achieved. It is unknown whether simply increasing *K* in this manner is an adequate solution to the local and regional scale problem; and thus, this procedure introduces model uncertainty that is difficult to assess.

Also, as discussed in the calibration section, one of the effects of using kriging to estimate and distribute values of hydraulic conductivity, *K*, is that in areas that are beyond the range of the variogram, an average value of *K* is assigned. For the areal distribution of *K* used initially in this study, the range of the variogram was about 4.5 mi (David C. Leeth, U.S. Geological Survey, written commun., 2004). Thus, in areas more than 4.5 mi from an aquifer-performance test location, kriging assigned an average value of *K* from all the available values, and these average values are subject to considerable uncertainty.

Most of the recharge to the Upper Floridan aquifer in the model area is from above, through direct infiltration of precipitation or through leakage from the overlying upper semiconfining unit. Few data are available to characterize these processes adequately, even though they may compose large parts of the ground-water budget. Thus, values used in the model of head in the upper semiconfining unit, vertical hydraulic conductance of the upper semiconfining unit, and rate of infiltration of rainfall are little better than educated guesses, and are subject to large uncertainty.

Irrigation pumpage for model input was estimated from measured daily pumpage at 192 irrigation systems in the model area, which is about 5 percent of the permitted irrigation systems (James E. Hook, National Environmentally Sound Production Agriculture Laboratory, written commun., 2003). Although efforts were made to ensure that the 192 systems were not a statistically biased sample, the variability of the daily pumpage rates among the systems was substantial. For simplicity, the daily irrigation pumpage data were used to determine a single average value of application depth for each month of the 12-month transient simulation. These monthly averages were applied evenly to all the permitted systems to develop model input, a procedure that does not account for the large variation in pumping rates between the systems and the short-term variation in pumping rates of each individual system.

Ground-Water Flow Direction

Directions of ground-water movement in the Upper Floridan aquifer are shown by elemental flow vectors for the October 1999 calibrated model (fig. 21). Because the higher density and smaller size of elements in subbasin 03130008 (lower Flint River) cause the ground-water flow vectors in figure 21 to become obscured, larger-scale flow-vector maps for the northern and southern parts of subbasin 03130008 are provided in figures 22 and 23, respectively. Flow vectors are oriented according to the direction of specific discharge at each element and are colored according to the values of specific discharge times the elemental thickness—blue for lower values (from 0 to 50 feet squared per day [ft^2/d]), purple for intermediate values (from 50 to 200 ft^2/d), and red for higher values (200 ft^2/d and greater). Following the fundamental characteristic of a ground-water flow net, the flow vectors typically are perpendicular to the contours of the potentiometric surface, because the ground-water flow system is simulated as isotropic. This representation conforms to the directions of ground-water movement that were described earlier during conceptualization of the flow system. In the Upper Floridan model, ground water flows into the northern and central parts of the lower ACF River Basin as regional flow across the eastern and western model boundaries and from the updip limit along the northern model boundary. Ground-water discharge from the Upper Floridan aquifer occurs as stream-aquifer flow along surface-water features, and as regional flow along parts of the eastern and southern model boundaries. The general patterns depicted in figures 21–23 do not change during transient simulation of an irrigation season, there are only relatively small changes in hydraulic head (usually less than 10 ft), and commensurately small changes in gradient.

The magnitude of the stream-aquifer flow to and, in rare cases, from simulated streams, is indicated in figure 24 by color of simulated flow rate; red colors indicate discharge from the Upper Floridan aquifer to streams (gaining streams), and blue colors indicate recharge to the Upper Floridan aquifer from streams (losing streams). Dark red indicates high discharge, primarily to the Apalachicola, Chattahoochee, and Flint Rivers. Ground-water flow into and out of the model area also is indicated in figure 24 at lateral head-dependent flux boundaries to the northeast, southeast, and southwest.

Simulated vertical leakage between the Upper Floridan aquifer and the overlying upper semiconfining unit and Lakes Seminole and Blackshear is shown in figure 25. Orange to red colors on the map indicate where the Upper Floridan discharges water to the upper semiconfining unit and blue colors indicate where the upper semiconfining unit recharges the Upper Floridan aquifer. White areas on the map indicate where the upper semiconfining unit is either missing or too thin to support a water table; in most of the white map areas, the aquifer is recharged by infiltration at a rate of 0.00298 ft/d (13.1 in/yr) for the October 1999 calibrated model.

Primary areas where the Upper Floridan aquifer discharges to the upper semiconfining unit are near the northwest boundary of the model, along Big Slough and the southernmost reach of the Flint River, and directly north of Lake Seminole. Near the northwest boundary, the upper semiconfining unit is thin and areas where there are upward gradients correspond to naturally low, swampy areas; for example, the Chickasawhatchee Swamp in western Dougherty and eastern Calhoun Counties and the area between Spring and Dry (B) Creeks in Early County. Ground-water levels in the Upper Floridan aquifer southeast of Big Slough and the southernmost reach of the Flint River are high because ground water flows from elevated parts of the aquifer across the Pelham Escarpment and underlying the Tifton Upland. As noted by Sever (1965a, p. Q4), "[many] small streams flow northwestward down the * * * [Pelham] Escarpment and into caves and sinkholes along the eastern edge of the Dougherty Plain." Big Slough is an intermittent stream that is affected by karst topography—there are numerous sinkholes along the stream trace, and the typical low flows are known to disappear into and reappear from the sinkholes. "* * * [It] is actually a linear array of disjointed karstic drainage developed parallel to the base of the Pelham Escarpment * * * [that drains] * * * in opposite directions in different areas" (Beck, 2002). Big Slough was essentially dry during the calibration period, as it often is. The hydrologic interaction between Big Slough and the shallow ground-water system is not well understood and cannot be adequately simulated using the current model. North of Lake Seminole, the surface topography is flat and ground-water levels in the Upper Floridan aquifer are maintained high because of the impoundment and southward regional ground-water flow (fig. 21), resulting in an upward gradient between the aquifer and the upper semiconfining unit, which fills numerous shallow depressions in the area.

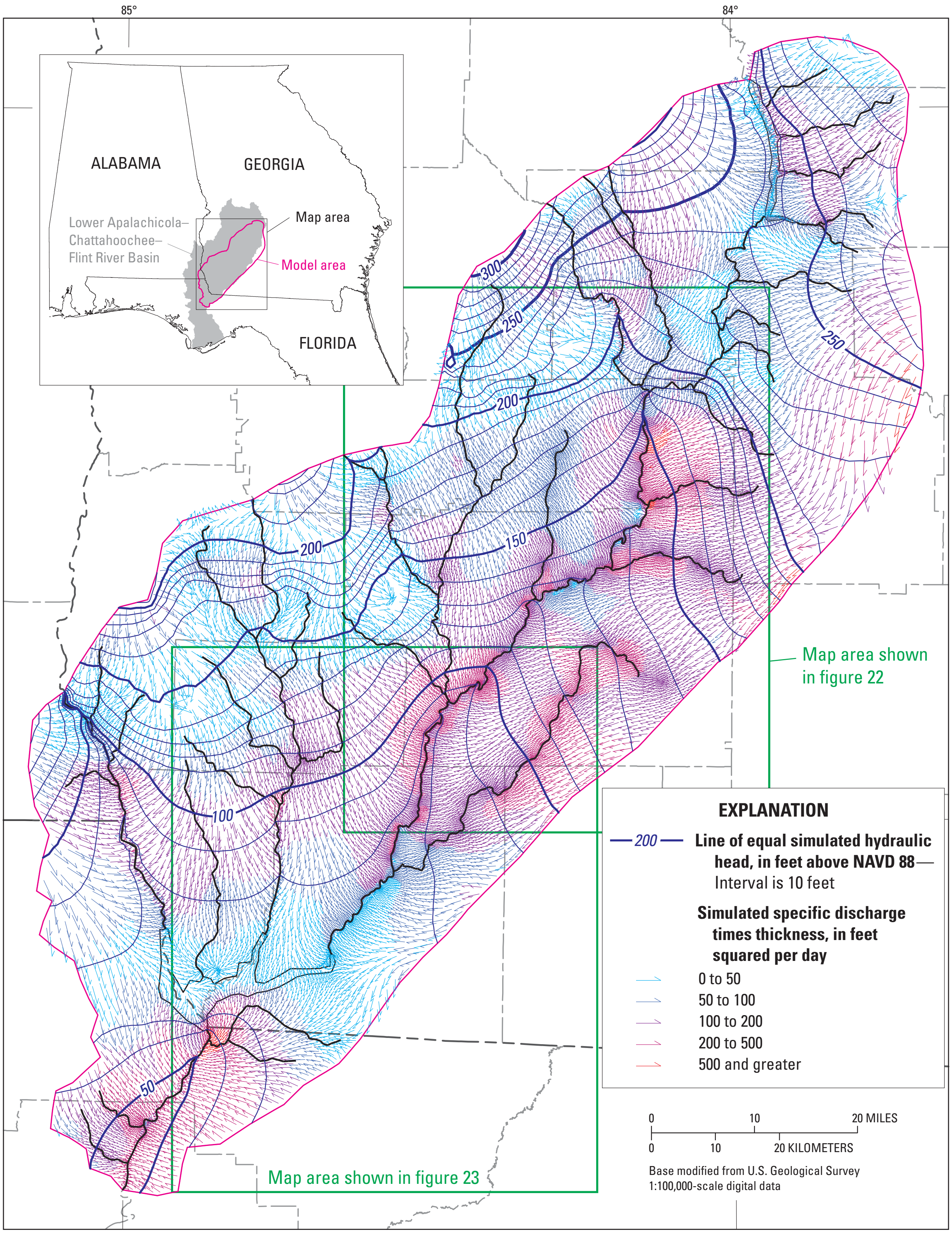

Figure 21. Simulated hydraulic head and ground-water flow direction in the Upper Floridan aquifer by element from the October 1999 calibrated model in southwest Georgia and adjacent parts of Alabama and Florida.

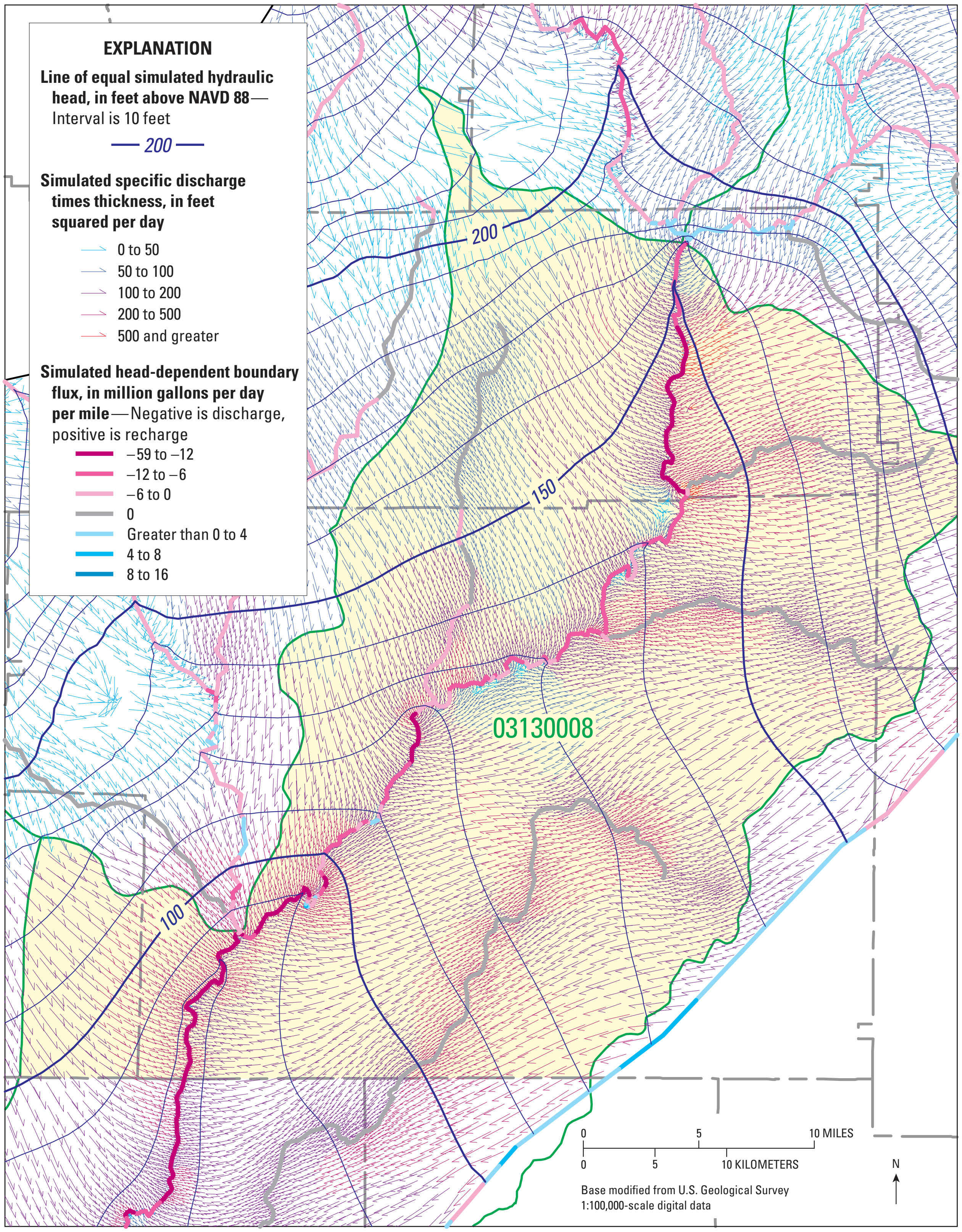

Figure 22. Simulated hydraulic head, ground-water flux by element, and head-dependent boundary flux by element side in the northern part of subbasin 03130008 from the October 1999 calibrated model. (See figure 21 for map area.)

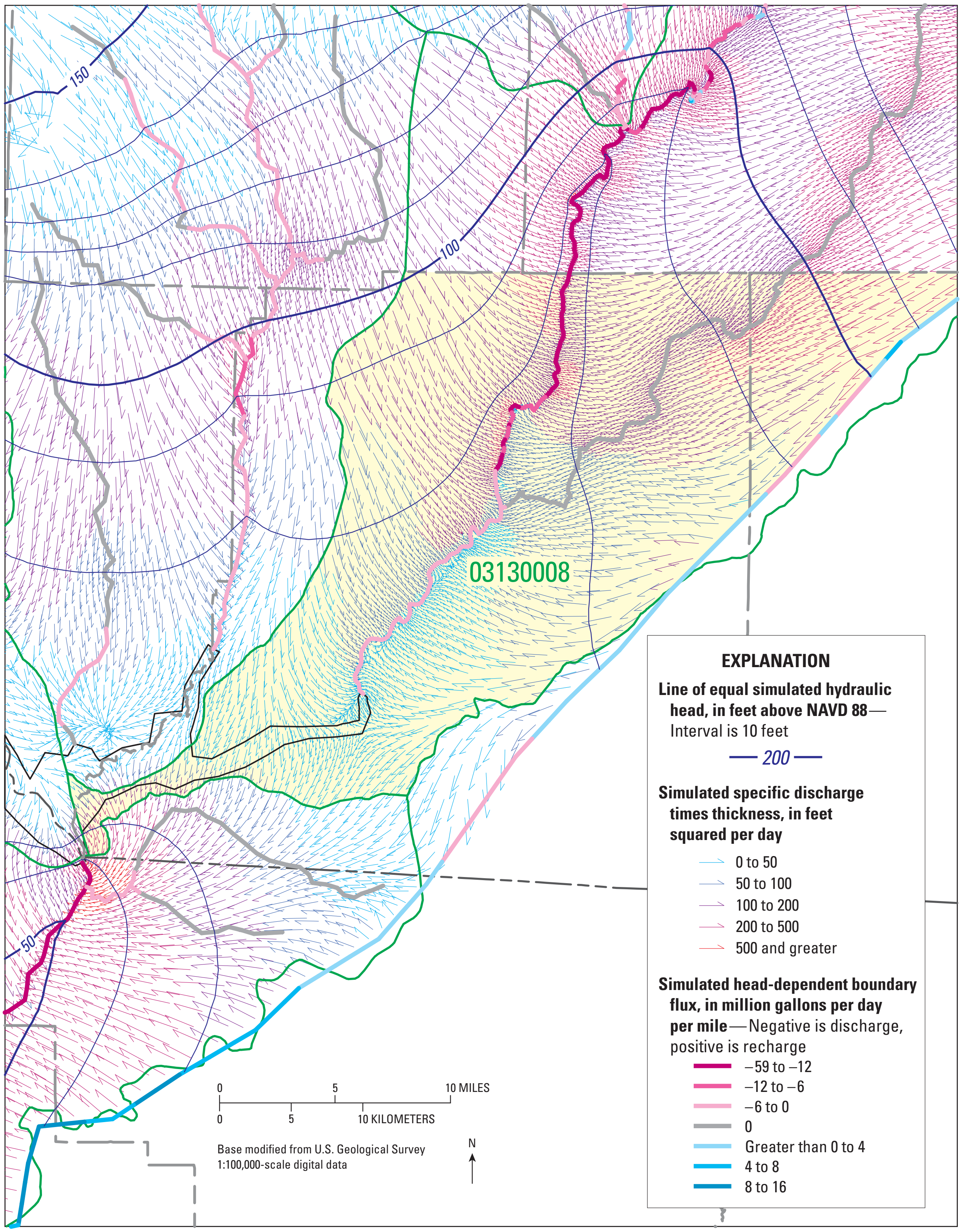

Figure 23. Simulated hydraulic head, ground-water flux by element, and head-dependent-boundary flux by element side in the southern part of subbasin 03130008 from the October 1999 calibrated model. (See figure 21 for map area.)

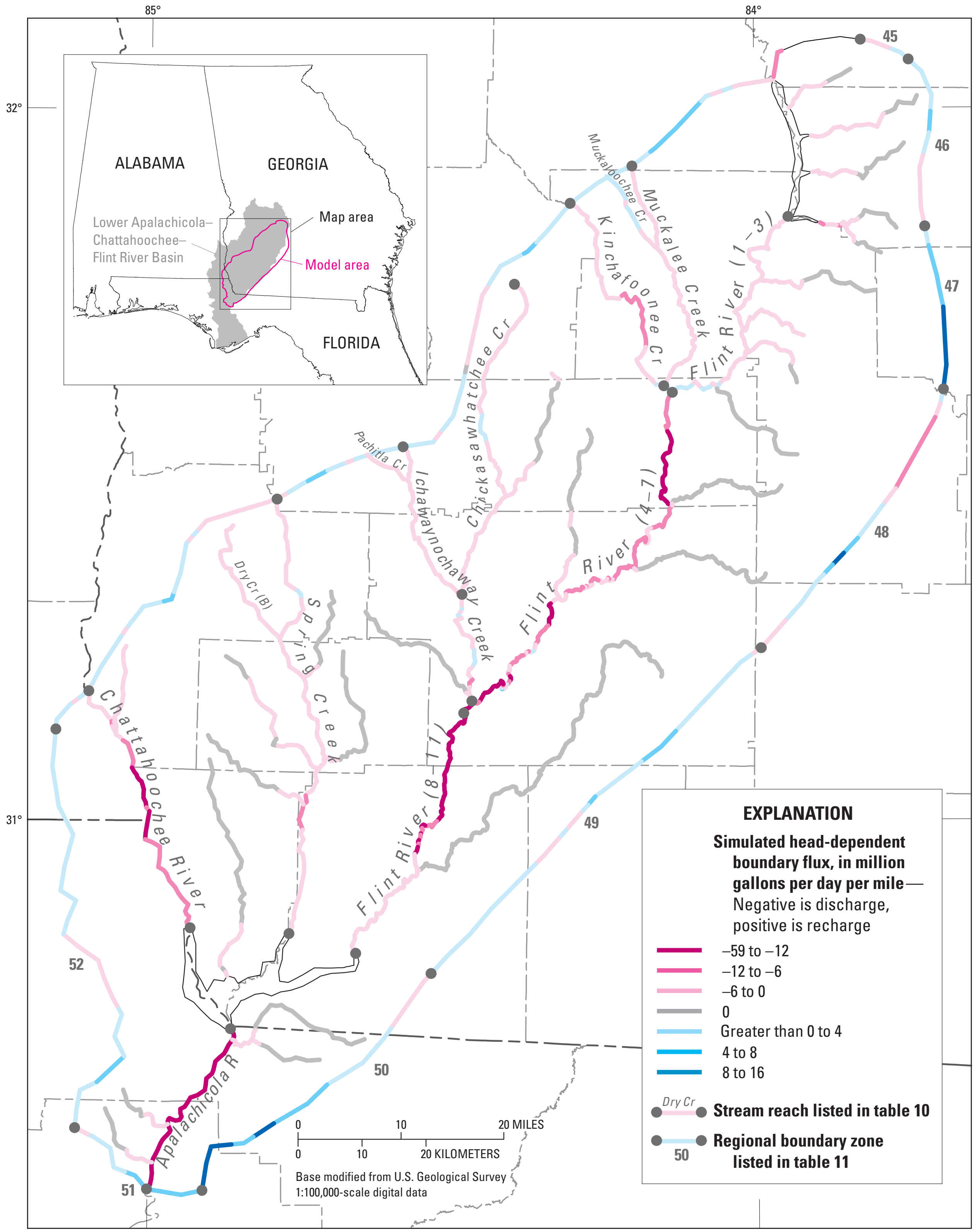

Figure 24. Simulated head-dependent boundary flux and specified-head boundary flux by element side from the October 1999 calibrated model in southwest Georgia and adjacent parts of Alabama and Florida. (Stream reach flows are given in table 10; regional boundary zone flows are given in table 11.)

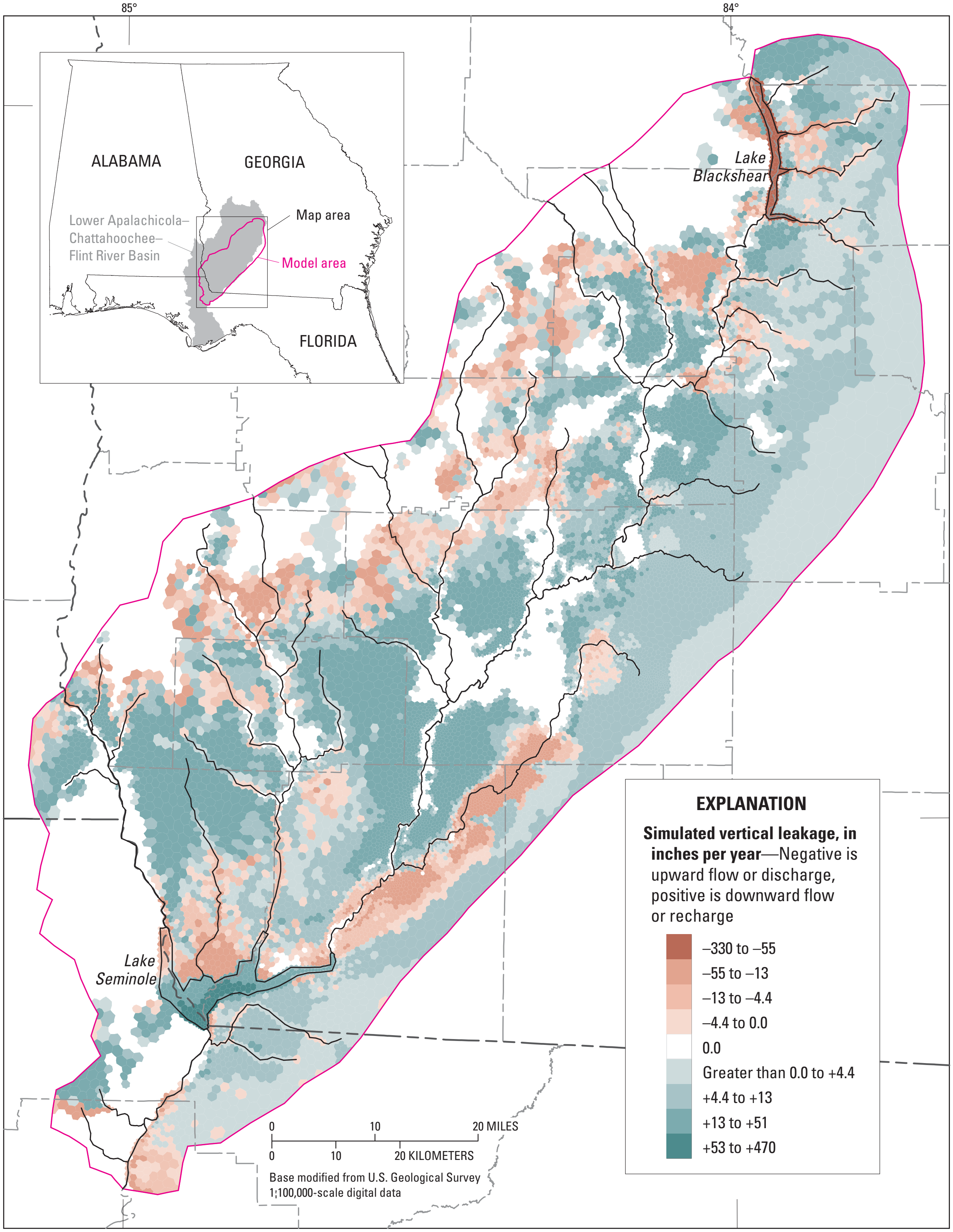

Figure 25. Vertical leakage between the Upper Floridan aquifer and the overlying upper semiconfining unit and Lakes Seminole and Blackshear by nodal area from the October 1999 calibrated model in southwest Georgia and adjacent parts of Alabama and Florida.

Although there are some isolated areas where the vertical-leakage rate between the upper semiconfining unit and the Upper Floridan aquifer is relatively high, the average rate of recharge from above, including leakage to and from the upper semiconfining unit and infiltration, which is discussed in a subsequent section on Water-Budget Components, is reasonable.

The highest rates of vertical leakage occur between the Upper Floridan aquifer and Lakes Seminole and Blackshear. Except in the northernmost impoundment arms of the Flint River and Spring Creek, Lake Seminole recharges the Upper Floridan aquifer at a total rate of 126 ft^3/s. Below Lake Seminole at streamgage 02358000 (Apalachicola River at Chattahoochee, Fla.), the measured flow was 6,400 ft^3/s on October 18, 1999. Conversely, Lake Blackshear, which has a pool elevation about 150 ft higher than Lake Seminole, but is in a region having more topographic relief, gains water from the Upper Floridan aquifer at a total rate of 105 ft^3/s. Below Lake Blackshear at streamgage 02350405 (Flint River near Warwick, Ga.), the measured flow was 851 ft^3/s on October 21, 1999.

Transient Simulation, March 2001–February 2002

Based on available daily pumpage data from the Ag Water Pumping study (James E. Hook, National Environmentally Sound Production Agriculture Laboratory, written commun., 2003), the period March 2001 through February 2002 was chosen as a typical dry-weather 12-month irrigation season and off-season suitable for a 1-year transient simulation. Maintaining all the aquifer characteristics of the October 1999 calibrated model, 12 monthly datasets were prepared based on the best available estimates of five time-varying parameters: (1) irrigation pumpage; (2) infiltration in areas where the upper semiconfining unit is absent or thin; (3) head in the upper semiconfining unit and lake levels; (4) stream stage in major streams simulated as linear head-dependent flux boundaries; and (5) stream stage in minor streams simulated as nonlinear head-dependent flux boundaries. Considering that the first simulated month, March 2001, is at the beginning of the annual irrigation season, a start-up period of six monthly stress periods, during which no irrigational pumpage was applied, was used to establish initial conditions. During the start-up stress periods, the other time varying parameters, (2) through (5) above, were kept the same as the October 1999 calibrated model. Twelve additional stress periods were then used to represent the 12-month simulation period March 2001–February 2002. Experimentation indicated that 15 time steps, increasing incrementally in duration by a factor of $\sqrt{2}$ per monthly stress period were sufficient to ensure a stable solution for each stress period. Additional time steps produced essentially the same stress-period result.

Continuous ground-water level recorders were operated in 20 selected wells in the model area during March 2001–February 2002. Average monthly measured water levels were calculated from the mean daily water levels recorded at each of these wells. Simulated monthly water levels at each well location at the end of each stress period were calculated using the same interpolation procedure as at the 275 well locations used for the October 1999 model calibration. The average differences between the average monthly measured and simulated monthly water levels or average monthly ground-water-level residuals were plotted during the 12-month simulation period (fig. 26). The color of the data points shown on the map in figure 26 are based on the value of the average monthly ground-water level residual at each well.

Although 20 well locations is probably an insufficient number for statistical reliability, calibration statistics were calculated based on the ground-water level residuals for each monthly stress period. The values of *RMS* of ground-water level residuals, ranging from 8.35 ft during December 2001 to 13.61 ft during April 2001 (fig. 27), were higher than the *RMS* of residuals for the October 1999 calibrated model (8.18 ft). During the last 6 months of the simulation period (September 2001–February 2002), however, the values of *RMS* of residuals were below the water-level error criteria of 9.4 ft. One possible explanation for the transient model performing more poorly during March–August 2001 than during September 2001–February 2002 is that average irrigation pumpage was much greater—monthly average of 1.22 inches (about 450 Mgal/d) during March–August 2001 compared with a monthly average of 0.24 inch (about 90 Mgal/d) during September 2001–February 2002. Irrigation pumpage during September 2001–February 2002 was much nearer 0.35 inch (about 130 Mgal/d) for the October 1999 calibrated model. Another possible explanation for the larger *RMS* of ground-water level residuals for the period March–August 2001 is that daily measured ground-water levels, from which the average monthly levels were derived, were far more variable during March–August 2001 than during September 2001–February 2002, because of variable irrigation pumping stress. For the 20 wells, the monthly average standard deviation of ground-water levels for March–August 2001 was about 1.6 ft, compared with about 0.4 ft for September 2001–February 2002. The calibrated model, which uses monthly stress periods, is less capable of simulating actual ground-water levels during periods of widely varying stress, such as March–April 2001, than during periods of relatively constant stress such as September 2001–February 2002.

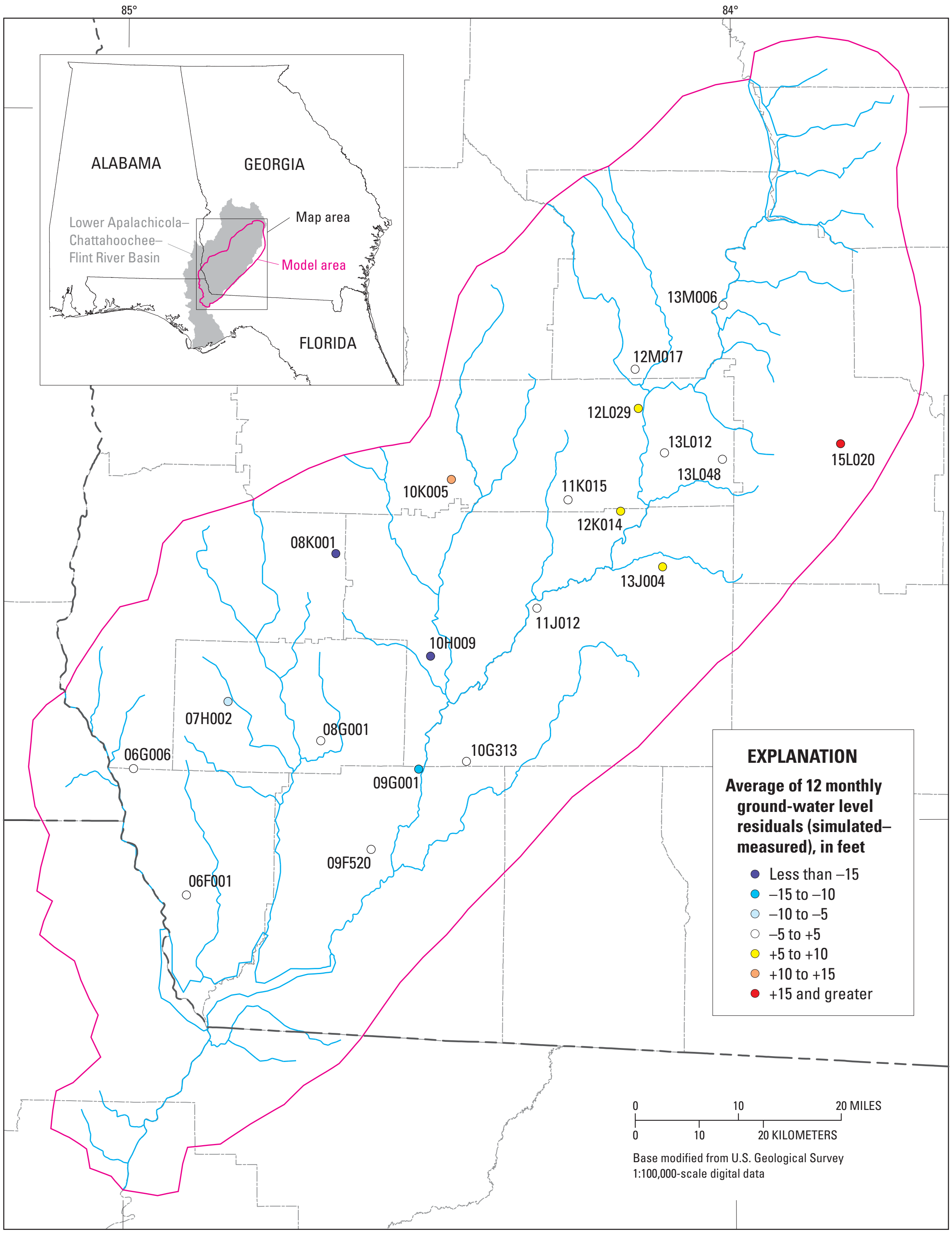

Figure 26. Average of 12 monthly ground-water level residuals (simulated minus measured) from the March 2001–February 2002 transient simulation in southwest Georgia and adjacent parts of Alabama and Florida.

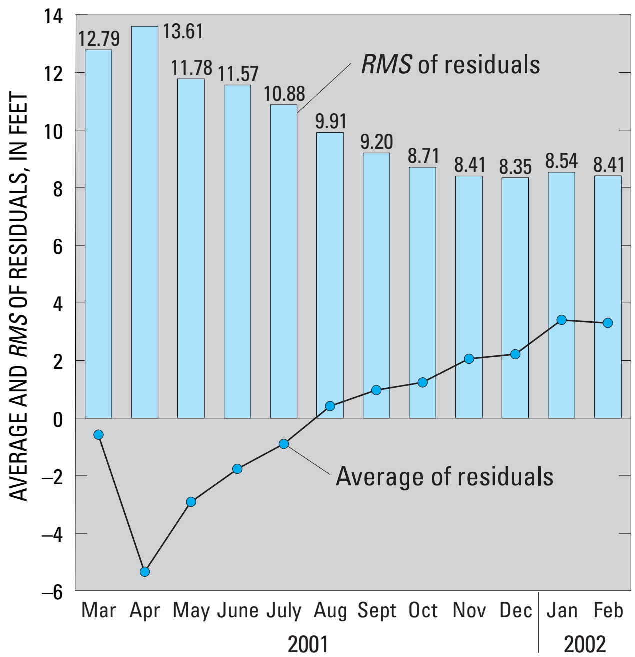

Figure 27. Root-mean square (*RMS*) and average of 20 ground-water-level residuals (simulated minus measured) from the March 2001–February 2002 transient simulation.

Water-Budget Components

A simulated ground-water budget was prepared from the October 1999 calibrated model (table 9). The total simulated volumetric flow rate through the Upper Floridan aquifer for October 1999 was about 2,850 Mgal/d. Because the October 1999 calibrated model is steady-state, recharge is equal to discharge, and there is no gain or loss of water stored in the Upper Floridan aquifer. Recharge to the aquifer was composed of leakage from the upper semiconfining unit (about 1,350 Mgal/d, or 48 percent of the total); infiltration of precipitation in areas where the upper semiconfining unit is absent or thin (about 650 Mgal/d, or 23 percent of the total); inflow from the regional flow system along the northeast, southeast, and southwest boundaries of the model (about 610 Mgal/d, or 21 percent of the total); inflow from the updip limit of the Upper Floridan aquifer along the northwest boundary of the model (about 140 Mgal/d, or 5 percent of the total); leakage from Lake Seminole (about 81 Mgal/d, or 3 percent of the total); and inflow from losing streams (about 16 Mgal/d, or 1 percent of the total). Discharge from the aquifer was primarily to streams and in-channel springs (about 2,050 Mgal/d, or 72 percent of the total)—other discharge components from the Upper Floridan aquifer were: leakage to the upper semiconfining unit (about 400 Mgal/d, or 14 percent of the total); outflow

Table 9. Ground-water budget components for the October 1999 calibrated model and the subbasin 03130008.

[Volumetric flow rate, in million gallons per day; —, component not simulated; totals may be inexact due to rounding]

Budget component	Calibrated model		Subbasin 03130008	
	Volumetric flow rate	Percentage of total	Volumetric flow rate	Percentage of total
Recharge to Upper Floridan aquifer				
Upper semiconfining unit	1,353.4	47.5	550.2	48.7
Infiltration	652.3	22.9	124.3	11.0
Regional flow	605.7	21.2	127.3	11.3
Upper Floridan aquifer updip limit	142.4	5.0	—	—
Lake Seminole	81.2	2.8	—	—
Streams	15.7	0.6	2.2	0.2
Interbasin flow	—	—	326.7	28.9
TOTAL	**2,850.8**	**100**	**1,130.7**	**100**
Discharge from Upper Floridan aquifer				
Streams and in-channel springs	2,045.6	71.8	918.6	80.9
Upper semiconfining unit	403.1	14.1	105.4	9.3
Regional flow	130.4	4.6	20.9	1.8
Irrigation pumpage	127.3	4.5	53.7	4.7
Lake Blackshear	68.0	2.4	—	—
Upper Floridan aquifer updip limit	43.9	1.5	—	—
Municipal pumpage and springs	30.1	1.1	24.8	2.2
Lake Seminole	2.4	0.1	—	—
Interbasin flow	—	—	12.2	1.1
TOTAL	**2,850.8**	**100**	**1,135.6**	**100**

from the regional flow system along the northeast, southeast, and southwest boundaries of the model (about 130 Mgal/d, or 5 percent of the total); withdrawal from irrigation wells (about 130 Mgal/d, or 4 percent of the total); leakage to Lake Blackshear (about 68 Mgal/d, or 2 percent of the total); outflow to the updip limit of the Upper Floridan aquifer along the northwest boundary of the model (about 44 Mgal/d, or 2 percent of the total); municipal pumpage (about 30 Mgal/d, or 1 percent of the total); nearly negligible leakage to Lake Blackshear (about 2 Mgal/d); and a nearly negligible outflow at off-channel springs (less than 1 Mgal/d).

The average rate of net recharge from above, including leakage to and from the upper semiconfining unit and infiltration, can be calculated from the budget terms in table 9 as 1,602.6 Mgal/d (= 1,353.4 Mgal/d + 652.3 Mgal/d – 403.1 Mgal/d). Dividing the average rate of net recharge from above by the area of the entire model (4,632 square miles) minus the combined area of Lakes Seminole and Blackshear (about 72 square miles), results in an average rate of net recharge from above of 7.4 in/yr, or about 15 percent of annual rainfall of about 50 inches. Despite isolated areas of high vertical-leakage rates, the average net-recharge rate is reasonable.

A similar budget was prepared for subbasin 03130008 (table 9) from the October 1999 calibrated model. To determine the balance of recharge to and discharge from this part of the entire model, it was necessary to estimate the flow of ground water to and from subbasin 03130008 along the internal boundary with other subbasins. This interbasin flow was approximated by dividing the model into nine zones of elements roughly corresponding to the seven subbasins in table 1 that are in the ACF River Basin, Lake Seminole, and Lake Blackshear. These element zones are shown in figure 28; and net interbasin flow rates along the boundary of subbasin 03130008 are indicated by blue arrows. The elemental flow vectors shown in figures 22 and 23, and the interbasin flow rates shown in figure 28, indicate that the Flint River is a regional drain; in October 1999, subbasin 03130008 collected a simulated total of about 325 Mgal/d of interbasin flow from subbasins 03130006, 03130007, 03130009, and 03130010, most of which eventually discharges to the Flint River. Based on simulation, during October 1999, subbasin 03130008 also received about 1 Mgal/d from Lake Seminole and discharged about 12 Mgal/d to subbasin 03130011.

To understand better the stream-aquifer flow system (shown in fig. 21), flows to and from selected major streams and stream reaches, shown in figure 24, are listed in table 10. Discharge is listed before recharge in table 10, because discharge has a much larger total flow, and the selected major streams are ordered by the magnitude of recharge or discharge. The Flint River is divided into three reaches (labeled in fig. 24): zones 1–3 (fig. 5), from Lake Blackshear to the Georgia Power Company dam near Albany; zones 4–7, from the Georgia Power Company dam to streamgage 02355660 (Flint River near Camilla, Ga.) just downstream from the confluence with Ichawaynochaway Creek; and zones 8–11, from streamgage 023556660 to Lake Blackshear. Most of the discharge from the Upper Floridan aquifer to streams (about 78 percent of total discharge to streams) occurs along the Apalachicola River, the Chattahoochee River, and the second (zones 4–7) and third (zones 8–11) reaches of the Flint River.

The regional-flow components of the ground-water budget (shown in fig. 24) are subdivided by zone (see fig. 5) along the lateral boundaries of the model (table 11), except at the Upper Floridan updip limit, which is a specified-head boundary. The zones are listed in clock-wise order around the lateral boundary in table 11, beginning at the northern model boundary and ending at the southwestern model boundary. About half of the recharge to the Upper Floridan aquifer from regional flow (about 50 percent of total recharge from the regional boundary) occurs along the eastern and southeastern boundary zones (zones 47 and 50, respectively). Most of the discharge from the Upper Floridan aquifer to regional flow (about 79 percent) occurs along the north Pelham boundary (zone 48).

Table 10. Stream-aquifer flow from the October 1999 calibrated model.

[Volumetric flow rate, in millions of gallons per day; totals may be inexact due to rounding; major streams shown in figure 24; minor streams are in table 4; other streams: Muckaloochee, Pachitla, and Dry (B) Creeks]

Stream reach	Volumetric flow rate	Percentage of total
Discharge from Upper Floridan aquifer		
Flint River (zones 4–7)	582.1	28.5
Apalachicola River	437.1	21.4
Flint River (zones 8–11)	334.2	16.3
Chattahoochee River	246.4	12.0
Kinchafoonee Creek	95.8	4.7
Minor streams	88.0	4.3
Spring Creek	85.7	4.2
Ichawaynochaway Creek	67.1	3.3
Muckalee Creek	52.3	2.6
Other streams	23.4	1.1
Flint River (zones 1–3)	17.2	0.8
Chickasawhatchee Creek	16.3	0.8
TOTAL	**2,045.6**	**100**
Recharge to Upper Floridan aquifer		
Other streams	4.6	29.1
Ichawaynochaway Creek	4.4	28.1
Flint River (zones 4–7)	2.2	13.7
Muckalee Creek	2.1	13.6
Flint River (zones 1–3)	2.1	13.0
Chickasawhatchee Creek	0.2	1.3
Kinchafoonee Creek	0.2	1.1
Spring Creek	0	0.1
Flint River (zones 8–11)	0	0
Apalachicola River	0	0
Chattahoochee River	0	0
Minor streams	0	0
TOTAL	**15.7**	**100**

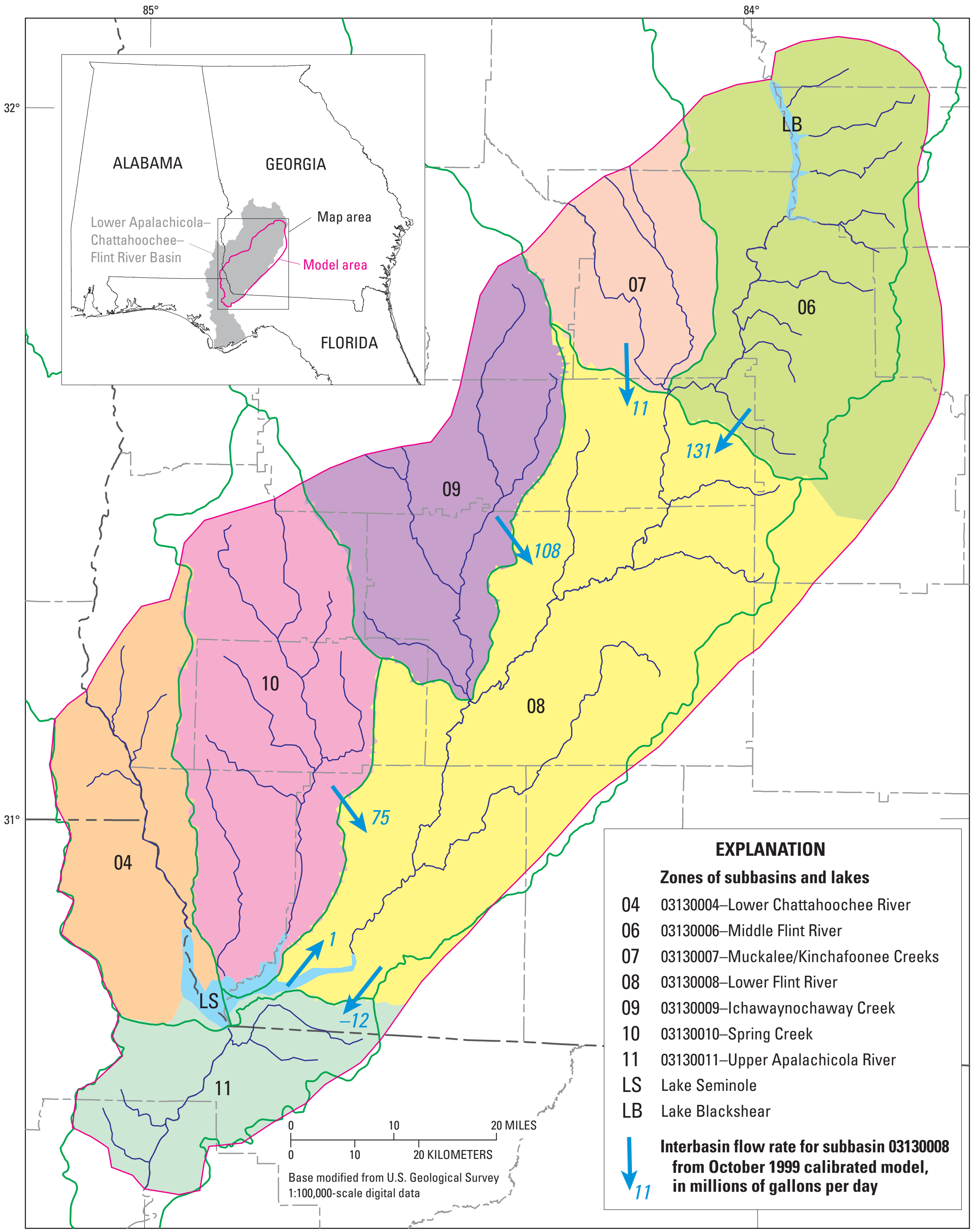

Figure 28. Zones of elements in the model representing subbasins in the lower Apalachicola–Chattahoochee–Flint River Basin and Lakes Seminole and Blackshear in southwest Georgia and adjacent parts of Alabama and Florida, and interbasin flow rates for subbasin 03130008 from the October 1999 calibrated model.

Table 11. Regional boundary flow from the October 1999 calibrated model.

[Volumetric flow rate, in millions of gallons per day; regional boundary zones are shown in figure 24; totals may be inexact due to rounding]

Regional boundary zone	Volumetric flow rate	Percentage of total
Recharge to Upper Floridan aquifer		
45. Northern	2.0	0.3
46. Northeastern	26.1	4.3
47. Eastern	150.2	24.8
48. North Pelham	58.0	9.6
49. South Pelham	76.2	12.6
50. Southeastern	155.0	25.6
51. Southern	61.3	10.1
52. Southwestern	77.0	12.7
TOTAL	**605.7**	**100**
Discharge from Upper Floridan aquifer		
45. Northern	2.4	1.9
46. Northeastern	9.9	7.6
47. Eastern	0.1	0
48. North Pelham	102.8	78.8
49. South Pelham	4.6	3.5
50. Southeastern	4.6	3.5
51. Southern	0.3	0.3
52. Southwestern	5.7	4.4
TOTAL	**130.4**	**100**

Essentially all of the discharge along the north Pelham boundary comes from recharge to the eastern boundary zone (zone 47) directly to the north; thus, about 100 Mgal/d of regional groundwater flow forms a short circuit along the lateral boundary of the model in this area (see flow direction indicated in fig. 21).

Water budgets also were computed from the March 2001–February 2002 transient simulation—volumetric flow rates of recharge and discharge components of the water budget for each of the 12 monthly stress periods are in table 12. In transient mode, the amount of water stored in the Upper Floridan aquifer is allowed to change from one stress period to the next—if recharge is greater than discharge, then net storage in the Upper Floridan aquifer increases, and if discharge is greater than recharge, then net storage in the aquifer decreases. Storage effects are included in table 12 under discharge components as storage gain, and under recharge components as storage loss.

Similar to table 10, monthly flows to and from selected major streams and stream reaches (shown in fig. 24) from the March 2001–February 2002 transient simulation are listed in table 13. Discharge components are given first, and the stream reaches are listed in the same order as in table 10, and the Flint River is divided into the same reaches. The four reaches receiving the most discharge from the Upper Floridan aquifer, the Apalachicola River, the Chattahoochee River, and the second (zones 4–7) and third (zones 8–11) reaches of the Flint River receive from about 69 percent to about 82 percent of the total discharge from the Upper Floridan aquifer to streams.

Table 12. Ground-water budget components and changes in storage in the Upper Floridan aquifer from the March 2001–February 2002 transient simulation.

[Totals may be inexact due to rounding]

Budget component	2001										2002	
	Mar.	Apr.	May	June	July	Aug.	Sept.	Oct.	Nov.	Dec.	Jan.	Feb.
Recharge to Upper Floridan aquifer, in million gallons per day												
Upper semiconfining unit	1,253	1,403	1,518	1,391	1,539	1,531	1,395	1,377	1,445	1,547	1,471	1,493
Regional flow	447	506	607	557	621	628	611	617	580	568	562	559
Infiltration	1,286	146	135	429	208	157	503	237	314	242	579	423
Upper Floridan aquifer updip limit	147	176	186	175	185	188	175	183	171	167	150	145
Lakes Seminole and Blackshear	46	68	83	75	85	84	77	79	72	71	71	72
Streams	164	100	57	69	62	54	44	40	42	57	52	59
Storage loss	2	143	614	33	424	350	66	155	126	59	38	37
TOTAL	**3,346**	**2,542**	**3,200**	**2,729**	**3,124**	**2,993**	**2,872**	**2,687**	**2,751**	**2,712**	**2,922**	**2,787**
Discharge from Upper Floridan aquifer, in million gallons per day												
Streams and in-channel springs	1,213	1,567	1,870	1,651	1,739	1,772	1,896	1,917	1,916	1,846	1,873	1,770
Upper semiconfining unit	526	389	312	364	308	309	384	372	370	330	384	388
Regional flow	163	144	127	136	124	123	131	131	144	148	151	147
Irrigation pumpage	4	155	750	311	826	667	195	127	137	51	11	14
Lake Blackshear	60	57	54	55	53	52	54	53	53	57	61	64
Upper Floridan aquifer updip limit	49	33	32	33	32	31	33	31	34	35	43	46
Municipal pumpage and springs	30	30	30	30	30	30	30	30	30	30	30	30
Lake Seminole	9	2	1	2	1	1	3	2	4	4	5	4
Storage gain	1,292	165	25	146	13	8	147	24	65	212	363	323
TOTAL	**3,346**	**2,542**	**3,200**	**2,729**	**3,124**	**2,993**	**2,872**	**2,687**	**2,753**	**2,712**	**2,922**	**2,786**

Table 13. Stream-aquifer flow from the March 2001–February 2002 transient simulation.

[Major streams shown in figure 24; minor streams in table 4; other streams: Muckaloochee, Pachitla, and Dry (B) Creeks; totals may be inexact due to rounding]

Stream reach	2001										2002	
	Mar.	Apr.	May	June	July	Aug.	Sept.	Oct.	Nov.	Dec.	Jan.	Feb.
Discharge from Upper Floridan aquifer, in million gallons per day												
Flint River (zones 4–7)	274	459	607	479	534	549	564	576	556	501	487	438
Apalachicola River	141	294	421	359	418	425	449	454	464	446	429	379
Flint River (zones 8–11)	251	286	293	272	264	272	301	312	322	316	318	309
Chattahoochee River	195	207	207	198	197	195	215	214	218	214	220	219
Minor streams	81	69	69	71	67	68	76	74	78	79	90	90
Kinchafoonee Creek	87	88	93	91	91	90	89	88	85	98	102	101
Spring Creek	59	37	18	36	17	23	48	48	51	52	65	68
Ichawaynochaway Creek	48	51	62	56	61	56	61	56	52	44	54	58
Muckalee Creek	40	46	58	52	51	53	51	54	49	53	57	56
Other streams	8	8	17	12	12	13	13	14	13	14	20	21
Flint River (zones 1–3)	14	15	16	15	16	16	16	16	16	17	17	17
Chickasawhatchee Creek	15	7	9	11	10	10	13	11	11	11	15	15
TOTAL	**1,213**	**1,567**	**1,870**	**1,651**	**1,739**	**1,772**	**1,896**	**1,917**	**1,916**	**1,846**	**1,873**	**1,770**
Recharge to Upper Floridan aquifer, in million gallons per day												
Other streams	20	13	3	8	7	5	6	4	7	11	8	9
Ichawaynochaway Creek	23	11	1	5	2	4	4	5	7	11	9	9
Flint River (zones 4–7)	57	7	1	5	3	3	3	2	2	4	4	5
Muckalee Creek	1	2	2	2	2	2	2	2	2	2	2	2
Flint River (zones 1–3)	1	2	2	2	2	2	2	2	2	2	2	2
Chickasawhatchee Creek	0	2	2	1	1	2	1	1	1	2	1	1
Kinchafoonee Creek	0	0	0	0	0	1	0	1	1	1	1	1
Spring Creek	2	6	8	4	7	6	2	2	1	1	0	0
Flint River (zones 8–11)	0	0	1	0	2	1	0	0	0	0	0	0
Apalachicola River	0	0	0	0	0	0	0	0	0	0	0	0
Chattahoochee River	0	0	0	0	0	0	0	0	0	0	0	0
Minor streams	59	56	36	42	36	29	23	21	19	24	25	29
TOTAL	**164**	**100**	**57**	**69**	**62**	**54**	**44**	**40**	**42**	**57**	**52**	**59**

The annual variation of the net discharge (discharge minus recharge) to individual stream reaches, in response to natural and anthropogenic time-varying boundary stresses, indicate the relative sensitivity of the stream to those stresses. For example, monthly net discharge from the Upper Floridan aquifer to two select stream reaches, the second reach of the Flint River (zones 4–7) and Spring Creek, demonstrate distinctly different variational patterns during March 2001–February 2002, indicating sensitivity to different time-varying boundary stresses. Net discharge to the second reach of the Flint River (zones 4–7, fig. 29) has a variational pattern that generally is inversely related to variations in rainfall; that is, in months having above average rainfall (March and June 2001), the associated high stream stages reduce the hydraulic gradient between the aquifer and the Flint River, thereby reducing discharge to the second reach of the River (zones 4–7). In this large collector stream, the effect of irrigation pumpage (indicated by fig. 6) is not readily apparent. The variational pattern of net discharge from the Upper Floridan aquifer to Spring Creek (fig. 30), however, is different, and generally is inversely related to variations in irrigation pumpage, as indicated by the average irrigated depth; the months having highest pumpage (May, July, and August 2001) have the lowest net discharge to Spring Creek. From March 2001 to February 2002, variation in discharge to the second reach of the Flint River (zones 4–7) is controlled primarily by climatic factors, whereas variation in discharge to Spring Creek is controlled primarily by irrigation pumpage.

Similar to table 11, monthly flows at regional boundaries from the March 2001–February 2002 transient simulation are separated by zone in table 14. Many of the same observations about regional-flow boundaries made for the October 1999 calibrated model are also true of results of the transient simulation, including the persistent short circuiting of about 100 Mgal/d in zones 47 and 48. In addition, the transient simulation provides an estimation of annual variation of regional-boundary recharge and discharge, in response to natural and anthropogenic time-varying boundaries. Total regional-boundary recharge to the Upper Floridan aquifer during March 2001–February 2002 (fig. 31) has a pattern that generally is inversely related to rainfall.

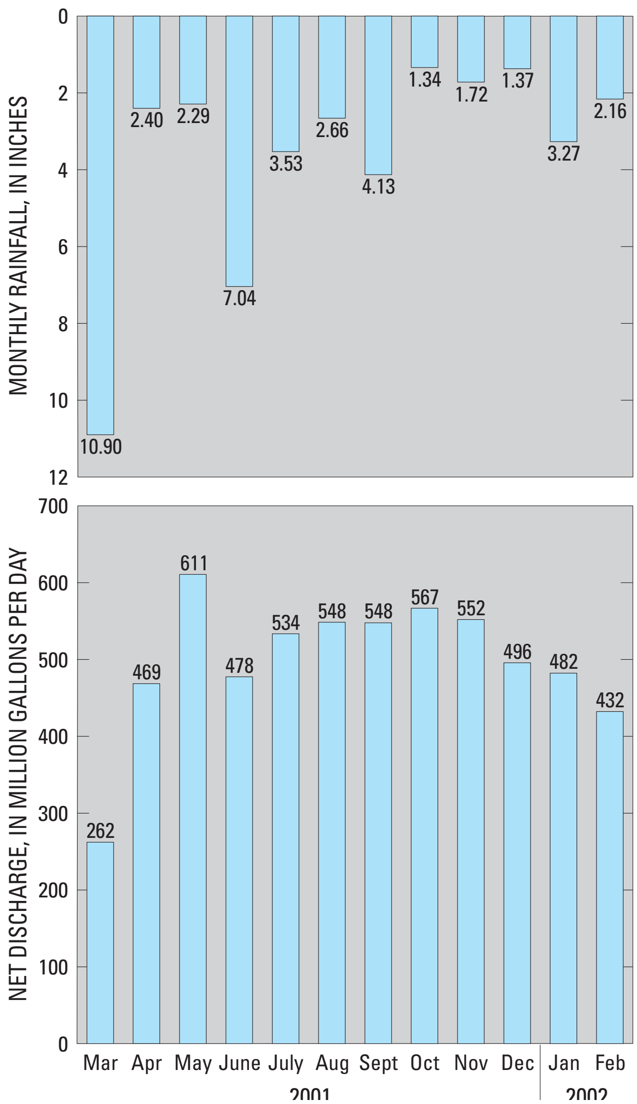

Figure 29. Simulated monthly net discharge from the Upper Floridan aquifer to the second reach of the Flint River (zones 4–7) from the March 2001–February 2002 transient simulation and average monthly rainfall in the model area.

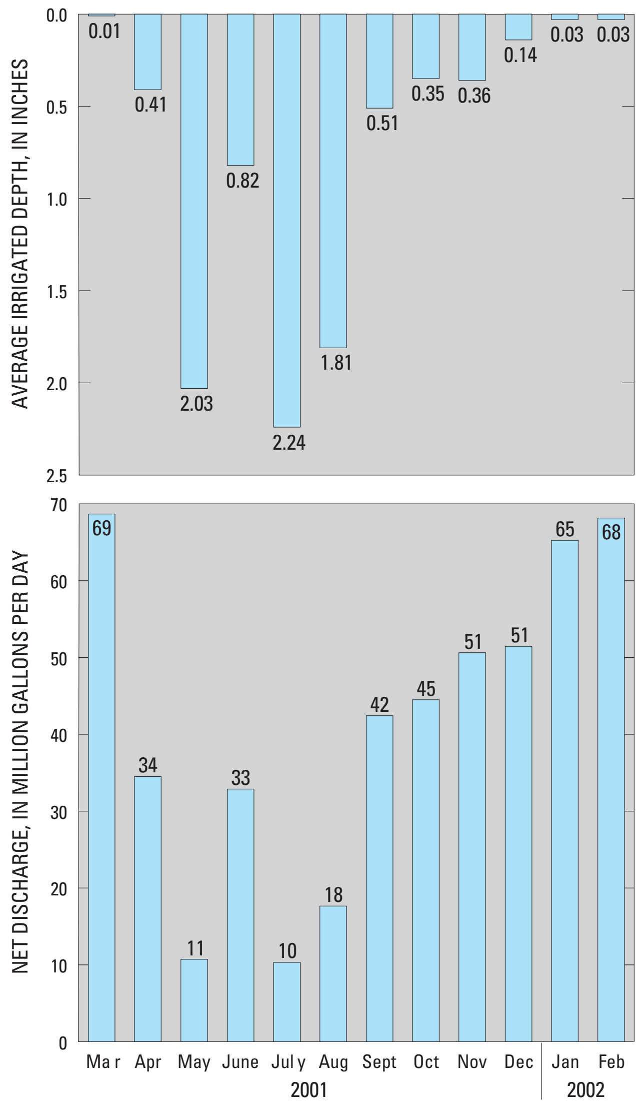

Figure 30. Simulated monthly net discharge from the Upper Floridan aquifer to Spring Creek from the March 2001–February 2002 transient simulation and average monthly irrigated depth in th emodel area.

Although the annual variation is not as pronounced as the variation in net discharge to the second reach of the Flint River (zones 4–7, fig. 29) the pattern is the same, indicating that high stream stage and infiltration in wet months (March and June 2001) in turn cause aquifer water levels to rise sufficiently to decrease the gradient at the regional boundaries, and thus, reduce regional-boundary inflow or recharge. In contrast, total regional-boundary discharge from the Upper Floridan aquifer during March 2001–February 2002 (fig. 32) has a pattern that is a less pronounced version of the variation in discharge to Spring Creek (fig. 30), which is inversely related to irrigational pumpage as indicated by the average irrigated depth. Therefore, regional boundary recharge is controlled primarily by climatic factors, whereas regional boundary discharge is controlled primarily by seasonal irrigation pumpage.

Source of Seasonal Ground-Water Pumpage

Paired, stacked bar graphs in figure 33 indicate balance between recharge (left-side bars) and discharge (right-side bars) components of the simulated ground-water budget from the October 1999 calibrated model. To determine the source of irrigation pumpage among the other components of the ground-water budget, the steady-state October 1999 calibrated model was executed without irrigation pumpage. Budget components from the steady-state simulations with and without irrigation pumpage (“calibrated simulation,” and “no irrigation pumpage,” respectively, in fig. 33) are shown in paired, stacked bar graphs for the entire model and for subbasin 03130008.

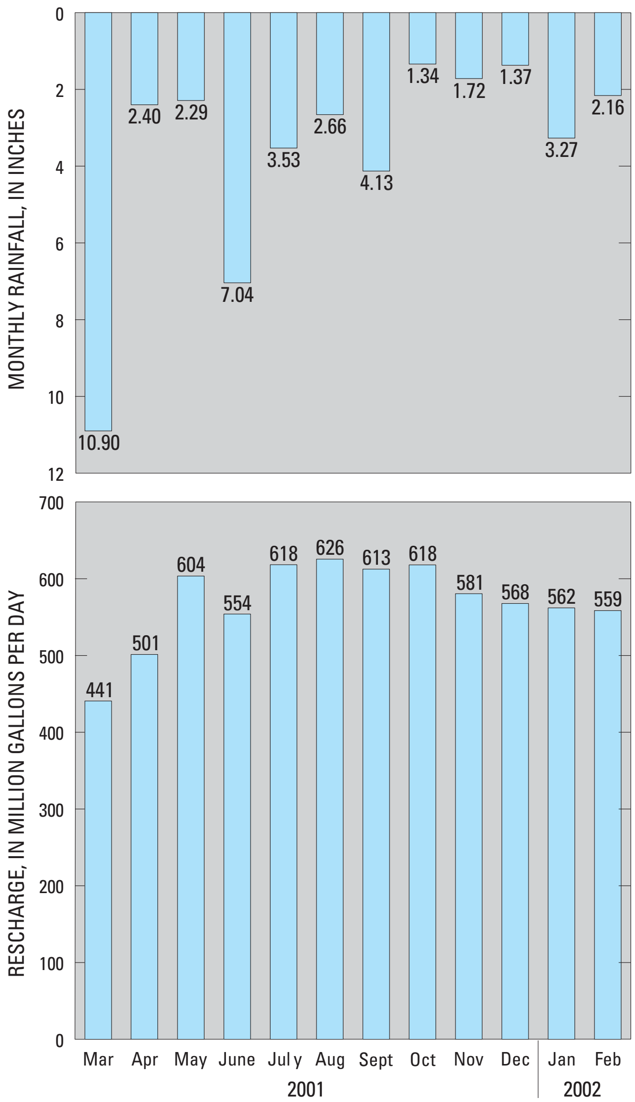

Figure 31. Simulated monthly total regional boundary recharge to the Upper Floridan aquifer from the March 2001–February 2002 transient simulation and monthly rainfall in the model area.

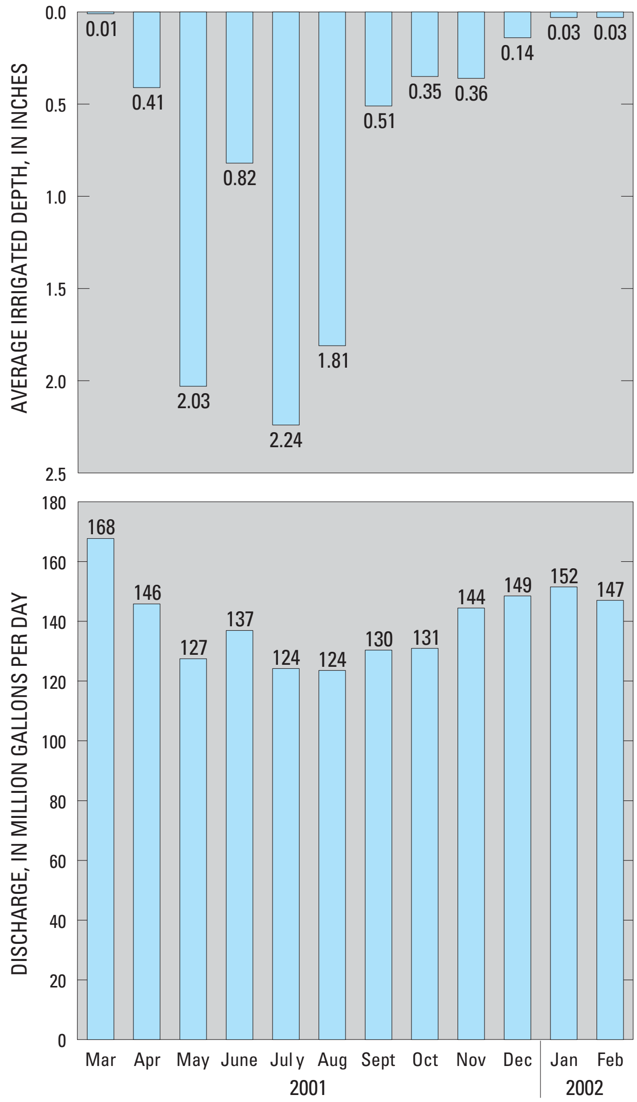

Figure 32. Simulated monthly total regional-boundary discharge to the Upper Floridan aquifer from the March 2001–February 2002 transient simulation and average monthly irrigated depth in the model area.

Individual contributions of the various ground-water budget components to irrigation pumpage can be determined from the change in the budgets from the October 1999 calibrated model and from a similar simulation in which no irrigation pumpage was applied ("calibrated simulation," and "no irrigation pumpage," respectively, in fig. 33). Paired, stacked bar graphs in figure 34 illustrate the change caused by irrigation pumpage by having the right-side bar represent increased discharge (irrigation pumpage) and the left-side bars represent increased recharge and decreased discharge. For each affected ground-water budget component, the relative contributions to irrigation pumpage, which was 127.3 Mgal/d for the October 1999 calibrated model, are the percentages of total change in the right-side bars (indicated in fig. 34). From the calibrated October 1999 simulation, the contributions to irrigation pumpage are increased recharge from and decreased discharge to: streams (about 44 percent), the upper semiconfining unit (about 39 percent), regional flow (about 14 percent), Lakes Seminole and Blackshear (about 2 percent), and the Upper Floridan aquifer updip limit (about 1 percent).

With respect to contributions to irrigation pumpage, the budget component of primary concern is decreased discharge from the Upper Floridan aquifer to streams (or increased recharge to the aquifer from streams). By subdividing the streams in the model area into the same reaches that are detailed in table 10 and calculating the difference in stream-aquifer flow from the October 1999 calibrated model and the simulation having no irrigation pumpage, the 44 percent of irrigation pumpage contributed by decreased discharge to and increased recharge from streams can be discussed in similar detail (table 15).

Table 14. Regional boundary flow from the March 2001–February 2002 transient simulation.

[Regional boundary zones are shown in figure 24; totals may be inexact due to rounding]

Regional boundary zone	2001										2002	
	Mar.	Apr.	May	June	July	Aug.	Sept.	Oct.	Nov.	Dec.	Jan.	Feb.
Recharge to Upper Floridan aquifer, in million gallons per day												
45. Northern	1	1	2	2	2	2	2	2	2	2	2	1
46. Northeastern	23	24	25	25	26	26	26	25	25	24	22	21
47. Eastern	146	148	154	150	155	154	150	149	146	145	141	141
48. North Pelham	55	55	56	56	57	58	57	57	57	56	56	56
49. South Pelham	58	64	90	74	96	94	78	76	62	58	60	67
50. Southeastern	78	109	144	129	147	151	155	159	143	139	141	140
51. Southern	6	25	51	41	53	56	61	64	61	58	56	49
52. Southwestern	81	80	84	81	85	87	84	85	86	86	84	83
TOTAL	**447**	**506**	**607**	**557**	**621**	**628**	**611**	**617**	**580**	**568**	**562**	**559**
Discharge from Upper Floridan aquifer, in million gallons per day												
45. Northern	4	3	3	3	3	3	3	3	3	3	3	3
46. Northeastern	14	13	11	12	11	11	12	13	15	16	18	19
47. Eastern	0	0	0	0	0	0	0	0	0	1	1	1
48. North Pelham	106	105	103	103	101	100	101	102	103	104	105	106
49. South Pelham	10	8	3	5	3	3	5	5	10	12	10	7
50. Southeastern	12	8	4	7	4	4	5	5	10	11	9	7
51. Southern	11	2	1	1	1	1	0	0	0	0	0	1
52. Southwestern	8	4	2	4	2	2	3	3	3	3	4	4
TOTAL	**163**	**144**	**127**	**136**	**124**	**123**	**131**	**131**	**144**	**148**	**151**	**147**

For comparison to table 10, the streams in table 15 are listed in the same order and decreased discharge is tabulated before increased recharge. About 23 percent of irrigation pumpage was derived from decreased discharge to the middle (zones 4–7) and lower (zones 8–11) reaches of the Flint River. Decreased discharge to the Chattahoochee River and to Spring Creek each accounted for about 6 percent of irrigation pumpage.

In subbasin 03130008, increased discharge for irrigation pumpage and a small interbasin flow component (about 0.4 percent of total) are balanced against increased recharge and decreased discharge of the other affected components (fig. 34). Considering that the increased discharge and decreased recharge component of interbasin flow is small compared to increased discharge to irrigation wells, the relative contributions to irrigation pumpage of the other affected components is close to the percentages of total change in the right-side bars. In subbasin 03130008, the approximate contributions to irrigation pumpage are increased recharge from and decreased discharge to: streams (about 56 percent), the upper semiconfining unit (about 26 percent), regional flow boundaries (about 18 percent), and interbasin flow (less than 1 percent).

Paired, stacked bar graphs in figure 35 indicate balance for each monthly stress period, one bar of each representing recharge components and storage loss (left-side bars), and the other bar representing discharge components and storage gain (right-side bars). During March 2001, the first month of the transient simulation, monthly precipitation was the highest for the 12-month period and irrigation pumpage was minimal. Consequently, there was above-average infiltration (green bar on left), which was offset by above-average gain in storage (light red bar on right). Above-average irrigation pumpage rates during May, July, and August 2001 (light yellow bars on right) were offset by losses in storage (light red bar on left). Using the same technique, simulated monthly ground-water budget components and storage changes are depicted for subbasin 03130008 in figure 36. Interbasin flow is presented as both a recharge and discharge component; each month subbasin 03130008 received substantially more water across its subbasin boundaries (large orange bars on left) than was lost (small orange bars on right), resulting in a large net recharge.

Similar to figures 35 and 36, except applied to the transient simulation in which no irrigation pumpage was applied, paired, stacked bar graphs of simulated monthly recharge components and storage loss (left-side bars) and discharge components and storage gain (right-side bars) are presented in figures 37 and 38, for the entire model and for subbasin 03130008, respectively.

To determine the individual contributions of the various ground-water budget components to seasonal irrigation pumpage, the same procedure that was applied to results from the steady-state October 1999 calibrated model, described above and shown in figure 34, was applied to each monthly stress period of the March 2001–February 2002 transient simulation.

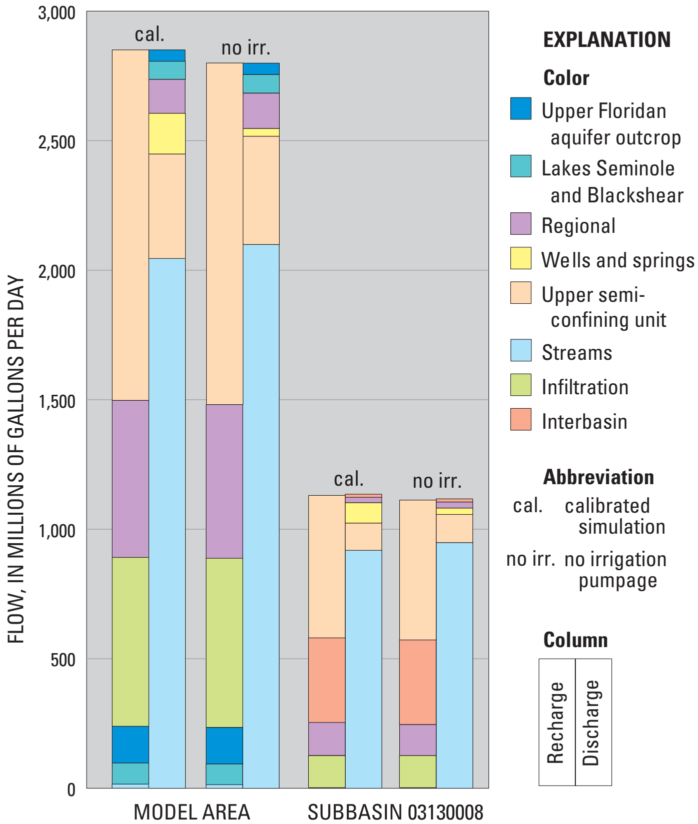

Figure 33. Simulated ground-water budget components in the Upper Floridan aquifer in the model area and in subbasin 03130008 from the October 1999 calibrated model and from a simulation applying no irrigation pumpage.

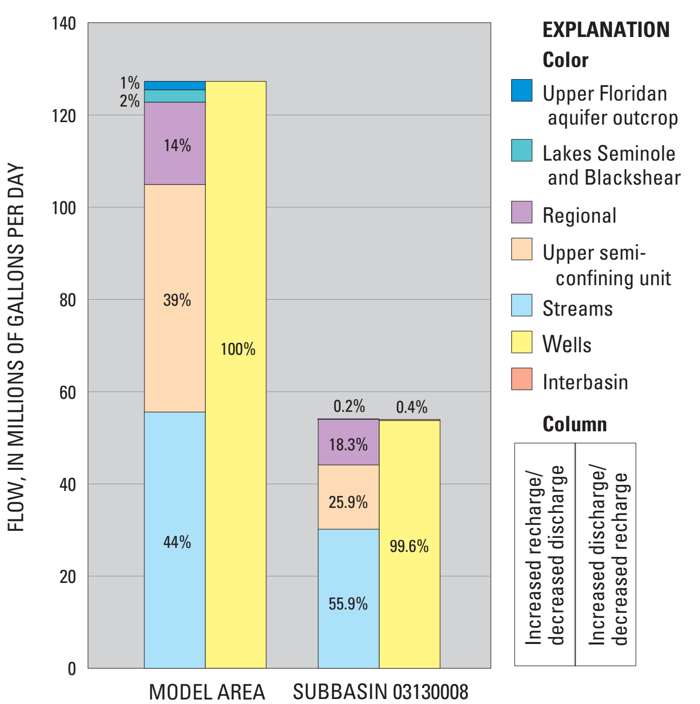

Figure 34. Simulated change in ground-water budget components in the Upper Floridan aquifer due to irrigation pumpage in the model area and in subbasin 03130008 from the October 1999 calibrated model.

Table 15. Changes in stream-aquifer flow from the October 1999 calibrated model.

[Change in volumetric flow rate, in millions of gallons per day; major streams shown in figure 24; minor streams are in table 4; other streams: Muckaloochee, Pachitla, and Dry (B) Creeks; totals may be inexact due to rounding]

Stream reach	Change in volumetric flow rate	Percentage of irrigation pumpage
Decreased discharge from Upper Floridan aquifer		
Flint River (zones 4–7)	15.6	12.3
Apalachicola River	0.2	0.2
Flint River (zones 8–11)	14.0	11.0
Chattahoochee River	8.1	6.3
Kinchafoonee Creek	1.1	0.9
Minor streams	3.0	2.3
Spring Creek	7.0	5.5
Ichawaynochaway Creek	3.2	2.5
Muckalee Creek	0.9	0.7
Other streams	0.6	0.5
Flint River (zones 1–3)	0.1	0.1
Chickasawhatchee Creek	0.2	0.2
TOTAL	**54.1**	**42.5**
Increased recharge to Upper Floridan aquifer		
Other streams	0.1	0.1
Ichawaynochaway Creek	1.0	0.8
Flint River (zones 4–7)	0.3	0.3
Muckalee Creek	0	0
Flint River (zones 1–3)	0	0
Chickasawhatchee Creek	0	0
Kinchafoonee Creek	0	0
Spring Creek	0	0
Flint River (zones 8–11)	0	0
Apalachicola River	0	0
Chattahoochee River	0	0
Minor streams	0	0
TOTAL	**1.5**	**1.2**
Decreased discharge + increased recharge	**55.6**	**43.7**

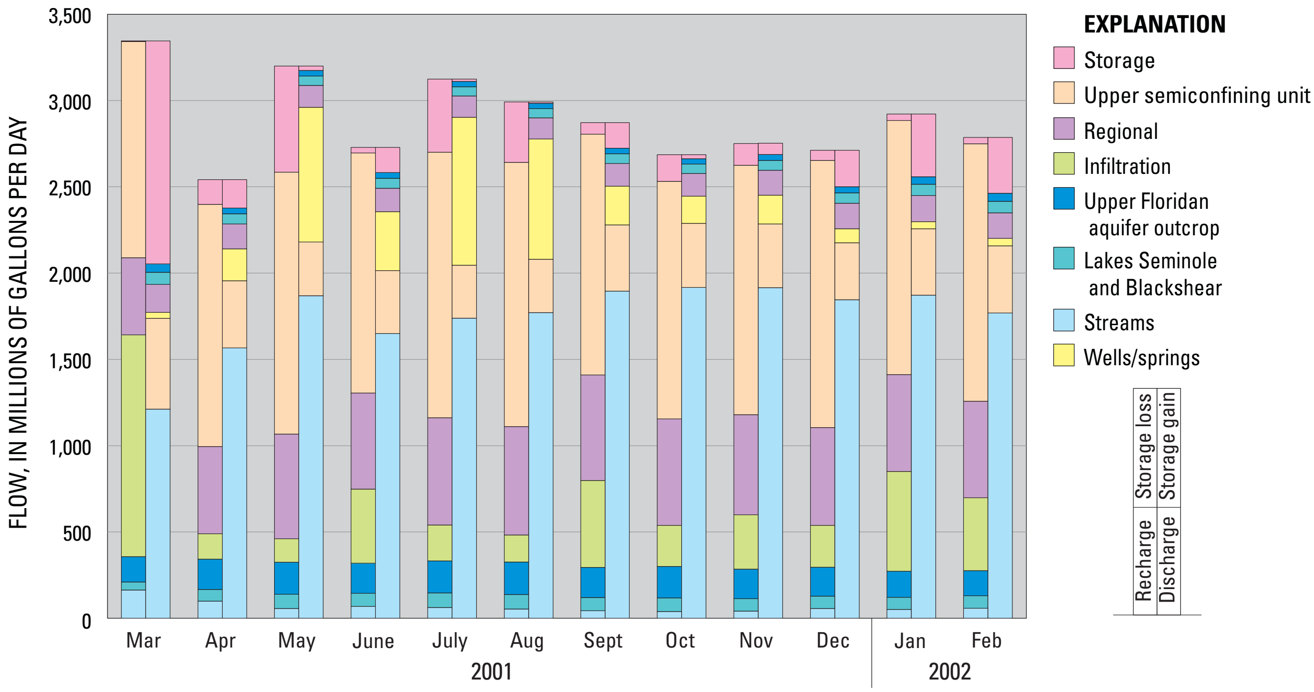

Figure 35. Simulated monthly ground-water budget components and storage change in the Upper Floridan aquifer from the March 2001–February 2002 transient simulation.

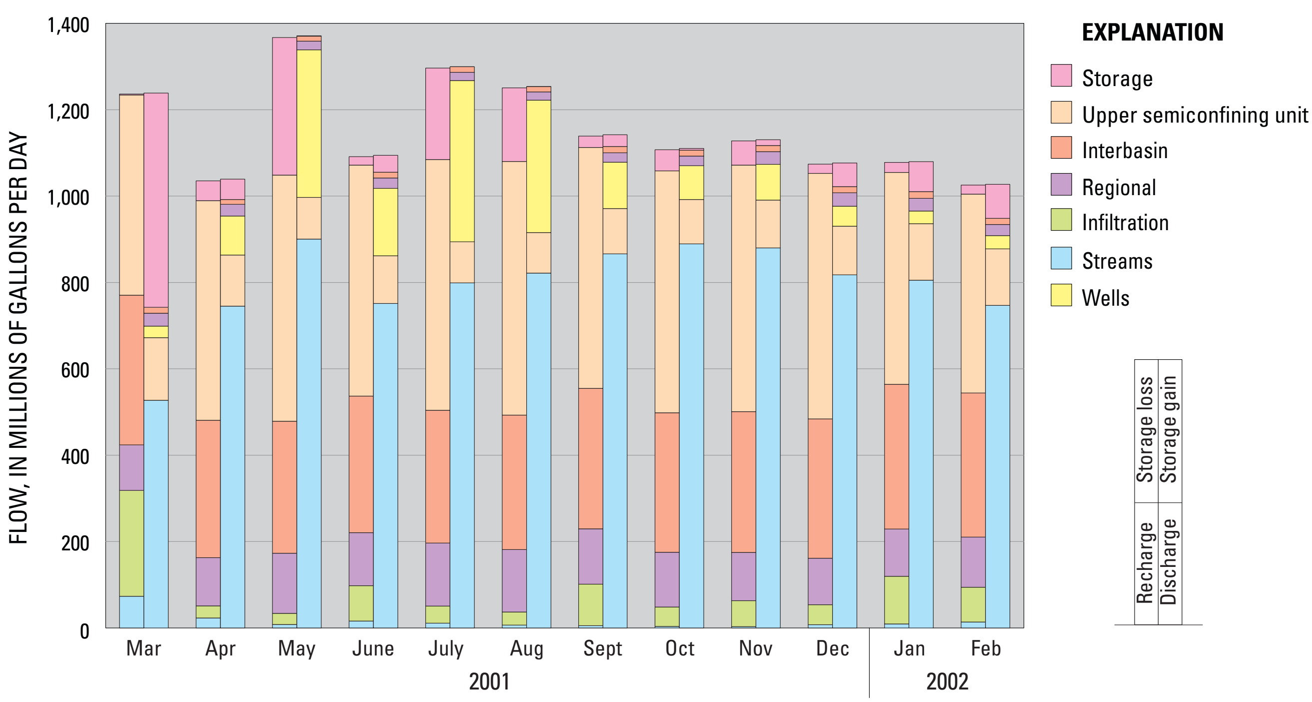

Figure 36. Simulated monthly ground-water budget components and storage change in the Upper Floridan aquifer in subbasin 03130008 from the March 2001–February 2002 transient simulation.

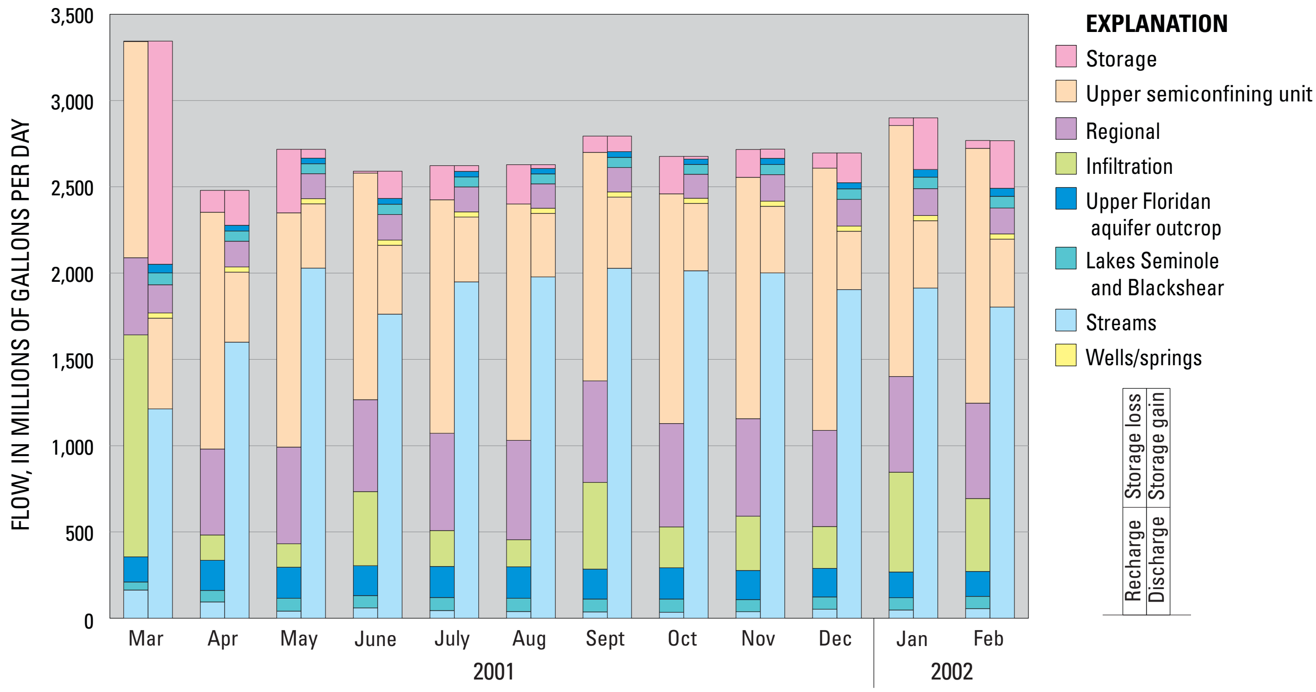

Figure 37. Simulated monthly ground-water budget components and storage change in the Upper Floridan aquifer from the March 2001–February 2002 transient simulation, applying no irrigation pumpage.

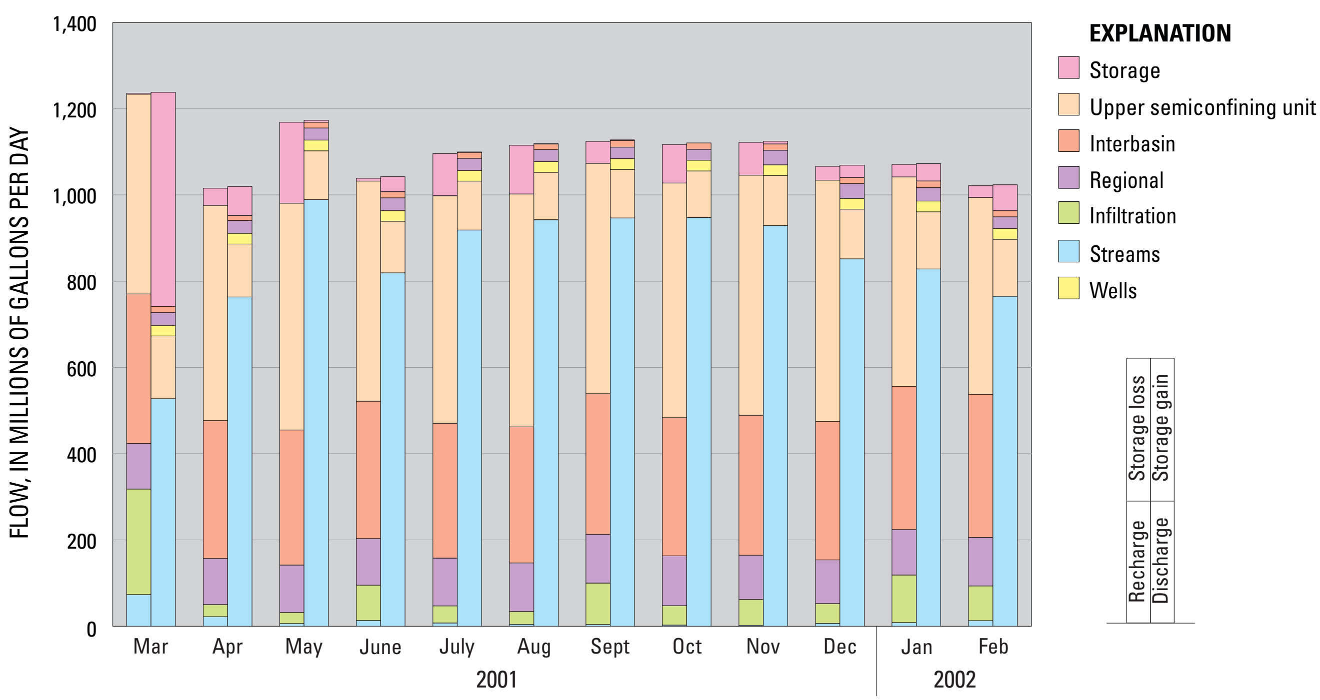

Figure 38. Simulated monthly ground-water budget components and storage change in the Upper Floridan aquifer in subbasin 03130008 from the March 2001–February 2002 transient simulation, applying no irrigation pumpage.

In figure 39 is the difference between simulated ground-water budget components from the March 2001–February 2002 transient simulation and the transient simulation having no irrigation pumpage. The only difference between figures 34 and 39 is that in a transient simulation, storage effects must be applied to the appropriate side of the stacked bars to achieve a water balance. When there is a decreased loss or increased gain of storage, the storage effect is applied to the left-side bar representing increased discharge (and decreased recharge), and when there is a decreased gain or increased loss of storage, the storage effect is applied to the right-side bar representing decreased discharge and increased recharge. Figure 40 quantifies the relative contribution of each of the components of the ground-water budget to the volume of irrigation pumpage based on each of the right-side bars shown in figure 39.

For the first 6 months of the simulation, from March 2001 through August 2002 (most of the irrigation season), the bar graph shown in figure 40 indicates the percentage contribution to irrigation pumpage by either a decreased discharge or increased recharge in some other budget component. About 84 percent of the 12-month total irrigation pumpage occurred during the first 6-month period, March–August 2001. During this period, the percentage contributions to irrigation pumpage from increased recharge and decreased discharge of other components ranged: from about 23 to 39 percent for stream-aquifer flow; from about 30 to 36 percent for leakage to or from the upper semiconfining unit; from about 8 to 11 percent for regional flow; from about 1 to 2 percent for leakage to or from Lakes Seminole and Blackshear; and about 1 percent for flow at the Upper Floridan aquifer updip limit.

During the second 6 months of the simulation period, September 2001–February 2002, there was an increased gain or decreased loss in storage in the Upper Floridan aquifer. The storage-effect portion of the total of irrigation pumpage and storage effects (right-side column) ranged from about 25 percent during November 2001 to about 87 percent during January 2002 (fig. 39). Consequently, increased recharge or decreased discharge of the other budget components during this second 6-month period are balanced against increased irrigation pumpage and substantial storage effects. As such, the percentage contributions of other budget components from the second 6-month period, September 2001–February 2002, are not directly comparable to the percentage contributions of the same components from the first 6-month period, March–August 2001. During the second 6-month period, the percentage contribution to irrigation pumpage and storage effects ranged: from about 49 to 55 percent for stream-aquifer flow; from about 28 to 35 percent for leakage to or from the upper semiconfining unit; from about 13 to 14 percent for regional flow; from about 1 to 3 percent for flow at the Upper Floridan aquifer updip limit; and from about 1 to 2 percent for leakage to or from Lakes Seminole and Blackshear.

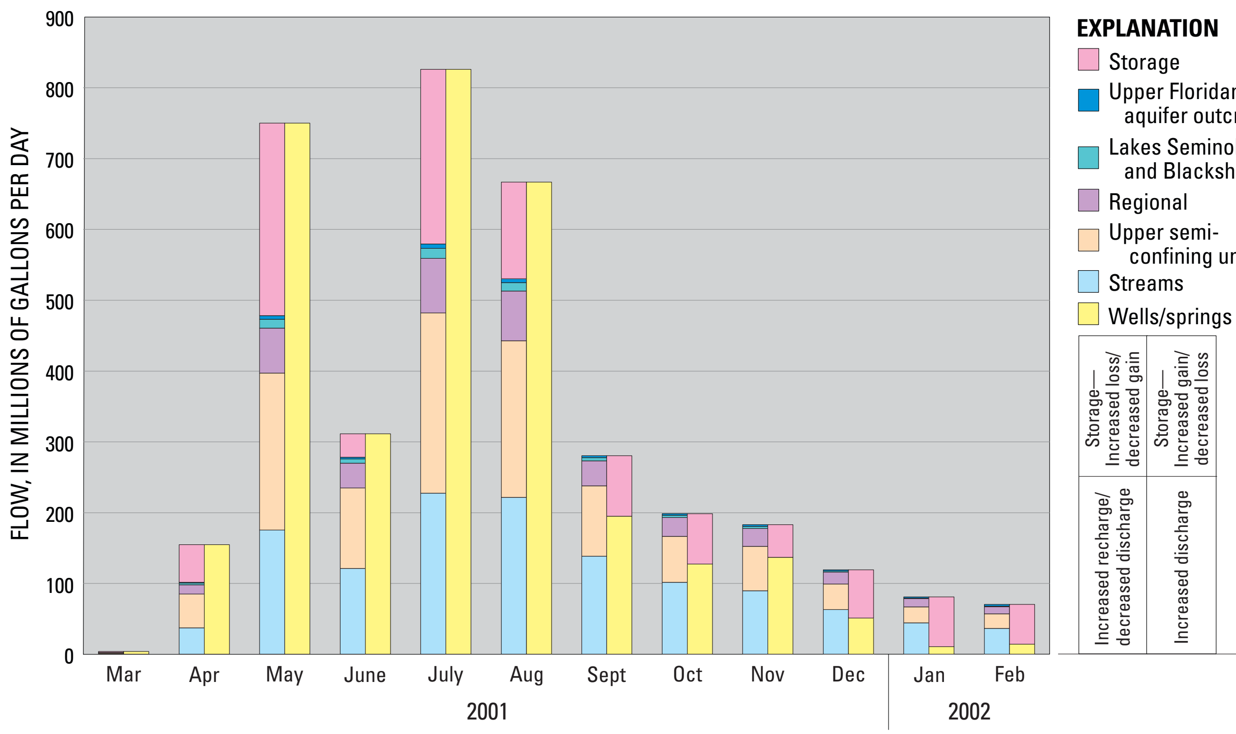

Figure 39. Simulated change in ground-water budget components and net increased storage loss or gain in the Upper Floridan aquifer due to irrigation pumpage from the March 2001–February 2002 transient simulation.

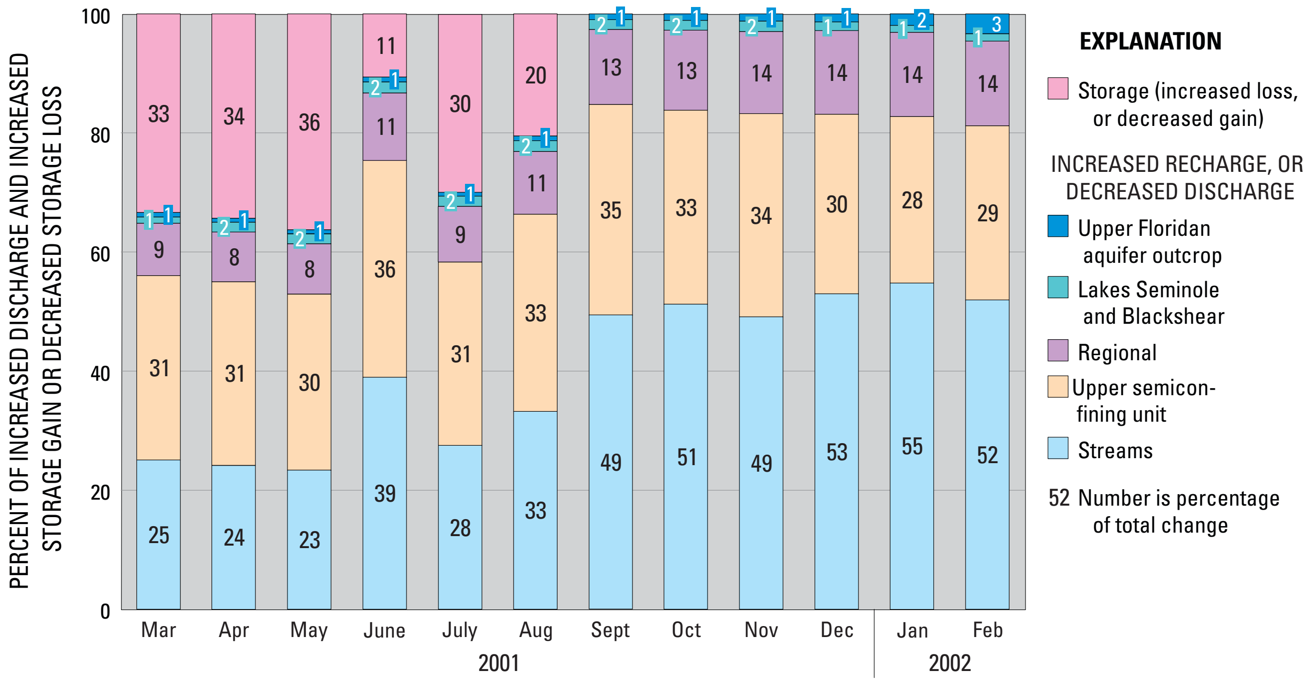

Figure 40. Simulated percentage of increased discharge for irrigation pumpage and net increased storage gain by increased recharge or decreased discharge of each affected ground-water budget component and net increased storage loss in the Upper Floridan aquifer from the March 2001–February 2002 transient simulation.

It should be noted that each of the monthly percentage contributions to irrigation pumpage are subject not only to the change in storage gains and losses, which are included in the bar graphs, but also are affected by the overall monthly change in storage in the ground-water system. For example, the percentages presented in figure 40 for June 2001 do not account for the 113 Mgal/d net gain in storage in the Upper Floridan aquifer (table 12) during June. The gain in aquifer storage during June is about 36 percent of the irrigation pumpage in that month. To minimize the effects of the change in aquifer storage month to month, 12-month totals of the changes in water budget terms associated with irrigation pumpage were considered. During the entire 12-month transient simulation, from March 2001 to February 2002, about 100 billion gallons were pumped from the Upper Floridan aquifer in the model area for irrigation. Of that total, the percentage of increased recharge or decreased discharge in: stream-aquifer flow was about 39 percent; leakage from or to the upper semiconfining unit was about 36 percent; regional flow was about 12 percent; leakage from or to Lakes Seminole and Blackshear was about 2 percent; and flow at the Upper Floridan aquifer updip limit was about 1 percent. Net increased loss or decreased gain in storage in the Upper Floridan aquifer accounted for about 11 percent of the total irrigation pumpage.

In a manner similar to table 15, changes in stream-aquifer flow to and from selected major streams and stream reaches are presented in table 16 for each month of the March 2001–February 2002 transient simulation. For comparison to table 15, the streams are in the same order and decreased discharge is listed before increased recharge. During the four-month period May–August 2001 about 79 percent of the 12-month total irrigation volume occurred. During this period, the percentage of irrigation pumpage that was derived from decreased discharge to and increased recharge from the middle (zones 4–7) and lower (zones 8–11) reaches of the Flint River ranged from about 12 to 22 percent. During the same period, decreased discharge to and increased recharge from Spring Creek ranged from about 5 to 6 percent of irrigation pumpage, and decreased discharge to the Chattahoochee River ranged from about 2 to 4 percent of irrigation pumpage.

Stacked, paired bar graphs similar to figures 39 and 40 also were prepared for changes in simulated water-budget components in subbasin 03130008 (lower Flint River) and are shown in figures 41 and 42. Considering the change in water-budget components associated with irrigation pumpage for subbasin 03130008, the same situation exists for storage effects. The storage effects are associated with the increase in irrigation pumpage for the second 6-month period, September 2001–February 2002; and are associated with the increased recharge or decreased discharge in the other budget component for the first 6-month period, March 2001–August 2001.

Table 16. Changes in stream-aquifer flow from the March 2001–February 2002 transient simulation.

[Major streams shown in figure 24; minor streams in table 4; totals may be inexact due to rounding; other streams: Muckaloochee, Pachitla, and Dry (B) Creeks; +, plus]

Stream reach	2001										2002	
	Mar.	Apr.	May	June	July	Aug.	Sept.	Oct.	Nov.	Dec.	Jan.	Feb.
Decreased discharge from Upper Floridan aquifer, in million gallons per day												
Flint River (zones 4 to 7)	0	8	39	33	56	59	43	32	27	20	14	11
Apalachicola River	0	0	1	0	1	1	1	0	0	0	0	0
Flint River (zones 8 to 11)	0	10	49	34	63	62	37	26	22	14	9	7
Chattahoochee River	0	3	18	14	26	27	20	17	15	12	9	8
Minor streams	0	2	7	5	9	8	5	3	3	1	1	1
Kinchafoonee Creek	0	1	2	2	4	4	3	2	2	1	1	1
Spring Creek	0	7	32	16	36	31	13	7	8	3	1	1
Ichawaynochaway Creek	0	2	8	5	12	11	8	6	6	4	4	3
Muckalee Creek	0	0	2	1	3	3	2	1	1	1	1	1
Other streams	0	0	1	1	1	1	1	1	1	1	1	1
Flint River (zones 1 to 3)	0	0	0	0	1	0	0	0	0	0	0	0
Chickasawhatchee Creek	0	0	1	0	1	1	0	0	0	0	0	0
TOTAL	**1**	**33**	**160**	**112**	**210**	**207**	**132**	**97**	**86**	**59**	**41**	**34**
Increased recharge to Upper Floridan aquifer, in million gallons per day												
Other streams	0	0	1	1	1	1	0	0	0	0	0	0
Ichawaynochaway Creek	0	0	1	1	1	2	2	2	2	2	2	1
Flint River (zones 4 to 7)	0	0	0	2	1	1	1	1	1	1	1	1
Muckalee Creek	0	0	0	0	0	0	0	0	0	0	0	0
Flint River (zones 1 to 3)	0	0	0	0	0	0	0	0	0	0	0	0
Chickasawhatchee Creek	0	0	0	0	0	0	0	0	0	0	0	0
Kinchafoonee Creek	0	0	0	0	0	0	0	0	0	0	0	0
Spring Creek	0	1	6	2	5	4	1	1	0	0	0	0
Flint River (zones 8 to 11)	0	0	1	0	2	1	0	0	0	0	0	0
Apalachicola River	0	0	0	0	0	0	0	0	0	0	0	0
Chattahoochee River	0	0	0	0	0	0	0	0	0	0	0	0
Minor streams	0	2	6	3	6	5	2	1	1	0	0	0
TOTAL	**0**	**4**	**15**	**9**	**17**	**15**	**6**	**5**	**4**	**4**	**3**	**3**
Decreased discharge + increased recharge	**1**	**37**	**175**	**121**	**227**	**221**	**138**	**102**	**90**	**63**	**44**	**37**

During the first 6-month period, March 2001–August 2001, in subbasin 03130008, the percentage contributions to irrigation pumpage and small, increased interbasin discharge from increased recharge or decreased discharge of other components ranged: from about 28 to 52 percent for stream-aquifer flow; from about 19 to 26 percent for leakage to or from the upper semiconfining unit; from about 11 to 15 percent for regional flow; and about 2 percent or less for interbasin flow. Also in the first 6-month period in subbasin 03130008, the percentage contribution to irrigation pumpage and small, increased interbasin discharge from an increased loss or decreased gain in storage in the Upper Floridan aquifer ranged from about 6 to 41 percent. During the second 6-month period, September 2001–February 2002, the storage-effect portion of the total of irrigation pumpage and storage effects for subbasin 03130008 ranged from about 32 percent during November 2001 to about 89 percent during January 2002 (fig. 41). Also in the later period, in subbasin 03130008 the percentage contribution to irrigation pumpage and storage effects from increased recharge or decreased discharge of other components ranged: from about 58 to 61 percent for stream-aquifer flow; from about 18 to 24 percent for leakage to or from the upper semiconfining unit; from about 15 to 17 percent for regional flow; and from about 1 to 7 percent for interbasin flow.

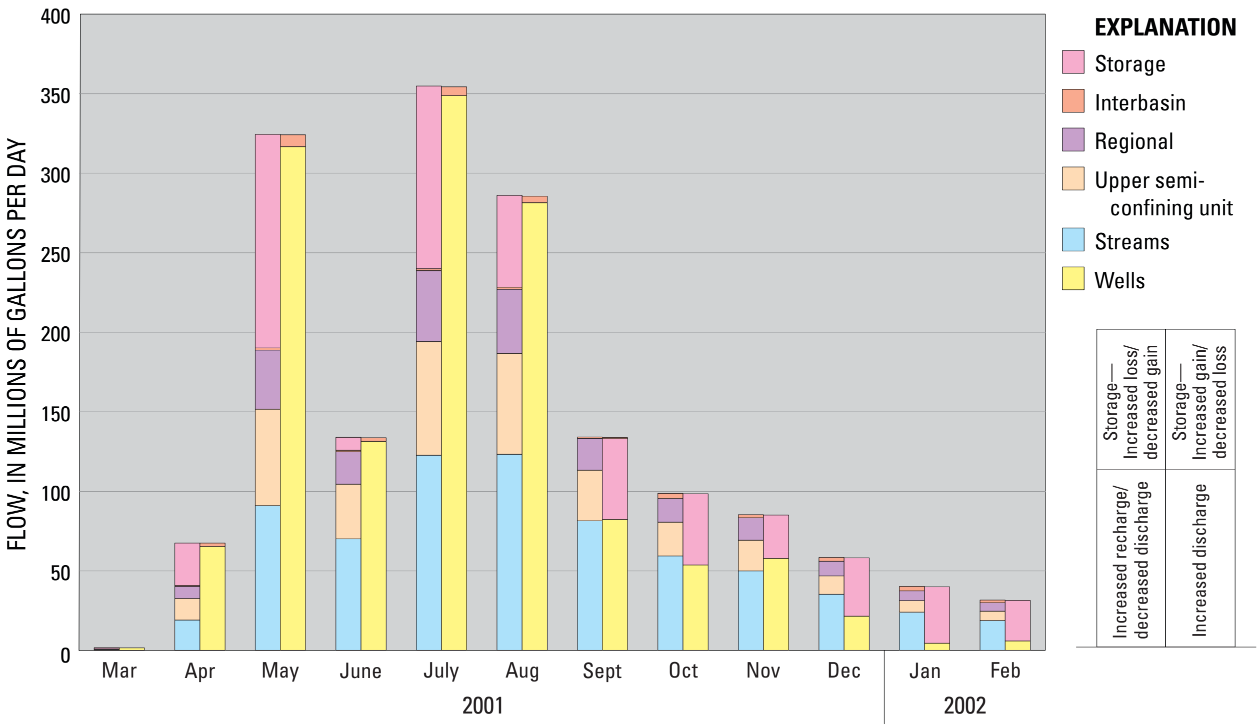

Figure 41. Simulated change in ground-water-budget components and net increased storage loss or gain in the Upper Floridan aquifer in subbasin 03130008 due to irrigation pumpage from the March 2001–February 2002 transient simulation.

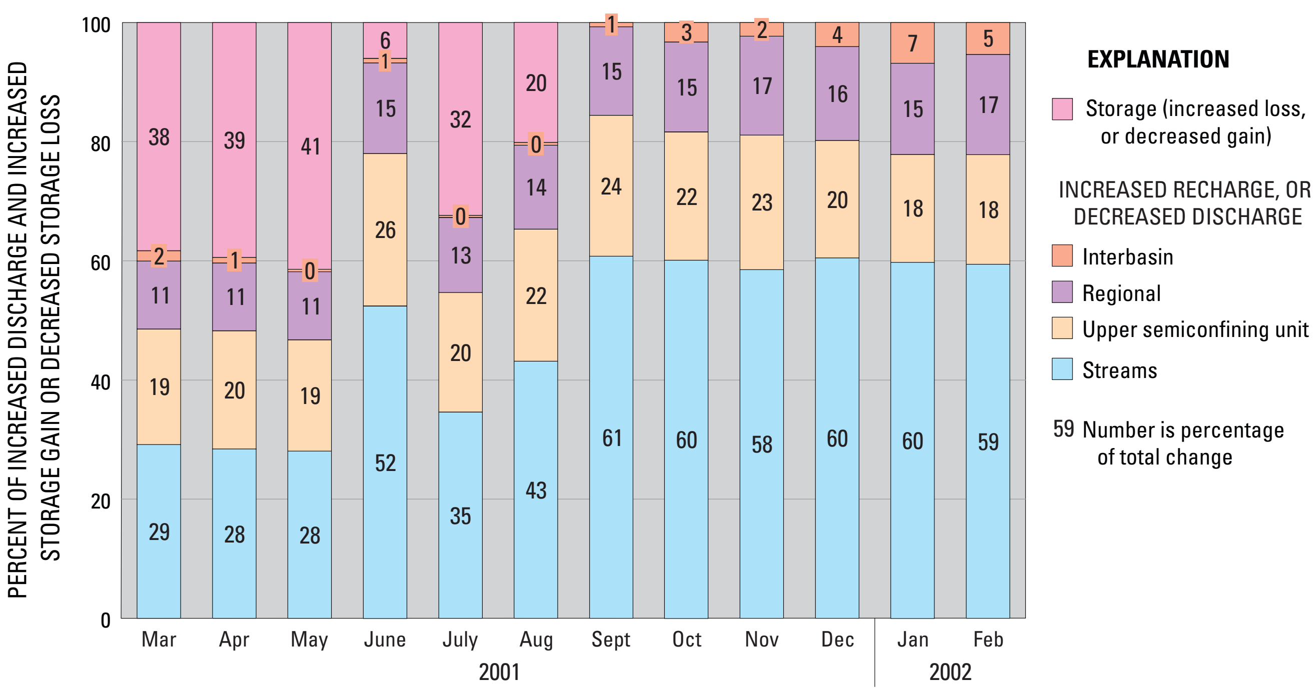

Figure 42. Simulated percentage of increased discharge for irrigation pumpage and net increased storage gain by increased recharge or decreased discharge of each affected ground-water-budget component and net increased storage loss in the Upper Floridan aquifer in subbasin 03130008 from the March 2001–February 2002 transient simulation.

Model Limitations

Several types of limitations affect the ability of the model application to represent components of the stream-lake-aquifer flow system in a manner that simulates actual conditions. One type is associated with finite-element numerical approximation of partial-differential equations that are assumed to govern ground-water flow and stream-lake-aquifer interaction. Model limitations associated with numerical approximation are endemic to any model and affect numerical accuracy of the model solution. These limitations are manifested as approximation error, are a permanent part of the solution, and generally are small. Any textbook that develops the finite-element method, such as Strang and Fix (1973), addresses approximation of equations.

Limitations related to the mathematical representation of ground-water flow in the lower ACF River Basin and time, such as the design of the finite-element mesh, geometric representation of hydrologic components using nodes (points), element sides (lines), or elements (areas), and finite-element or finite-difference approximation of time vary according to how the model is used to represent spatial and temporal aspects of a specific flow problem. These limitations result in an inability of the model to simulate the correct physics of the flow system or the correct aquifer or boundary-condition geometry, areal extent, or time-varying hydrologic processes that occur in the study area. Errors related to mesh design, finite-element representation of time, and the configuration of hydrologic components have been minimized during model development in the lower ACF River Basin by performing preliminary simulations and analyzing model results. Details of these analyses are beyond the scope of this report; design considerations for developing a finite-element mesh and applying the model are given in Torak (1996). The transfer value of design considerations and development of similar models for the lower ACF River Basin by Torak and others (1993, 1996) and Torak and McDowell (1996) greatly assisted in the development of the current model by minimizing model limitations inherent to mathematical representation of flow-system processes in space and time.

Limitations related to model representation of specific hydrologic components and observed conditions in the flow system are evaluated with regard to two criteria (1) the ability of hydrologic data to support an alternate representation of a hydrologic component in the model, and (2) the sufficiency of data to discern changes in model performance caused by changes in component representation. These limitations address the agreement of simulation capabilities with hydrologic processes that have been conceptualized to occur in the lower ACF River Basin. Model application is limited by hydrologic data, which not only support flow-system conceptualization and substantiate the selection of specific model capabilities that simulate hydrologic components, but also validate acceptable model performance.

Lack of accurate hydrologic data defining several flow-system components, listed below in no particular order, limit the ability to develop the current model: (1) irrigation pumpage; (2) impermeable base of the model (Lisbon Formation); (3) controlling head at regional (lateral) flow boundaries; (4) hydraulic conductance and head of the upper semiconfining unit; (5) water-bearing units above the Upper Floridan south of the escarpment and Lake Seminole; and (6) principal water-bearing layer in the Upper Floridan aquifer.

The adequacy of the sample representing irrigation pumpage upon which ground-water withdrawal was developed as a model input has been evaluated by the authors of the sampling technique and the Ag Water Pumping Program at the University of Georgia (Hook and others, 2005). A statistically valid sample of irrigation pumpage was obtained in the lower ACF River Basin for use in the current study. Additional information such as crop type and distribution, irrigation schedules, and discharge rates for all wells represented in the model would have provided the detail necessary to improve the statistically derived estimates of irrigation pumpage used in the model.

Representing the underlying confining unit as wholly impermeable and not allowing leakage to deeper parts of the flow system, flow-system component 2 listed above, poses no model limitation and has been addressed in the companion geohydrology report by Torak and Painter (2006). Data compiled for the current study and regional modeling by Faye and Mayer (1996) do not refute an impermeable or nearly impermeable base to the Upper Floridan aquifer.

Assessment of limitations associated with the current model application to flow-system components 2–6, listed previously, presupposes that hydrologic data exist to support alternate representations of each component and that these data can be used to discern differences in the goodness of fit between models developed using alternate-component representations. Without sufficient hydrologic data to fulfill these criteria, components 2–6 pose no model limitation. The model is capable of simulating an impermeable base of the Upper Floridan aquifer, regional flow-system boundaries, an upper semiconfining unit having hydraulic conductance and a source-layer head, water-bearing units above the Upper Floridan aquifer, and a single model layer. The current model is limited, however, by a lack of hydrologic data to support an alternate flow-system conceptualization that would be mirrored by an alternate model application, which improves the goodness of fit between the computed solution and field data.

The inability of data to define possible effects on the Upper Floridan aquifer resulting from simulating an unconfined aquifer in the undifferentiated overburden, components 4 and 5 listed previously, should not be confused with a lack of data or a model limitation. Existing hydrologic data do not define the undifferentiated overburden to the Upper Floridan aquifer as "an active unconfined aquifer" above the Upper Floridan aquifer; such data would give cause for simulation as a model layer (or several layers). Attributes of an active unconfined aquifer—such as the release or uptake of water from storage in the unconfined aquifer, delayed yield, areally extensive water-bearing zones, water-table fluctuations with stream interaction, indications of lateral flow, and importance as a viable water source—are not defined with hydrologic data collected in the upper semiconfining unit. This lack of physical substantiation of the upper semiconfining unit to behave as an aquifer permits the various geologic units that compose the upper semiconfining unit to be represented as a single hydrologic unit for model application. Areally extensive shallow well-bore data rule out the occurrence of a continuous water-table aquifer overlying the Upper Floridan aquifer (Torak and Painter, 2006); preliminary simulations indicate a negligible amount of water released from or taken up by aquifer storage; the lithology and genesis of the residuum contacting the limestone of the Upper Floridan aquifer dictates that laterally discontinuous water-bearing zones above the residuum supply water to the aquifer below by vertical leakage; and lateral-flow processes usually represented with a distinct model for simulation do not apply to the overburden.

A "true" model limitation arises from data that support an alternate conceptualization in which the model is incapable of representing, and a different, less "acceptable" flow-system concept is represented instead. A true model limitation can be quantified with data that not only define the alternate flow-system concept, but that confirm an "unacceptable" model application; model acceptance is gauged with various statistical moments and residuals of ground-water levels (simulated minus measured) described previously. True model limitations do not exist in the current model, which adequately and correctly simulates all flow-system processes that are contained in the flow-system conceptualization and that are defined and supported by hydrologic data.

Improvements to the model would address problems inherent to data deficiencies and sources of parameter uncertainty discussed previously. The most prominent data deficiency prohibits model calibration during wet periods and transient conditions. A wet-period calibration could be addressed by conducting another intensive data-collection effort during a wetter part of the year or climate cycle, as was performed during October 1999 when water levels were measured in about 275 wells and streamflow was determined at more than 60 streamgaging stations. Transient calibration would require collection of long-term continuous ground-water and surface-water levels, stream discharge, and precipitation data. Continued short-term measurement and compilation of irrigation pumpage, as provided by the Ag Water Pumping Program (James E. Hook, National Environmentally Sound Production Agriculture Laboratory, written commun., 2003) is critical for developing a transient ground-water model to assess the effects of pumpage on hydrologic conditions in the area.

Uncertainty of model results and the assessment of goodness of fit, or model acceptability, could be alleviated by obtaining more precise estimates of land-surface altitude for wells and streamgaging stations than exist at locations where altitude has been estimated from topographic maps. Uncertainty associated with the amount of recharge that the Upper Floridan aquifer receives from infiltration of precipitation and vertical downward leakage could be addressed by monitoring ground-water levels in closely spaced, vertically nested, shallow wells in the undifferentiated overburden. Many of the shallow wells installed during aquifer performance tests in a related study (Torak and Painter, 2006) could serve as an initial distribution of nested-well locations.

Summary and Conclusions

The finite-element ground-water flow model of the Upper Floridan aquifer in the lower Apalachicola–Chattahoochee–Flint River Basin developed for this study simulates ground-water withdrawal from irrigation, municipal, and industrial wells; flow between the aquifer and area streams and lakes; vertical leakage to and from the overlying upper semiconfining unit; regional ground-water flow at the lateral model boundaries; and areally distributed infiltration where the aquifer is at or near land surface. The steady-state calibration to drought conditions of October 1999 adequately simulated 275 measured ground-water levels and changes in streamflow along 53 reaches defined by upstream and downstream flow measurements. A transient simulation during the period from March 2001 to February 2002 accounted for time-varying input of irrigation pumpage, stream and lake stage, head in the overlying upper semiconfining unit, and infiltration rates.

The finite-element model simulating ground-water flow with stream-lake-aquifer interaction represents an improvement from previous models in the lower ACF River Basin by Torak and others (1993, 1996) and Torak and McDowell (1996) in the following developmental and functional areas:

- Data defining hydrologic heterogeneity of the Upper Floridan aquifer;
- Versatile and selective use of gradational detail in the finite-element mesh for representing locations of wells, stream reaches, and geometrically complex flow-system boundaries;
- Spatial and temporal distribution of irrigation pumpage;
- Hydrologic data supporting steady-state calibration to October 1999 drought conditions and simulation of transient conditions of March 2001–February 2002; and
- Capability of quantifying time-varying (transient) effects of recharge, irrigation pumpage, and hydrologic drought conditions on ground-water levels in the Upper Floridan aquifer and on streamflow to mainstem streams and tributaries.

Compilation of recent data on the hydraulic properties of the stream-lake-aquifer flow system with existing hydrologic information (Torak and Painter, 2006) enabled hydrologic heterogeneity of the Upper Floridan aquifer and upper semiconfining unit to be represented with detailed inputs to the model. Data refinements to the areal distribution of aquifer hydraulic conductivity, thickness, transmissivity, and storage properties; upper semiconfining unit thickness and water level; and to the areal extent of the ground-water flow system contributing water to lakes and streams in the lower ACF River Basin provided the basis for improved and detailed model inputs for simulating ground-water flow with stream-lake-aquifer interactions, when compared with previous models developed for selected parts of the basin by Torak and others (1993, 1996) and Torak and McDowell (1996).

The continuous and smoothly gradational finite-element mesh consisting of nearly equilateral triangular finite elements improved the representation of well locations, stream reaches, and the extent and geometric complexity of the basin area contributing ground water to the stream-lake-aquifer flow system compared to meshes designed for previous studies by Torak and others (1993, 1996) and Torak and McDowell (1996). Equilateral-triangular elements minimize approximation error associated with simulating flow-system processes within an element based on values computed at the element's bounding nodes. The mesh design incorporates smooth transitions of variously sized equilateral triangular elements to represent detailed and complex flow-system geometry, such as meandering streams, irregular lakeshore, aquifer outcrop, and external model boundaries.

The detailed distribution of irrigation wells in the lower ACF River Basin during October 1999 and the temporal variation of pumping rates and well locations during March 2001–February 2002, compiled for model input from data provided by the State of Georgia, represent major improvements to simulating stream-lake-aquifer interaction with the current model, in comparison with the well and pumping-rate distributions used in previous models developed by Torak and others (1993, 1996) and Torak and McDowell (1996). Previous models simulated only steady-state conditions based on pumping rates derived from reported pump, well, and irrigation-system capacity, and therefore overestimated irrigation pumpage during drought conditions of October 1986. Model inputs incorporating detailed estimates of pumping rates and data defining transient hydrologic conditions for recharge and streamflow, together with a refined finite-element mesh, resulted in a model capable of simulating the effects of hydrologic heterogeneity and temporal variations in irrigation pumpage and recharge on ground-water levels and streamflow for the transient conditions that existed during the period from March 2001 to February 2002, in addition to simulating steady-state October 1999 conditions.

Computed water budgets from the calibrated steady-state October 1999 and transient March 2001–February 2002 simulations of the Upper Floridan aquifer provide estimates of the relative contributions to irrigation pumpage of hydrologic components in the stream-lake-aquifer flow system. Under steady-state October 1999 conditions, irrigation pumpage reduced simulated ground-water flow to streams by a rate of about 56 million gallons per day (Mgal/d), which is equivalent to about 44 percent of the October 1999 pumping rate of about 127 Mgal/d. This percentage (44 percent) represents the *aggregate streamflow reduction* for all streams simulated in the model of the lower ACF River Basin; it does not represent the streamflow reduction of a specific stream in the model area. Pumpage-induced flow reductions for specific streams may not equal 44 percent because of complexities in the ground-water flow system caused by heterogeneous aquifer-hydraulic properties and the location of pumped wells and boundary conditions proximate to streams in each subbasin. For example, in subbasin 03130008 (lower Flint River), simulated-streamflow reduction caused by irrigation pumpage equals about 56 percent of the total pumping rate.

The current level of refinement of hydrologic data in the lower ACF River Basin and of simulation of the stream-lake-aquifer flow system with the finite-element model, MODFE (Cooley, 1992; Torak, 1993a, b), represents an improved understanding of the effects of irrigation pumpage on streamflow from the previous understanding derived from data and models used by Torak and others (1993, 1996) and Torak and McDowell (1996). As an improved flow-system model, the current simulated pumpage-induced streamflow reduction of 44 percent of the steady-state, October 1999 pumping rate represents a 16-percent decrease in the effect of pumpage on streamflow from that simulated by Torak and McDowell (1996, tables 14–19) for similar steady-state drought conditions of October 1986. Pumpage-induced vertical leakage to the Upper Floridan aquifer increased, however, by 15 percent to 39 percent of the October 1999 pumping rate, when compared with similar leakage in the model by Torak and McDowell (1996, tables 14–19) for steady-state, October 1986 conditions. Increased data definition of aquifer hydrologic heterogeneity and a detailed finite-element mesh resulted in these differences in flow-system response to irrigation pumpage.

For water-management considerations, simulation of pumpage-induced streamflow reduction at the subbasin level allows detailed model results to document the cause-and-effect relations of irrigation (or any) pumpage on the stream-lake-aquifer flow system. Detailed simulation of ground-water flow in a subbasin is possible with the current model provided that all pumping stress affecting the subbasin flow system is represented in the subbasin water budget. Because subbasin boundaries are based on surface-water divides and not ground-water divides, which change with time to accommodate changes in hydrologic conditions, subbasin boundaries and flow conditions along them must be able to account for inflow and outflow resulting from pumpage changes on either side of the subbasin boundary. Flow across subbasin boundaries affect streamflow and indicate a smaller or larger area contributing ground-water flow (or baseflow) to streams than the area represented within the subbasin of interest. Management scenarios for determining pumpage-induced streamflow reduction in a specific subbasin must address not only temporal variations in pumping rates of existing wells and inclusion of new wells, but time-varying changes in hydrologic conditions, including pumping rates, on either side of subdivision boundaries. Analysis of ground-water flow directions derived from transient simulations can identify possible changes in the area contributing ground water to streams (or baseflow), as defined by simulated ground-water flow directions.

Model results for the transient simulation of March 2001–February 2002 conditions indicate that effects of aquifer storage minimally affect streamflow reduction caused by pumpage, and that results of a steady-state simulation are acceptable for most water-management considerations. The 44-percent reduction in streamflow in accordance with the simulation of steady-state, October 1999 conditions is only slightly more conservative (that is, more of a worse-case scenario) than percent streamflow reductions derived from the transient simulation of March 2201–February 2002 conditions. Streamflow reductions simulated during the growing season, March–August 2001, range from 23 to 39 percent of the pumping rate, in comparison with the 44-percent reduction computed by the steady-state simulation of October 1999 conditions.

Simulations demonstrating flow-system sensitivity indicate that the lower ACF River Basin and Upper Floridan aquifer responds linearly to plausible changes in values of selected model parameters. Specifically, discharge and recharge components, including flow to and from streams, respond linearly to changes in irrigation pumpage that are one-half or twice the steady-state, October 1999 pumping rate of about 127 Mgal/d, that is, between about 64–314 Mgal/d. Linear stream-aquifer response to pumpage is important from a water-management perspective in that the effect of proposed pumpage changes within this range can be calculated easily by expressing the change in pumpage as a multiple (or multiplier) of the October 1999 rate. Linear flow-system response to changes in pumping rate has been demonstrated for the lower ACF River Basin in previous models by Torak and others (1993, 1996) and Torak and McDowell (1996) using pumping rates of nearly 7.5 times the October 1999 rates used in the current model, indicating the possibility of a larger range of linear flow-system response to pumpage than simulated here.

References Cited

Arthur, J.D., and Rupert, F.R., 1989, Selected geomorphic features of Florida, *in* The lithostratigraphy and hydrostratigraphy of the Floridan aquifer system in Florida, field trip guidebook T185, Tampa to Tallahassee, Florida, July 1–7, 1989: American Geophysical Union, p. T185:10–14.

Bear, Jacob, 1979, Hydraulics of groundwater: New York, McGraw-Hill, 569 p.

Beck, B.F., 2002, Integrating science, overview of background resources on karst research emphasizing obscure and “gray area” documents, *in* U.S. Geological Survey karst interest group proceedings, Shepardstown, West Virginia, August 20–22, 2002, Eve L. Kuniansky, ed.: U.S. Geological Survey Water-Resources Investigations Report 02-4174, p. 7.

Bush, P.W., and Johnston, R.H., 1988, Ground-water hydraulics, regional flow, and ground-water development of the Floridan aquifer system in Florida and in parts of Georgia, South Carolina, and Alabama: U.S. Geological Survey Professional Paper 1403-C, 80 p.

Clark, W.Z., and Zisa, A.C., 1976, Physiographic map of Georgia: Georgia Department of Natural Resources, 1 sheet, scale 1:2,000,000.

Cooke, C.W., 1939, Scenery of Florida interpreted by a geologist: Florida Geological Survey Bulletin 17, 118 p.

Cooke, C.W., 1943, Geology of the Coastal Plain of Georgia: U.S. Geological Survey Bulletin 941, 121 p.

Cooley, R.L., 1983, Analysis of an incongruity in the standard Galerkin finite-element method: Water Resources Research, v. 19, no. 1, p. 289–291.

Cooley, R.L., 1992, A MODular Finite-Element model (MODFE) for areal and axisymmetric ground-water flow problems, Part 2—Derivation of finite-element equations and comparisons with analytical solutions: U.S. Geological Survey Techniques of Water-Resources Investigations, Book 6, Chap. A4, 108 p.

Faye, R.E., and Mayer, G.C., 1996, Simulation of ground-water flow in southeastern Coastal Plain clastic aquifers in Georgia and adjacent parts of Alabama and South Carolina: U.S. Geological Survey Professional Paper 1410-F, 77 p.

Georgia Environmental Protection Division, 2006, Flint River Basin Regional Water Development and Conservation Plan, dated March 20, 2006, 227 p., accessed April 6, 2006, at *http://www.gadnr.org/frbp/Assets/Documents/Plan22.pdf*

Gotvald, A.J., Fisher, J.T., Oberst, C.E., and Calhoun, D.L., 2005, Water resources data—Georgia, 2004, Volume 1—Continuous water-level, streamflow, water-quality data, and periodic water-quality data, Water Year 2004, McCallum, B.E., and Alhadeff, D.V. (compilers): Reston, Va., U.S. Geological Survey Water-Data Report GA-04-1, 2253 p.

Hayes, L.R., Maslia, M.L., and Meeks, W.C., 1983, Hydrology and model evaluation of the principal artesian aquifer, Dougherty Plain, southwest Georgia: Georgia Geologic Survey Bulletin 97, 93 p.

Hendricks, E.L., and Goodwin, M.H., Jr., 1952, Water-level fluctuations in limestone sinks in southwestern Georgia: U.S. Geological Survey Water-Supply Paper 1110-E, 89 p.

Herrick, S.M., 1961, Well logs of the Coastal Plain of Georgia: Georgia Geologic Survey Bulletin 70, 462 p.

Hicks, D.W., Gill, H.E., and Longsworth, S.A., 1987, Hydrogeology, chemical quality, and availability of ground water in the Upper Floridan aquifer, Albany, Georgia: U.S. Geological Survey Water-Resources Investigations Report 87–4145, 52 p.

Hicks, D.W., Krause, R.E., and Clarke, J.S., 1981, Geohydrology of the Albany area, Georgia: Georgia Geologic Survey Information Circular 57, 31 p.

Hook, J.E., Harrison, K.A., and Hoogenboom, Gerrit, 2005, Statewide irrigation monitoring, executive summary: The University of Georgia Project Report 52, UGA ID 25-21-RF327-107, 6 p., accessed March 17, 2005, at *http://nespal.cpes.peachnet.edu/awp/2005.01.AWP_ExecSum.pdf*

Jones, L.E., and Torak, L.J., 2004, Simulated effects of impoundment of Lake Seminole on ground-water flow in the Upper Floridan aquifer in southwestern Georgia and adjacent parts of Alabama and Florida: U.S. Geological Survey Scientific Investigations Report 2004-5077, 18 p.

Kwader, Thomas, and Schmidt, Walter, 1978, Top of the Floridan aquifer of northwest Florida: Northwest Florida Water Management District in cooperation with the Florida Bureau of Geology Map Series No. 86, 1 sheet.

MacNeil, F.S., 1947, Geologic map of the Tertiary and Quaternary Formations of Georgia: U.S. Geological Survey Oil and Gas Inventory (Preliminary) Map 72.

McCallie, S.W., 1898, A preliminary on the artesian-well system of Georgia: Georgia Geologic Survey Bulletin 7, 214 p.

Moore, W.E., 1955, Geology of Jackson County, Florida: Florida Geological Survey Bulletin 37, 101 p.

Mosner, M.S., 2002, Stream-aquifer relations and the potentiometric surface of the Upper Floridan aquifer in the lower Apalachicola–Chattahoochee–Flint River Basin in parts of Georgia, Florida, and Alabama, 1999–2000: U.S. Geological Survey Water-Resources Investigations Report 02–4244, 45 p.

National Oceanic and Atmospheric Administration, 2002, Climatological data annual summary, 2001: National Oceanic and Atmospheric Administration, v. 105, no. 13, 28 p.

National Oceanic and Atmospheric Administration, 2003, Climatological data annual summary, 2002: National Oceanic and Atmospheric Administration, v. 106, no. 13, 28 p.

Norrie, D.H., and deVries, Gerard, 1973, The finite element method: New York, Academic, 322 p.

Peck, M.F., Clarke, J.S., Ransom, Camille, III, and Richards, C.J., 1999, Potentiometric surface of the Upper Floridan aquifer in Georgia and adjacent parts of Alabama, Florida, and South Carolina, May 1998; and water-level trends in Georgia, 1990–1998: Georgia Geologic Survey Hydrologic Atlas 22, 1 sheet.

Pollard, L.D., Grantham, R.G., and Blanchard, H.E., 1978, A preliminary appraisal of the impact of agriculture on ground-water availability in southwest Georgia: U.S. Geological Survey Water-Resources Investigations 80–771, 40 p.

Puri, H.S., and Vernon, R.O., 1964, Summary of the geology of Florida and a guidebook to the classic exposures: Florida Geological Survey, Special Publication 5 revised, 312 p.

Rovey, C.W., II, and Cherkauer, D.S., 1995. Scale dependency of hydraulic conductivity measurements: Ground Water, v. 33, no. 5, p. 769–780.

Rupert, F.R., 1990, Geology of Gadsden County, Florida: Florida Geological Survey Bulletin 62, 61 p.

Schmidt, Walter, 1978, Environmental geology series Apalachicola sheet: Florida Bureau of Geology Map Series No. 90, 1 sheet.

Schmidt, Walter, 1979, Environmental geology series Tallahassee sheet: Florida Bureau of Geology Map Series No. 84, 1 sheet.

Schmidt, Walter, 1984, Neogene stratigraphy and geologic history of the Apalachicola Embayment, Florida: Florida Bureau of Geology Bulletin 58, 146 p.

Schmidt, Walter, and Clark, M.W., 1980, Geology of Bay County, Florida: Florida Bureau of Geology Bulletin 57, 96 p.

Schmidt, Walter, Clark, M.W., and Bolling, Sharon, 1980, Miocene carbonate of the Florida Panhandle, *in* Scott, T.M., and Upchurch, S.B., eds., Miocene of the Southeastern United States—A symposium, Tallahassee, Fla., 1980: Southeastern Geological Society in cooperation with the Florida Bureau of Geology, Special Publication No. 25, p. 224–234.

Schmidt, Walter, and Coe, Curtis, 1978, Regional structure and stratigraphy of the limestone outcrop belt in the Florida panhandle: Florida Department of Natural Resources, Bureau of Geology Report of Investigation No. 86, 25 p.

Seaber, P.R., Kapinos, F.P., and Knapp, G.L., 1987, Hydrologic unit maps: U.S. Geological Survey Water-Supply Paper 2294, 63 p.

Sever, C.W., 1965a, Ground-water resources and geology of Seminole, Decatur and Grady Counties, Georgia: U.S. Geological Survey Water-Supply Paper 1809-Q, 30 p.

Sever, C.W., 1965b, Ground-water resources of Bainbridge, Georgia: Georgia Geological Survey Information Circular 32, 10 p.

Shelton, Stacy, 2005, Water war waged in different courts, neighbors try to invalidate Georgia deal: The Atlanta Journal-Constitution, accessed January 9, 2005, at *http://www.ajc.com/metro/content/metro/index.html*

Stephenson, L.W., and Veatch, J.O., 1915, Underground waters of the Coastal Plain of Georgia, and a discussion of the quality of the waters, by Dole, R.B.: U.S. Geological Survey Water-Supply Paper 341, 539 p.

Stokes, W.R., III, McFarlane, R.K., and Buell, G.R., 1990, Water resources data Georgia, water year 1989: U.S. Geological Survey Water-Data Report GA-89-1, 513 p.

Strang, Gilbert, and Fix, G.J., 1973, An analysis of the finite element method: Englewood Cliffs, New Jersey, Prentice-Hall, Inc., 306 p.

Torak, L.J., 1993a, A MODular Finite-Element model (MODFE) for areal and axisymmetric ground-water flow problems, Part 1—Model description and user’s manual: U.S. Geological Survey Techniques of Water-Resources Investigations, Book 6, Chap. A3, 136 p.

Torak, L.J., 1993b, A MODular Finite-Element model (MODFE) for areal and axisymmetric ground-water flow problems, Part 3—Design philosophy and programming details: U.S. Geological Survey Techniques of Water-Resources Investigations, Book 6, Chap. A5, 243 p.

Torak, L.J., and McDowell, R.J., 1996, Ground-water resources of the lower Apalachicola–Chattahoochee–Flint River Basin in parts of Alabama, Florida, and Georgia—Subarea 4 of the Apalachicola–Chattahoochee–Flint and Alabama–Coosa–Tallapoosa River Basins: U.S. Geological Survey Open File Report 95-321, 145 p.

Torak, L.J., and Painter, J.A, 2006, Geohydrology of the lower Apalachicola–Chattahoochee–Flint River Basin, southwestern Georgia, northwestern Florida, and southeastern Alabama, U.S. Geological Survey Scientific Investigations Report 2006-5070, 80 p.

Torak, L.J., Crilley, D.M., and Painter, J.A., 2006, Physical and hydrochemical evidence of lake leakage near Jim Woodruff Lock and Dam and assessment of karst features in and near Lake Seminole, southwestern Georgia and northwestern Florida: U.S. Geological Survey Scientific Investigations Report 2005-5084, 90 p.

Torak, L.J., Davis, G.S., Strain, G.A., and Herndon, J.G., 1993, Geohydrology and evaluation of water-resource potential of the Upper Floridan aquifer in the Albany area, southwestern Georgia: U.S. Geological Survey Water-Supply Paper 2391, 59 p.

Torak, L.J., Davis, G.S., Strain, G.A., and Herndon, J.G., 1996, Geohydrology and evaluation of stream-aquifer relations in the Apalachicola–Chattahoochee–Flint River Basin, southeastern Alabama, northwestern Florida, and southwestern Georgia: U.S. Geological Survey Water-Supply Paper 2460, 94 p.

U.S. Army Corps of Engineers, 1948, Definite project report on Jim Woodruff Dam (formerly Junction Project), Apalachicola River, Florida: U.S. Army Corps of Engineers, Mobile District, Mobile, Ala., v. II, appendixes II and III, 63 p.

U.S. Army Corps of Engineers, 1973, Survey report on Apalachicola, Chattahoochee, and Flint Rivers, Alabama, Florida, and Georgia: Mobile, Ala., U.S. Army Engineer District, Mobile Corps of Engineers, Office of the District Engineer, 44 p.

U.S. Army Corps of Engineers, 1997, Sharing the water in Alabama, Florida, and Georgia—ACT and ACF River Basins EISs: U.S. Army Corps of Engineers, Mobile District, Mobile, Ala., October 1997 newsletter, 4 p., accessed March 18, 2005, at *http://www.sam.usace.army.mil/pd/actacfeis/files/1097.pdf*

Vernon, R.O., 1951, Geology of Citrus and Levy Counties, Florida: Florida Geological Survey Bulletin 33, 256 p.

Wait, R.L., 1963, Geology and ground-water resources of Dougherty County, Georgia: U.S. Geological Survey Water-Supply Paper 1539-P, 102 p.

Zienkiewicz, O.C., 1977, The finite element method: New York, McGraw-Hill, 787 p.

Appendix A. Maps of Streamgaging-Station and Well Locations, Model-Sensitivity Plots, and Water-Level and Streamflow Data

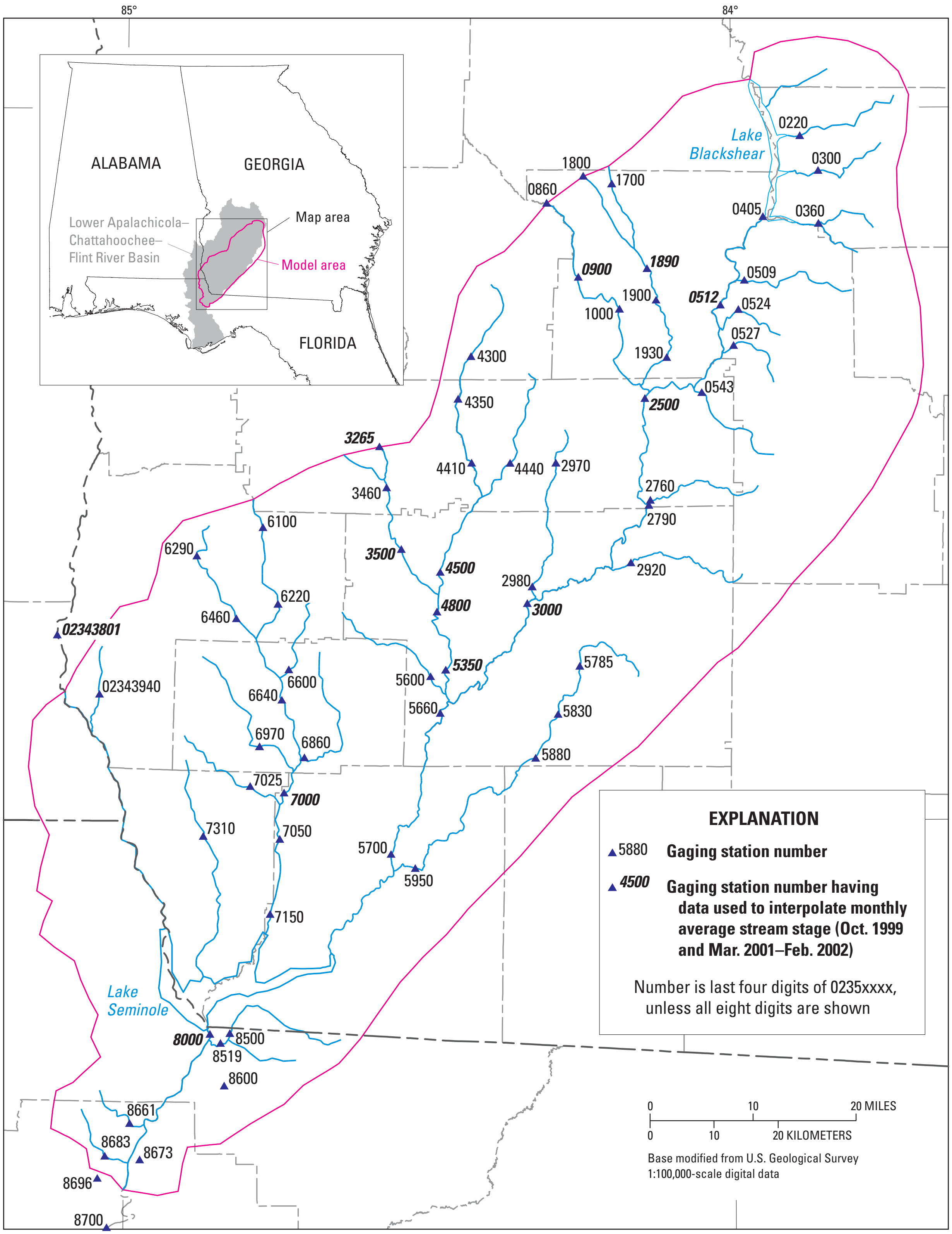

Figure A1. Locations of streamgaging stations in the lower Apalachicola–Chattahoochee–Flint River Basin in southwest Georgia and adjacent parts of Alabama and Florida that were measured and used for the October 1999 model calibration and stations used for interpolating average monthly stream stages for October 1999 and the March 2001–February 2002 transient simulation. (Station names listed in table A1.)

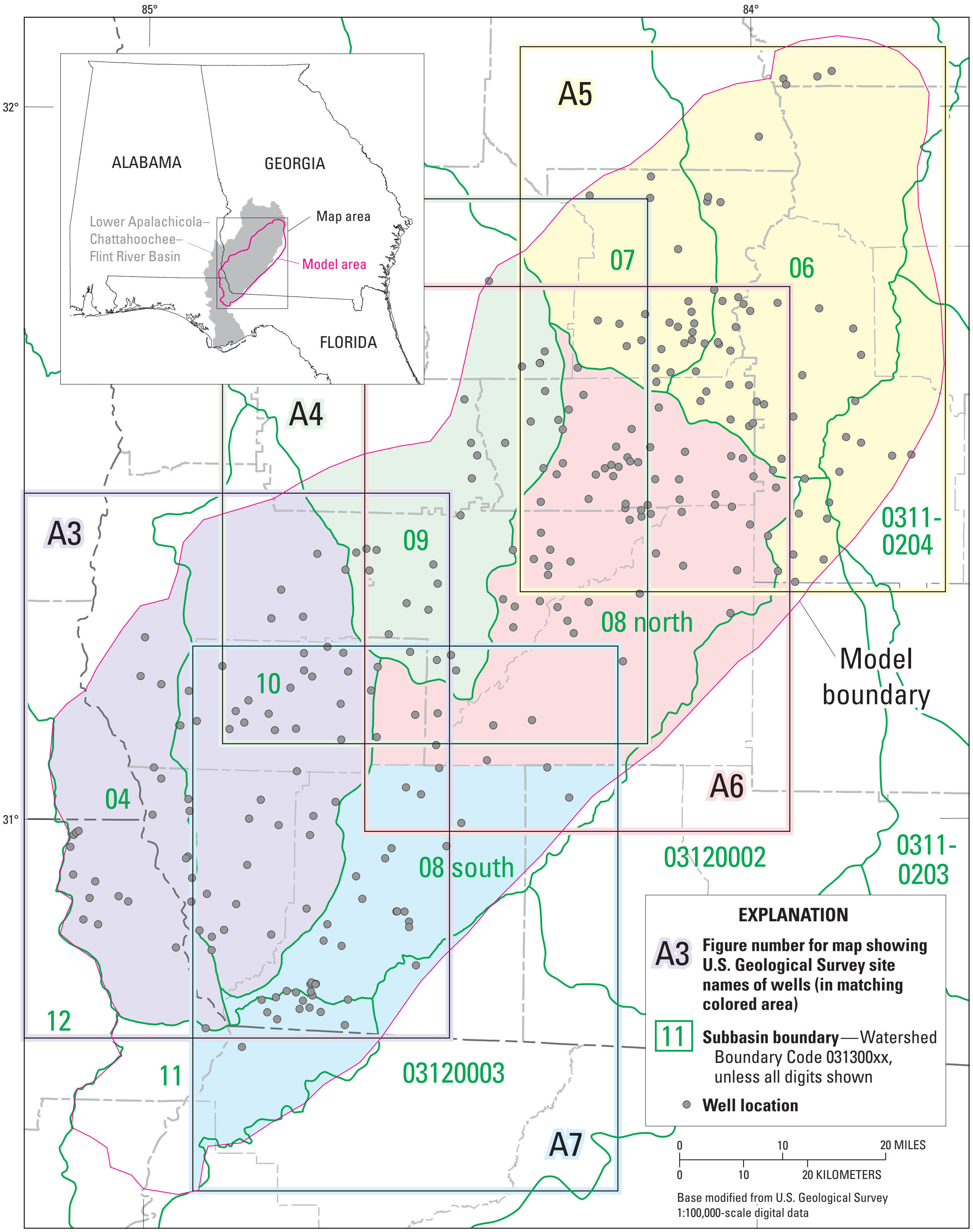

Figure A2. Locations of wells that were measured and water levels simulated for the October 1999 model calibration in southwest Georgia and adjacent parts of Alabama and Florida, and color-coded areas of detail maps (figures A3–A7) that show well numbers. (Wells listed in table A4.)

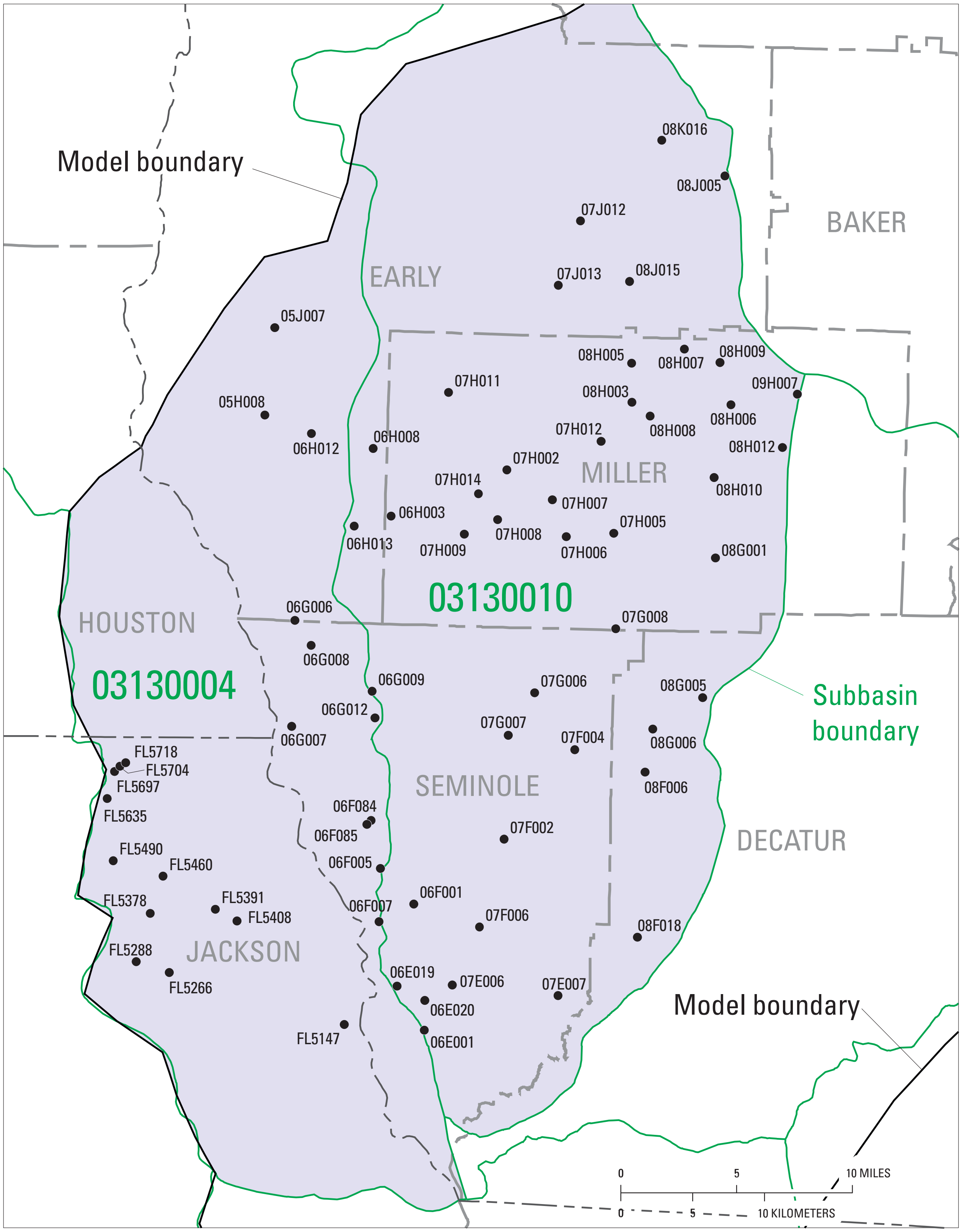

Figure A3. U.S. Geological Survey site names of wells in subbasins 03130004 and 03130010 that were measured and water levels simulated for the October 1999 model calibration. (See figure A2 for map area; wells listed in table A4.)

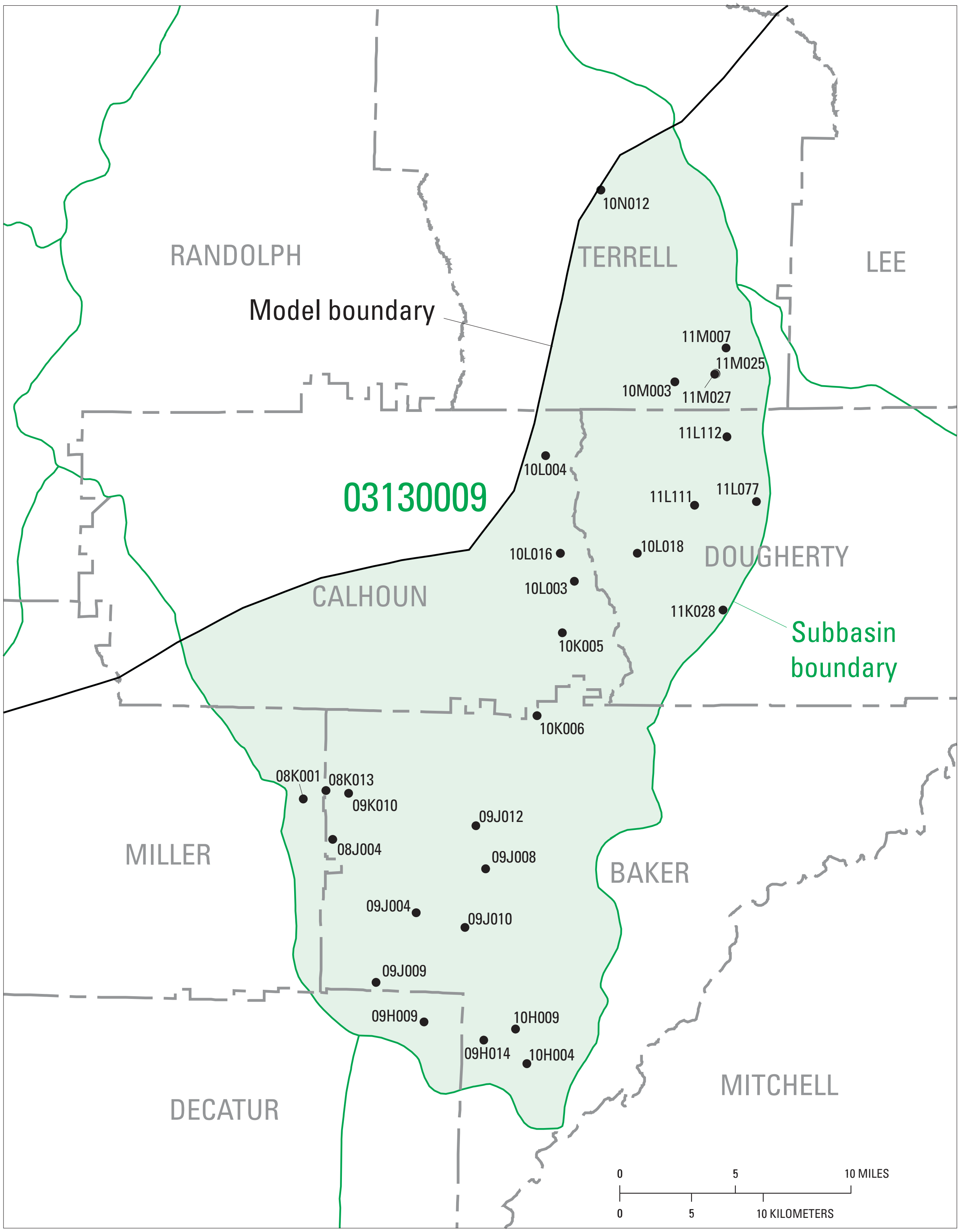

Figure A4. U.S. Geological Survey site names of wells in subbasin 03130009 that were measured and water levels simulated for the October 1999 model calibration. (See figure A2 for map area; wells listed in table A4.)

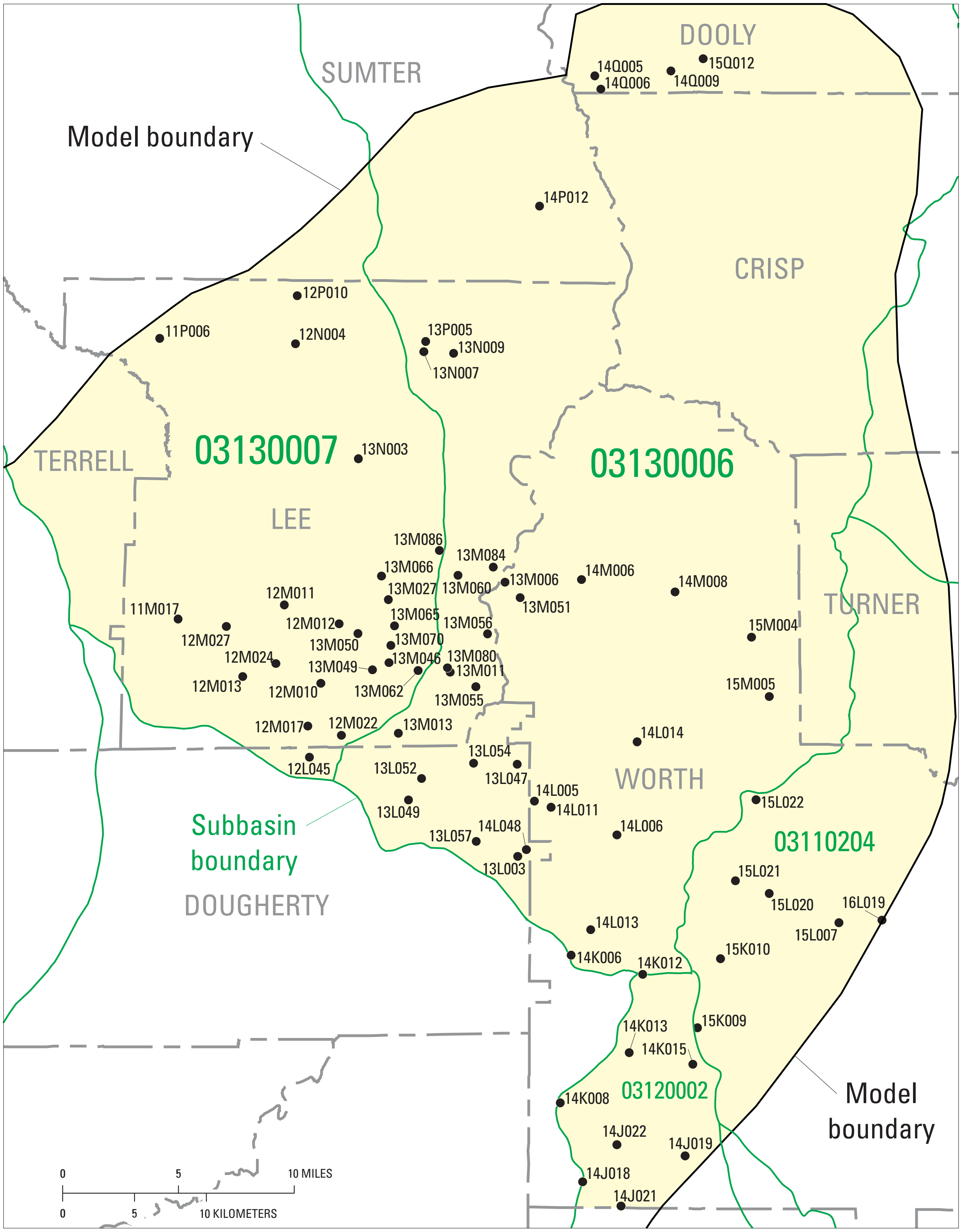

Figure A5. U.S. Geological Survey site names of wells in subbasins 03110204, 03120002, 03130006, and 03130007 that were measured and water levels simulated for the October 1999 model calibration. (See figure A2 for map area; wells listed in table A4.)

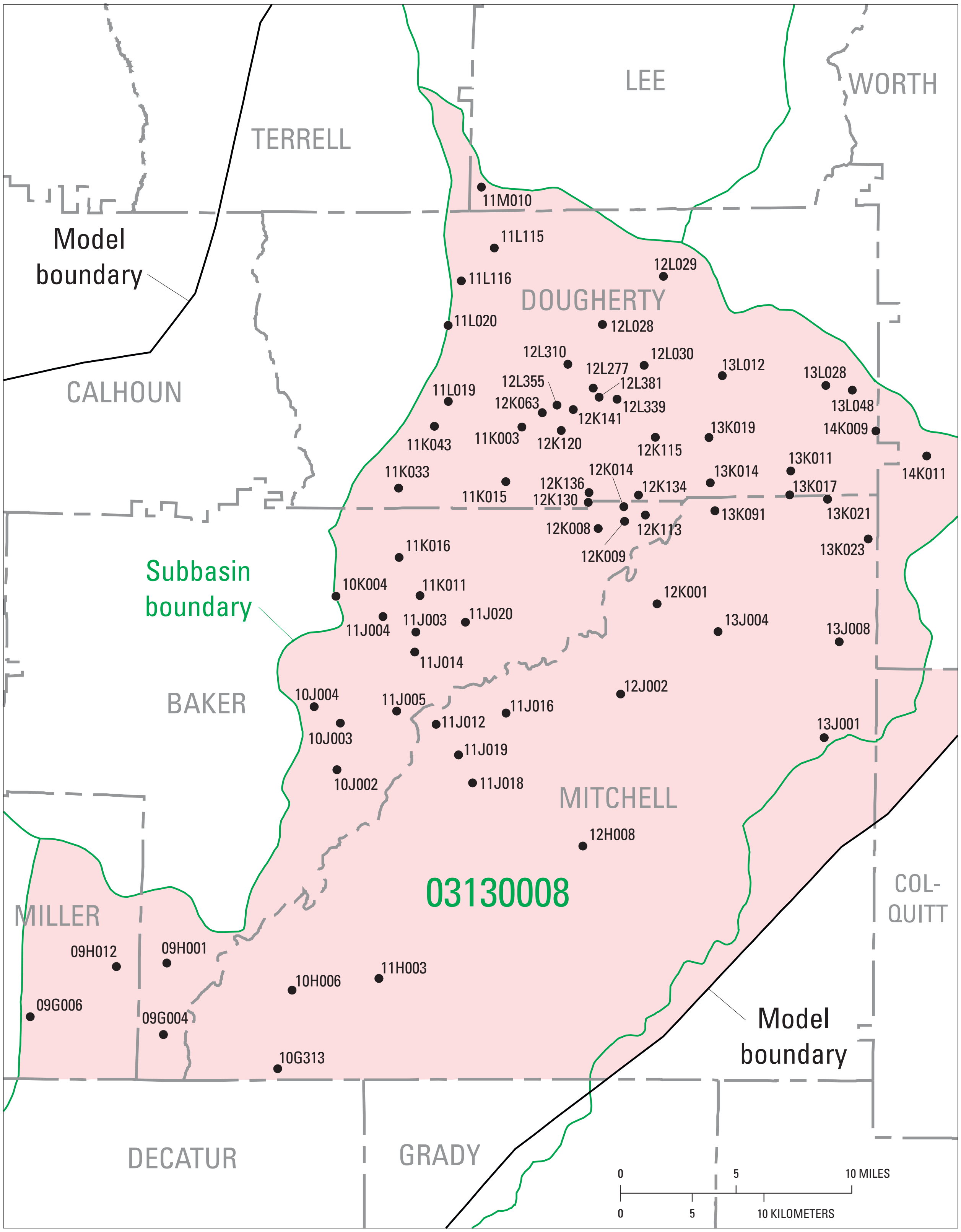

Figure A6. U.S. Geological Survey site names of wells in the northern part of subbasin 03130008 that were measured and water levels simulated for the October 1999 model calibration. (See figure A2 for map area; wells listed in table A4.)

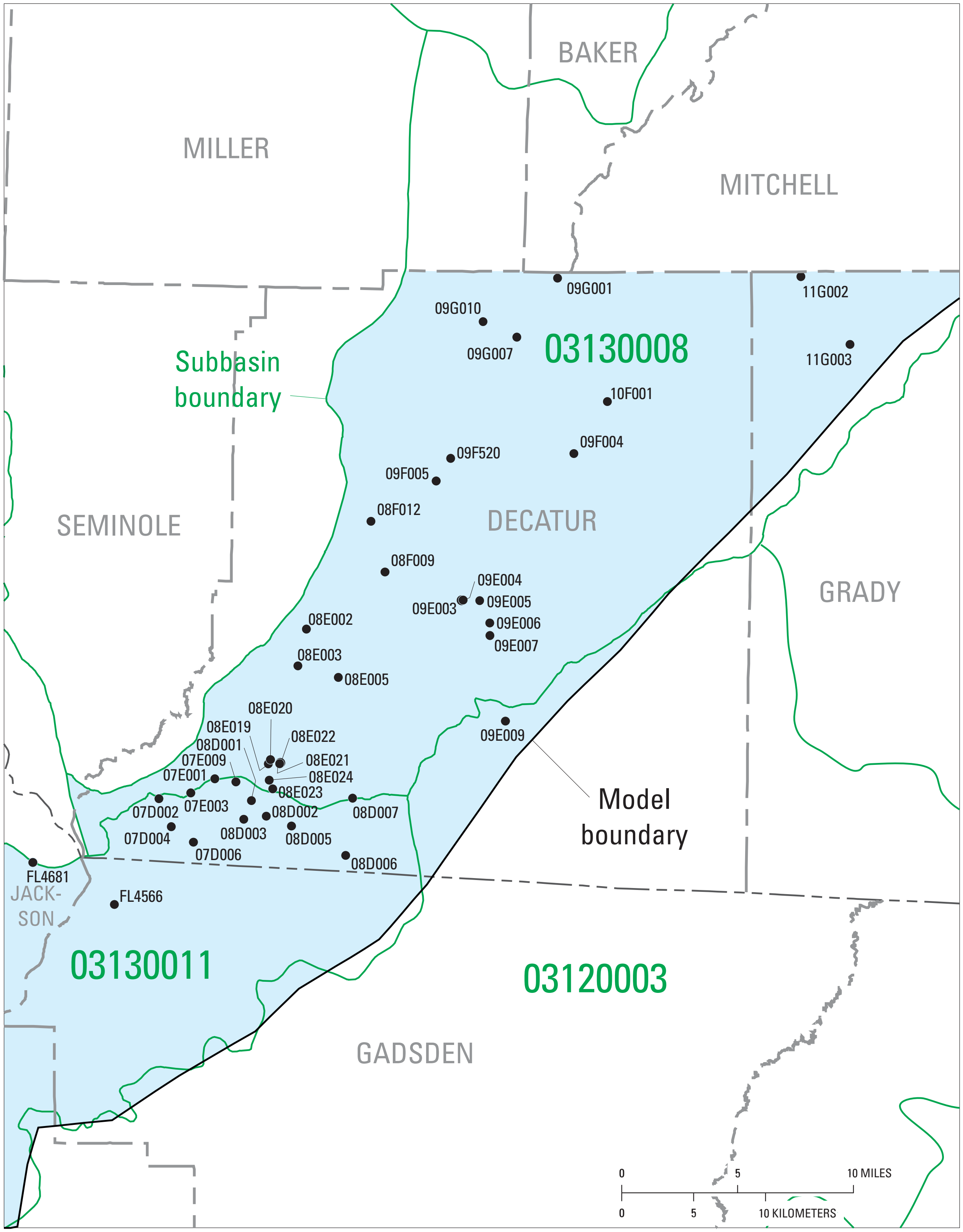

Figure A7. U.S. Geological Survey site names of wells in the southern part of subbasin 03130008 and subbasins 03120003 and 03130011 that were measured and water levels simulated for the October 1999 model calibration. (See figure A2 for map area; wells listed in table A4.)

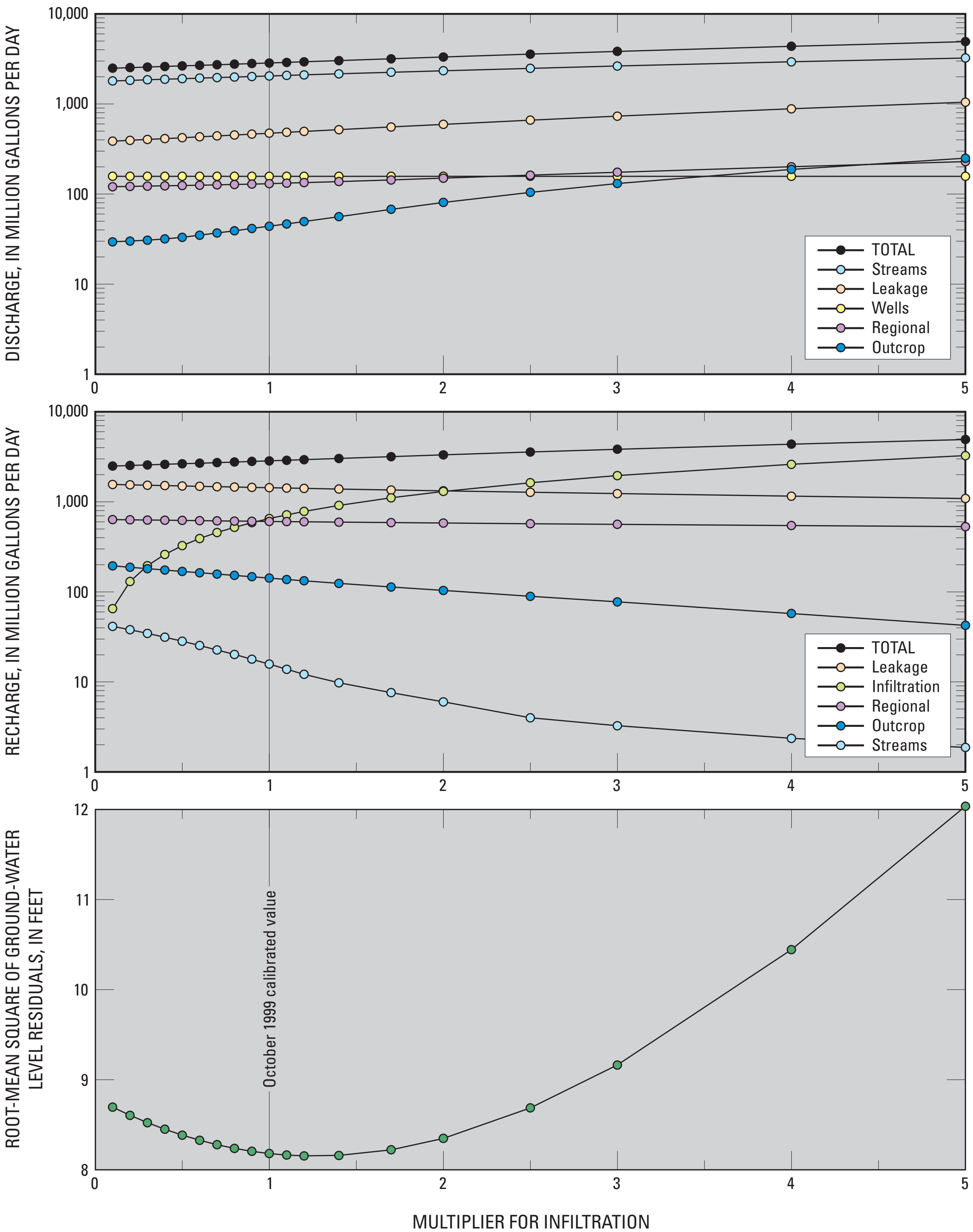

Figure A8. Changes in budget components and root-mean square of ground-water level residuals (simulated minus measured) with respect to simulated changes in infiltration rates.

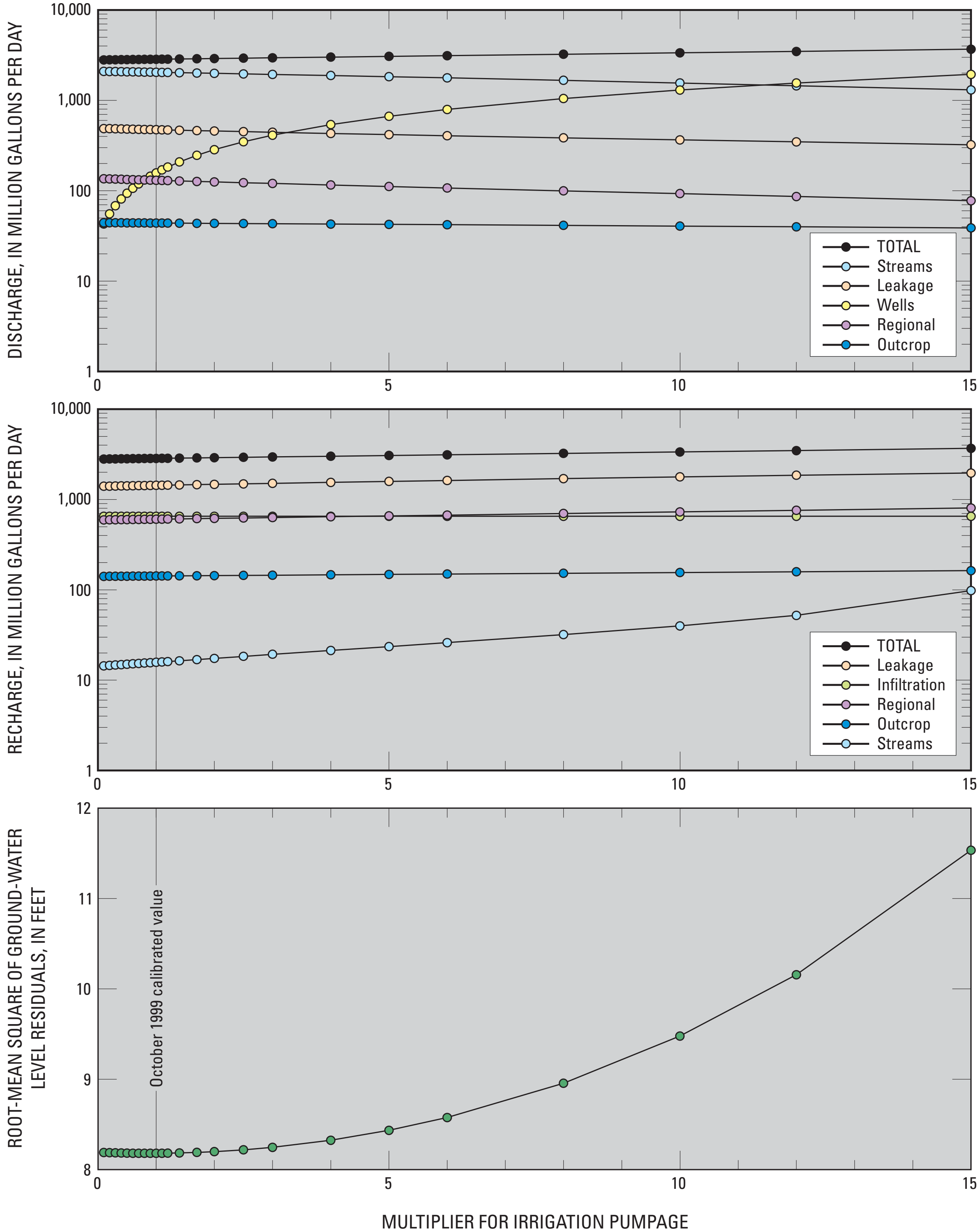

Figure A9. Changes in budget components and root-mean square of ground-water level residuals (simulated minus measured) with respect to simulated changes in irrigation pumpage.

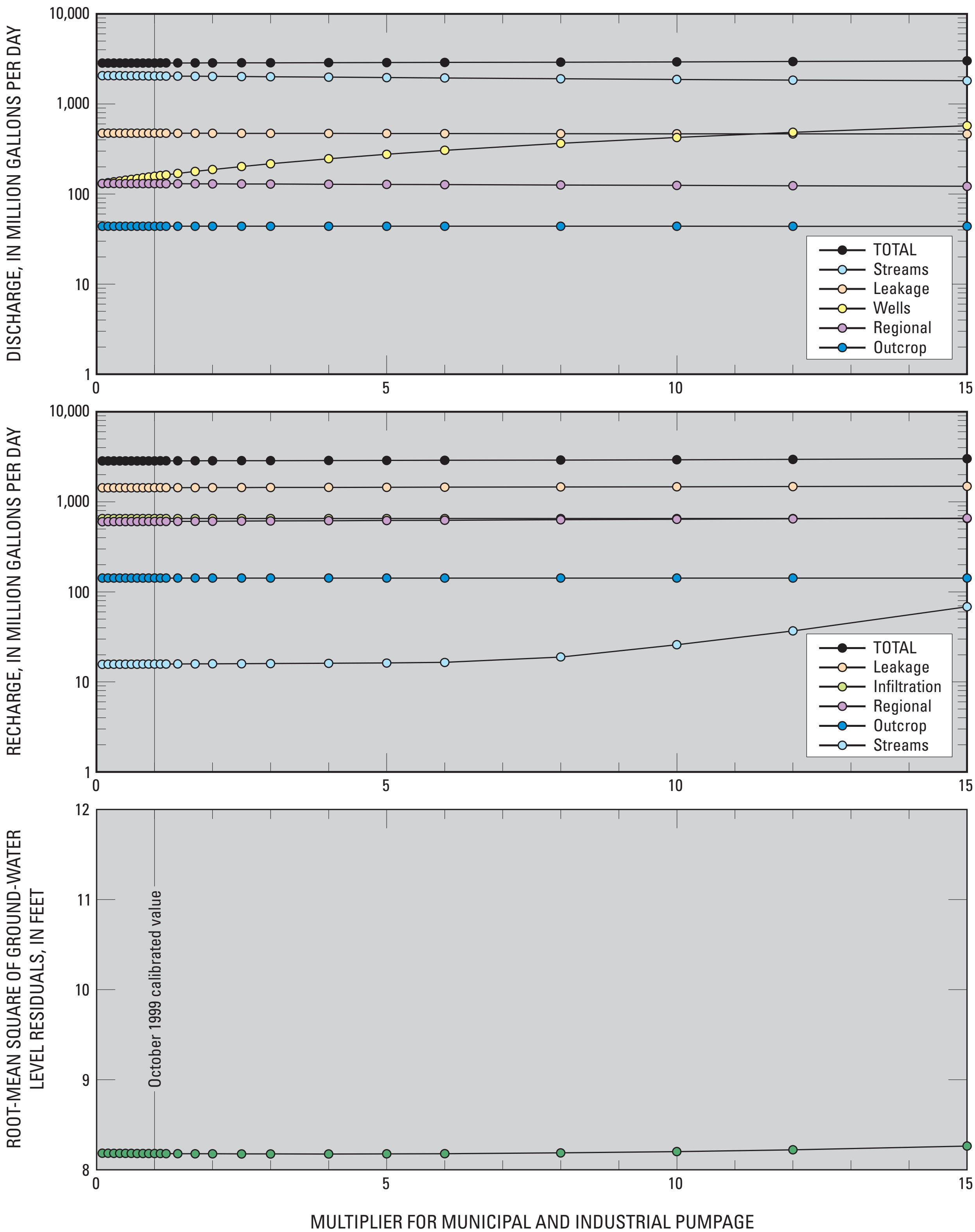

Figure A10. Changes in budget components and root-mean square of ground-water level residuals (simulated minus measured) with respect to simulated changes in municipal and industrial pumpage.

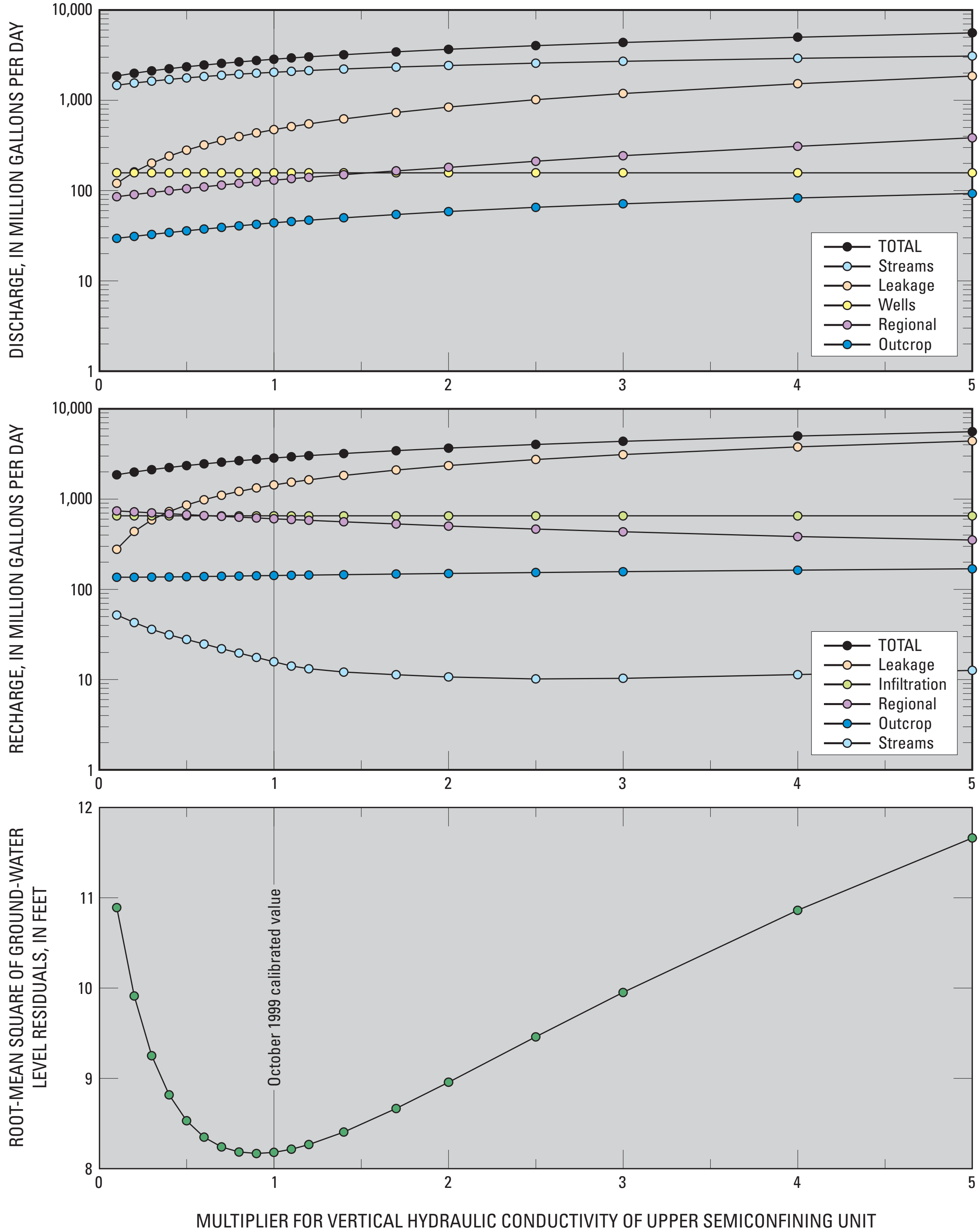

Figure A11. Changes in budget components and root-mean square of ground-water level residuals (simulated minus measured) with respect to simulated changes in vertical hydraulic conductivity of the upper semiconfining unit.

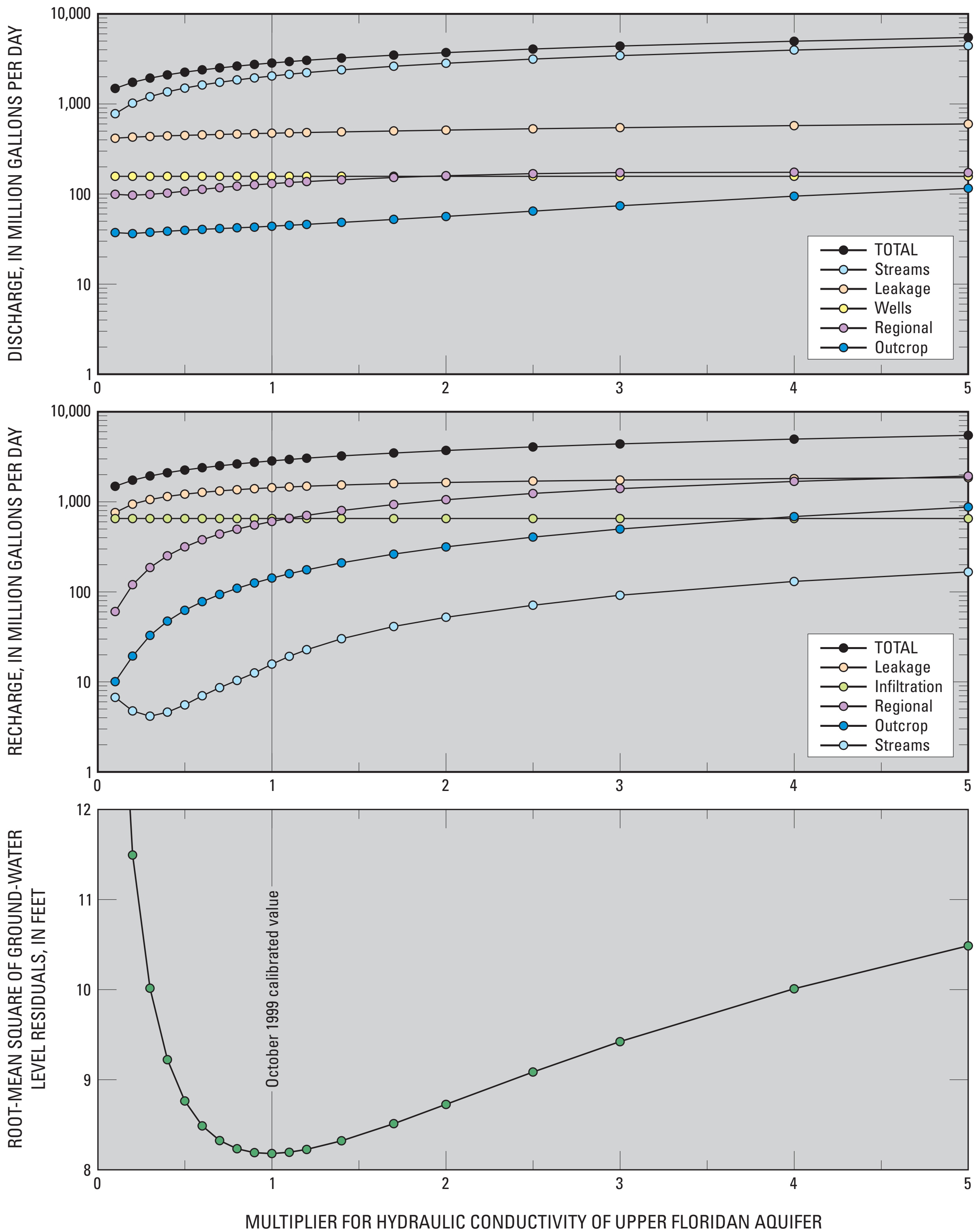

Figure A12. Changes in budget components and root-mean square of ground-water level residuals (simulated minus measured) with respect to simulated changes in hydraulic conductivity of the Upper Floridan aquifer.

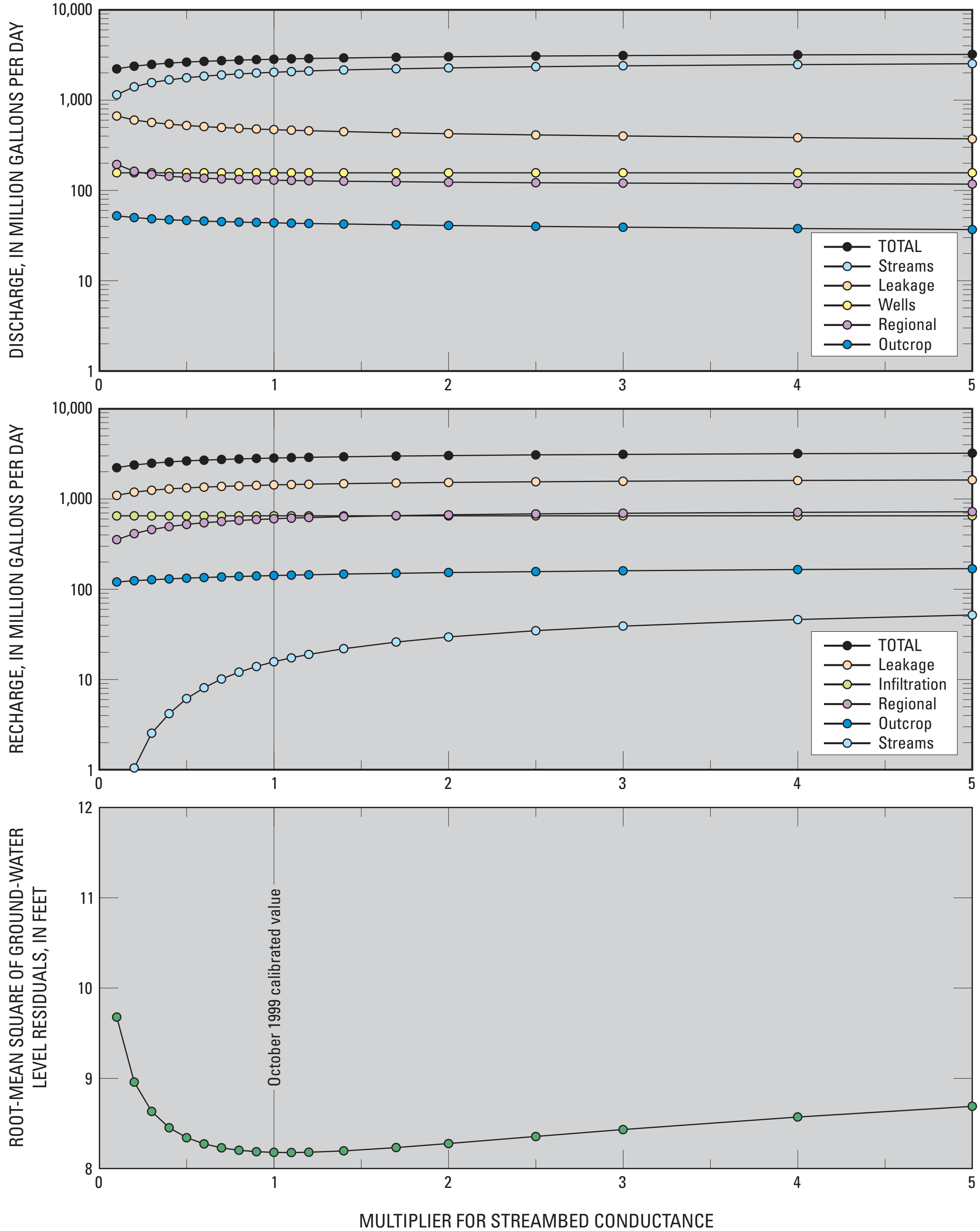

Figure A13. Changes in budget components and root-mean square of ground-water level residuals (simulated minus measured) with respect to simulated changes in streambed conductance, α.

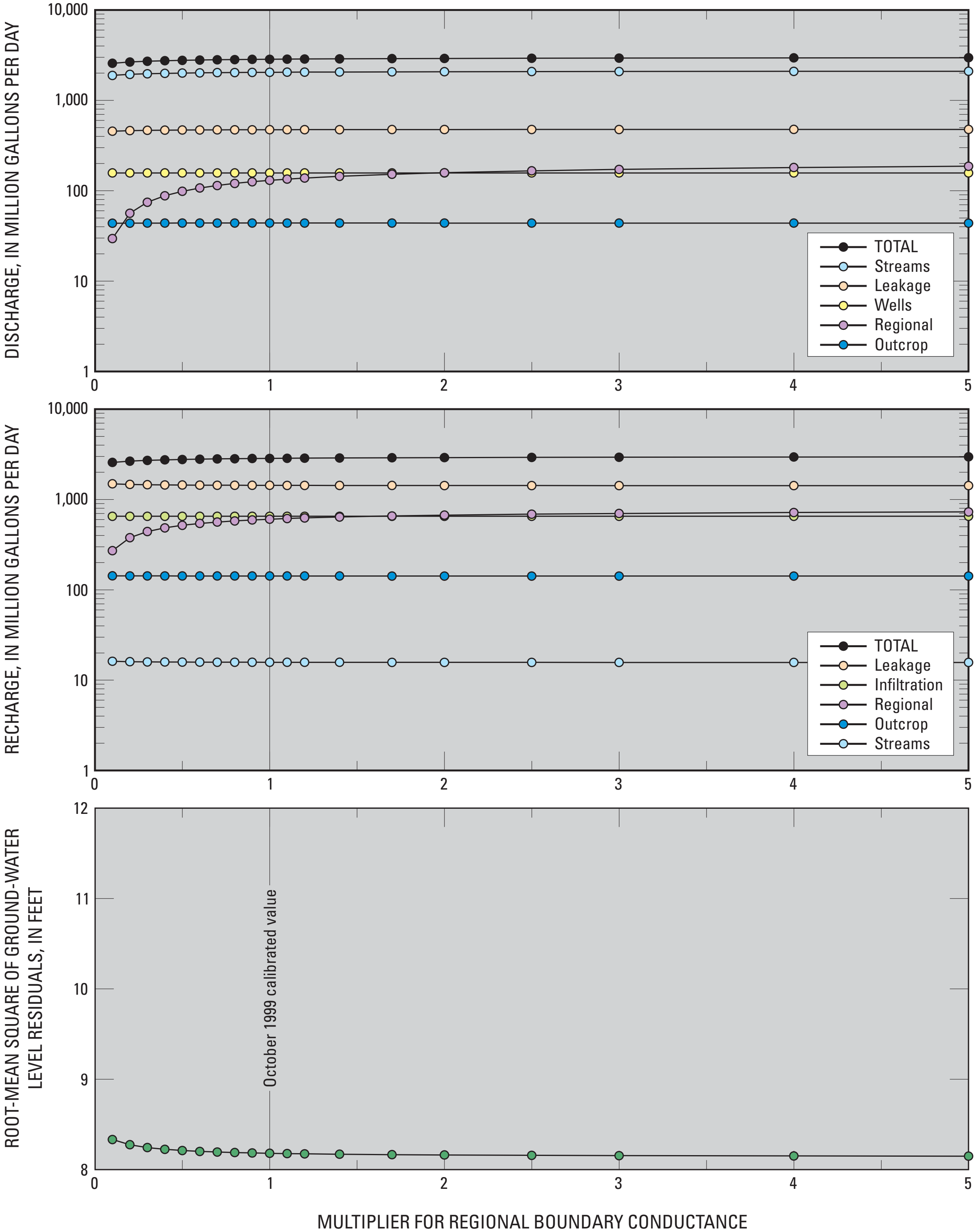

Figure A14. Changes in budget components and root-mean square of ground-water level residuals (simulated minus measured) with respect to simulated changes in regional boundary conductance, α.

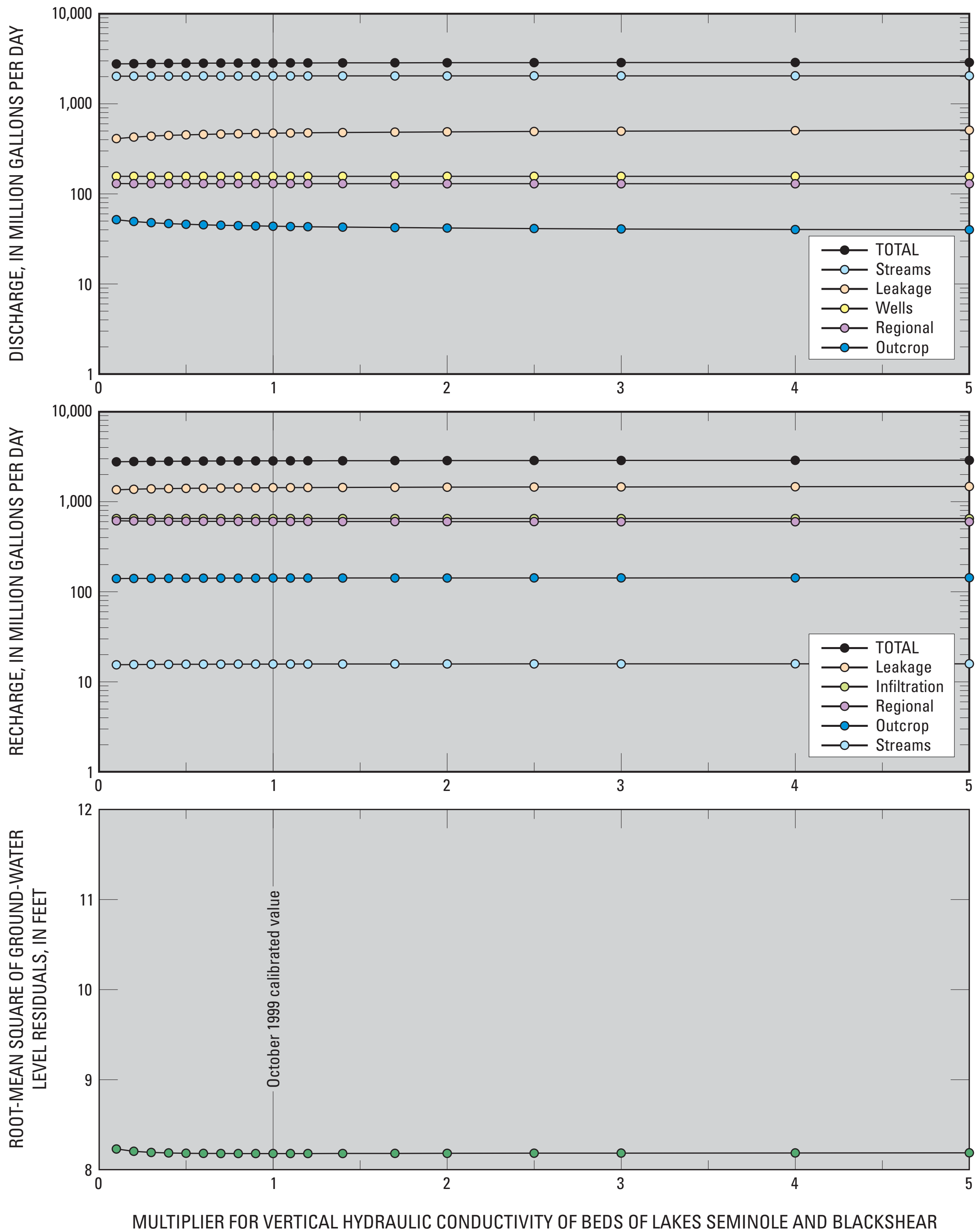

Figure A15. Changes in budget components and root-mean square of ground-water level residuals (simulated minus measured) with respect to simulated changes in vertical hydraulic conductivity of beds of Lakes Seminole and Blackshear.

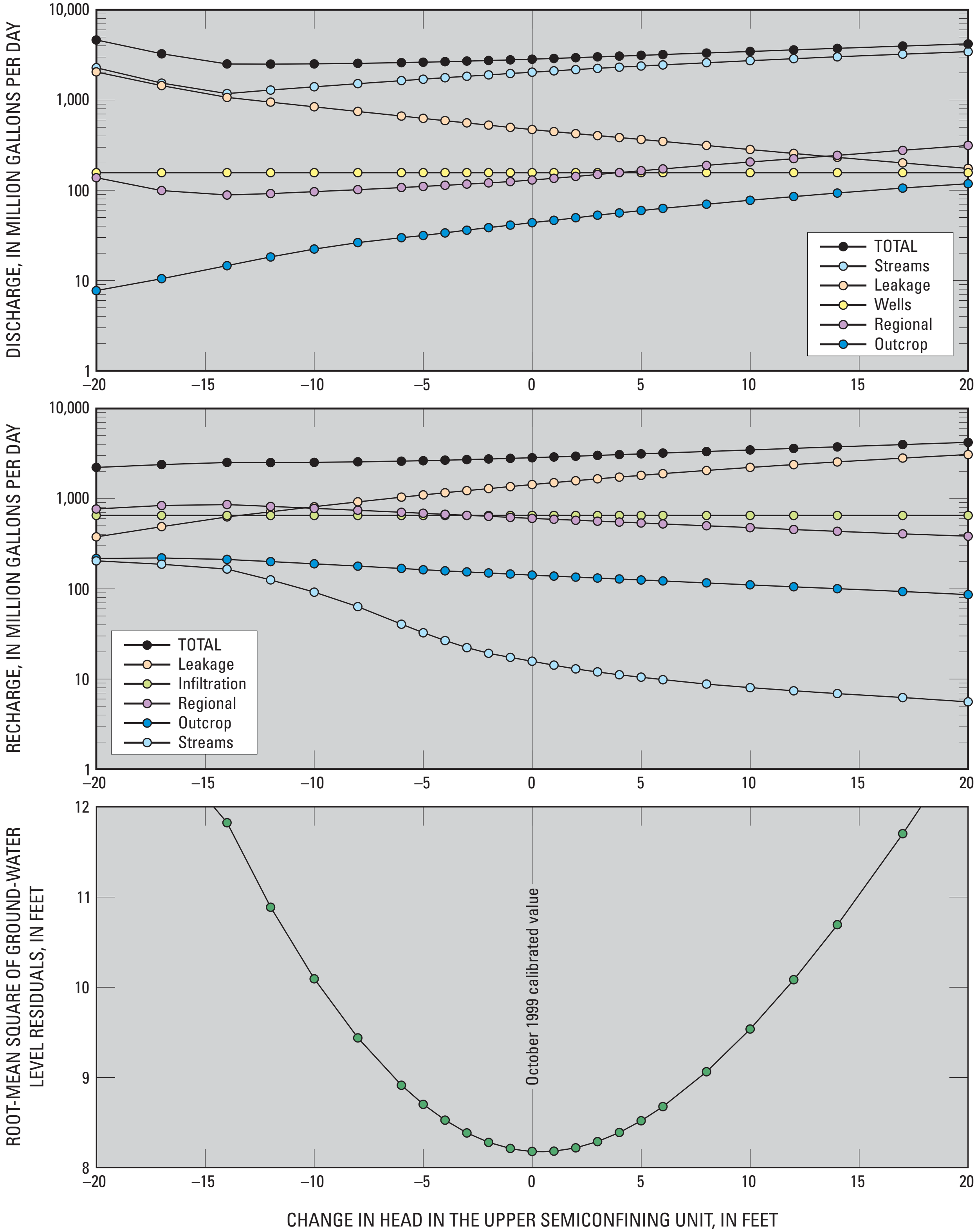

Figure A16. Changes in budget components and root-mean square of ground-water level residuals (simulated minus measured) with respect to simulated changes in head in the upper semiconfining unit.

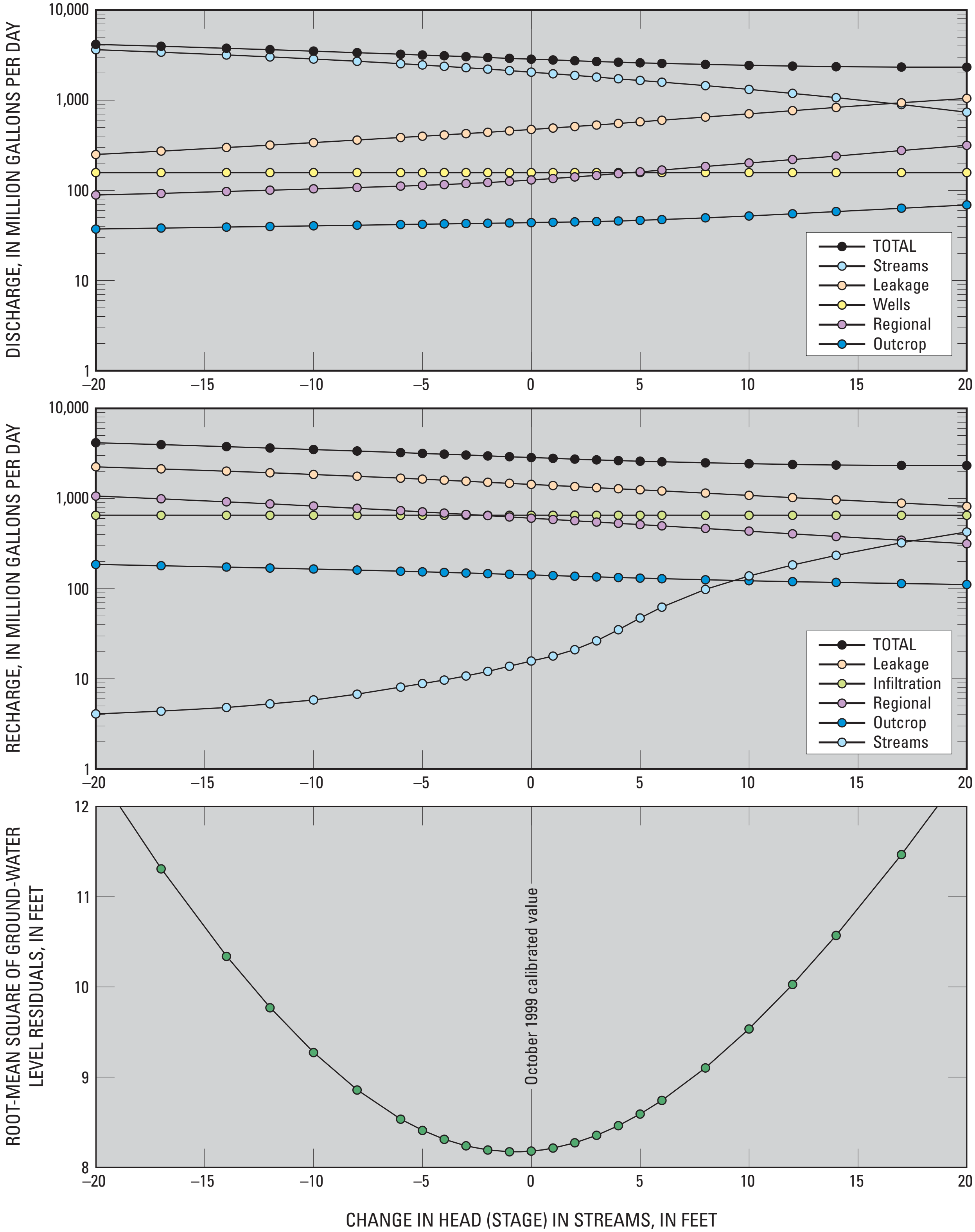

Figure A17. Changes in budget components and root-mean square of ground-water level residuals (simulated minus measured) with respect to simulated changes in head (stage) in streams.

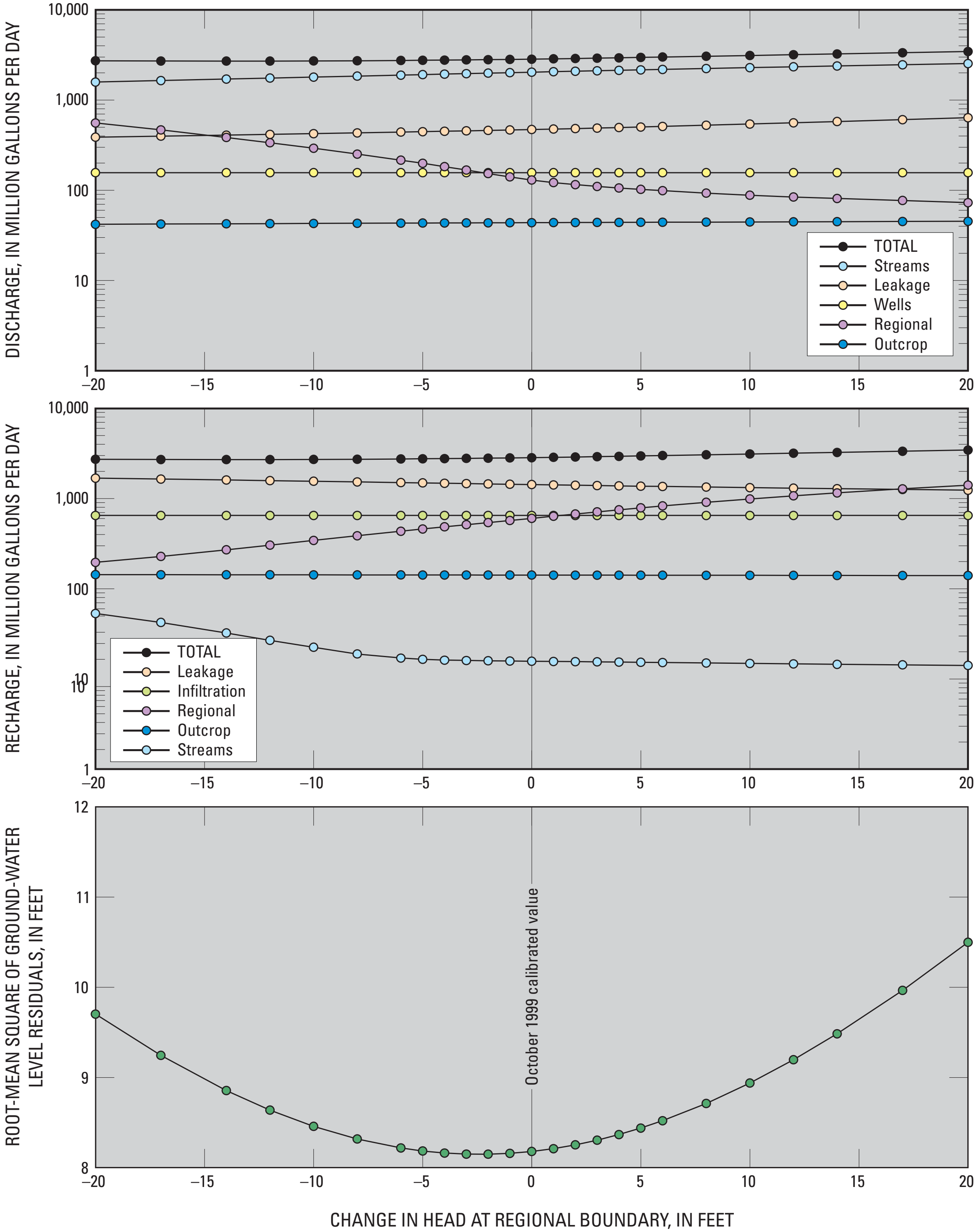

Figure A18. Changes in budget components and root-mean square of ground-water level residuals (simulated minus measured) with respect to simulated changes in head at regional boundary.

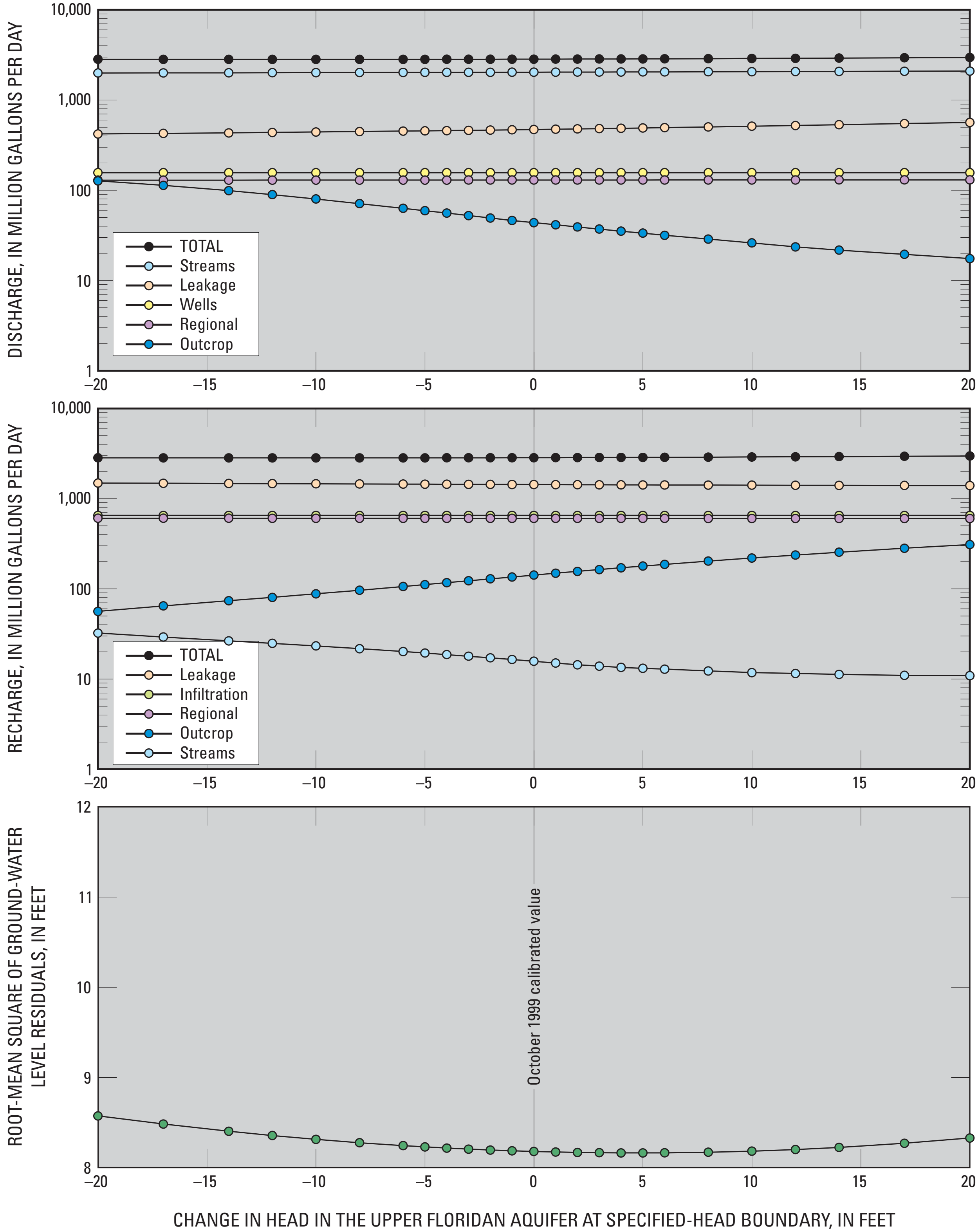

Figure A19. Changes in budget components and root-mean square of ground-water level residuals (simulated minus measured) with respect to simulated changes in head in the Upper Floridan aquifer at the specified-head boundary.

Table A1. Weather stations used for model input.

NOAA, National Oceanic and Atmospheric Administration (2002; 2003); USACE, U.S. Army Corps of Engineers, Mobile District, Water Management Section, accessed January 18, 2004, at, *http://water.sam.usace.army.mil/gage/jwrain.htm*); GAEMN, Georgia Automated Environmental Monitoring Network, the University of Georgia, College of Agriculture and Environmental Sciences, Griffin Experiment Station, Griffin, Ga., accessed September 23, 2003, at *http://georgiaweather.net/*.

Station number (figure 1)	Agency	Station name (index number)
1	NOAA	Cordele (2266)
2	NOAA	Dawson (2570)
3	NOAA	Bainbridge Intl Paper (0586)
4	USACE	Woodruff Lock and Dam
5	NOAA	Albany 3 SE (0140)
6	GAEMN	Arlington, Tony Smith Farm
7	GAEMN	Newton, Jones Center
8	NOAA	Camilla 3 SE (1500)
9	GAEMN	Cordele, Catahoula Farm
10	GAEMN	Dawson, USDA Peanut Lab
11	NOAA	Morgan 5 NW (6043)
12	GAEMN	Lake Seminole, Sneads Landing

Table A2. Streamgaging stations measured for the October 1999 model calibration.

[streamflow in cubic foot per second; °, degree; ', minute; ", second]

Station number	Station name	Latitude (north)	Longitude (west)	Date measured, during 1999	Streamflow
02343801	Chattahoochee River near Columbia, Ala.	31°15'33"	85°06'37"	Oct. 18	[1]2,780
02343940	Sawhatchee Creek at Cedar Springs, Ga.	31°10'41"	85°02'37"	Oct. 18	10.6
02350220	Gum Creek (U.S. Hwy. 280) at Coney, Ga.	31°57'41"	83°53'05"	Oct. 19	10.1
02350300	Cedar Creek near Cordele, Ga.	31°54'46"	83°51'18"	Oct. 19	1.43
02350360	Swift Creek near Warwick, Ga.	31°50'21"	83°51'18"	Oct. 19	10.9
02350405	Flint River near Warwick, Ga.	31°50'57"	83°56'50"	Oct. 21	851
02350509	Jones Creek near Oakfield, Ga.	31°45'34"	83°58'42"	Oct. 18	4.69
02350512	Flint River at Ga. 32, near Oakfield, Ga.	31°43'31"	84°01'07"	Oct. 18	880
02350524	Abrams Creek near Oakfield, Ga.	31°43'08"	83°59'19"	Oct. 18	9.62
02350527	Mill Creek near Albany, Ga.	31°40'05"	83°59'48"	Oct. 18	10.8
02350543	Piney Woods Creek above Albany, Ga.	31°36'09"	84°02'58"	Oct. 18	0.00
02350860	Kinchafoonee Creek (Ga. 118) near Smithville, Ga.	31°52'07"	84°18'18"	Oct. 20	148
02350900	Kinchafoonee Creek near Dawson, Ga.	31°45'53"	84°15'12"	Oct. 20	138
02351000	Kinchafoonee Creek (Ga. Hwy. 32) near Leesburg, Ga.	31°43'11"	84°11'08"	Oct. 18	210
02351700	Muckalee Creek near Smithville, Ga.	31°53'44"	84°11'52"	Oct. 20	85.3
02351800	Muckaloochee Creek at Smithville, Ga.	31°54'20"	84°14'44"	Oct. 20	23.2
02351890	Muckalee Creek at Ga. 195, near Leesburg, Ga.	31°46'35"	84°08'22"	Oct. 18	151
02351900	Muckalee Creek near Leesburg, Ga.	31°43'56"	84°07'30"	Oct. 18	149
02351930	Muckalee Creek below Leesburg, Ga.	31°39'06"	84°06'27"	Oct. 22	126
02352500	Flint River at Albany, Ga.	31°35'40"	84°08'39"	Oct. 21	1,060
02352760	Dry Creek near Putney, Ga.	31°27'05"	84°08'07"	Oct. 18	0.00
02352790	Flint River (Putney Intake) near Putney, Ga.	31°26'40"	84°08'16"	Oct. 22	1,370

Table A2. Streamgaging stations measured for the October 1999 model calibration.—Continued

[streamflow in cubic foot per second; °, degree; ', minute; ", second]

Station number	Station name	Latitude (north)	Longitude (west)	Date measured, during 1999	Streamflow
02352920	Raccoon Creek at Ga. Hwy. 3 near Baconton, Ga.	31°21'49"	84°10'04"	Oct. 18	0.00
02352970	Cooleewahee Creek near Albany, Ga.	31°30'14"	84°17'28"	Oct. 19	0.00
02352980	Cooleewahee Creek near Newton, Ga.	31°19'49"	84°19'50"	Oct. 18	1.93
02353000	Flint River at Newton, Ga.	31°18'25"	84°20'19"	Oct. 22	1,600
02353265	Ichawaynochaway Creek at Ga. 37, Near Morgan, Ga.	31°31'38"	84°34'58"	Oct. 19	122
02353460	Ichawaynochaway Creek at State Rt. 62 near Leary, Ga.	31°28'10"	84°34'15"	Oct. 19	211
02353500	Ichawaynochaway Creek at Milford, Ga.	31°22'59"	84°32'52"	Oct. 18	239
02354300	Chickasawhatchee Creek near Dawson, Ga.	31°39'11"	84°25'46"	Oct. 20	13.0
02354350	Chickasawhatchee Creek near Albany, Ga.	31°35'38"	84°27'12"	Oct. 19	17.2
02354410	Chickasawhatchee Creek near Leary, Ga.	31°30'14"	84°25'50"	Oct. 19	2.97
02354440	Kiokee Creek near Pretoria, Ga.	31°30'14"	84°22'01"	Oct. 19	0.00
02354500	Chickasawhatchee Creek at Elmodel, Ga.	31°21'03"	84°28'57"	Oct. 18	8.50
02354800	Ichawaynochaway Creek near Elmodel, Ga.	31°17'43"	84°29'17"	Oct. 18	292
02355350	Ichawaynochaway Creek below Newton, Ga.	31°12'49"	84°28'24"	Oct. 18	307
02355600	Big Cypress Creek near Newton, Ga.	31°12'15"	84°29'53"	Oct. 18	0.00
02355660	Flint River near Camilla, Ga.	31°09'09"	84°28'57"	Oct. 21	2,270
02355700	Flint River (Aux.) above Bainbridge, Ga.	30°57'16"	84°33'47"	Oct. 21	2,750
02355785	Big Slough (SR 97) near Camilla, Ga.	31°13'07"	84°15'08"	Oct. 18	0.00
02355830	Big Slough (SR 65) below Camilla, Ga.	31°09'03"	84°17'19"	Oct. 18	0.00
02355880	Big Slough at Ga. 179 near Pelham, Ga.	31°05'25"	84°19'32"	Oct. 18	0.00
02355950	Big Slough at Ga. Hwy. 97 near Bainbridge, Ga.	30°56'06"	84°31'23"	Oct. 18	0.00
02356100	Spring Creek near Arlington, Ga.	31°24'48"	84°46'33"	Oct. 18	0.30
02356220	Spring Creek at Ga. Hwy. 200 at Damascus, Ga.	31°18'21"	84°44'59"	Oct. 18	3.62
02356290	Dry Creek near Blakely, Ga.	31°22'23"	84°52'59"	Oct. 18	1.17
02356460	Dry Creek at Hentown, Ga.	31°17'03"	84°49'10"	Oct. 18	7.64
02356600	Long Branch near Colquitt, Ga.	31°12'50"	84°43'54"	Oct. 18	0.00
02356640	Spring Creek at U.S. 27, at Colquitt, Ga.	31°10'15"	84°44'34"	Oct. 18	25.6
02356860	Big Drain Creek (SR 310) near Boykin, Ga.	31°05'24"	84°42'20"	Oct. 19	0.00
02356970	Aycocks Creek below Colquitt, Ga.	31°06'20"	84°46'46"	Oct. 19	0.00
02357000	Spring Creek near Iron City, Ga.	31°02'24"	84°44'18"	Oct. 19	34.2
02357025	Dry Creek near Iron City, Ga.	31°02'58"	84°47'40"	Oct. 19	0.00
02357050	Spring Creek (U.S. Hwy. 84) at Brinson, Ga.	30°58'31"	84°44'44"	Oct. 19	88.4
02357150	Spring Creek near Reynoldsville, Ga.	30°54'14"	84°44'57"	Oct. 19	158
02357310	Fishpond Drain near Donalsonville, Ga.	30°58'45"	84°52'17"	Oct. 19	0.00
02358000	Apalachicola River at Chattahoochee, Fla.	30°42'04"	84°51'33"	Oct. 18	5,630
02358500	North Mosquito Creek at Chattahoochee, Fla.	30°42'08"	84°49'35"	Oct. 18	44.4
02358519	Mosquito Creek at Chattahoochee, Fla.	30°41'19"	84°50'30"	Oct. 18	46.2
02358600	Flat Creek near Chattahoochee, Fla.	30°37'43"	84°50'06"	Oct. 18	18.6
02358661	Ocheesee Creek near Altha, Fla.	30°34'31"	84°59'22"	Oct. 18	7.74
02358673	Sweetwater Creek near Rock Bluff, Fla.	30°31'29"	84°58'22"	Oct. 18	31.0
02358683	Graves Creek at Selman, Fla.	30°31'44"	85°01'48"	Oct. 18	14.9
02358696	Stafford Creek near Selman, Fla.	30°29'54"	85°02'31"	Oct. 18	6.63
02358700	Apalachicola River near Blountstown, Fla.	30°25'30"	85°01'53"	Oct. 18	6,400

[1]Stage only used for estimating nodal stream stages

Table A3. Average monthly stream-stage and lake-level altitudes from March 2001 to February 2002 at continuous-record streamgaging stations used to estimate stage at nodes representing head-dependent flux boundary streams.

[NAVD 88, North American Vertical Datum of 1988; gage datums of station numbers in italics estimated from topographic maps and are different than the datums in Gotvald and others (2005).]

Station number or lake	Altitude of average monthly stream stage or lake level, in feet above NAVD 88											
	2001										2002	
	Mar.	Apr.	May	June	July	Aug.	Sept.	Oct.	Nov.	Dec.	Jan.	Feb.
02343801	89.97	81.51	78.35	80.63	78.18	78.14	77.16	76.79	76.70	76.78	77.79	79.40
02350512	198.20	193.71	189.77	192.17	189.82	188.98	188.84	188.51	188.82	189.34	189.91	190.90
02350900	220.93	218.33	215.37	216.50	215.34	214.81	215.05	214.51	215.18	215.89	216.02	216.64
02351890	221.86	219.90	216.53	218.03	217.55	216.79	217.26	216.34	217.05	217.96	217.99	218.36
02352500	163.3	157.92	153.44	155.53	153.73	152.89	152.9	152.38	152.47	153.33	153.80	154.67
02353000	124.88	120.73	115.77	117.79	115.91	114.69	114.58	114.01	113.94	115.13	115.68	116.78
02353265	196.00	195.00	194.00	193.64	192.28	192.23	192.78	192.44	192.77	193.6	194.16	193.82
02353500	153.49	152.64	151.58	151.88	151.08	151.05	151.44	151.28	151.51	151.82	151.86	151.90
02354500	142.00	141.03	138.11	138.63	137.68	137.49	137.46	137.42	137.39	137.65	137.98	138.16
02354800	130.57	129.29	126.59	127.25	125.91	125.71	125.93	125.68	125.80	126.33	126.51	126.71
02355350	105.87	104.66	101.99	102.59	101.27	100.99	101.18	100.90	100.99	101.58	101.78	102.01
02357000	102.34	101.55	97.12	97.61	96.23	95.78	95.38	95.14	95.07	95.36	95.63	96.01
02358000	57.08	49.66	42.69	45.59	42.43	41.73	40.40	39.79	39.68	40.51	41.35	43.69
Lake Blackshear	236.6	236.6	236.7	236.8	236.9	236.7	236.8	236.8	236.9	237.0	236.9	236.6
Lake Seminole	77.36	77.29	76.82	77.39	76.99	76.78	76.67	76.43	76.24	76.30	76.61	76.72

Table A4. Measured, simulated, and residual water levels and location of wells measured for the October 1999 model calibration.

[USGS, U.S. Geological Survey; NAVD 88, North American Vertical Datum of 1988; °, degree; '. minute; ", second; –, minus]

USGS site name	Latitude (north)	Longitude (west)	Date measured, during 1999	Water level, in feet above NAVD 88		
				Measured	Simulated	Residual
05H008	31°21'08"	84°37'59"	Oct. 18	162.62	151.01	–11.61
05J007	31°06'25"	84°31'23"	Oct. 17	166.40	169.54	3.14
06E001	31°09'06"	84°31'14"	Oct. 17	77.21	76.47	–0.74
06E019	31°13'36"	84°31'19"	Oct. 19	75.68	77.58	1.90
06E020	31°18'23"	84°34'18"	Oct. 26	80.53	77.18	–3.35
06F001	31°20'02"	84°31'14"	Oct. 26	76.71	80.33	3.62
06F005	31°15'46"	84°36'04"	Oct. 17	86.48	81.91	–4.57
06F007	31°17'50"	84°32'09"	Oct. 17	77.97	78.74	0.77
06F084	31°21'39"	84°31'40"	Oct. 18	91.95	85.60	–6.35
06F085	31°22'52"	84°37'17"	Oct. 19	78.54	85.04	6.50
06G006	31°12'43"	84°29'25"	Oct. 18	94.03	95.8	1.77
06G007	31°14'01"	84°29'55"	Oct. 06	84.35	83.96	–0.39
06G008	31°16'21"	84°23'45"	Oct. 25	93.86	95.62	1.76
06G009	31°18'06"	84°23'36"	Oct. 18	97.76	99.78	2.02
06G012	31°18'43"	84°24'45"	Oct. 18	102.90	97.24	–5.66
06H003	31°22'52"	84°23'47"	Oct. 18	137.67	143.53	5.86
06H008	31°21'31"	84°20'16"	Oct. 19	153.05	150.11	–2.94
06H012	31°18'33"	84°21'07"	Oct. 19	153.88	151.77	–2.11

Table A4. Measured, simulated, and residual water levels and location of wells measured for the October 1999 model calibration.—Continued

[USGS, U.S. Geological Survey; NAVD 88, North American Vertical Datum of 1988; °, degree; '. minute; ", second; –, minus]

USGS site name	Latitude (north)	Longitude (west)	Date measured, during 1999	Water level, in feet above NAVD 88		
				Measured	Simulated	Residual
06H013	31°20'46"	84°20'19"	Oct. 25	135.36	141.59	6.23
07D002	31°22'53"	84°20'05"	Oct. 19	73.63	73.30	–0.33
07D004	31°25'23"	84°12'13"	Oct. 19	70.79	71.52	0.73
07D006	31°26'12"	84°11'05"	Oct. 19	69.98	71.62	1.64
07E001	31°25'53"	84°10'08"	Oct. 19	66.65	75.20	8.55
07E003	31°26'22"	84°12'39"	Oct. 19	68.67	74.24	5.57
07E006	31°28'54"	84°27'51"	Oct. 05	78.04	77.42	–0.62
07E007	31°30'50"	84°27'19"	Oct. 20	69.71	77.19	7.48
07E009	31°31'53"	84°27'56"	Oct. 20	75.42	75.30	–0.12
07F002	30°44'21"	84°50'00"	Oct. 20	85.89	85.86	–0.03
07F004	30°44'55"	84°48'29"	Oct. 20	78.30	93.34	15.04
07F006	30°43'16"	84°47'00"	Oct. 22	73.82	79.65	5.83
07G006	30°43'56"	84°47'59"	Oct. 27	96.91	102.56	5.65
07G007	30°43'17"	84°46'59"	Oct. 27	100.67	98.78	–1.89
07G008	30°45'40"	84°46'03"	Oct. 20	104.66	106.01	1.35
07H002	30°45'08"	84°47'06"	Oct. 20	148.49	141.58	–6.91
07H005	30°45'51"	84°45'45"	Oct. 21	142.16	120.63	–21.53
07H006	30°45'33"	84°45'08"	Oct. 21	134.74	123.96	–10.78
07H007	30°44'51"	84°44'27"	Oct. 20	135.46	132.97	–2.49
07H008	30°44'16"	84°43'48"	Oct. 27	130.90	136.19	5.29
07H009	30°44'09"	84°44'47"	Oct. 27	129.72	135.74	6.02
07H011	30°43'54"	84°42'42"	Oct. 27	147.79	152.26	4.47
07H012	30°42'48"	84°40'20"	Oct. 27	136.68	136.95	0.27
07H014	30°44'57"	84°40'02"	Oct. 27	134.54	140.87	6.33
07J012	30°51'18"	84°42'04"	Nov. 17	164.85	164.77	–0.08
07J013	30°49'55"	84°42'26"	Oct. 21	147.41	152.04	4.63
08D001	30°49'29"	84°40'40"	Nov. 17	72.21	74.94	2.73
08D002	30°46'14"	84°43'43"	Oct. 20	88.05	74.77	–13.28
08D003	30°46'23"	84°43'37"	Oct. 20	66.74	74.25	7.51
08D005	30°46'16"	84°43'12"	Oct. 20	74.29	74.95	0.66
08D006	30°46'14"	84°43'13"	Oct. 20	75.40	75.38	–0.02
08D007	30°45'18"	84°43'31"	Oct. 21	73.83	75.89	2.06
08E002	30°45'37"	84°43'40"	Oct. 27	77.82	77.59	–0.23
08E003	30°45'34"	84°48'31"	Oct. 20	71.98	77.00	5.02
08E005	30°45'18"	84°44'22"	Oct. 20	74.91	76.41	1.50
08E019	30°45'57"	84°42'16"	Oct. 27	81.83	75.90	–5.93
08E020	30°58'49"	84°43'48"	Oct. 19	77.98	75.98	–2.00
08E021	30°53'27"	84°38'38"	Oct. 21	68.65	75.93	7.28
08E022	30°55'21"	84°39'15"	Nov. 17	67.14	75.92	8.78
08E023	30°52'37"	84°44'07"	Oct. 21	63.12	75.43	12.31
08E024	31°01'37"	84°41'17"	Oct. 19	89.31	75.58	–13.73
08F006	30°52'23"	84°34'29"	Oct. 26	81.60	86.59	4.99
08F009	30°51'32"	84°34'03"	Oct. 26	82.47	77.76	–4.71
08F012	30°51'04"	84°34'02"	Oct. 26	76.89	80.26	3.37
08F018	30°48'24"	84°33'30"	Oct. 26	76.83	78.28	1.45
08G001	30°47'51"	84°33'21"	Oct. 26	110.66	112.93	2.27

Table A4. Measured, simulated, and residual water levels and location of wells measured for the October 1999 model calibration.—Continued

[USGS, U.S. Geological Survey; NAVD 88, North American Vertical Datum of 1988; °, degree; '. minute; ", second; –, minus]

USGS site name	Latitude (north)	Longitude (west)	Date measured, during 1999	Water level, in feet above NAVD 88		
				Measured	Simulated	Residual
08G005	30°57'54"	84°30'22"	Oct. 20	91.99	93.48	1.49
08G006	30°56'52"	84°36'24"	Oct. 20	81.52	91.06	9.54
08H003	30°57'43"	84°35'46"	Oct. 19	123.09	138.27	15.18
08H005	31°04'29"	84°31'05"	Oct. 19	155.87	144.56	–11.31
08H006	31°02'16"	84°32'52"	Oct. 28	128.51	131.81	3.30
08H007	31°02'51"	84°34'21"	Nov. 04	146.20	147.31	1.11
08H008	30°44'58"	84°29'01"	Oct. 21	120.51	135.51	15.00
08H009	30°59'51"	84°28'54"	Oct. 20	152.12	141.82	–10.30
08H010	32°02'28"	83°56'45"	Oct. 19	119.69	124.08	4.39
08H012	32°01'58"	83°56'29"	Oct. 19	122.30	123.57	1.27
08J004	32°02'38"	83°53'22"	Oct. 19	197.15	182.92	–14.23
08J005	32°03'05"	83°51'56"	Oct. 19	205.99	186.24	–19.75
08J015	31°31'53"	84°24'32"	Oct. 25	151.54	151.69	0.15
08K001	31°29'12"	84°15'34"	Oct. 19	211.47	194.12	–17.35
08K013	31°27'09"	84°16'17"	Oct. 19	188.27	193.81	5.54
08K016	31°29'45"	84°20'45"	Oct. 20	193.45	195.94	2.49
09E003	31°26'55"	84°21'01"	Oct. 20	78.99	76.38	–2.61
09E004	31°29'14"	84°19'26"	Oct. 20	79.46	76.40	–3.06
09E005	31°30'10"	84°18'49"	Oct. 19	77.33	76.66	–0.67
09E006	31°33'01"	84°18'49"	Oct. 19	65.69	77.12	11.43
09E007	31°33'49"	84°19'16"	Oct. 19	86.69	77.26	–9.43
09E009	31°36'15"	84°20'34"	Oct. 19	73.99	77.50	3.51
09F004	31°35'55"	84°16'46"	Oct. 20	76.58	80.10	3.52
09F005	31°34'41"	84°18'14"	Oct. 19	72.64	80.42	7.78
09F520	31°29'44"	84°14'40"	Oct. 21	77.25	80.81	3.56
09G001	31°28'48"	84°09'41"	Oct. 21	89.78	79.63	–10.15
09G004	31°29'04"	84°13'50"	Oct. 21	79.53	84.36	4.83
09G006	31°26'44"	84°12'37"	Oct. 21	94.25	109.00	14.75
09G007	31°29'51"	84°13'18"	Oct. 04	75.47	83.28	7.81
09G010	31°33'03"	84°12'00"	Oct. 19	88.34	88.46	0.12
09H001	31°34'51"	84°09'18"	Oct. 19	107.99	93.48	–14.51
09H007	31°31'30"	84°10'10"	Oct. 19	126.25	127.46	1.21
09H009	31°36'59"	84°09'32"	Oct. 20	127.59	122.85	–4.74
09H012	31°30'39"	84°12'25"	Oct. 04	94.26	103.77	9.51
09H014	31°30'15"	84°11'22"	Oct. 19	118.50	111.33	–7.17
09J004	31°30'01"	84°14'01"	Oct. 20	141.27	142.81	1.54
09J008	31°30'19"	84°12'10"	Sept. 02	134.27	137.69	3.42
09J009	31°27'31"	84°03'43"	Oct. 20	152.51	143.11	–9.40
09J010	31°27'05"	84°07'16"	Oct. 19	124.02	138.68	14.66
09J012	31°26'37"	84°03'46"	Oct. 20	144.32	145.09	0.77
09K010	31°28'47"	84°07'19"	Oct. 20	187.90	188.98	1.08
10F001	31°31'06"	84°06'43"	Oct. 19	90.07	81.90	–8.17
10G313	31°30'43"	84°02'09"	Oct. 20	87.70	89.39	1.69
10H004	31°36'41"	84°00'21"	Oct. 20	110.22	103.52	–6.70
10H006	31°30'32"	84°00'59"	Oct. 19	99.27	91.77	–7.50
10H009	31°35'22"	84°05'10"	Oct. 19	125.31	109.96	–15.35

Table A4. Measured, simulated, and residual water levels and location of wells measured for the October 1999 model calibration.—Continued

[USGS, U.S. Geological Survey; NAVD 88, North American Vertical Datum of 1988; °, degree; '. minute; ", second; –, minus]

USGS site name	Latitude (north)	Longitude (west)	Date measured, during 1999	Water level, in feet above NAVD 88		
				Measured	Simulated	Residual
10J002	31°36'10"	84°04'35"	Oct. 20	120.84	118.06	–2.78
10J003	31°36'44"	84°02'17"	Oct. 19	130.41	127.14	–3.27
10J004	31°33'48"	84°02'11"	Oct. 20	138.16	131.67	–6.49
10K004	31°29'00"	83°59'57"	Oct. 20	147.21	150.21	3.00
10K005	31°33'29"	83°59'58"	Oct. 26	167.71	179.81	12.10
10K006	31°12'10"	85°00'33"	Oct. 16	170.70	169.85	–0.85
10L003	31°15'27"	85°00'08"	Oct. 18	183.90	185.82	1.92
10L004	31°04'28"	84°59'11"	Oct. 17	219.53	212.99	–6.54
10L016	31°08'14"	84°56'11"	Oct. 17	192.73	190.66	–2.07
10L018	31°10'56"	84°55'47"	Oct. 17	181.05	185.81	4.76
10M003	31°11'08"	84°56'43"	Oct. 16	245.97	234.36	–11.61
10N012	31°11'29"	84°58'30"	Oct. 16	293.50	296.10	2.60
11G002	31°08'01"	84°56'36"	Oct. 17	97.49	98.33	0.84
11G003	31°19'30"	84°46'42"	Oct. 18	94.23	100.24	6.01
11H003	31°17'05"	84°47'40"	Oct. 18	98.39	102.10	3.71
11J003	31°21'12"	84°40'21"	Oct. 19	146.88	140.01	–6.87
11J004	31°17'14"	84°44'32"	Oct. 18	142.00	144.32	2.32
11J005	31°22'39"	84°39'17"	Oct. 19	122.28	122.56	0.28
11J012	31°22'58"	84°38'17"	Oct. 19	115.36	118.85	3.49
11J014	31°22'32"	84°43'08"	Oct. 19	138.59	136.31	–2.28
11J016	31°04'32"	84°20'25"	Oct. 20	124.59	126.31	1.72
11J018	31°01'59"	84°18'16"	Nov. 17	130.28	121.70	–8.58
11J019	30°52'36"	84°12'52"	Oct. 19	125.79	120.69	–5.10
11J020	31°38'12"	84°17'20"	Oct. 20	122.77	139.03	16.26
11K003	31°42'11"	84°15'19"	Oct. 20	162.09	157.70	–4.39
11K011	31°52'42"	84°16'06"	Oct. 21	142.43	144.89	2.46
11K015	31°39'45"	84°09'01"	Oct. 20	158.60	153.32	–5.28
11K016	31°42'42"	84°10'37"	Oct. 20	142.28	151.14	8.86
11K028	31°41'59"	84°08'12"	Oct. 20	172.55	170.71	–1.84
11K033	31°40'01"	84°12'28"	Oct. 20	166.10	160.23	–5.87
11K043	31°38'09"	84°09'36"	Oct. 19	169.18	165.44	–3.74
11L019	31°37'48"	84°08'07"	Oct. 20	165.31	166.81	1.50
11L020	31°40'30"	84°11'00"	Oct. 20	183.05	180.77	–2.28
11L077	31°41'54"	84°13'11"	Oct. 20	183.88	185.90	2.02
11L111	31°52'29"	84°10'05"	Oct. 20	192.10	188.89	–3.21
11L112	31°54'17"	84°10'00"	Oct. 21	211.8	205.36	–6.44
11L115	31°40'09"	84°03'18"	Oct. 20	192.03	192.42	0.39
11L116	31°37'52"	84°05'36"	Oct. 20	185.64	187.88	2.24
11M007	31°42'53"	84°06'01"	Oct. 20	235.51	231.56	–3.95
11M010	31°40'31"	84°06'00"	Oct. 21	212.84	214.91	2.07
11M017	31°40'15"	84°06'44"	Oct. 21	241.65	214.44	–27.21
11M025	31°41'37"	84°07'22"	Oct. 21	234.28	229.49	–4.79
11M027	31°39'36"	84°02'10"	Oct. 21	234.84	229.51	–5.33
11P006	31°41'35"	84°01'38"	Oct. 21	279.01	274.81	–4.20
12H008	31°40'13"	84°04'43"	Oct. 21	124.31	129.05	4.74
12J002	31°41'54"	84°05'45"	Oct. 21	131.16	137.75	6.59

Table A4. Measured, simulated, and residual water levels and location of wells measured for the October 1999 model calibration.—Continued

[USGS, U.S. Geological Survey; NAVD 88, North American Vertical Datum of 1988; °, degree; '. minute; ", second; –, minus]

USGS site name	Latitude (north)	Longitude (west)	Date measured, during 1999	Water level, in feet above NAVD 88		
				Measured	Simulated	Residual
12K001	31°43'46"	84°06'19"	Oct. 21	138.59	141.24	2.65
12K008	31°41'10"	84°05'55"	Oct. 21	138.66	144.36	5.70
12K009	31°40'19"	84°03'25"	Oct. 21	135.12	143.62	8.50
12K014	31°44'05"	84°01'22"	Oct. 21	136.51	145.05	8.54
12K063	31°44'43"	84°03'45"	Oct. 21	152.26	157.80	5.54
12K113	31°48'10"	84°07'19"	Oct. 21	140.36	142.99	2.63
12K115	31°52'10"	84°04'24"	Oct. 21	146.03	144.57	–1.46
12K120	31°52'06"	84°03'05"	Oct. 21	162.98	154.49	–8.49
12K130	31°52'33"	84°04'19"	Oct. 21	140.90	147.42	6.52
12K134	31°08'24"	84°54'59"	Oct. 17	133.68	144.45	10.77
12K136	31°04'12"	84°45'06"	Oct. 17	145.62	148.02	2.40
12K141	31°10'09"	84°49'54"	Oct. 19	157.80	155.94	–1.86
12L028	31°07'47"	84°45'12"	Oct. 10	160.90	164.59	3.69
12L029	31°07'39"	84°47'17"	Oct. 10	148.27	159.19	10.92
12L030	31°09'02"	84°47'54"	Oct. 17	151.45	151.54	0.09
12L045	31°08'17"	84°50'18"	Oct. 18	181.08	183.34	2.26
12L277	31°07'44"	84°51'46"	Oct. 18	152.45	156.88	4.43
12L310	31°13'03"	84°52'29"	Oct. 18	164.01	162.38	–1.63
12L339	31°11'14"	84°45'46"	Oct. 18	149.87	152.59	2.72
12L355	31°09'15"	84°51'09"	Oct. 18	160.65	157.66	–2.99
12L381	31°06'52"	84°40'44"	Oct. 19	155.00	155.07	0.07
12M010	31°12'42"	84°44'25"	Oct. 18	208.03	201.56	–6.47
12M011	31°14'10"	84°44'26"	Oct. 18	201.63	204.46	2.83
12M012	31°12'37"	84°40'04"	Oct. 18	211.27	209.99	–1.28
12M013	31°14'42"	84°42'07"	Oct. 18	187.33	202.39	15.06
12M017	31°12'11"	84°43'37"	Oct. 17	189.61	191.40	1.79
12M022	31°14'12"	84°40'33"	Oct. 18	170.43	192.14	21.71
12M024	31°09' 53"	84°40'48"	Oct. 18	173.39	194.56	21.17
12M027	31°11'01"	84°37'48"	Oct. 18	205.80	208.75	2.95
12N004	31°05'12"	84°35'31"	Oct. 17	259.84	256.70	–3.14
12P010	31°07'05"	84°37'14"	Oct. 17	270.62	268.56	–2.06
13J001	31°13'01"	84°37'09"	Oct. 19	153.61	156.40	2.79
13J004	31°14'17"	84°33'57"	Oct. 19	137.23	147.82	10.59
13J008	31°08'58"	84°33'27"	Oct. 19	169.79	161.47	–8.32
13K011	31°05'08"	84°26'22"	Oct. 22	150.98	158.56	7.58
13K014	31°08'05"	84°25'44"	Oct. 22	145.64	146.11	0.47
13K017	31°08'31"	84°21'55"	Oct. 21	157.80	157.64	–0.16
13K019	31°18'03"	84°19'23"	Oct. 22	144.73	147.46	2.73
13K021	31°18'28"	84°16'18"	Oct. 21	165.18	163.17	–2.01
13K023	31°15'51"	84°17'47"	Oct. 21	171.80	172.03	0.23
13K091	31°16'54"	84°18'24"	Oct. 21	136.77	146.30	9.53
13L003	31°13'28"	84°12'56"	Oct. 22	184.80	181.81	–2.99
13L012	31°19'10"	84°11'15"	Oct. 22	148.91	152.56	3.65
13L028	31°22'33"	84°09'38"	Oct. 22	171.61	166.61	–5.00
13L047	31°17'30"	84°02'18"	Oct. 22	192.72	207.86	15.14
13L048	31°21'30"	84°06'57"	Oct. 22	178.49	171.62	–6.87

Table A4. Measured, simulated, and residual water levels and location of wells measured for the October 1999 model calibration.—Continued

[USGS, U.S. Geological Survey; NAVD 88, North American Vertical Datum of 1988; °, degree; '. minute; ", second; –, minus]

USGS site name	Latitude (north)	Longitude (west)	Date measured, during 1999	Water level, in feet above NAVD 88		
				Measured	Simulated	Residual
13L049	31°19'18"	84°02'58"	Oct. 22	162.71	169.23	6.52
13L052	31°21'06"	84°01'37"	Oct. 22	182.07	177.13	–4.94
13L054	31°26'27"	84°02'06"	Oct. 22	174.49	190.05	15.56
13L057	31°24'57"	84°00'19"	Oct. 22	159.89	169.88	9.99
13M006	31°26'02"	84°07'04"	Oct. 22	227.10	225.48	–1.62
13M011	30°49'06"	84°53'26"	Oct. 27	229.15	215.07	–14.08
13M013	30°50'45"	84°54'38"	Oct. 19	199.38	198.40	–0.98
13M027	30°50'13"	84°53'25"	Oct. 27	206.78	216.51	9.73
13M046	30°53'50"	84°53'55"	Sept. 14	213.25	209.46	–3.79
13M049	30°55'10"	84°55'23"	Oct. 19	207.94	207.72	–0.22
13M050	30°53'10"	84°55'26"	Oct. 27	220.48	210.45	–10.03
13M051	30°56' 58"	84°55'48"	Oct. 27	219.75	224.36	4.61
13M055	30°56' 49"	84°55'59"	Oct. 27	208.80	214.38	5.58
13M056	31°00'29"	84°59'18"	Oct. 27	221.37	219.13	–2.24
13M060	31°03'32"	84°58'28"	Oct. 27	232.09	223.49	–8.60
13M062	31°01'49"	84°55'47"	Oct. 27	218.49	212.76	–5.73
13M065	31°00'49"	84°55'39"	Oct. 27	226.11	214.62	–11.49
13M066	30°50'48"	84°52'13"	Oct. 27	213.79	218.41	4.62
13M070	30°50'25"	84°47'35"	Oct. 27	220.56	211.87	–8.69
13M080	30°56'17"	84°49'58"	Oct. 27	228.32	215.36	–12.96
13M084	30°59'39"	84°46'53"	Oct. 27	210.73	226.63	15.9
13M086	30°52'59"	84°51'02"	Oct. 27	230.74	224.49	–6.25
13N003	31°02'50"	84°47'27"	Oct. 27	235.58	233.82	–1.76
13N007	31°01'47"	84°48'39"	Oct. 19	271.12	249.35	–21.77
13N009	31°00'11"	84°49'48"	Oct. 27	286.43	247.37	–39.06
13P005	31°57'36"	83°59'14"	Oct. 21	259.59	250.80	–8.79
14J018	31°38'19"	84°22'52"	Oct. 20	180.37	179.85	–0.52
14J019	31°45'31"	84°26'08"	Oct. 20	195.11	203.56	8.45
14J021	31°39'35"	84°20'36"	Oct. 20	180.10	184.17	4.07
14J022	31°38'37"	84°21'04"	Oct. 20	208.71	190.99	–17.72
14K006	31°38'36"	84°21'06"	Oct. 20	205.57	193.64	–11.93
14K008	31°39'19"	83°38'07"	Oct. 20	180.69	181.54	0.85
14K009	31°43'31"	84°00'51"	Oct. 18	191.25	178.46	–12.79
14K011	31°42'56"	84°00'11"	Oct. 18	204.29	193.33	–10.96
14K012	31°21'01"	83°57'34"	Oct. 18	211.25	208.91	–2.34
14K013	31°21'58"	83°53'03"	Oct. 18	188.84	200.78	11.94
14K015	31°20'06"	83°55'53"	Oct. 18	197.08	209.89	12.81
14L005	31°22'24"	83°56'03"	Oct. 18	211.28	204.69	–6.59
14L006	31°29'31"	83°58'01"	Oct. 18	202.81	219.50	16.69
14L011	31°23'59"	83°58'32"	Oct. 18	205.17	208.92	3.75
14L013	31°28'03"	83°57'43"	Oct. 18	207.16	201.06	–6.10
14L014	31°28'47"	83°54'52"	Oct. 18	236.23	236.32	0.09
14L048	31°25'51"	83°55'29"	Oct. 18	188.83	187.27	–1.56
14M006	31°25'24"	83°52'41"	Oct. 18	232.63	235.92	3.29
14M008	31°35'18"	83°59'36"	Oct. 18	249.32	246.78	–2.54
14P012	31°34'01"	83°55'58"	Oct. 18	240.42	248.52	8.10

Table A4. Measured, simulated, and residual water levels and location of wells measured for the October 1999 model calibration.—Continued

[USGS, U.S. Geological Survey; NAVD 88, North American Vertical Datum of 1988; °, degree; '. minute; ", second; –, minus]

USGS site name	Latitude (north)	Longitude (west)	Date measured, during 1999	Water level, in feet above NAVD 88		
				Measured	Simulated	Residual
14Q005	31°35'04"	83°58'52"	Oct. 18	242.78	248.27	5.49
14Q006	31°30'28"	83°57'09"	Oct. 18	245.69	249.25	3.56
14Q009	31°37'30"	83°55'03"	Oct. 18	250.66	269.27	18.61
15K009	31°21'55"	83°51'19"	Oct. 19	205.68	211.89	6.21
15K010	31°22'50"	83°50'35"	Oct. 19	209.28	216.71	7.43
15L007	31°26'46"	83°52'28"	Oct. 19	216.28	220.84	4.56
15L020	31°29'21"	83°51'26"	Oct. 19	208.35	223.06	14.71
15L021	31°30'40"	83°46'12"	Oct. 19	200.70	223.40	22.70
15L022	31°31'47"	83°49'16"	Oct. 19	242.73	234.09	–8.64
15M004	31°32'16"	83°50'45"	Oct. 19	264.75	251.68	–13.07
15M005	31°35'18"	83°49'49"	Oct. 19	259.28	247.83	–11.45
15Q012	31°41'24"	83°49'58"	Oct. 19	262.06	274.62	12.56
16L019	31°25'27"	83°42'35"	Oct. 19	208.66	220.21	11.55
FL4566	30°40'56"	84°50'25"	Oct. 20	62.07	59.69	–2.38
FL4681	30°42' 30"	84°53'59"	Oct. 19	74.42	64.85	–9.57
FL5147	30°49'18"	84°56'56"	Oct. 19	77.48	78.21	0.73
FL5266	30°51'13"	85°04'36"	Oct. 19	82.66	85.26	2.60
FL5288	30°51'37"	85°06'03"	Nov. 17	81.52	86.82	5.30
FL5378	30°53'26"	85°05'27"	Nov. 18	83.18	90.05	6.87
FL5391	30°53'36"	85°02'36"	Nov. 17	97.84	86.85	–10.99
FL5408	30°53'10"	85°01'39"	Nov. 17	91.28	85.13	–6.15
FL5460	30°54'50"	85°04'54"	Nov. 17	89.77	91.61	1.84
FL5490	30°55'24"	85°07'05"	Nov. 17	90.09	95.47	5.38
FL5635	30°57'44"	85°07'22"	Nov. 17	105.02	101.00	–4.02
FL5697	30°58'45"	85°07'03"	Nov. 18	107.11	103.09	–4.02
FL5704	30°58'57"	85°06'49"	Nov. 18	108.11	102.60	–5.51
FL5718	30°59'05"	85°06'34"	Nov. 18	107.24	101.92	–5.32

Manuscript approved for publication, September 15, 2006

Prepared by USGS Georgia Water Science Center

Edited by Patricia L. Nobles

For more information concerning the research in this report, contact
USGS Georgia Water Science Center, Atlanta,
telephone: 770-903-9100